CHANGES IN THE VISUAL SYSTEM OF TELEOST FISHES DURING GROWTH AND SETTLEMENT: AN ECOLOGICAL PERSPECTIVE

Thesis submitted by

JULIA SHAND BSc. (Hons) (Durham)

for the degree of Doctor of Philosophy in

the Department of Marine Biology at

James Cook University of North Queensland

March 1994

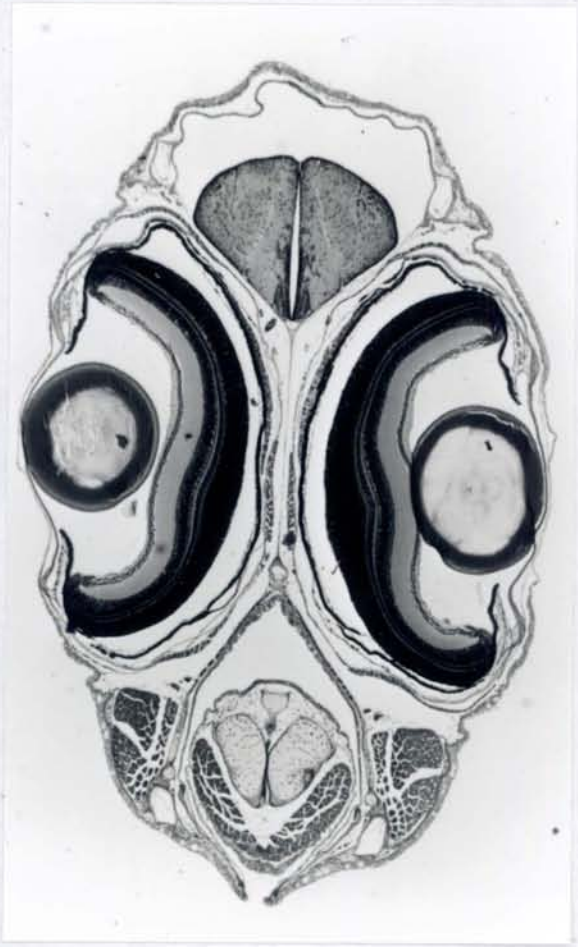

Transverse section through the head of a newly-settled fish, the labrid *Stethojulis strigiventer*, standard length 5.7 mm.

Statement on Access to Thesis

I, the undersigned, the author of this thesis, understand that James Cook University of North Queensland will make it available for use within the University Library and, by microfilm or other photographic means, allow access to users in other approved libraries. All users consulting this thesis will have to sign the following statement:

> "In consulting this thesis I agree not to copy or closely paraphrase it in whole or in part without the written consent of the author; and to make proper written acknowledgement for any assistance which I have obtained from it."

Beyond this, I do not wish to place any restriction on access to this thesis.

27th March 1994

ABSTRACT

Nearly all tropical teleost fishes have a pelagic larval phase. Species that settle to a demersal reef-associated mode of life experience dramatic changes in habitat and light environment at this time. In many cases, behaviour associated with feeding, predator avoidance and diel activity also changes. These changes are often rapid, overnight, events. The growth of the eye and extent to which the visual system of larval fishes alters during settlement was investigated in fish with ecologically differing adult lifestyles.

The ocular morphology of 18 species of tropical teleosts caught from a variety of locations across the northern Great Barrier Reef, Australia, was examined prior to and following settlement. Detailed retinal cell counts of 6 species with differing post-settlement lifestyles were carried out on fish covering a range of developmental stages. These were: the reef fish *Stethojulis strigiventer* (Family Labridae), a microcarnivore; *Pomacentrus moluccensis* and *Pomacentrus bankanensis* (Family Pomacentridae), a planktivore and herbivore respectively; *Apogon doederleini* (Family Apogonidae), a nocturnal planktivore; the inter-reef fish *Upeneus tragula* (Family Mullidae), a benthic carnivore; and the inshore planktivore *Ambassis vachelli* (Family Ambassidae). A microspectrophotometric investigation of the visual pigment compliment of *Upeneus tragula* was carried out over the settlement period. In addition microspectrophometric measurements obtained from the adults of four additional tropical teleosts are presented.

Fish that settled at small and intermediate sizes showed changes in retinal cell densities prior to settlement which appeared to be in anticipation of the post-settlement lifestyle. *Upeneus tragula*, a species that remained pelagic for an extended period was found to maintain adaptations for a pelagic lifestyle in both structural and visual pigment compliment. At settlement the retina of this species under went rapid changes in structure as a double layer of cones in the dorsal retina amalgamated to form a single layer. The loss of long-wavelength sensitivity also occurred at this time.

The theoretical ability of an eye to resolve fine detail improved rapidly as eye size increased. Mechanisms for increasing sensitivity in nocturnal species were found. These included an increase in rod densities and a lowering of Matthiessen's ratio. The ocular features found in the variety of fish examined were considered in relation to the light environment and behaviours of the fish at respective phases of their life history.

ACKNOWLEDGMENTS

This thesis would not have been completed without the help and encouragement of many colleagues and friends. To all, I extend my sincere gratitude. My supervisors Howard Choat, Dave Williams and Chris Alexander have always been ready to give advice and assistance. Bill Muntz, who took on the role of an honorary supervisor, also provided much advice and helpful discussion. Invaluable help with field work and the provision and identification of specimens has been given by Mark McCormick, Mark Meekan, Rob McCauley, Mike Cappo, Tony Fowler and Bridgid Kerrigan. Similarly, help with laboratory techniques has been received from Leigh and Heather Winsor, Zollie Florian and the staff of the Marine Biology Department at James Cook University. The setting up of the microspectrophotometer would not have been possible without the skills of Julian Partridge who also advised on analysis of visual pigment data. Additional data analysis has been carried out with considerable assistance from Rob McCauley. Drafts of the thesis have been read by Chris Alexander, Rob McCauley and Julian Partridge. Ann Sharp has always been willing to help with smoothing the way on administrative matters.

Financial assistance was provided by a Commonwealth Scholarship and student grants from the Australian Coral Reef Society and James Cook University.

A very special thanks is owed to Rob McCauley for his friendship, patience and encouragement throughout. Without his continued support my task would have been immeasurably more difficult.

I was first introduced to the world of animal vision by John Lythgoe and it was he who encouraged me to come to Australia and undertake this work. His influence has always been present. Sadly, I am prevented from expressing my gratitude. To his memory I humbly dedicate this thesis.

CONTENTS

List of Figures

Part I

Part II

List of Plates

List of Tables

DECLARATION

I declare that this thesis is my own work and has not been submitted in any form for another degree or diploma at any university or other institution of tertiary education. Information derived from the published or unpublished work of others has been acknowledged in the text and a list of references is given.

Julia Shand
27th March 1994

GENERAL INTRODUCTION

The eyes of vertebrates are designed to capture light and resolve images, hence providing information to the animal about its surroundings and allowing it to carry out essential functions such as food gathering or predator avoidance. The laws of physics governing the behaviour of light have a profound influence on the design of all eyes and every eye has to operate within the framework of these laws (Lythgoe, 1979; Land 1981; Duncan, 1990; Goldsmith, 1990). The effects of these laws can be seen in the optical design of eyes such as the size of apertures, in the size of photoreceptors and in the spectral sensitivity of visual pigments contained in these cells. Although the "camera" vertebrate eye is of a conservative design when compared with the enormous variety of eye designs found in invertebrates, there are, within this basic design, many adaptations and specialisations (Walls, 1942). These specialisations can often be correlated with the mode of life of particular groups of animals. For example most fish possess a spherical lens with a graded internal refractive index to overcome the lack of refractive power at the cornea and the problem of spherical aberration. This enables an image to be focussed on the retina of the aquatic eye (Land, 1987 for review). The extent to which species will go to improve sensitivity or resolving power usually appear to weighted against the "costs" of such specialisations in terms of metabolic demand or space and although some eyes could be considered inferior in, say, resolving power they will usually be found to meet the requirements of the animal for the behavioural tasks it needs to carry out in a particular habitat (Land, 1981).

In the aquatic situation the behaviour of light is affected by the natural variation in the colour and turbidity of different bodies of water and by the loss of intensity and spectral attenuation with any increase in depth (see Lythgoe, 1979; 1988; Loew and McFarland, 1990; Partridge, 1990 for reviews relating to vision). Thus, the study of the visual system of fishes can be particularly rewarding when examining the adaptations to different photic conditions and indeed the eyes of

fishes show many morphological and biochemical specialisations which can be correlated with mode of life and habitat. For example, the retinae of many deep-sea fishes show structural specialisations to maximise photon capture (Locket, 1977; Pankhurst, 1987) and they may also possess visual pigments that have the wavelength of maximum absorption located in a region of the spectrum that corresponds to the predominant wavelengths of the down welling light (Denton and Warren, 1957; Munz, 1958; Partridge *et al.*, 1988). Diurnal shallow-living species on the other hand can show variations in retinal topography that can be related to visual axis (Tamura and Wisbey, 1963), feeding mode (Pankhurst, 1989) or foraging ecology (Williamson and Keast, 1988; Collin and Pettigrew, 1989a, b; Browman *et al.*, 1990; Zaunreiter *et al.*, 1991). In addition, the wavelengths of maximum absorption of the visual pigments contained in the cones of many species have been shown to be related to the spectral composition of the ambient light (Lythgoe, 1984; Lythgoe and Partridge, 1989; Bowmaker, 1990 for reviews). Although other sensory systems, such as lateral line and hearing, become increasingly important in environments not well suited to vision it is only in some cave dwelling species that the sense of vision is abandoned. For the fish inhabiting the clear waters of the tropics vision is an important, and often the primary, sensory system (McFarland, 1991).

Vision is also important during larval life, influencing feeding ability and predator avoidance (e.g. Blaxter, 1986 for review). The eyes of coral reef species are prominent at hatching and occupy a large volume of the head throughout the larval stages, as can be seen in Plate 1 (front piece). Following hatching, the eye undergoes enormous changes in structure as a result of growth (Powers and Raymond, 1990 for review) while still maintaining visual function (Fernald, 1985; 1990a). At a time when the development of the eye is still in progress many larval reef fish undergo settlement from the pelagic environment to the reef and the changes in habitat can also be accompanied by changes in feeding behaviour (Victor, 1991 for review). Thus a complete change in the light environment and the nature of visual tasks is experienced.

It is known that fish that migrate from one spectral type of water to another, such as eels and salmon, undergo changes in retinal structure and visual pigment compliment prior to or concomitant with changes in habitat or feeding strategy (Carlisle and Denton, 1959; Beatty, 1984; Pankhurst, 1982; Pankhurst and Lythgoe, 1983). However, changes in the visual system during early ontogenetic stages have not been extensively investigated in fish that undergo a rapid transition from a pelagic to reef environment, such as those taking place at the time of settlement in many coral reef species.

This thesis examines the retinal structure of a number of species of tropical larval and juvenile fishes. Detailed changes in the visual system of five coral reef and one inshore fish species, as they undergo settlement from the plankton to ecologically differing reef-associated modes of life are investigated. An investigation of the visual pigments of one species during settlement was also undertaken. Visual pigment results for four additional adult species, which have not been previously published, are also presented.

The thesis is divided into two sections, the first dealing with the morphological aspects of the investigation. The introduction to the first section gives a summary of the structure of the teleost eye and introduces the terminology used throughout the thesis. The second section introduces the factors affecting the nature of ambient light in the aquatic environment and the role of visual pigments in the adaptation of the visual system to different photic conditions. The thesis is concluded with a general discussion.

Copies of papers published during time the thesis was being prepared are given in the appendices.

PART I

Morphology of the Teleost Eye and Changes in Retinal Structure During Growth and Settlement

Generalised structure of the teleost eye

The structure of a teleost eye is shown in Fig. I.1A. Fig. I.1B shows a transverse section through the wall of the eye. There are considerable interspecific differences in the arrangement of many of the structures but a general pattern is followed. This is described briefly here to introduce the terminology used in this thesis. The following summary is taken mainly from Walls (1942) and Nicol (1989).

The eye is completely surrounded by layers of tough fibrous bundles of collagen and elastic fibres, collectively known as the sclera. This is only penetrated by the optic nerve. The sclera is transparent over the front of the eye, forming a layer of the cornea. An exterior transparent dermal component of the cornea is continuous with the epidermis surrounding the eye. Multilayer structures, of alternating refractive index, that bring about iridescent colouration of the cornea can be located in a number of different sites within the cornea (Lythgoe, 1975; Shand, 1988). Carotenoid pigments, responsible for the yellow colour of some teleost corneas, are found in the corneal stroma.

The layers inside the sclera are pigmented and richly vascular and known as the choroid. The black pigment, which absorbs light entering from directions other than the front of the eye, is melanin. In addition a silvery layer of guanine crystals in the outer region of the choroid, the stratum argenteum, reflects light away from the back of the eye. This layer may also act as reflective camouflage, similar to that often surrounding the gut, in transparent larval fish (McFall-Ngai, 1990). In many teleosts there are areas of the choroid particularly rich in blood vessels, those occurring above the optic nerve being known as choroid glands and those below as lentiform bodies. Teleosts possess an embryonic fissure, formed by apposition of the lips of the optic cup, running in a ventro-nasal direction from

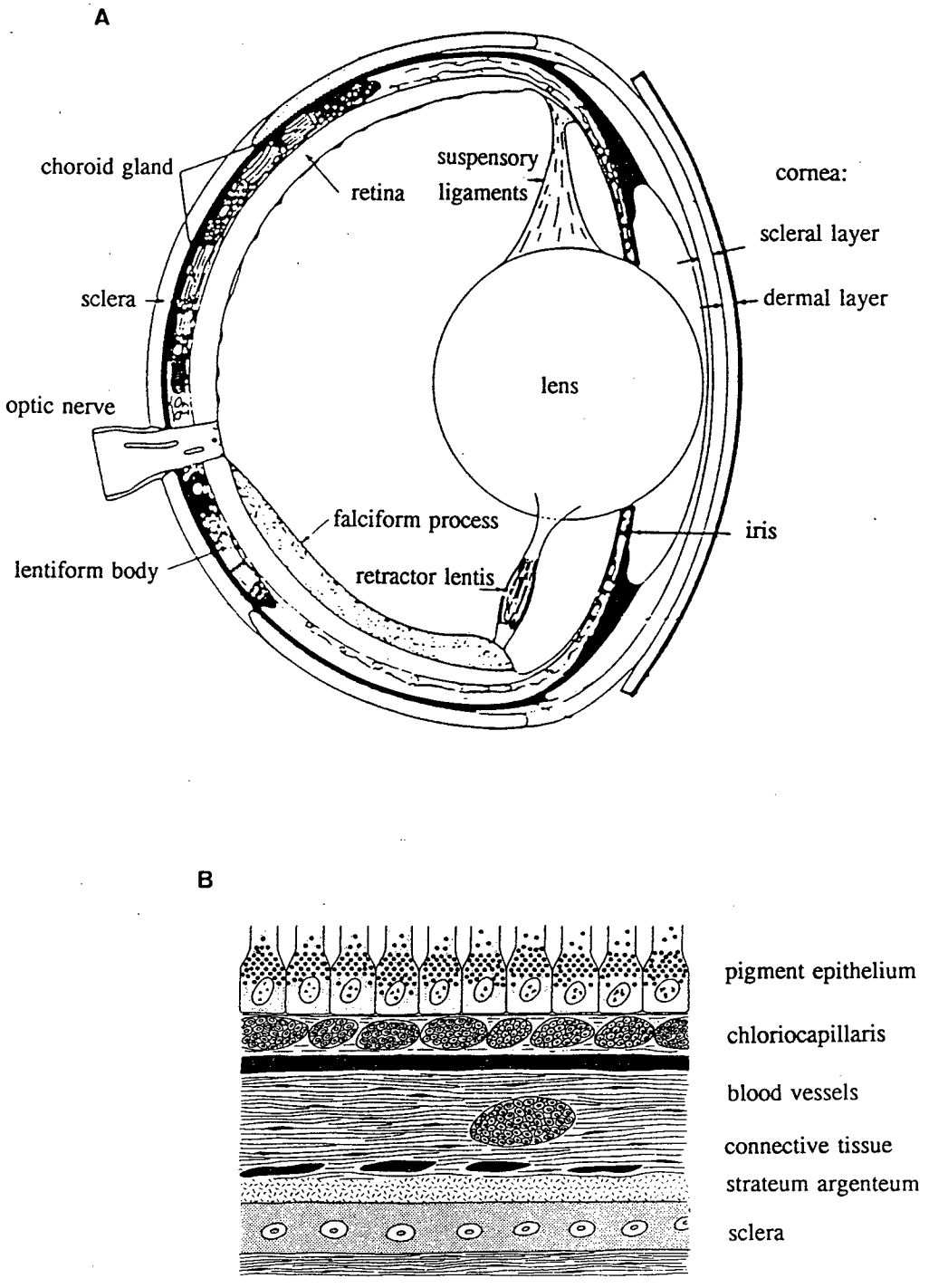

Fig. I.1. Vertical sections through a generalised teleost eye: **A)** the whole eye (after Walls, 1942); **B)** details of the layers in the back wall of the eye (after Nicol, 1989).

the optic nerve head. This often gives rise to a fold of choroidal connective tissue, protruding upward into the vitreous cavity, called the falciform process. Several of the choroid layers continue beneath part of the cornea as the iris but leave a central aperture which forms the pupil. Muscles responsible for pupillary movement are located within the iris although alteration of the size of the pupil is not a common feature in teleosts. The iris is also continuous with the retinal pigment epithelium and the sensory retina. The retina forms the internal lining of the eye cup. A more detailed description of the structure of the retina is given below. The reflecting tapetum (or tapeta lucida), a layer of stacked guanine crystals that reflect light back through the retina in some teleosts, can be located at the back of the retina or in the choroid. This layer of crystals is responsible for eye shine and is most common in species that are nocturnal or live in low-light conditions.

The crystalline lens, lying behind the pupil, focuses light onto the retina. This is spherical in almost all teleosts and is held in place by suspensory ligaments and the retractor lentis muscles. Accommodation, or changes in focal length of the lens for focusing, are also brought about by these muscles. The interior of the eye is divided into two fluid filled chambers, that in front of the lens containing the aqueous humour and that behind, the gelatinous vitreous humour. The pressure of the fluids within these chambers is largely responsible for keeping the eye distended and rigid.

Generalised structure of the teleost retina

Figure I.2 shows a schematic representation of a transverse section of a teleost retina. Plate I.2 shows photomicrographic views of a) light-adapted and b) dark adapted teleost retina.

The Pigment Epithelium: The external layer of cells, next to the choroid, form the pigment epithelium. Processes of these cells containing melanin granules extend

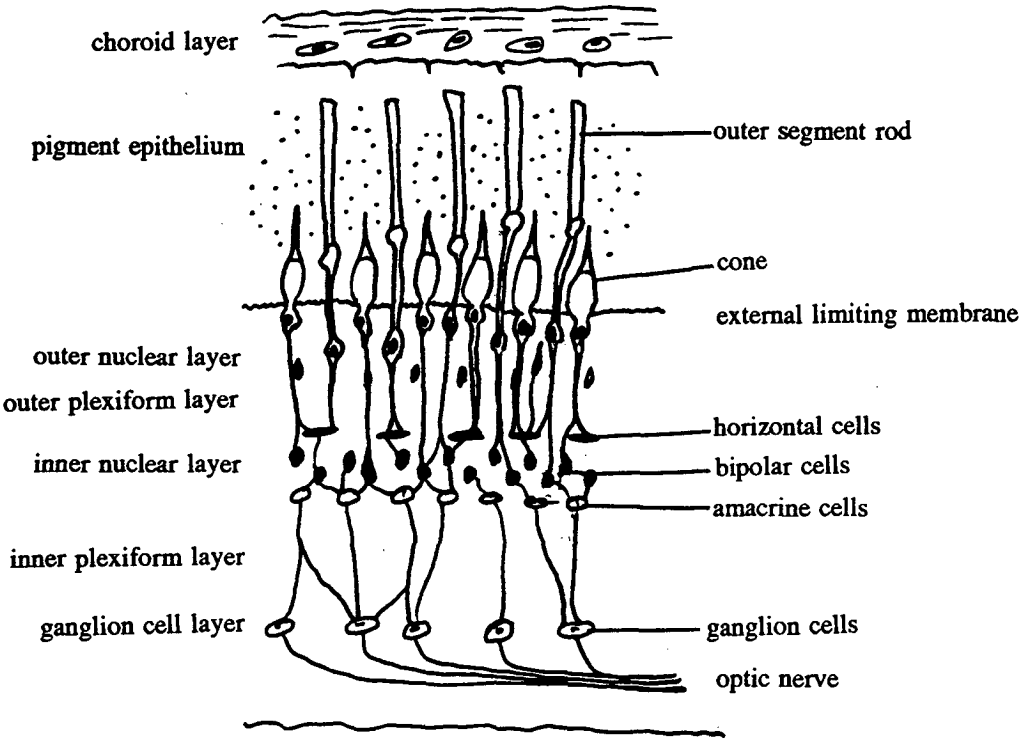

Fig. I.2. Schematic drawing of a radial section through a generalised teleost retina. See Plate I.2 for a photomicrographic view.

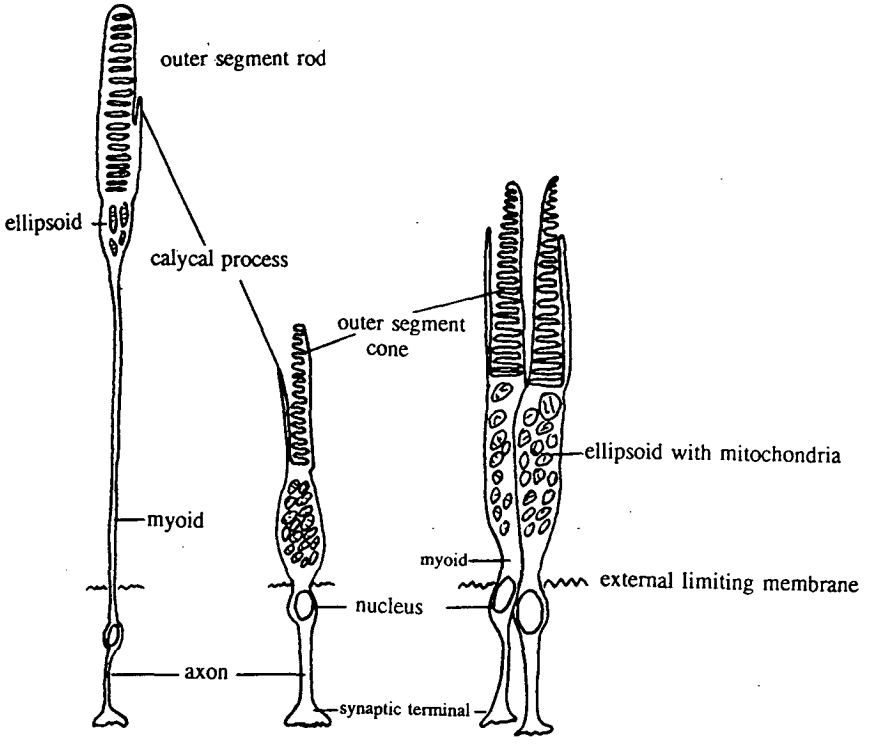

Fig. I.3. Schematic drawing of a typical rod, single cone and double cone. Note the discs within the rod outer segment are isolated whereas those within the cones are continuous.

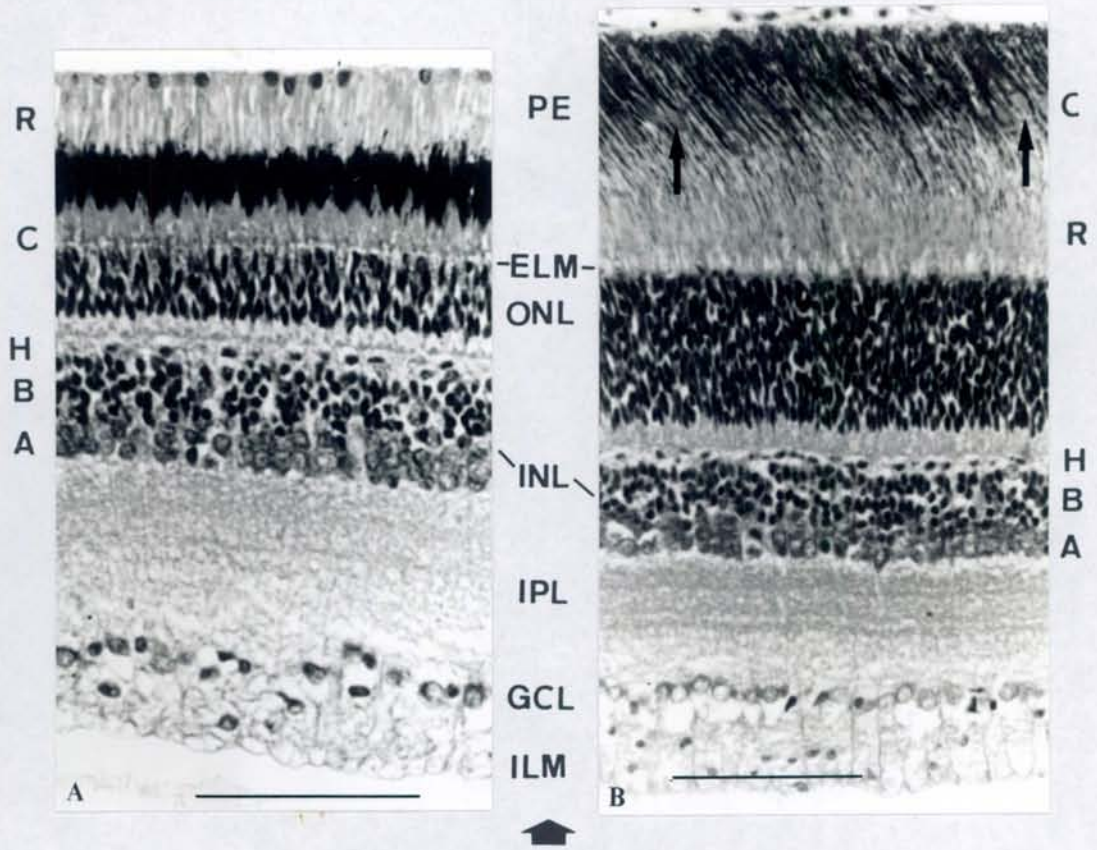

Plate I.2. Radial sections through the retinae of 2 teleosts: **A)** *Chromis atripectoralis* in the light-adapted condition. The cone inner segments are in a vitread position aligned along the external limiting membrane with the outer segments protruding into the melanin of the pigment epithelium. The rods are displaced to a sclerad position at the back of the eye and shielded from excess light by the melanin; **B)** *Neoniphon sammara* in the dark adapted condition. The pigment epithelium is retracted in a sclerad position and the rods are in a vitread position next to the external limiting membrane. The cone inner and outer segments have moved in a sclerad direction and only a few can be seen amongst the melanin of the pigment epithelium (arrows). *N. sammara* is a nocturnal species with high rod densities, as reflected by the thickness of the outer nuclear layer. PE, pigment epithelium; R, rod outer segments; C, cone ellipsoids; ELM, external limiting membrane; ONL, outer nuclear layer; INL; inner nuclear layer; H, horizontal cell bodies; B, bipolar cell bodies; A, amacrine cell bodies; IPL, inner plexiform layer; GCL, ganglion cell layer; ILM, inner limiting membrane. The large arrow shows the direction from which light strikes the retina. Scale bars = 50 μm. See Fig. I.2 for a schematic representation.

inwards among the photoreceptors. The melanin absorbs much of the scattered light from around the photoreceptors and thus prevents backscattering and deterioration of image quality. The processes of the pigment epithelium around the photoreceptors can change in shape during light- and dark-adaptation (see below for further details). The pigment epithelium is also important in the renewal process of the photoreceptors as it is here that packets of outer segment discs from the photoreceptors are destroyed (see below for further details).

The Photoreceptors: A duplex retina contains photoreceptors of two basic kinds, rods and cones (Fig. I.3). Both have regions called: A) outer segments, which contain stacks of discs that are the site of the photolabile visual pigments; and B) inner segments that are composed of ellipsoids, containing mitochondria and other cell organelles. Rods have long, cylindrical outer segments and small ellipsoids, whereas cones appear shorter and conical with bulbous ellipsoids. Teleosts usually possess paired cones (or occasionally even triple or quadruple cones), the morphology of which is very variable between species. The two halves may be identical (so known as twin cones) or differ in the size of the outer segments and ellipsoids (so known as double cones). The cones are fused along the ellipsoid and myoid regions but the outer segments and nuclear regions remain distinct (Fig. I.3).

The arrangement of cones in teleosts usually follows a precise pattern known as the cone mosaic. When viewed in cross section the ellipsoids of the cones of a light-adapted retina are aligned in rows (Fig. I.4) with specific repeating patterns (arrays or units) of the double and single cones. A common arrangement is a square array in which four double cones surround one single cone (Fig. I.4). The significance of these arrays is not entirely clear but suggestions include movement discrimination (Lyall, 1957; Engstrom, 1963; Ahlbert, 1976), border enhancement (Browman *et al.*, 1990), resolution of colour (Fernald, 1989a) and detection of polarised light (Cameron and Pugh, 1991). The mosaic pattern can extend through to the layers of neural cells into the inner retina, thus forming physiological units (Wagner, 1978).

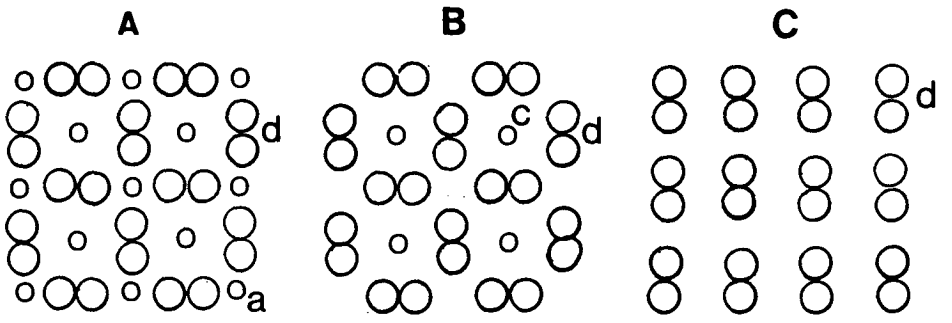

Fig. I.4. Schematic drawing of tangential sections through teleost retinae showing the most common mosaic patterns formed by the cones. **A)** Alternating rows of single and double cones with central single cones and additional single cones. **B)** A square array of double cones and central single cones. **C)** Rows of double cones only. Abbreviations: a, additional single cones; c, central single cone; d, double cone. After Boehlert (1978).

The arrangement of the membrane discs in the outer segments differs between rods and cones (Fig. I.3). In rods a stack of isolated discs is characteristic. These are formed at the inner end of the outer segment and lie free within the cytoplasm. In cones, the membranes are not regularly isolated to form discs but remain continuous so that the intra-disc spaces are in contact with the extracellular space (Fig. I.3). Continual renewal of the visual pigment, located within the membranes of both rods and cones, is brought about by the addition of cell membrane at the base of the outer segments and removal of bundles of discs from the tips of the cells by the pigment epithelium (Young, 1969).

Contractile myoids connect the photoreceptor inner segments to the nuclei. The nuclei of both the rods and cones form a distinct layer known as the outer nuclear layer (ONL) (Plate I.2). Between the ellipsoids and nuclei of the photoreceptors, and through which the myoids pass, is a boundary membrane known as the external limiting membrane (ELM). Axons lead from the nuclei to synaptic terminals in the outer plexiform layer (OPL), where connections with the neurones of the inner retina take place (Fig. I.2).

The majority of diurnal teleosts possess both rods and cones with, in general, the rods participating in scotopic (night) vision and cones in photopic (day) vision. It is possible double cones are concerned with vision at low light intensities. Cones are also the receptors for colour vision. The rods and cones participate in retinomotor movements around the times of change in ambient light intensity i.e. dawn and dusk. In a light-adapted retina (as in Plate I.2A) the cone myoids are contracted and the base of the cone ellipsoids lie along the external limiting membrane. The rod myoids are extended so that the rod ellipsoids and outer segments are displaced to the back of the eye amongst the processes of the pigment epithelial cells. The pigment granules of the pigment epithelium extend around the cone outer segments. In dim light and at night, retinomotor movements reverse the positions of the rods and cones and the pigment granules contract to the back of the eye (Plate I.2B). These movements ensure that light absorption by the rods is maximal at night and that they are protected from excess light by the pigment granules during the day, when the cones are in a position to best absorb light.

The Neural Cells: The cell bodies of the neural cells form a distinct band inside the outer plexiform layer (OPL), known as the inner nuclear layer (INL) (Fig. I.2, Plate I.2). Within this layer three main sub-layers containing the following cells can be recognised: A) Horizontal cells; B) Bipolar cells and; C) Amacrine cells. The connections between photoreceptors and neural cells, and between neural cells themselves, are not straight forward with a number of sub-types having been classified depending on position and pattern of connection. In

addition, neurones can be displaced from their usual positions, with for example, amacrine cells occurring in the ganglion cell layer and vice versa. Much variation between species exists (for reviews see Dowling, 1987; Wagner, 1978; 1990). In very general terms, rods and cones connect to both horizontal and bipolar cells and the horizontal cells connect to the bipolar dendrites in the OPL. Bipolar cells connect to amacrine cells, as well as directly to the synaptic terminals of the ganglion cells, in the inner plexiform layer (IPL). Amacrine cells also connect to ganglion cells in the IPL. The ganglion cell bodies lie in the ganglion cell layer (GCL), the axons from which form the nerve fibre layer that leads to the optic nerve. An internal limiting membrane (ILM) separates the retina from the vitreous humour.

Area centralis: Many fish have areas of retina where there is an increased density of cones, bipolar and ganglion cells. These areas usually correspond to the main visual axis of the fish and confer increased resolution. Rods densities are usually reduced in such areas.

Development of the teleost eye

At hatching the eyes of larval teleosts have usually reached a stage of development at which the optic cup is formed with the layers of the pigment epithelium and neurosensory retina differentiated (Walls, 1942; Nicol, 1989). The lens vesicle has separated from the ectoderm and the iris and corneal stroma are defined. Of the retinal cells the ganglion cells are the first to differentiate, followed by amacrine cells, bipolar and horizontal cells and finally the photoreceptors. The axons of the ganglion cells extend to where the optic cup joins the optic stalk, eventually giving rise to the optic nerve. Synapse formation follows the differentiation of the photoreceptors (Walls, 1942; Grun, 1982; Nicol, 1989). In general larval fish have a cone dominated retina at hatching with the rods being differentiated at later stages of development (Ali, 1959; Blaxter and Staines, 1970; Blaxter and Jones, 1967; Sandy and Blaxter, 1980; Sharma and

Ungar, 1980; Branchek and BreMiller, 1984; Raymond, 1985; Evans and Fernald, 1993). An exception is the eel, *Anguilla anguilla* in which the deep-sea leptocephalus larvae has rod-like receptors (Pankhurst, 1984). Although the timing and rate of development of photoreceptors varies between species, it appears that by the time fish become free-swimming and begin to feed, differentiation of the photoreceptors is well underway (Brancheck and Bremiller, 1984; Blaxter, 1988; Powers and Raymond, 1990). The eyes are, however, still very small and as a result the optics are inherently poor with the short focal length being a factor limiting the resolving power (Land, 1981). The rapid increase in eye size following hatching together with a period of rapid development of neuronal circuitry and proliferation of retinal projections to the brain allows for a rapid increase in visual resolution (Neave, 1984; Marguiles, 1989; Schmitt and Kunz, 1989; Pankhurst *et al.*, 1993).

The teleost eye, unlike that of birds and mammals, continues to grow during the lifetime of the animal and this is now known to be accomplished by both a stretching of the retinal tissue and cell neurogenisis at the retinal margins (Fernald, 1989a; Johns, 1981; Powers and Raymond, 1990 for reviews). As fish develop during larval and juvenile life, cone and ganglion cell densities decrease (Ali, 1964; Johns and Easter, 1977; Kock, 1982). However the densities of rods initially increase and are then maintained or may even continue to increase during adult growth (Powers *et al.*, 1988). The increase in rod density results from continual mitotic activity within differentiated areas of the retina (Scholes, 1976; Sandy and Blaxter, 1980; Johns and Fernald, 1981; Johns, 1982; Fernald, 1989b). Exactly how the visual function of the eye is maintained during the early stages of rapid growth, and its continued growth during adult life of the fish, is still unclear (Powers and Raymond, 1990). In addition to the changes resulting from growth, the structure of the retina can undergo changes in preparation for, or in response to, ontogenetic changes in habitat and behaviour (Noakes and Godin, 1988). For example shallow living larval and juvenile stages of deep-sea fish can lose cone classes as they migrate to deeper water (Boehlert, 1978; 1979; Munk, 1990). New types of photoreceptor have been found in the winter flounder

following metamorphosis (Evans and Fernald, 1993; Evans *et al.*, 1993). Changes in the distribution of areas of high cone density have been recorded during development of the salmon and trout (Ahlbert, 1976) and red sea bream (Kawamura *et al.*, 1984). In addition, as the feeding habits of the trout change, a class of small single cones is lost with a concomitant loss of ultraviolet sensitivity (Bowmaker and Kunz, 1987). Similarly, changes in sensitivity and acuity were found in three species of hake as their depth distribution and feeding behaviour changed during growth (Mas-Riera, 1991).

Coral reef fish, like most teleosts have larvae that hatch, whether from demersal or pelagic eggs, as relatively passive plankters. Larvae rely on their yolk sacs for initial sustenance and are without developed powers of mobility (e.g. Leis and Rennis, 1983; Kendall *et al.*, 1984). However within a number of days the yolk sac is absorbed and larvae begin to feed (Leis, 1991a). Generally, a period of development in the pelagic environment follows until notochord flexion is complete and the full fin ray compliment obtained. During this time they may possess morphological specialisations for pelagic life such as trailing guts or elongate fin spines (Moser, 1981). By post-flexion, many coral reef species have larvae that have changed from passive planktonic organisms to actively feeding and selecting their position within the water column (Leis, 1991b). This implies that their sensory systems, in particular the visual system, have developed sufficiently to allow these behavioural responses. At settlement, the larvae of many tropical reef fishes undergo an abrupt and dramatic transition in lifestyle, when in a matter of hours, they abandon their pelagic existence to begin the reef-associated mode of life (Victor, 1991). This transition, that can involve changes in body shape and colouration, and can be accompanied by changes in feeding behaviour is often termed transformation (Kendall *et al.*, 1984) or metamorphosis (Yousen, 1988). The stage of development at which this occurs can vary enormously between different species. For example, some members of the families labridae and scaridae settle out of the plankton at very small sizes e.g. 6 mm standard length (SL) in *Coris sp.* and *Stethojulis sp.* (Brothers *et al.*, 1983; Alison Green, personal communication) and 7.5 - 8 mm SL in *Scarus sp.*

(Bellwood and Choat, 1989). Larvae of the family Mullidae have a protracted pelagic stage and do not settle until much later (Caldwell, 1962) e.g. 27 mm SL for *Upeneus tragula* (McCormick, 1994). Whatever the stage of development, it is important to the subsequent survival of the fish that the sensory systems of newly settled juveniles are able to cope with the new range of environmental and behavioural cues to which they become exposed.

The structural investigation reported in this section examines the retina of eighteen species of teleosts. A wide range of species were examined before it became apparent which would be suitable for detailed examination over a size range encompassing settlement. The information obtained for all species is included. Six species with ecologically differing lifestyles as adults were chosen for detailed investigation of development of the eyes prior to, during, and following settlement, a time when the visual demands of the fish are changing. The extent to which changes in the retinal structure are related to behavioural and environmental influences, rather than growth alone is discussed.

Terminology

The following terms are used to describing regions and layers of the retina: vitread, towards the vitreous; sclerad, towards the sclera; or alternatively: proximal, towards the vitreous; distal, towards the sclera. Nasal and rostral, towards the nose; temporal and caudal, towards the tail. Planes of sections: transverse, right angles to the longitudinal axis of the fish; radial, normal to the retinal surface; tangential, parallel to the retinal surface.

The terminology of larval stages can often cause confusion (Leis and Rennis, 1983). That used by Leis and Rennis (1983), Kendall *et al.* (1984) and McCormick (1992) is followed in this thesis. By following this terminology, larva refers to all developmental stages from hatching to loss of larval characteristics. Thus, larval includes the following stages: yolk-sac (hatching to absorption of

yolk sac); pre-flexion (following yolk sac stage but prior to flexion of notochord); flexion (prior to complete flexion of notochord); post-flexion (notochord flexion complete and full caudal fin ray count obtained); late-stage pelagic (full external meristic compliment but with specialisations for pelagic life). Juvenile refers to fishes that have the appearance of small adults and, in the case of demersal species, have usually settled out of the pelagic environment.

Identification of species was carried out using a number of specialised texts e.g. for larvae: Leis and Rennis (1983); Leis and Trnski (1989); Okiyama, 1988. For juveniles and adults: Randall *et al.* (1990); Myers (1989); Allen and Swainston (1988); Allen and Burgess (1990); Bellwood and Choat (1989). The assistance of many fish biologists who are taxonomic specialists in different families was also obtained.

The authorities for the respective species used in this study are given in Table I.1.

Materials and Methods

Study species and collection techniques

Larval, juvenile and adult fish were collected between 1989 and 1993 from a variety of tropical marine habitats in the central and northern regions of the Great Barrier Reef and adjacent coastline (see Table I.1 and Fig. I.5 for a map showing the location of the sites). Table I.1 summarises the details of the species caught, the size range obtained, the location of capture, the method of capture and the type of results obtained from each species. Table I.2 summarises ecological data about the species investigated at the stages of their life cycle relevant to this study. Further details of the collection techniques are given below.

Hatching eggs: Newly hatched *Pomacentrus amboinensis* were obtained by bringing eggs, attached to shells or rocks, into the aquarium at Lizard Island Research Station a few hours before the estimated time of hatching. Following hatching, larvae were sampled at the following ages: 20 min; 14 hr; 24 hr; and 46 hr.

Plankton tows: Twenty min plankton tows were carried out around Lizard Island using a 800 μm mesh plankton net set at 5 m depth. The net was deployed from a 7.2 m aluminium dory travelling at an approximate speed of 0.25 - 0.5 kn. This method of capture did not obtain live fish as they were crushed in the cod end by large numbers of the scyphozoan *Aurelia*. Larvae in a reasonable condition were immediately transferred to Bouin's fixative.

Light traps: These are particularly efficient at catching larval fish in late stages of development and pelagic juveniles (Choat *et al.*, 1993). Traps were suspended at about 1 m depth. The control of the lights was fully automated and set for three collection times of 1 hr duration (21-2200 hrs; 24-0100 hrs and 03-0400 hrs) (see Doherty (1987) for design details). Fish were alive and in healthy condition the

Table I.1. List of species caught, the size range obtained, the location of capture, the method of collection and the type of results obtained. L, larvae; S, settled juvenile or adult; P, pelagic juvenile or adult; TBM, Townsville Breakwater Marina; AIMS, Australian Institute of Marine Science Breakwater; Morphology, external eye and lens measurements only; Retinal structure, general observations and characteristic of the species; Cell counts, detailed retinal cell densities over a size range of fish; MSP, microspectrophotometry; EM, electron microscopy. See Fig. I.5 for map showing location of collection sites.

Family Species	Size range (SL mm)	Where caught	How caught	Results obtained
Ambassidae				
Ambassis vachelli (Richardson)	L 5-12 S 12-48	TBM TBM, AIMS	Dip net	Shrinkage expt. Morphology Cell count MSP
Apogonidae				
Cheilodipterus quinquelineatus (Cuvier)	S 35-68	Davies Rf.	Diver - quinaldine Retinal structure	Morphology
Apogon doederleini (Jordan and Snyder)	L 9-11 S 11-45	Lizard Is., John Brewer Rf.	Light-trap Diver - quinaldine	Morphology Cell counts
Blenniidae				
Meiacanthus grammistes (Valenciennes)	L 8-21 S 32	Lizard Is. Lizard Is.	Rafts Diver - quinaldine	Morphology Retinal structure
Clupeidae				
Spratelloides delicatulus (Bennett)	P 32-40	GBR Lagoon	Light- trap	Morphology Retinal structure
Hemirhamphidae				
Hemirhamphus sp.	P 9-27 P 100	TBM AIMS	Dip net	Morphology MSP
Holocentridae				
Neoniphon sammara (Forskal)	L 23-29 S 32	Lizard Is.	Light-trap Aquarium settled	Morphology Retinal structure
Labridae				
Coris schroederi (Bleeker)	S 8-60	Lizard Is.	Diver - hand net, fence net	Morphology
Stethojulis strigiventer (Bennett)	S 5-63	Lizard Is. Cell counts	Diver - hand net, Fence net	Morphology Retinal structure
Thalassoma amblycephalum (Bleeker)	S 10-16	Myrmidon Rf.	Diver - quinaldine Retinal structure	Morphology

(Table I.1 continued)

Family Species	Size range (SL mm)	Where caught	How caught	Results obtained
Mullidae				
Parupeneus barberinus (Lacepede)	L 21-27 S 34-76	Lizard Is.	Light- trap Diver - fence net	Morphology
Upeneus moluccensis (Bleeker)	S 125	Cleveland Bay	Trawl	MSP
Upeneus tragula (Richardson)	L 8-30 S 28-75	Lizard Is.	Light-trap, rafts Diver- fence net	Morphology Cell counts, EM MSP
Pomacentridae				
Chromis atripectoralis (Welander and Schultz)	L 7-9 S 12-56	Lizard Is. Lizard Is., Davies Rf.	Light trap Diver- quinaldine, spear	Morphology Retinal structure
Pomacentrus *amboinensis* (Bleeker)	L 2-3 L 11-12 S 14-35	Lizard Is. Lizard Is.	Aquarium hatched Light trap Diver- quinaldine	EM Morphology Retinal structure
Pomacentrus bankanensis (Bleeker)	S 16-67	John Brewer Rf.	Diver- quinaldine	Morphology Cell counts
Pomacentrus lepidogenys (Fowler and Ball)	S 12-43	Davies Rf.	Diver quinaldine	Morphology Retinal structure
Pomacentrus moluccensis (Bleeker)	L 10-11 S 12-46	Lizard Is. Davies Rf.	Light trap Diver- quinaldine, spear	Morphology Cell count
Scaridae				
Scarus sp.	S 7-22	Lizard Is.	Diver- hand net	Retinal structure
Terapontidae				
Terapon theraps (Cuvier)	L 19-26	AIMS	Rafts	Morphology Retinal structure
	S 20-42	Cleveland Bay	Trawl	Shrinkage Expt.

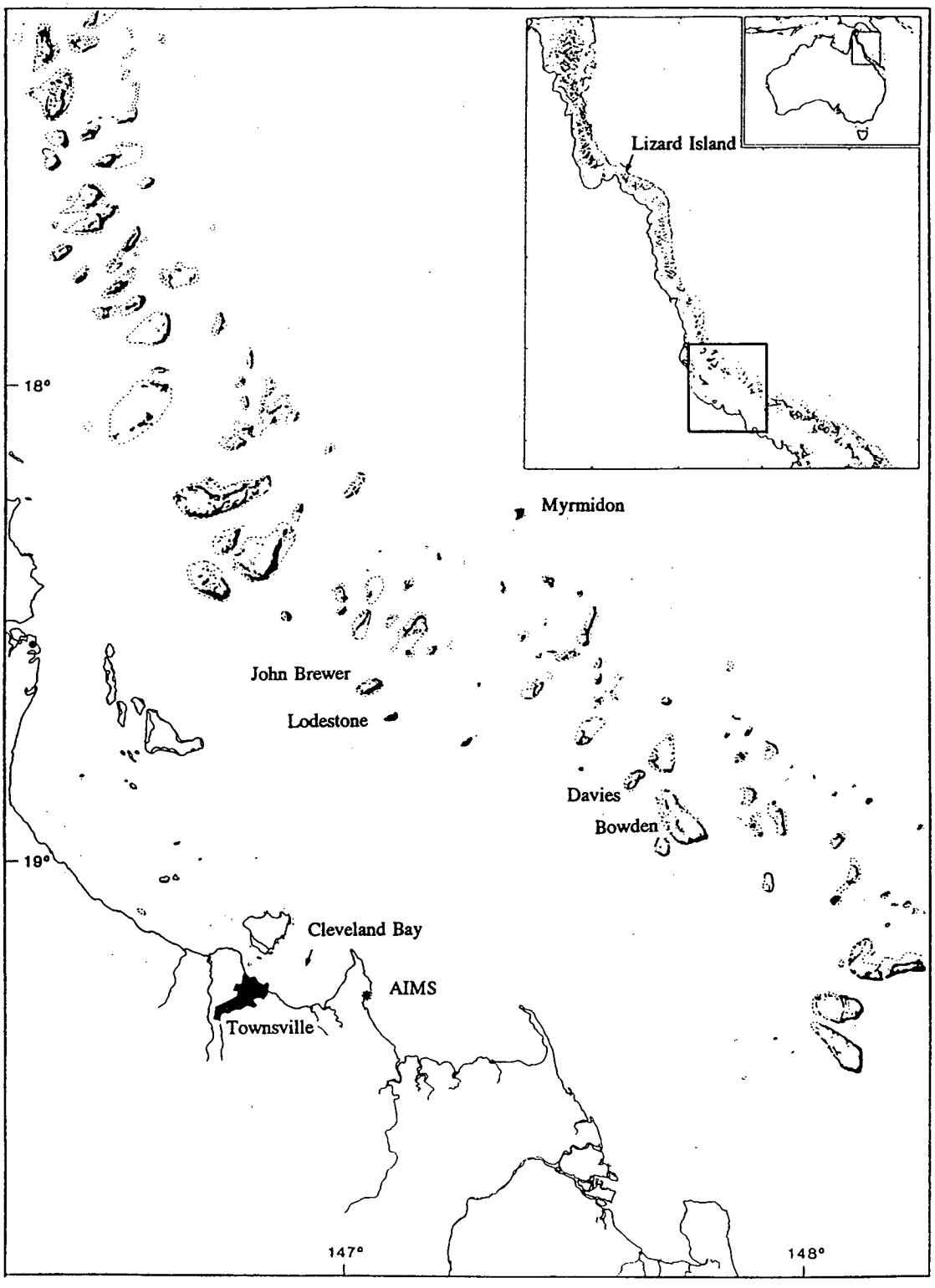

Fig. I.5. Map showing the location of collection sites in North-East Australia. Details of where each species was caught are given in Table I.1.

Table I.2. Ecological notes about the species investigated. L, larval; P, pelagic; S, settled; N, nocturnal; D, diurnal.

Family Species	Size (SL mm)	L/P/S	Settlement size (mm)	N/D	Depth range (m)	Water type	Food preference	Reference
Ambassidae								
Ambassis vachelli	5-12	L	10 - 12	D/N	0-1	inshore/	plankton	Allen and Burgess 1990
	12-48	S		N	0-3	estuarine	plankton	
Apogonidae								
Cheilodipterus quinquelineatus	38-68	S	?	N	1-40	coral reef	crustaceans/fish	Myers 1989
Apogon doederleini	9-11	L	10 - 12	D	1-?	inter reef		
	11-45	S		D/N	1-?	coral reef	zooplankton	Randall et al. 1990
Blenniidae								
Meiacanthus grammistes	8-21	L	20 - 28	D	0-1	inter reef	plankton	
	29-32	S		D	1-30	coral reef	benthic invertebrates	Myers 1989
Clupeidae								
Spratelloides delicatulus	32-40	P	-	D/N	?	inter reef reef margins	zooplankton	M. Cappo (pers comm) Myers 1989
Hemirhamphidae								
Hemirhamphus sp.	9-27	L	-	D	1-2	inshore	plankton	
	100	P		D/N	1-5		plankton	

Table I.2. continued

Family Species	Size (SL mm)	L/P/S	Settlement size (mm)	N/D	Depth range (m)	Water type	Food preference	Reference
Holocentridae								
Neoniphon sammara	23-29	L	28 -32	?	?	coral reef	plankton	
	32	S		N	2-40		zooplankton	Myers 1989
Labridae								
Coris schroederi	8-60	S	5 - 8	D	1-16	coral reef	benthic invertebrates	Myers 1989
Stethojulis strigiventer	5-63	S	5 - 8	D	1-6	coral reef	benthic invertebrates	Myers 1989
Thalassoma amblycephalum	10-16	S	?	D	1-15	coral reef	zooplankton	Myers 1989
Mullidae								
Parupeneus barberinus	21-27	L	28-34	D	1-6	inter reef	plankton	Leis 1991b
	34-76	S		D	5-40	coral reef	benthic invertebrates	McCormick 1992
Upeneus moluccensis	125	S	?	D	5-40	inter reef	benthic invertebrates	
Upeneus tragula	8-30	L	28 - 34	D	1-6	inter reef	plankton	Leis 1991b
	28-51	S		D	5-40	inter reef	benthic invertebrates using barbels	McCormick 1992
Pomacentridae								
Chromis atripectoralis	7-9	L	10 - 12	D		inter reef		
	12-56	S		D	1-5	coral reef	zooplankton	Hamner et al. 1988
Pomacentrus amboinensis	2-3	L						
	11-12	L	10 - 12	D		inter reef		
	14-35	S		D	1-10	coral reef	plankton	

Table I.2. continued

Family Species	Size (SL mm)	L/P/S	Settlement size (mm)	N/D	Depth range (m)	Water type	Food preference	Reference
Pomacentrus bankanensis	16-67	S	10 - 12	D	1-12	coral reef	benthic herbivore	Hamner et al. 1988
Pomacentrus lepidogenys	12-43	S	10 - 12	D	1-10	coral reef	zooplankton	Hamner et al. 1988
Pomacentrus moluccensis	10-11	L	10 - 12	D		inter reef		
	12-46	S		D	1-20	coral reef	plankton	Hamner et al. 1988
Scaridae								
Scarus sp.	7-22	S	5 - 8	D	?	coral reef	crustaceans/herbivore	Bellwood 1988
Terapontidae								
Terapon theraps	19-26	P	20 - 30	D	1-3	inshore	plankton	
	20-42	S		N	5-30	inshore	benthic invertebrates omnivores	R. McCauley (pers comm.)

following morning. With the exception of clupeids, fish obtained were part of the catch used by Meekan (1992) to assess the distribution and abundance of pre-settlement pomacentrid larvae and thus the traps were moored at the sites used by him about 300 m from shore on windward, lagoon and leeward habitats around Lizard Island. Light traps were an effective way of obtaining pre-settlement pomacentrids, apogonids and holocentrids. The light traps used to collect the clupeids were of similar design but left to drift off the back of Bowden Reef in the Central Great Barrier Reef. The lights were on for 1 hr and emptied immediately. Fish were killed immediately and transferred to fixative.

Floating aggregation devices (FADS): These attract late pelagic-stage larvae which appear to use them as shelter in the same way as rafts of sargassum seaweed or floating debris (Kingsford and Choat, 1985). They are 1 x 1 m plastic rafts either moored permanently or deployed for a number of hours and allowed to drift. Sites sampled around Lizard Island were those used by McCormick (1992) to investigate larval mullid distribution and settlement patterns. The fish were captured by surrounding the rafts with a 14 x 2 m plankton mesh purse seine net. The pursed net was pulled up to the windward side of the dinghy to allow removal of live fish to buckets of seawater (see Kingsford and Choat (1985) and McCormick and Milicich (1993) for further details of this technique). Mullids and blennies were obtained using this technique.

Hand held dip nets: Larval ambassids and garfish were caught by using plankton mesh nets (500 μm) from rocks around Townsville Breakwater marina and the Australian Institute of Marine Science (AIMS) breakwater.

Divers: Newly settled apogonids and pomacentrids were caught by divers with hand held nets. Anaesthetics such as quinaldine administered from wash bottles, to fish that retreated into coral heads or crevices, aided in capture. Spearing was required for the more mobile adult pomacentrids. Recently settled mullids and labrids were caught by divers herding fish into a 5 mm mesh fence net.

Trawling was used in Cleveland Bay, Townsville, to obtain adult Mullids. The nets were deployed from the RV James Kirby at depths of 10 - 20 m.

Fish maintained in laboratory aquaria were fed live *Artemia sp.*, dried flaked fish food, live mysids or chopped sardines according to the size of the fish. Newly hatched larvae were fed on ground flaked food.

Morphometrics

Fish were maintained on a natural light regime and killed during the day when in a fully light-adapted condition. Whole larval fish were fixed, but larger fish (> 2 cm) were killed by decapitation or cold shock, the head was bisected and the eyes pierced to facilitate penetration of the fixative.

The presence or absence of corneal structural colours (iridescence) and corneal pigmentation was noted prior to fixation of the eyes.

Measurements of standard length, horizontal eye diameter, horizontal and vertical pupil diameter and lens diameter were made following fixation or prior to embedding. Correction for shrinkage was made if appropriate. In an experiment to investigate specifically the amount of fixation and embedding induced shrinkage in eyes of different size it was found that small specimens shrank significantly more than large (details of this experiment are given in Appendix 1). The exponential curve (% shrinkage = $10.59e^{-0.3627ED}$; $r^2 = 0.36$; $F = 99.148$) derived from this experiment and used to calculate the correction factor for different size eyes is shown in Fig. I.6. The equation used for correcting the eye diameter following shrinkage was:

$$TED = ED\ (1\ (1 - (10.59 \times 10^{-2}\ e^{-0.3627ED}))) \qquad \text{Eqn. I.1}$$

where TED is the true eye diameter and ED is the measured eye diameter (see Appendix 1 for the method of calculating the correction factor). The ratio of eye diameter: lens diameter was obtained from the corrected measurements.

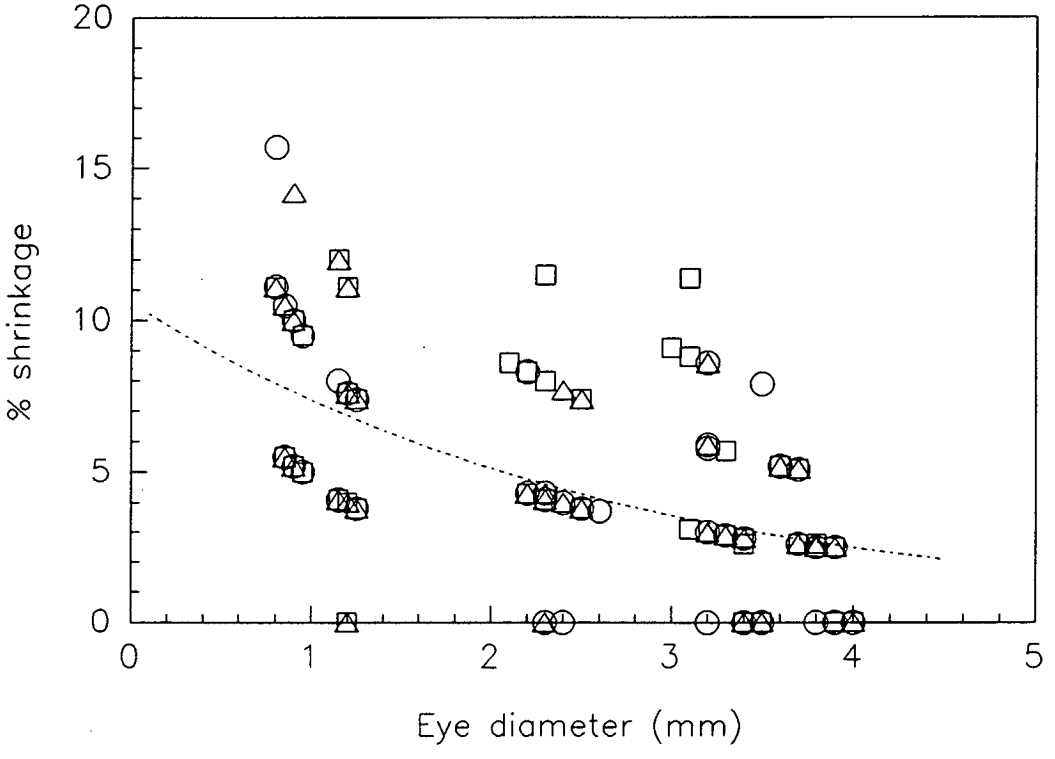

Fig. I.6. Graph showing the exponential decay regression curve that was used in calculating the correction factor for % shrinkage to eyes of different sizes. The data points were obtained from an experiment to investigate % shrinkage of the eye in fixative, as detailed in Appendix 1. See Appendix 1 for explanation of the symbols.

Preservation, embedding and sectioning techniques for histology

Light microscopy

Fixation: Initially trials with three fixatives were carried out: 1) "Seawater Bouin's" (4% formaldehyde; 5% glacial acetic acid and; 85% saturated picric acid in seawater). 2) Formaldehyde-acetic- alcohol (FAA) (4% formaldehyde; 50% of 95% ethanol; 2% acetic acid and; 38% water). 3) Heidenhains SUSA (65 ml saturated aqueous mercuric chloride; 20 ml formalin; 4 ml glacial acetic acid; 2 g trichloroacetic acid; 0.5 g sodium chloride and; water to 100 ml). Because Bouin's fluid penetrates rapidly and material fixed in this way sections easily, Bouin's was subsequently used for all light microscopy. The material was fixed for 24-48 hr, washed in several changes of 70% alcohol over 48 hr to remove the picric acid, and stored in 70% alcohol until further processing. Before processing the head was removed from smaller fish and the snout and lower jaw trimmed. The head of larger fish was bisected (if not already done so) and the lens removed, but the eye was always retained in the head to maintain orientation.

Embedding: A double embedding procedure adapted from Molnar (1974) and now detailed in Winsor (1994) was carried out on an automatic tissue-transfer processor (Shandon Duplex). The material was dehydrated in an ascending ethanol series followed by infiltration with 0.5% low viscosity nitrocellulose (LVN) in methyl salicylate (MS) for 12 hr followed by 24 hr in 1% LVN in MS. The material was then taken through toluene (1 hr) and 3 changes, 2 hr each, of paraffin wax (Paraplast) (melting point 56° C) before final embedding. Material prepared in this way was used for vertical sections of the eye.

To obtain tangential sections of the retina, portions of retina of approximately 1 mm^2 were removed from the Bouin's fixed eyes, dehydrated in an ethanol series and infiltrated with resin (Spurr, 1969), for 2 hr at a time, in increasing ratios of resin: absolute ethanol of 1:1 and 3:1 followed by 2 changes of full strength resin for 2-3 hours. The material was then cured in a 3 rd change of full strength resin

for 16 hr at 70° C.

Sectioning: Vertical serial sections of wax embedded material were cut at 3-4 μm from posterior to anterior on a motorised retracting microtome (Reichert-Jung 1140 Autocut). Sections were mounted on microscope slides and stained with Mayer's haematoxylin and Young's eosin-erythrosin following the procedure outlined by Winsor (1984). From the resin embedded material, 1 μm tangential sections of the retina were cut on an ultra microtome with a glass knife at the level of the photoreceptors. These were mounted on glass slides and stained in 1% toluidine blue in 1% borax.

Electron microscopy

The retina was removed and fixed in 2% glutaraldehyde in 0.1M cacodylate buffer (pH 7.4) for 1-2 hr at 24° C, washed in buffer and stored at 4° C until further processing up to 1 month later. Initial fixation was carried out in the field to ensure freshly killed material was used. Material was post-fixed in 1% Osmium tetroxide for 1 hr at 24° C, washed in buffer, dehydrated in an ethanol series and infiltrated and embedded with resin (Spurr, 1969) and cured for 16 hr at 70° C.

Ultra-thin sections were cut on an ultra-microtome using a glass knife, mounted on copper grids and stained with saturated uranyl acetate in acidified 50% ethanol for 10 mins followed by lead citrate for 2 mins (Reynolds, 1963) and examined with a Jeol FX 2000 transmission electron microscope.

Recording retinal structure and estimation of cell densities

From serial vertical sections, the position at which the optic nerve exits the retina was recorded, together with the presence or absence of a reflecting tapetum behind the retina. The arrangement of the retinal mosaic formed by the cones was recorded from the tangential sections cut at the level of the photoreceptors. The

fine structure of the retina of the post-hatching larvae of *Pomacentrus amboinensis* was recorded from material viewed by transmission electron microscopy.

From the vertical sections of wax embedded material, counts of the numbers of cells in each of the following retinal layers were made: double and single cone inner segments; outer nuclear layer (rod and cone nuclei); horizontal cell layer; bipolar cell layer; amacrine cell layer; and ganglion cell layer (no distinction was made between ganglion cells and displaced amacrine cells) (see Fig. I.2 and Plate I.2 for arrangement of cell layers). In each fish, counts began in a nasal position relative to the optic nerve in the mid-dorsal or mid-ventral retina. No samples were taken from a temporal position as in the smaller fish the plane of sectioning through the photoreceptors was too oblique to allow accurate counts. Counts were made using a graticule eye piece over a strip of retina 52 μm wide (see Plate I. 2A). Alternating sections were used for dorsal and ventral retinal counts over 20 serial sections, thus 10 dorsal and 10 ventral areas were sampled in each fish. Because the high densities of small cells made it impossible to follow profiles of cells from one section to the next (as reviewed by Coggeshall, 1992) the counts were corrected for section thickness using Abercrombie's correction (Abercrombie, 1946). This allows for extrapolation of cell numbers to a volumetric density by accounting for fragments which may be counted as whole cells in the section. The counts were initially multiplied by 1.9 to give the number of cells/100 μm. This was then corrected using Abercrombie's formula to correct for section thickness:

$$P = A(M/L+M) \qquad \text{Eqn. I.2}$$

where P is the corrected number of whole cells counted per section, A is the crude count of cells in a 100 μm strip of retina, M is the thickness of the section (in μm) and L is the average diameter (in μm) of the cells. The density per 100 μm^2 (0.01 mm^2) for each cell type in both dorsal and ventral areas of retina was then calculated by multiplying the corrected number of cells/100 μm by 100/section thickness. The density of rods in each area was calculated by subtracting the corrected number of cones per 0.01 mm^2 from the corrected number of external nuclear layer cells (the rod plus cone nuclei) per 0.01 mm^2.

All records were stored in the database, dBASE III PLUS (Aston-Tate). Mean values of each retinal cell type for both the dorsal and ventral areas were calculated for each fish and these data, together with the 95% confidence limits of the mean, incorporated into the Sigma Plot graphics program (Jandel Corporation).

Appropriate curves were fitted to the data using programs written for Sigma Plot. These were either linear, sigmoid, exponential decay to a minimum, exponential rise to a maximum or quadratic. The sigmoid curves have the equation:

$$f = (a-d/(1+(x/c)^b)) + d \qquad \text{Eqn. I.3}$$

where a is the maximum asymptote, b is the minimum asymptote and c is the point of inflexion. The exponential decay to a minimum curves have the equation:

$$f = ae^{-bx} + c \qquad \text{Eqn. I.4}$$

where 1/b is the time constant for the curve to drop half its range from x = 0 to x = infinity. Therefore the smaller the time constant the steeper the curve. The minimum asymptote is given by c. The exponential rise to a maximum curves have the equation:

$$f = a(1-e^{-bx}) + c \qquad \text{Eqn. I.5}$$

where 1/b is the time constant, and a + c is the maximum asymptote.

Where comparison between data sets was required, the procedures outlined by Zar (1984) were followed.

Visual acuity calculations

Visual acuity calculations were based on the Helmholtz hypothesis (Helmholtz, 1924-1925) in which cone density is assumed to be the limiting factor in resolving a grating of black and white bars. The grating is supposed to be resolved when an unstimulated row of cones occurs between those stimulated by the bright bars of the grating. The acuity was calculated using the formula given by Tamura (1957):

α (radians) = 2c/f Eqn. I.6

where α is the minimum separable angle (MSA), c is the distance between the centres of adjacent cones and f is the focal length of the lens. The density of cones (d) in this study is measured in numbers/0.01 mm^2 so the reciprocal of $10\sqrt{d}$ gives the cone separation (in mm). Shrinkage during processing was 12% so the formula was multiplied by 1.12 to account for this (see Appendix 1 for estimation of shrinkage). The focal length of the lens was calculated using Matthiessen's ratio in which the focal length divided by the lens radius equals 2.5. Thus the following expression was used:

$\alpha = ((2 \times 1.12) / (2.5r \times 10\sqrt{d})) \times (180 / \pi)$ degrees Eqn. I.7

There are several variations of the formula for calculating visual acuity and these need to be considered when comparing results presented by different authors. A detailed appraisal of the different formulae, together with other possible factors which could affect resolution, are considered in Appendix 2.

Results

External Morphology

Growth of the eye cup and lens

Measurements of eye diameter and lens diameter were obtained from 18 species of teleost at a range of developmental stages (see Table I.1 for the species investigated). In all fish, horizontal eye diameter and lens diameter were found to increase in a linear relationship with standard length with all curves having r^2 values >94%. Examples of changes in eye and lens diameter, from the six species that were used for the detailed retinal cell counts, are shown in Fig. I.7 and I.8 respectively. The equations for the regression lines for these species are given in Table I.3 and Table I.4. The slopes of the lines differ. For eye diameter the slopes range from 0.0635 to 0.1257 and for lens diameter from 0.0240 to 0.0568. These differences may in part result from the differences in body shape of the species e.g. *Upeneus tragula* has an elongated body (SL of 3.9-4.5 body depth) whereas the pomacentrids have short and squat bodies (SL of *Pomacentrus moluccensis* is 1.8 - 1.9 body depth) (Randall *et al.*, 1990).

Comparisons of the lens diameters of four species of pomacentrid with similar body shape are shown in Fig. I.9 and the equations for the regression lines given in Table I.5. The slopes of the lines are different (ANCOVA: $F = 60.94$; df 3,112; $p << 0.0001$). This implies that the size of the lenses of the three planktivores, *Pomacentrus moluccensis, P. amboinensis* and *P. lepidogenys*, increase at a greater rate than the size of the lenses of the herbivore *P. bankanensis.*

The size of the eyes at settlement varied between species as can be seen in Table I.6. They range from 0.65 mm diameter in the labrid, *Stethojulis strigiventer*, to 4 mm in the holocentrid, *Neoniphon sammara.*

Table I.3. Coefficients for the regression lines fitted to eye diameter (ED) during growth (SL) as shown opposite.

Species	Equation for regression line	r^2 value
P. moluccensis	ED = 0.4778 + 0.1020 SL	0.9639
S. strigiventer	ED = 0.6907 + 0.0584 SL	0.9679
P. bankanensis	ED = 1.4555 + 0.0635 SL	0.9636
U. tragula	ED = 0.3521 + 0.0725 SL	0.9523
A. vachelli	ED = 0.0857 + 0.1060 SL	0.9874
A. doederleini	ED = 0.0840 + 0.1257 SL	0.9934

Fig. I.7. Changes in eye diameter during the growth of *Pomacentrus moluccensis, Stethojulis strigiventer, Pomacentrus bankanensis, Upeneus tragula, Ambassis vachelli*, and *Apogon doederleini*. Open symbols, pre-settlement; filled symbols, settled; SL, standard length. Coefficients for the regression lines are given above.

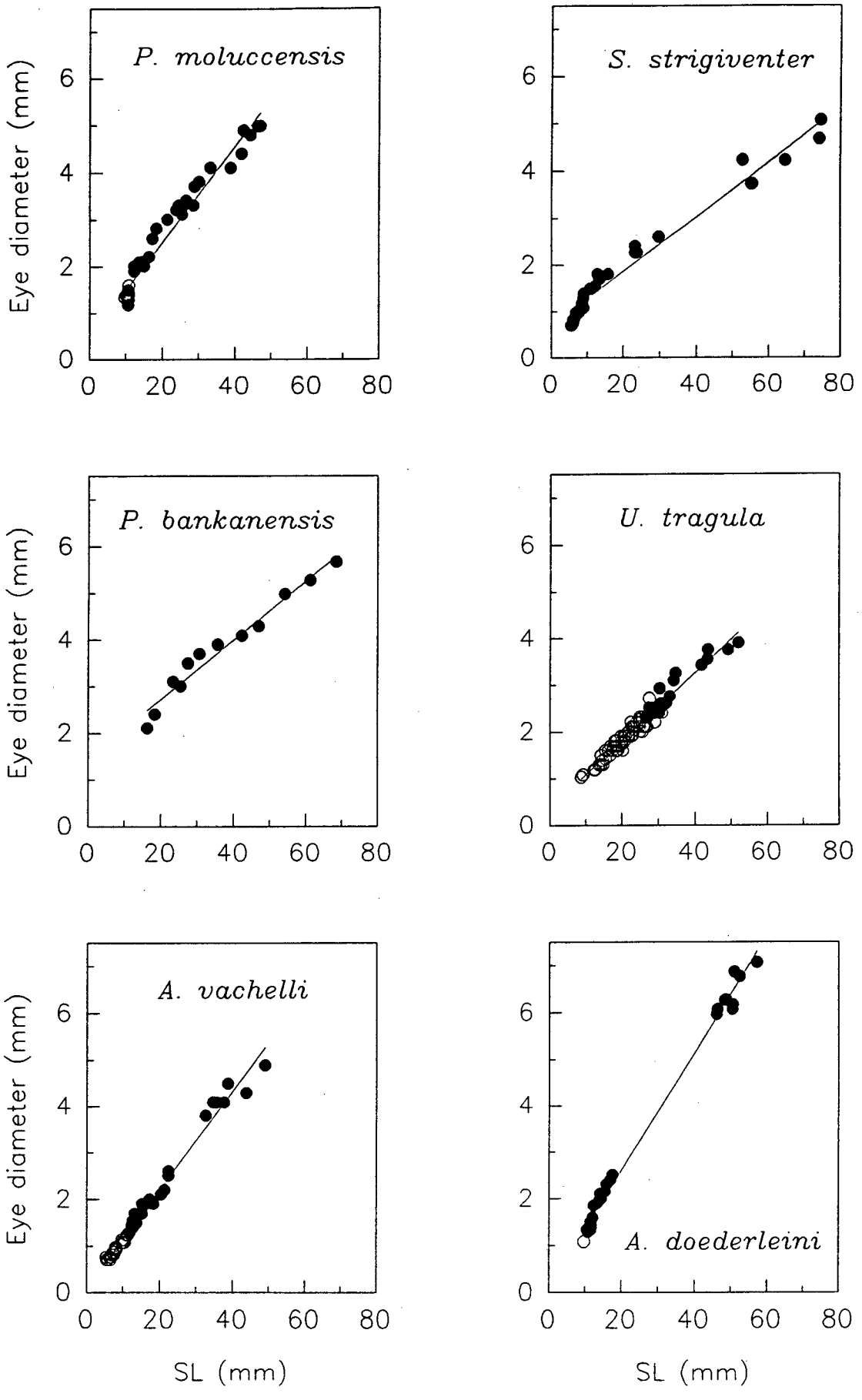
P. moluccensis
S. strigiventer
P. bankanensis
U. tragula
A. vachelli
A. doederleini
Eye diameter (mm)
SL (mm)
0
2
4
6
0
20
40
60
80

Table I.4. Coefficients for the regression lines fitted to the lens diameter (LD) during growth (SL) as shown opposite.

Species	Equation for regression line	r^2 value
P. moluccensis	LD = 0.1213 + 0.0428 SL	0.9559
S. strigiventer	LD = 0.1941 + 0.0266 SL	0.9773
P. bankanensis	LD = 0.5920 + 0.0241 SL	0.9429
U. tragula	LD = -0.0184 + 0.0330 SL	0.9536
A. vachelli	LD = -0.0367 + 0.0483 SL	0.9871
A. doederleini	LD = -0.0300 + 0.0568 SL	0.9944

Fig. I.8. Changes in lens diameter during the growth of *Pomacentrus moluccensis, Stethojulis strigiventer, Pomacentrus bankanensis, Upeneus tragula, Ambassis vachelli*, and *Apogon doederleini*. Open symbols, pre-settlement; filled symbols, settled; SL, standard length. Coefficients for the regression lines are given above.

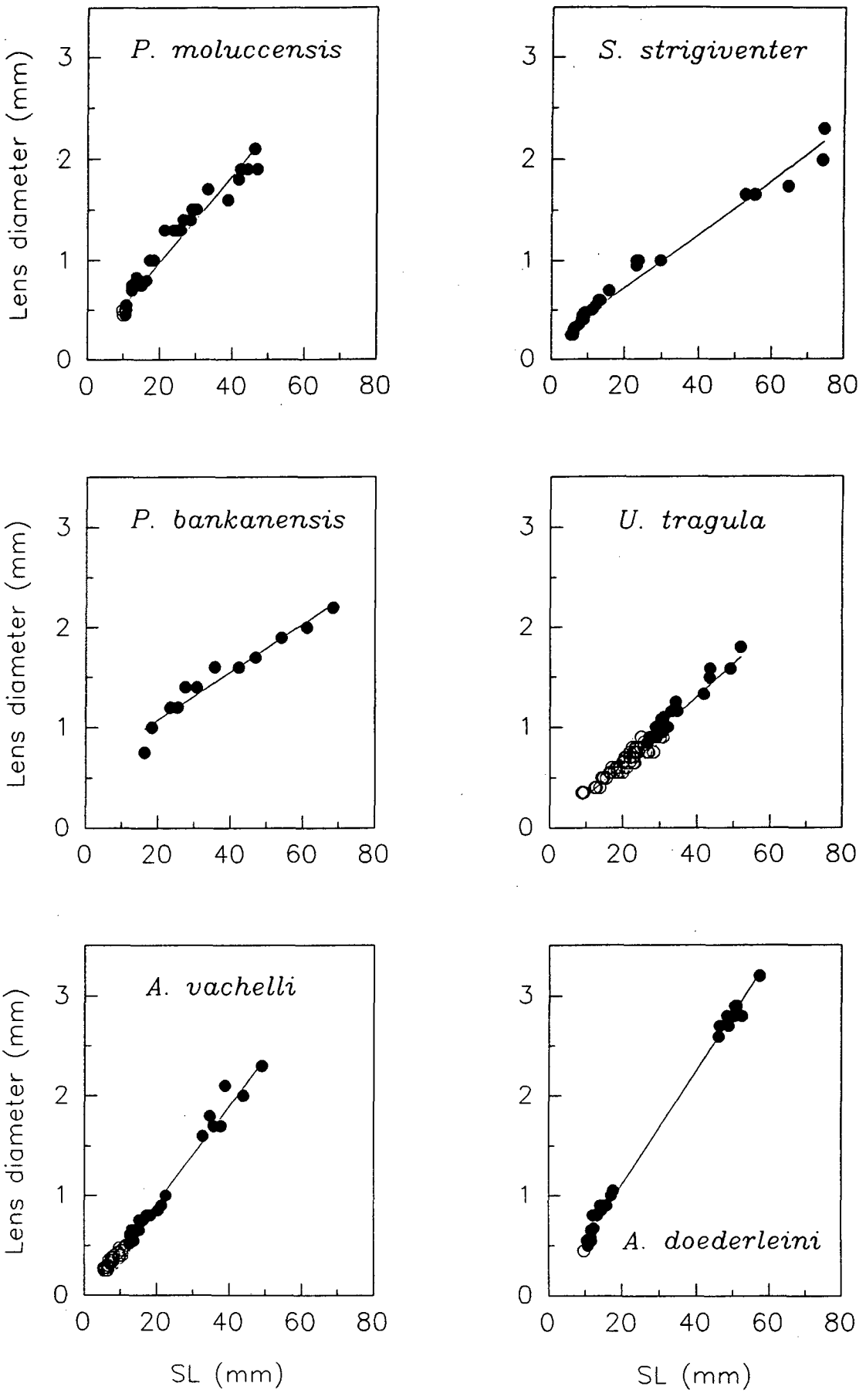
P. moluccensis
S. strigiventer
P. bankanensis
U. tragula
A. vachelli
A. doederleini
Lens diameter (mm)
SL (mm)
0
1
2
3
0
20
40
60
80

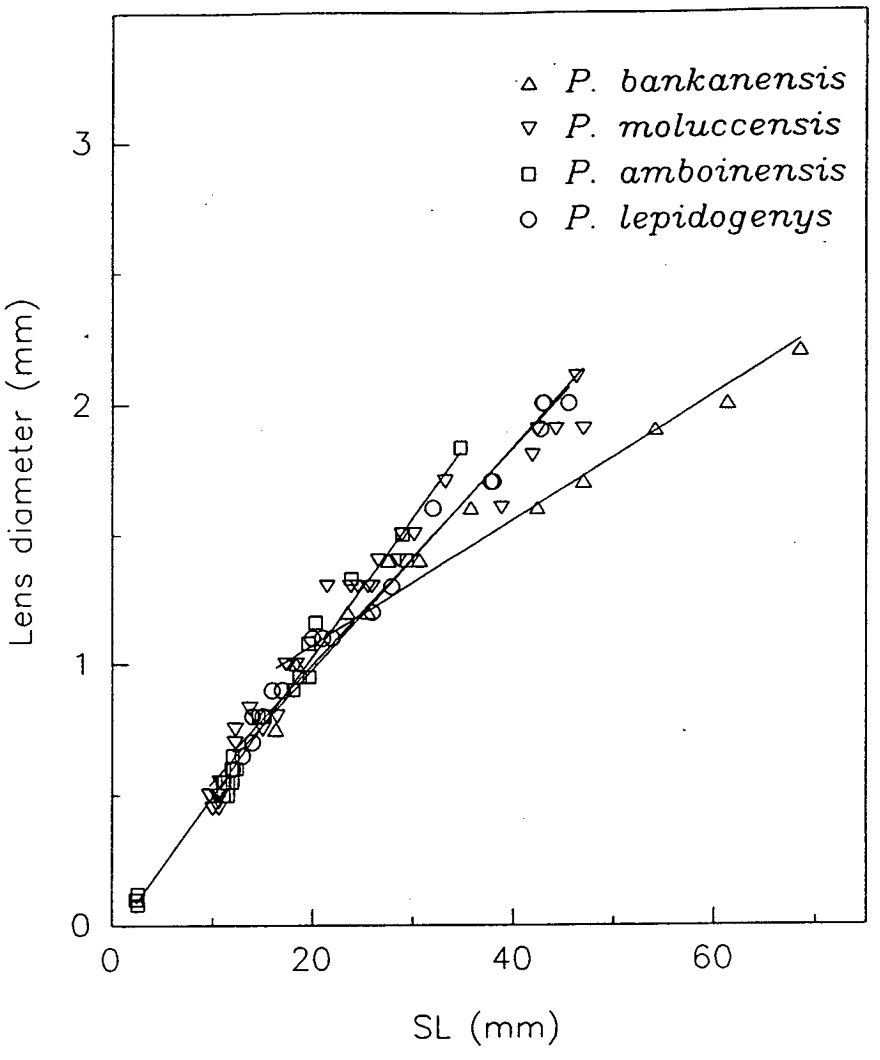

Fig. I.9. Comparison of the changes in lens diameter during the growth of four Pomacentrid species with similar body shapes. SL, standard length. The coefficients for the regression lines are given below.

Table I.5. Coefficients for the regression lines fitted to the lens diameter (LD) changes during growth (SL) as shown above.

Species	Equation for regression line	r^2 value
P. moluccensis	LD = 0.1213 + 0.0428 SL	0.9559
P. lepidogenys	LD = 0.1627 + 0.0416 SL	0.9875
P. amboinensis	LD = -0.0407 + 0.0534 SL	0.9859
P. bankanensis	LD = 0.5920 + 0.0241 SL	0.9429

Table I.6. The diameter of the eyes of 12 species of teleost at settlement, estimated from the largest pre-settlement and smallest settled size where appropriate.

Species	Size range (mm)
Stethojulis strigiventer	0.65 - 0.7
Coris schroederi	0.8 - 1.0
Pomacentrus moluccensis	1.2 - 1.3
Ambassis vachelli	1.2 - 1.3
Apogon doederleini	1.2 - 1.4
Pomacentrus amboinensis	1.4 - 1.5
Chromis atripectoralis	1.4 - 1.5
Meiacanthus grammistes	1.4 - 1.5
Pomacentrus lepidogenys	1.5
Parapeneus barberinus	2.25 - 2.4
Upeneus tragula	2.2 - 2.4
Neoniphon sammara	3.9 - 4.2

The ratio of eye diameter to lens diameter for six species over a range of sizes are shown in Fig. I.10. If it is assumed that the eye is hemispherical this ratio is equivalent to that between lens radius and the distance between the centre of the lens and the retina and thus gives an estimation of Matthiessen's ratio (see discussion for further explanation). The r^2 values of the 'exponential decay to a minimum' curves that have been fitted to the data are low (Table I.7) and for *Upeneus tragula* and *Ambassis vachelli* do not show where the relationship between eye and lens ratio becomes constant because more data from larger fish are required. In the case of *Apogon doederleini* there are not enough points in the

Table I.7 Coefficients for the regression lines fitted to the ratio of eye to lens diameter (ELR) during growth (SL) as shown opposite. The curves have the equation of an exponential decay to minimum. TC, time constant. See text for explanations of equations.

Species	Equation for regression line	r^2	notes
P. moluccensis	$ELR = 1.127e^{-0.1257SL} + 2.469$	0.5210	TC = 7.9554
S. strigiventer	$ELR = 0.8217e^{-0.04378SL} + 2.257$	0.5539	TC = 22.84
P. bankanensis	no correlation		
U. tragula	$ELR = 3.5041e^{-0.00584SL} - 0.296$	0.4064	TC = 171.23
A. vachelli	$ELR = 2.176e^{-0.006303SL} + 0.56$	0.2892	TC = 158.65
A. doederleini	not enough points to fit anything but straight line		

Fig. I.10. Changes in the ratio of eye to lens diameter during the growth of *Pomacentrus moluccensis, Stethojulis strigiventer, Pomacentrus bankanensis, Upeneus tragula, Ambassis vachelli*, and *Apogon doederleini*. Open symbols, pre-settlement; filled symbols, settled; SL, standard length.

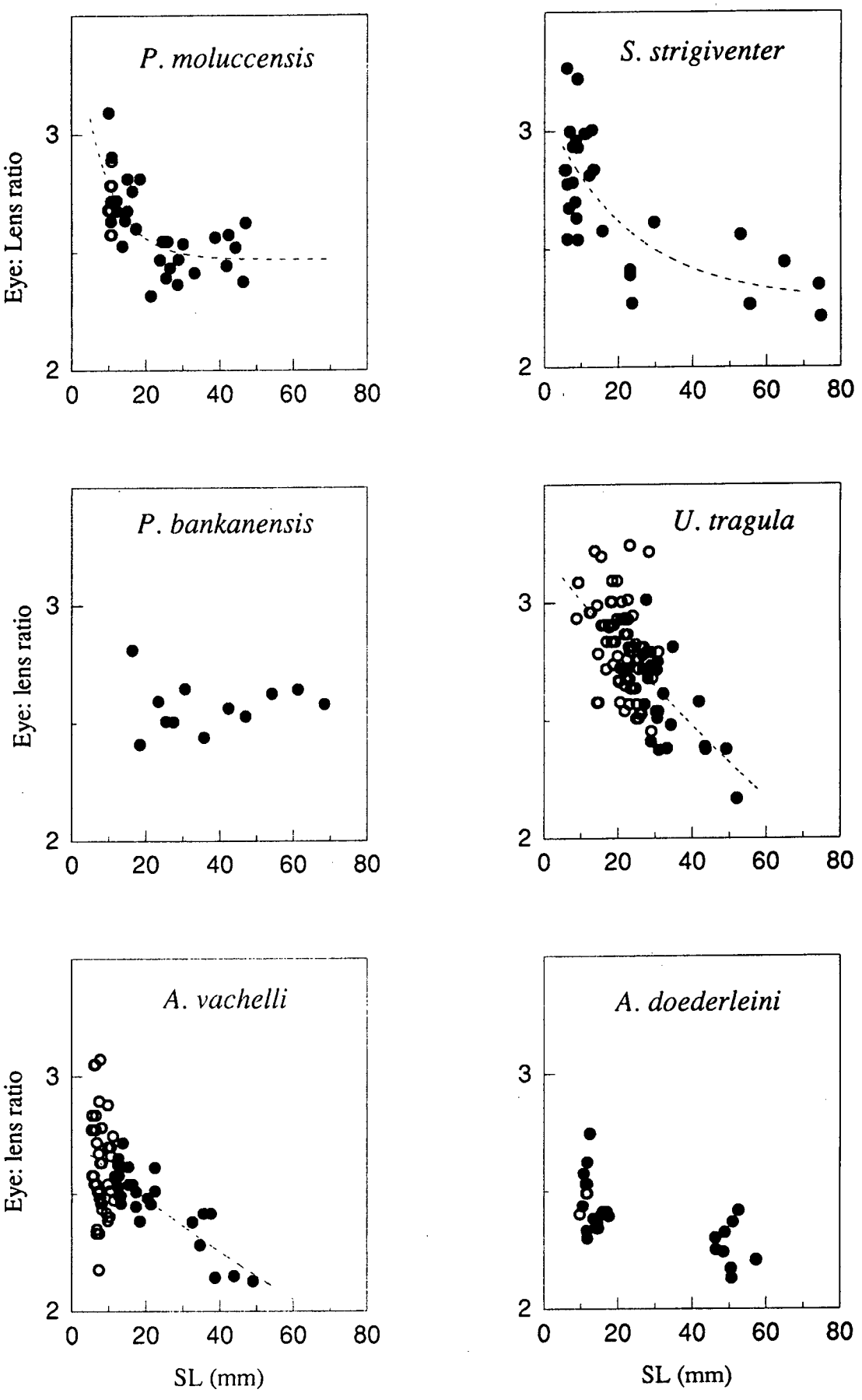
P. moluccensis
S. strigiventer
P. bankanensis
U. tragula
A. vachelli
A. doederleini
Eye: Lens ratio
Eye: lens ratio
SL (mm)
2
3
0
20
40
60
80

intermediate size range to fit a curve. Never-the-less smaller fish tend to have a higher ratio of eye to lens diameter. For the purposes of comparing the mean ratio of individual settled species a cut-off of lens size greater than 1 mm has been taken and results from fish with eyes greater than this averaged. This is equivalent to SL <20 mm for *P. moluccensis, P. bankanensis, A. vachelli and A. doederleini* and SL <30 mm for *S. strigiventer* and *U. tragula*. In the case of *U. tragula* the ratio continues to reduce over the size range of fish for which measurements were obtained so the mean value should be treated with caution. Mean values for the ratio between eye and lens diameter were obtained for 14 of the 18 species for which sufficient data on lens sizes greater than 1 mm diameter were available. The results are ranked and are presented in Table I.8. There is considerable variation in the values for each species but generally species with the lowest ratio of eye to lens size are nocturnal (see Table I.2 for further ecological notes about each species).

Iridescence and pigmentation of the cornea

The presence of an iridescent cornea was observed in the labrids and scarids (Table I.9). This was found in all fish, including the smallest individuals caught, all of which had settled. Pre-settlement specimens of labrids and scarids were not obtained so it is not known at what stage the iridescent cornea first develops. The labrids were also found to possess yellow pigmented corneas at all stages examined (post-settlement only). Note that settlement occurs at very small sizes, as small as 5 mm SL, in these fishes, (Table I.2).

Table I.8. Mean eye to lens ratios for 14 species of teleost. Calculated for species where sufficient fish with lens diameter greater than 1 mm available.

Species	Mean eye: lens ratio ± SE	n	Period of activity
Pomacentrus lepidogenys	2.62 ± 0.03	12	diurnal planktivore
Pomacentrus amboinensis	2.62 ± 0.05	6	diurnal planktivore
Coris schroederi	2.59 ± 0.05	7	diurnal microcarnivore
Pomacentrus bankanensis	2.56 ± 0.02	11	diurnal herbivore
Pomacentrus moluccensis	2.47 ± 0.02	18	diurnal planktivore
Parapeneus barberinus	2.46 ± 0.06	12	diurnal benthic
Upeneus tragula	2.45 ± 0.06	13	diurnal benthic
Terapon theraps	2.44 ± 0.03	9	nocturnal omnivore
Chromis atripectoralis	2.41 ± 0.02	12	diurnal planktivore
Stethojulis strigiventer	2.38 ± 0.04	9	diurnal microcarnivore
Cheilodipterus quinquelineatus	2.36 ± 0.23	4	nocturnal planktivore
Ambassis vachelli	2.34 ± 0.05	33	nocturnal planktivore
Apogon doederleini	2.32 ± 0.03	10	nocturnal planktivore
Neoniphon sammara	2.26 ± 0.22	7	nocturnal planktivore

Retinal Structure

The retinal structure of 17 of the 18 species investigated is summarised in Table I.9. The retinal structure of the settled fish followed the general structure of a teleost retina but with considerable variation in photoreceptor and neural cell density between species and sizes of fish. In addition, *Spratelloides delicatulus*, the labrid and scarid species and the pelagic stage of *Upeneus tragula* were found to have specialised areas of the retina. These specialisations will be described in more detail below.

General description for settled fish

As a rule the species known to be active at night were characterised by: 1) large cones in low densities; 2) high rod densities (thus high rod to cone ratios); 3) high rod to bipolar cell ratios; and 4) a reflecting tapetum. These species were (in order of descending rod to cone ratio for the dorsal retina of settled fish with similar eye sizes) *Neoniphon sammara* (25:1), *Terapon theraps* (25:1), *Apogon doederleini* (23:1), *Ambassis vachelli* (20:1), *Spratelloides delicatulus* (15:1 in the unspecialised area of retina) and *Cheiliodipterus quinquelineatus* (11:1). Plate I.3A shows an example of a 'nocturnal' retina.

The diurnal microcarnivores and planktivores were characterised by: 1) small cones in high densities; 2) low rod densities (and therefore low rod to cone ratios); and 3) low rod to bipolar cell ratios. These species were (in order of ascending rod to cone ratios for the dorsal retina of settled fish) *Thalassoma amblycephalum* (1:1), *Stethojulis strigiventer* (2:1), *Meiacanthus grammistes* (2:1), *Chromis atripectroralis* (3:1), *Pomacentrus lepidogenys* (3.5:1), *Pomacentrus moluccensis* (4:1) and *Pomacentrus amboinensis* (4.5:1). Plate I.3B shows a typical example of a 'planktivore' retina.

The herbivorous species were found to have intermediate rod and cone densities. The rod to cone ratios for the dorsal retina of the small scarid were 5:1, and for

Table I.9. Summary of the retinal morphology of the species investigated. L/P/S, larval/pelagic/settled; C, cone density/0.01 mm^2; Rods, rod density/0.01 mm^2; R:C, rod:cone ratio; R:B, rod:biploar cell ratio; R:GCL, rod:ganglion cell ratio, D, dorsal retina; V, ventral retina; MSA, minimum separable angle; ON, position of optic nerve; T, temporal retina; M, mid retina; irid, iridescent cornea; PE, pigment epithelium.

Family Species	Size (SL mm)	L/P/S	Retinal Morphology C	 Rods	 R:C	 R:B	 C:GCL	MSA (min)	Mosaic	ON	Lens/cornea	Comments
Ambassidae												
Ambassis vachelli	5	L	D489±8 V594±10	743±50 421±41	1.5±0.1 0.7±0.1	0.2±0.03 0.1±0.03	0.7±0.03 0.6±0.02	D101 V92	square	M/M	clear	
	38	S	D157±5 V228±9	3139±120 2529±85	20.2±1 11.3±0.6	4.9±0.5 2.4±0.14	1.7±0.13 2.3±0.2	D23 V19	square	M/M	clear	reflecting tapetum, ventral
Apogonidae												
Cheilodipterus quinquelineatus	38	S	D182±3.5 V257±5	1920±86 963±36	10.6±0.4 3.8±0.2	1.1±0.05 0.5±0.05	0.95±0.05 1.2±0.04	D28 V24	square	T/V	clear	reflecting tapetum
Apogon doederleini	10	L	D432±5 V689±7	905±34 207±27	2.1±0.1 0.3±0.04	0.5±0.02 0.1±0.01	0.56±0.02 0.78±0.02	D65 V51	square	M/V	clear	
	45	S	D166±3 V220±4	3746±59 3111±66	22.6±0.5 14.2±0.3	4.1±0.2 3.5±0.2	1.3±0.1 2.3±0.2	D17 V15	square	M/M	clear	reflecting tapetum
Blennidae												
Meiacanthus grammistes	14	L	D483±8 V568±8	704±29 331±35	1.5±0.06 0.58±.06	0.23±.01 0.13±.01	0.93±0.06 1.16±0.03	D45.8 V42.2	square	T/V	clear	
	32	S	D594±10 V551±8	1238±88 1043±38	2.1±0.1 1.9±0.1	0.3±0.02 0.3±0.01	0.96±0.05 1.4±0.1	D19 V19	square	T/V	clear	
Clupeidae												
Spratelloides delicatulus	34	P	D217±6 V186±8	3295±95 2714±63	15.2±0.5 14.7±0.9	2.4±0.2 3.2±0.2	1.5±0.1 1.5±0.1	D51 V55	square	T/V	clear	unspecialised area of retina

Table I.9 continued

Family / Species	Size (SL mm)	L/P/S	Retinal Morphology C	Rods	R:C	R:B	C:GCL	MSA (min)	Mosaic	ON	Lens/cornea	Comments
Hemirhamphidae												
Hemirhamphus sp.	27	P	D310±6	2073±57	6.7±0.3	1.0±0.1	1.0±0.1	D57	square	M/V	clear	dorsal PE 4x wider
			V374±25	780±25	2.1±0.1	0.6±0.04	1.3±0.2	V52				than ventral PE
Holocentridae												
Neoniphon sammara	26	L	D317±8	4616±189	14.9±.8	1.6±0.1	0.7±0.05	D26	square	M/M	clear	dorsal PE 2x wider
			V551±8.5	1840±185	3.3±0.3	0.7±0.06	1.2±0.05	V20				than ventral PE
	33	S	D226±7	5652±170	25.1±0.98	2.6±0.1	0.6±0.04	D20	square	M/M	clear	dorsal PE 1.5x wider
			V349±17	5257±228	15.2±1.4	2.7±0.3	1.2±0.05	V16				than ventral PE
Labridae												
Stethojulis strigiventer	6	S	D597±10	695±62	1.2±0.1	0.2±0.01	0.4±0.02	D99	square	T/D	yellow/irid	area centralis
			V716±9	576±61	0.8±0.1	0.2±0.02	0.6±0.02	V90				
	54	S	D370±3	853±118	2.3±0.1	0.4±0.02	1.8±0.1	D19	square	T/D	yellow/irid	area centralis
			V486±5	645±29	1.3±0.1	0.3±0.01	2.3±0.1	V16				
Thalassoma amblycephalum	13.5	S	D417±8	516±37	1.24±.09	0.2±.02	0.87±.03	D49.3	square	T/D	yellow/irid	area centralis
			V644±14	568±38	0.88±.05	0.2±.01	1.31±.04	V39.7				
Mullidae												
Upeneus tragula	12	L	D518±7	992±40	1.9±0.1	0.7±0.03	0.9±0.03	D66	square	T/V	clear	double layer of cones dorsal
			V621±7	550±35	0.9±0.1	0.4±0.02	1.1±0.04	V61				in pre-settlement fish >15 mm
	41	S	D208±3.3	3280±94	15.9±0.6	2.6±0.06	1.3±0.06	D31	square	T/V	clear	double layer of cones absent
			V276±4	3439±141	12.5±0.5	2.3±0.07	1.7±0.08	V27				in settled fish
Pomacentridae												
Chromis atripectoralis	9	L	D506±7.8	1207±66	2.4±0.1	0.3±0.03	0.5±0.02	D60	square	M/D	clear	
			V500±16	1840±178	3.7±0.5	3.7±0.5	0.6±0.1	V60				
	26	S	D435±6	1378±123	3.2±0.3	0.5±0.05	1.2±0.05	D24	square	T/D	clear	
			V421±7	1867±53	4.4±0.2	0.7±0.1	1.7±0.05	V24				

Table I.9 continued

Family / Species	Size (SL mm)	L/P/S	Retinal Morphology C	Rods	R:C	R:B	C:GCL	MSA (min)	Mosaic	ON	Lens/cornea	Comments
Pomacentrus amboinensis	2.5	L	cones only									
	11	L	D428±8	1734±31	4±0.05	0.48±0.04	0.7±0.01	D58	square	M/M	clear	
			V551±9	1348±68	2.5±0.2	0.3±0.01	0.7±0.02	V51				
	29	S	D351±6.9	1642±100	4.7±0.2	0.5±0.05	1.3±0.1	D23	square	M/D	clear	
			V482±9	1603±90	3.3±0.2	0.5±0.03	2.4±0.1	V20				
Pomacentrus bankanensis	46	S	D242±4	2283±90	9.5±0.4	1.2±0.1	1.8±0.1	D23	square	T/D	clear	
			V330±4	2333±130	7.1±0.4	0.9±0.1	2.4±0.2	V20				
Pomacentrus lepidogenys	26	S	D325±7	1121±86	3.5±0.3	0.45±0.1	1.2±0.04	D28	square	T/D	clear	
			V442±8	1350±92	3.1±0.2	0.3±0.02	1.1±0.05	V24				
Pomacentrus moluccensis	10	L	D418±4	847±43	2.0±0.1	0.4±0.02	0.8±0.03	D59	square	T/D	clear	
			V621±7	597±56	1.0±0.1	0.2±0.02	1.1±0.05	V48				
	41	S	D356±5	1417±55	4.0±0.1	0.6±0.1	1.9±0.1	D18	square	T/D	clear	
			V325±5	1178±41	3.4±0.1	0.5±0.1	1.7±0.1	V19				
Scaridae												
Scarus sp.	11	S	D360±8	616±33	1.7±.08	0.22±.01	0.66±.05	D64	square	T/D	-/irid	area centralis
			V459±8	737±53	1.6±.12	0.25±.02	0.85±.05	V56				
	22	S	D289±13	1381±51	4.8±0.4	0.55±.03	0.8±.05	D39	square	T D	-/irid	area centralis
			V431±12	1332±118	3.1±.4	0.4±.06	1.3±.04	V32				
Terapontidae												
Terapon theraps	26	P	D253±12	4454±179	17.8±1.5	3.4±0.2	1.4±0.2	D34.5	square	T/V	clear	
			V351±7	3356±63	9.6±0.3	1.4±0.1	1.5±0.1	V29				
	41	S	D199±5	4961±142	25±0.9	3.5±0.3	1.2±0.2	D27	square	T/M	clear	
			V226±8	3179±96	14.1±0.5	1.8±0.1	1.3±0.2	V25				

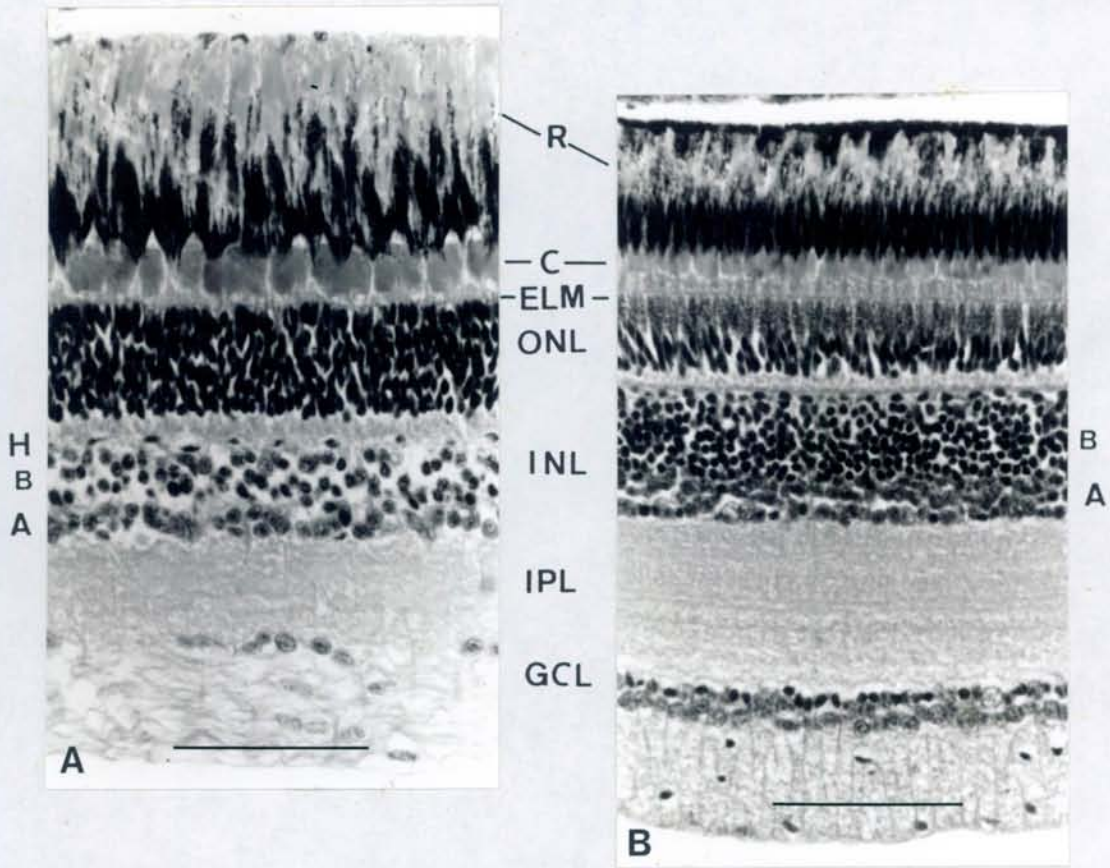

Plate I.3. Radial sections through the retinae of 2 teleosts of similar developmental stage: **A)** *Apogon doederleini*, a nocturnal fish with a rod dominated retina and large cones. The individual rod outer segments cannot be visualised but an indication of their density can be gained from the thickness of the outer nuclear layer. The density of cells in the inner nuclear layer and ganglion cell layer is low, indicating high convergence ratios of photoreceptors to neural processing cells; **B)** *Pomacentrus moluccensis*, a diurnal planktivore. In this species the cones are small and numerous and the rods are low in density (as indicated by the cell numbers in the outer nuclear layer). The densities of the cells in the inner nuclear layer and the ganglion cell layer are high compared with those in A. R, rods; C, cones; ELM, external limiting membrane; ONL, outer nuclear layer; INL; inner nuclear layer; H, horizontal cell bodies; B, bipolar cell bodies; A, amacrine cell bodies; IPL, inner plexiform layer; GCL, ganglion cell layer. Scale bars = 50 μm.

Pomacentrus bankanensis, 9.5:1. *Upeneus tragula*, a benthic species, was found to have ratios of 16:1. This species moves to deeper water between reefs following settlement. The ratios used in all these examples were obtained from settled fish with similar eye size but should not be considered definitive values adults because changes in rod to cone ratios can occur during the growth of the eye (see discussion).

Variation within the retina

Cell densities often showed regional variation. As a general rule the dorsal retina had the higher rod and lower cone densities. These differences were usually found to be greater in nocturnal species. In many planktivores e.g. *Pomacentrus moluccensis* there was little or no difference between the ventral and dorsal regions. *Chromis atripectoralis* was the only settled species found to have a higher rod to cone ratio in the ventral retina (see Table I.9).

Development and Growth

Retina of a newly hatched fish

The retina of *Pomacentrus amboinensis* was investigated from several minutes to 2 days after hatching. Initially, the pigment epithelium lacked pigment granules and single cones were the only photoreceptors present (Plate I.4). By day 2 the pigment epithelium contained melanin granules and a second type of photoreceptor could be distinguished (Plate I.5). This was thought to be a rod. No double cones were found although the close arrangement of the inner segments (Plate I.6B) may provide the sites for fusion between single cones as suggested by Ahlbert (1973). A tangential section of the retina showed the cones were arranged in rows (Plate I.6A and B). Pre-settlement fish obtained from light traps of approximately 19 days old (Brothers *et al.* 1983; Thresher *et al.* 1989) were found to have a well developed duplex retina with single and double cones arranged in a square

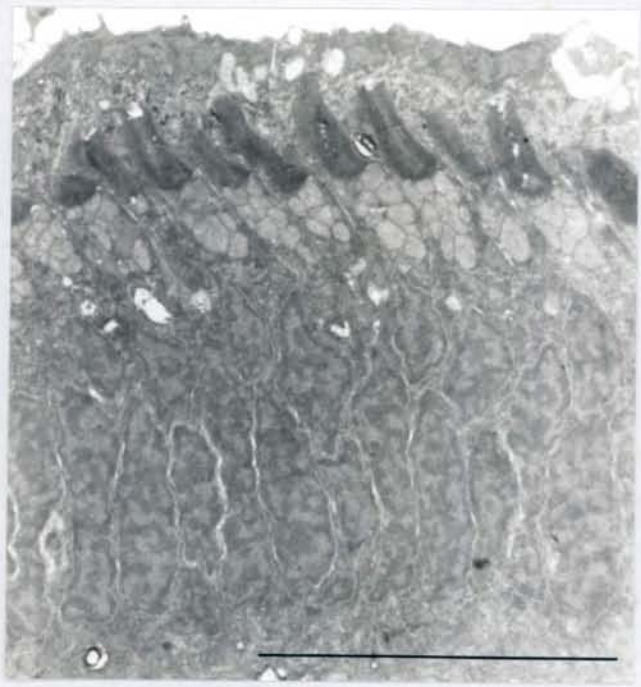

Plate I.4. Electron micrograph of a radial section through the retina of a 20 min. hatched *Pomacentrus amboinensis* larva. The pigment epithelium contains virtually no melanin granules and the only photoreceptors are single cones. The nuclear layers are not well defined. C, cones; Scale bar = 20 μm.

A

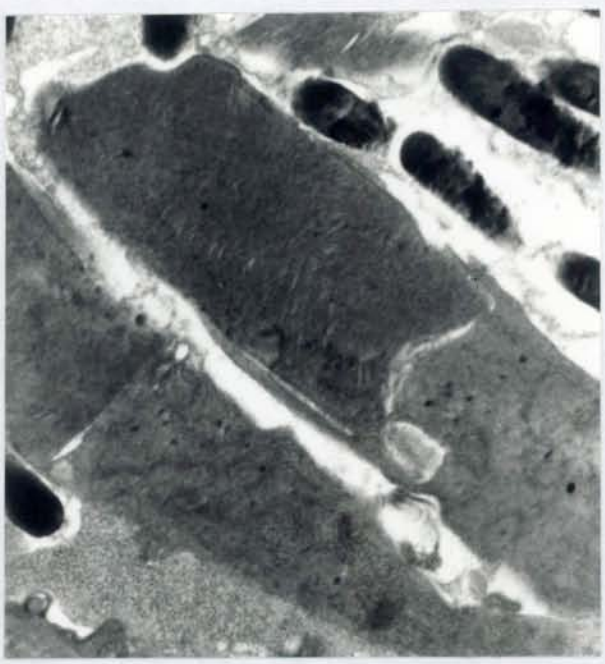

B

Plate I.5. Electron micrographs of the photoreceptors in the retina of a 2 day-hatched *Pomacentrus amboinensis*: **A)** cones, scale bar = 5 μm; **B)** rods, scale bar = 4 μm.

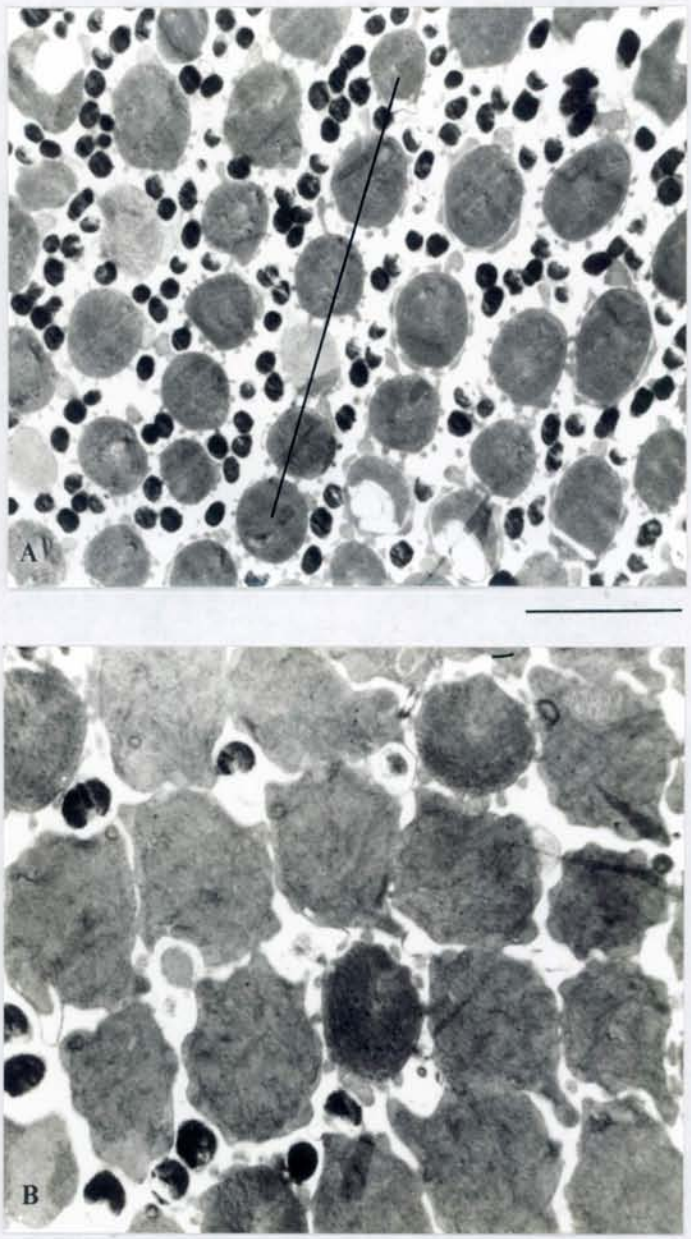

Plate I.6. Electron micrographs of tangential sections through the retina of a 2 day-hatched *Pomacentrus amboinensis*: **A)** at the level of the outer segments. An alignment of the cells into rows can be detected (line). Numerous melanin granules surround the outer segments. **B)** at the level of the inner segments. Scale bars = 5 μm.

mosaic. Relatively high rod densities in the dorsal retina were also found in these fish. For example an 11 mm SL specimen has rod densities of 1734/ 0.01mm^2 (Table I.9).

Retinal cell counts during growth

Detailed retinal cell counts over a range of developmental stages were obtained for 6 species (the dietary notes refer to settled fish):

Pomacentrus moluccensis	planktivore
Stethojulis strigiventer	microcarnivore
Pomacentrus bankanensis	herbivore
Upeneus tragula	benthic carnivore using barbels
Ambassis vachelli	inshore nocturnal planktivore
Apogon doederleini	nocturnal planktivore

Graphs of the changes in density of cones, rods, cells in the inner nuclear layer (INL) and cells in the ganglion cell layer (GCL) are shown in Fig. I.11-14 respectively.

Cell densities in each retinal layer tend to be higher in the younger fish, with the exception of the rods. Taking each type of cell individually:

Cones (Fig. I.11): In all six species the ventral retina has higher cone densities than the dorsal. Five species, for which records were obtained from fish smaller than 10 mm SL, were found to have cone densities in the ventral retina of at least 600 cones/ 0.01 mm^2. The decline in the cone densities varied between species with the greatest in the nocturnal species, *Ambassis vachelli* and *Apogon doederleini* and the least in the diurnal microcarnivore *Stethojulis strigiventer* and planktivore *Pomacentrus moluccensis.* Thus the cone densities in nocturnal species asymptote at lower values than those for the diurnal microcarnivore and

Table I.10. Equations and regression coefficients for the curves fitted to the changes in cone density (CD) during growth (SL) as shown opposite. The curves are either: exponential decay to a minimum (EDM), with time constant (TC), minimum asymptote (MIN) or: sigmoid (SIG), with maximum asymptote (MAX), minimum asymptote (MIN), point of inflection (IN). D, dorsal; V, ventral. See text for equations and explanations of curves.

Species	Curve type	Equation	r^2	Notes
P. moluccensis	EDM	D CD = $206.7e^{-0.0589SL} + 295.3$	0.6654	TC = 19.99
				MIN = 295
		V CD = $1003e^{-0.1039SL} + 289$	0.9512	TC = 7.19
				MIN = 289
S. strigiventer	EDM	D CD = $280.2e^{-0.0596SL} + 370.7$	0.8603	TC = 16.77
				MIN = 370
		V CD = $359.8e^{-0.033SL} + 428.6$	0.8893	TC = 30.3
				MIN = 428
P. bankanensis	no correlation			
U. tragula	SIG	D CD=$(281/(1+(SL/27.1)^{17.28}))+203$	0.9718	MAX = 484.0
				MIN = 203.1
				IN = 27.1
		V CD=$(376/(1+(SL/27.47)^{6.476})+234$	0.9500	MAX = 609.9
				MIN = 234
				IN = 27.4
A. vachelli	EDM	D CD = $745.7e^{-0.1589SL} + 174.4$	0.9521	TC = 6.29
				MIN = 174
A. doederleini	EDM	D CD = $1891e^{-0.2061SL} + 176.6$	0.9330	TC = 5.29
				MIN = 177
		V CD = $4022e^{-0.2276SL} + 238.8$	0.9598	TC = 4.39
				MIN = 239

Fig. I.11. Changes in the cone density during the growth of *Pomacentrus moluccensis, Stethojulis strigiventer, Pomacentrus bankanensis, Upeneus tragula, Ambassis vachelli* and *Apogon doederleini.* Open symbols, dorsal retina; filled symbols, ventral retina; circles, pre-settlement; triangles, settled; SL, standard length. The error bars give the 95% confidence limits.

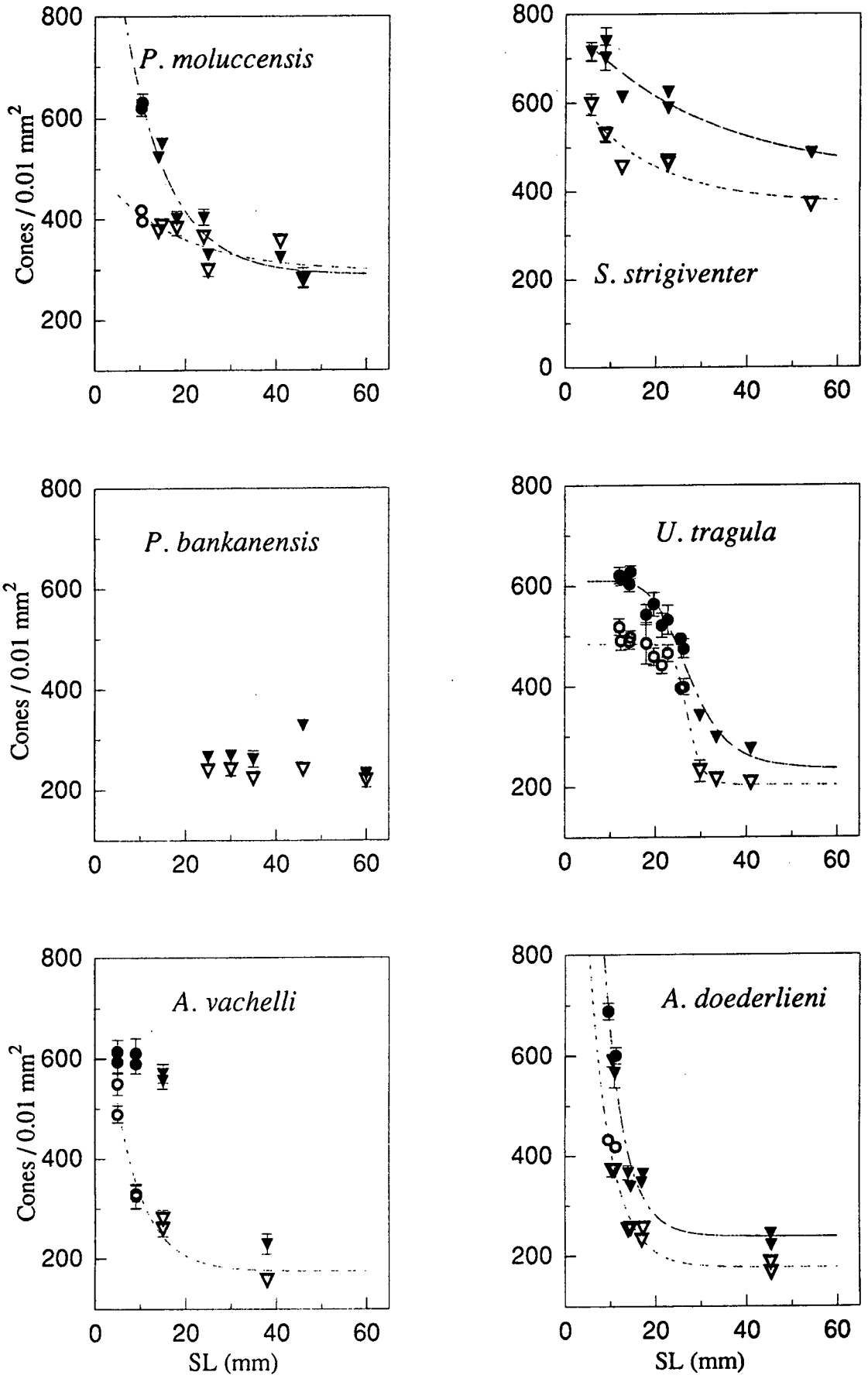
P. moluccensis
S. strigiventer
P. bankanensis
U. tragula
A. vachelli
A. doederlieni
Cones / 0.01 mm2
SL (mm)
800
600
400
200
0
20
40
60

planktivore (Table I.10). Decline in cone density was most rapid early in development with the exception of *Upeneus tragula* in which the most rapid period of decline was over the later settlement period. The asymptote for the densities in this species then occurred at values approaching those of the nocturnal species. The herbivore, *Pomacentrus bankanensis* had a constant density of cones for fish >20 mm which was similar in value to that for *U. tragula*. Fish <20 mm were unavailable for comparisons during the settlement phase.

Rods (Fig. I.12): Rod densities in pre-settlement fish of about 10 mm SL were less than 1000/0.01 mm^2 and increased in density in *Pomacentrus bankanensis, Upeneus tragula, Ambassis vachelli*, and *Apogon doederleini*. However little or no increase in rod density occurred in *Stethojulis strigiventer* or *Pomacentrus moluccensis*. The curves fitted to the data show that the increase in density was most rapid in the dorsal retina of *A. vachelli and A. doederleini* during early development. In *U. tragula* the greatest rate of rod addition occurred over the later settlement period, following which the values asymptote at values similar to those of the nocturnal species, between 3000 and 4000/0.01 mm^2 (Table I.11). Intermediate values of approximately 2000/0.01 mm^2 were obtained from *P. bankanensis*.

Cells of the inner nuclear layer (Fig. I.13): The density of cells in the INL tended to be higher in younger fish and declined most rapidly during the early stages of development to about 20 mm SL with the exception of *Upeneus tragula*. Like cone densities, the most rapid rate of decline was in *Ambassis vachelli* and *Apogon doederleini* and the highest densities were maintained in *Stethojulis strigiventer* and *Pomacentrus moluccensis*. INL densities did not decline in *Upeneus tragula* until after settlement (SL 24-30 mm). *Pomacentrus bankanensis* showed a constant density of INL cells although data for small fish were not available. Of the three cell types found in this layer the bipolar cells were the most numerous and were mainly responsible for the changes in cell densities. This is examined in more detail below for *Upeneus tragula*. Horizontal cells were not found to vary significantly in density in the species for which estimates were

Table I.11. Equations and regression coefficients for the curves fitted to the changes in rod density (RD) during growth (SL) as shown opposite. The curves are either: exponential rise to a maximum (ERM), with time constant (TC), maximum asymptote (MAX) or: sigmoid (SIG), with maximum asymptote (MAX), minimum asymptote (MIN), point of inflection (IN). D, dorsal; V, ventral. See text for equations and explanations of curves.

Species	Curve type	Equation	r^2	Notes
P. moluccensis	no correlation			
S. strigiventer	no correlation			
P. bankanensis	not enough points to fit curve			
U. tragula	SIG	D $RD=(2379/(1+(SL/26)^{-5.622}))+902$	0.9334	MIN = 901.9
				MAX = 3281
				IN = 26.0
		V $RD=(2870/(1+(SL/29)^{-9.751}))+601$	0.9762	MIN = 600.6
				MAX = 3471
				IN = 28.8
A. vachelli	ERM	D $RD = 7134(1-e^{-0.1896SL}) - 3682$	0.9122	TC = 5.27
				MAX = 3452
A. doederleini	ERM	D $RD = 12590(1-e^{-0.1481SL}) - 8772$	0.9748	TC = 6.75
				MAX = 3818
		V $RD = 14550(1-e^{-0.1558SL}) - 11330$	0.9766	TC = 6.42
				MAX = 3220

Fig. I.12. Changes in the rod density during the growth of *Pomacentrus moluccensis, Stethojulis strigiventer, Pomacentrus bankanensis, Upeneus tragula, Ambassis vachelli*, and *Apogon doederleini*. Open symbols, dorsal retina; filled symbols, ventral retina; circles, pre-settlement; triangles, settled; SL, standard length. The error bars give the 95% confidence limits.

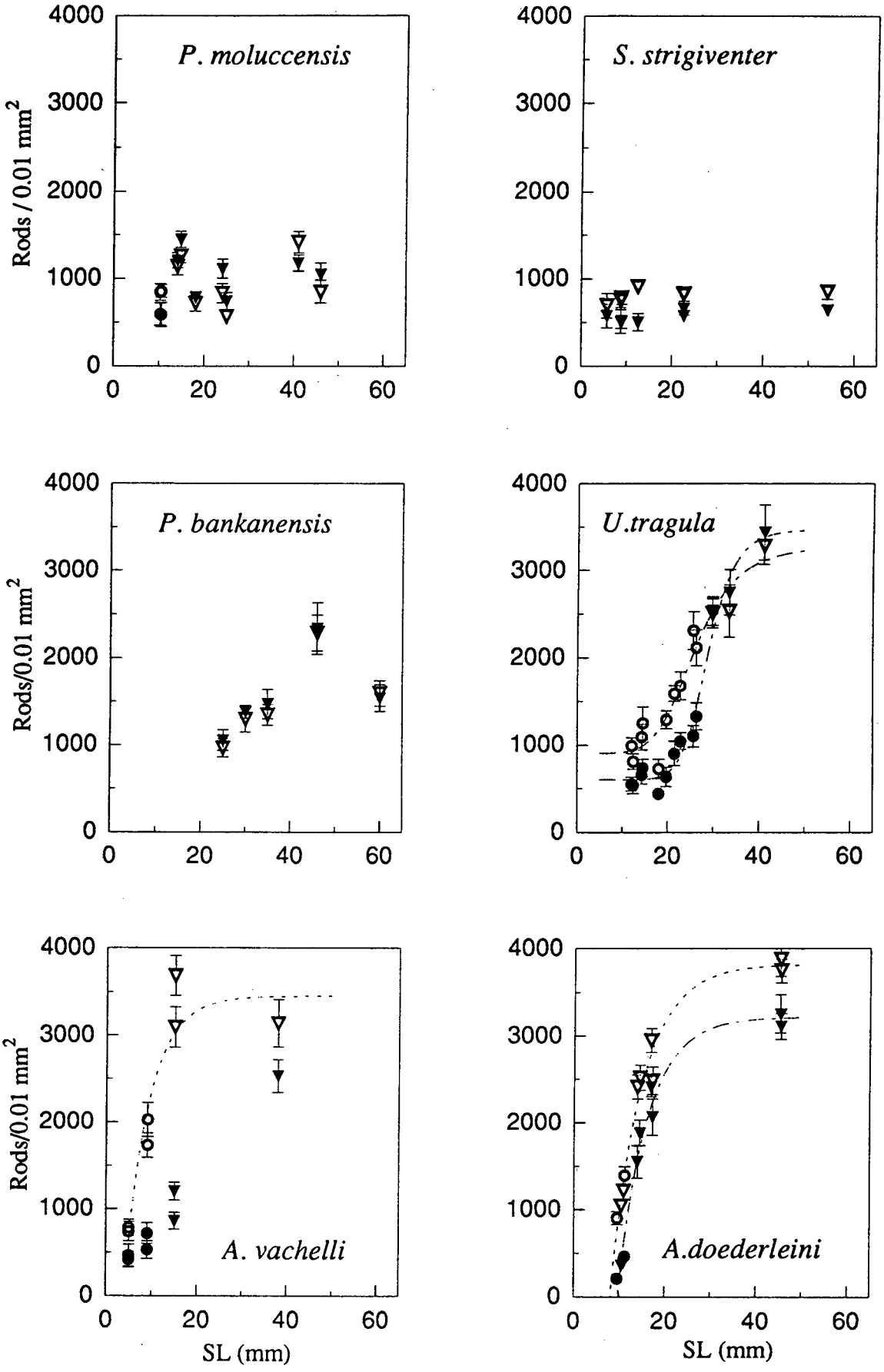
P. moluccensis
S. strigiventer
P. bankanensis
U.tragula
A. vachelli
A.doederleini
Rods / 0.01 mm2
Rods/0.01 mm2
SL (mm)
0
1000
2000
3000
4000
0
20
40
60

Table I.12. Equations and regression coefficients for the curves fitted to the changes in inner nuclear layer cells (INL) during growth (SL) as shown opposite. The curves are either: exponential decay to a minimum (EDM), with time constant (TC), minimum asymptote (MIN) or; quadratic (QUAD). D, dorsal; V, ventral. See text for equations and explanations of curves.

Species	Curve type	Equation	r^2	Notes
P. moluccensis	EDM	D INL = $2667e^{-0.0582SL} + 2266$	0.6454	TC = 17.18
				MIN = 2266
		V INL = $4906e^{-0.08707SL} + 2149$	0.8126	TC = 11.48
				MIN = 2149
S. strigiventer	no curve fitted			
P. bankanensis	no correlation			
U. tragula	QUAD	D INL = $79.48SL - 1.81SL^2 + 1586$	0.3755	
		V INL = $145.9SL - 2.98SL^2 + 1178$	0.6268	
A. vachelli	EDM	D INL = $3335e^{-0.08561SL} + 1037$	0.9215	TC = 11.68
				MIN = 1037
A. doederleini	EDM	D INL = $6781e^{-0.1473SL} + 1288$	0.9514	TC = 6.79
				MIN = 1288
		V INL = $3627e^{-0.06351SL} + 1154$	0.96	TC = 15.74
				MIN = 1154

Fig. I.13. Changes in the density of cells in the inner nuclear layer during the growth of *Pomacentrus moluccensis, Stethojulis strigiventer, Pomacentrus bankanensis, Upeneus tragula, Ambassis vachelli*, and *Apogon doederleini*. Open symbols, dorsal retina; filled symbols, ventral retina; circles, pre-settlement; triangles, settled; SL, standard length. The error bars give the 95% confidence limits.

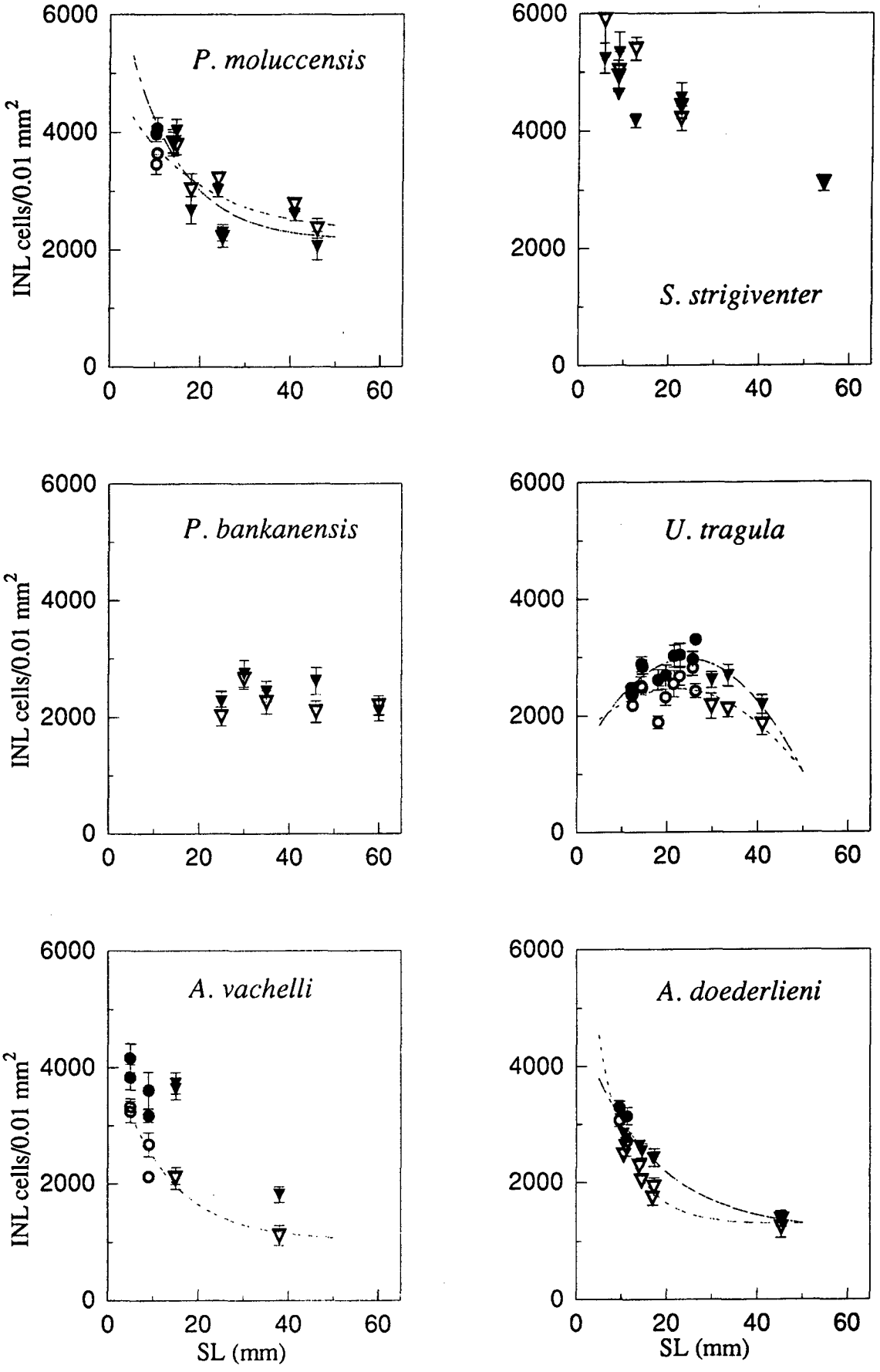
P. moluccensis
S. strigiventer
P. bankanensis
U. tragula
A. vachelli
A. doederlieni
INL cells/0.01 mm2
SL (mm)
0
2000
4000
6000
0
20
40
60

obtained.

Cells in the ganglion cell layer (Fig. I.14): These cells decreased in density during growth in all species for which data for small fish was available. The best curve fitted has an exponential decay to a minimum equation which implies the greatest rate of reduction in ganglion cells occurs early in development. The asymptote values are lowest in the nocturnal species (Table I.13).

Rod to cone ratios: Changes of the ratios between the two photoreceptor types during growth are shown in Fig. I.15. Because of the reduction in cone densities and increase in rod densities there is usually an increase in this ratio i.e. all fitted curves have positive slopes (Table I.14). The increase is greatest in the nocturnal species which have the highest rod densities. *Upeneus tragula* also shows a sharp increase after settlement (>25 mm SL as the fish moves to deeper water (in excess of 20 m)). *Pomacentrus moluccensis* and *Stethojulis strigiventer*, diurnal species which remain in the first 20 m of the water column, show little or no increase in this ratio as their rod densities remain low throughout the size range of fish.

Changes in the ratios of photoreceptors to neural cells

Since the degree of convergence of photoreceptors to neural cells is likely to affect the degree of information maintained, processed and subsequently transmitted to the optic lobes of the brain, the ratios of various cell types were analysed during growth of the six species for which detailed cell counts were obtained.

Cones to cells in the inner nuclear layer (Fig. I.16): This ratio does not vary during growth and is similar in all species, with the exception of *Upeneus tragula.* The densities of cones and cells in the INL must therefore decline in proportion to each other. The exception to this pattern is *U. tragula* in which the ratio is greater

Table I.13 Coefficients for the regression lines fitted to changes in density of cells in the ganglion cell layer (GCL) during growth (SL) as shown opposite. All curves are exponential decay to a minimum (EDM), with time constant (TC) and minimum asymptote (MIN). Dorsal and ventral points have been combined for the *Pomacentrus moluccensis, Stethojulis strigiventer* and *Upeneus tragula* curves. D, dorsal; V, ventral. See text for equations and explanations of curves.

Species	Equation for regression line	r^2	notes
P. moluccensis	$GCL = 1815e^{-0.1665SL} + 220.4$	0.9252	TC = 6.00
			MIN = 220.4
S. strigiventer	$GCL = 3283e^{-0.1879SL} + 275.7$	0.9656	TC = 5.29
			MIN = 275.7
P. bankanensis	no correlation		
U. tragula	$GCL = 2450e^{-0.154SL} + 181.3$	0.9316	TC = 6.49
			MIN = 181.3
A. vachelli	$D\ GCL = 1914e^{-0.2359SL} + 154.8$	0.9600	TC = 4.23
			MIN = 154.8
	$V\ GCL = 1440e^{-0.1140SL} + 103.7$	0.9803	TC = 8.77
			MIN = 103.7
A. doederleini	$D\ GCL = 16650e^{-0.3517SL} + 151.5$	0.9297	TC = 2.84
			MIN = 151.5
	$V\ GCL = 5707e^{-0.2116SL} + 108.3$	0.9806	TC = 4.73
			MIN = 108.3

Fig. I.14. Changes in the density of cells in the ganglion cell layer during the growth of *Pomacentrus moluccensis, Stethojulis strigiventer, Pomacentrus bankanensis, Upeneus tragula, Ambassis vachelli* and *Apogon doederleini*. Open symbols, dorsal retina; filled symbols, ventral retina; circles, pre-settlement; triangles, settled; SL, standard length. The error bars give the 95% confidence limits.

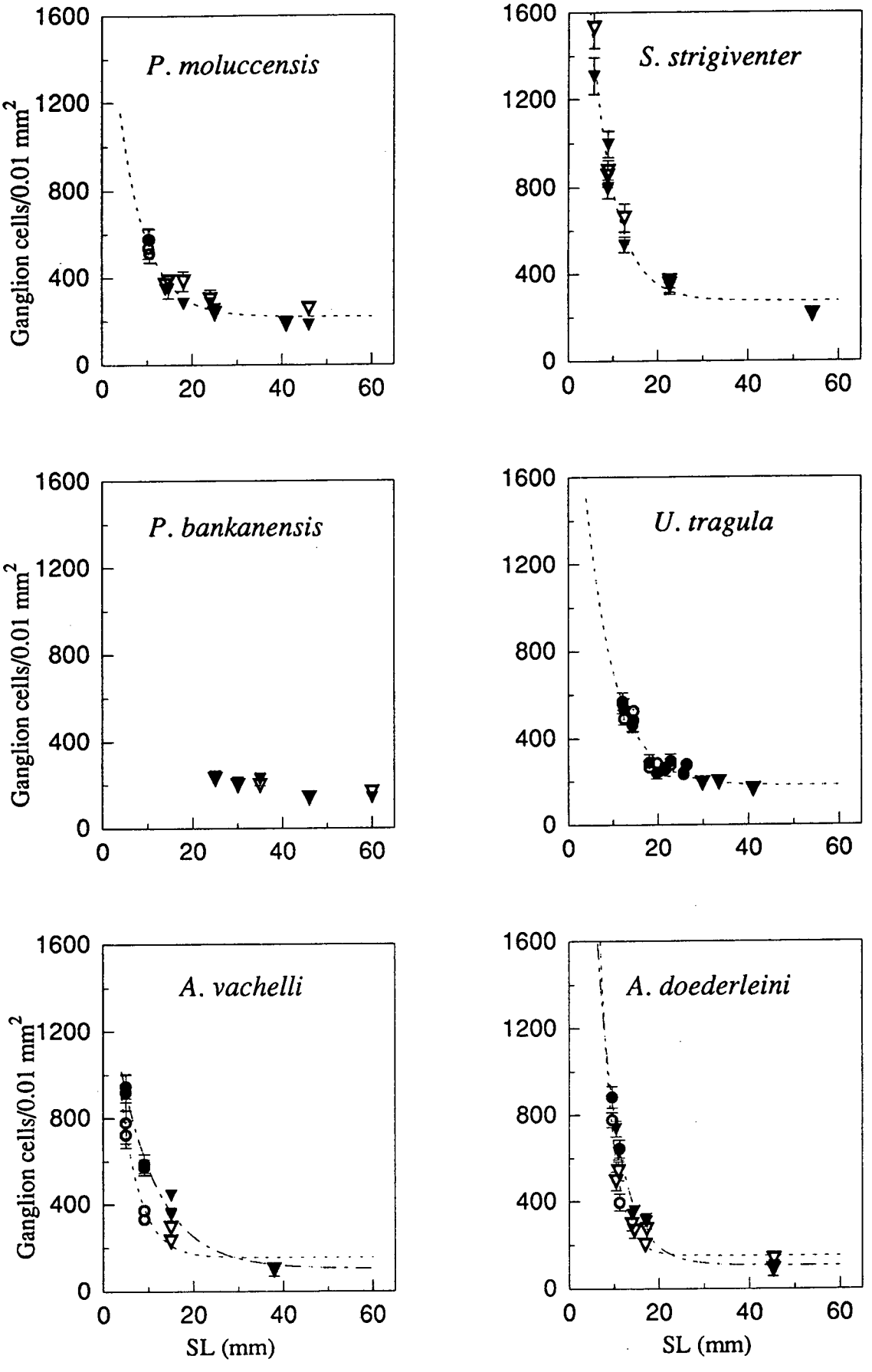
P. moluccensis
S. strigiventer
P. bankanensis
U. tragula
A. vachelli
A. doederleini
Ganglion cells/0.01 mm2
SL (mm)
0
400
800
1200
1600
0
20
40
60

Table I.14. Equations and regression coefficients for the curves fitted to the changes in the ratio of rod to cone densities (RC) during growth (SL) as shown opposite. The curves are either: exponential rise to a maximum (ERM), with time constant (TC), maximum asymptote (MAX) or: sigmoid (SIG), with maximum asymptote (MAX), minimum asymptote (MIN), point of inflection (IN). Dorsal and ventral curves are combined for the *Pomacentrus bankanensis* curve. D, dorsal; V, ventral. See text for equations and explanations of curves.

Species	Curve type	Equation	r^2	Notes
P. moluccensis	no correlation			
S. strigiventer	no correlation			
P. bankanensis	ERM	$RC = 45.1(1-e^{-0.0985SL})-37.4$	0.7335	TC = 10.15
				MAX = 7.7
U. tragula	SIG	$D\ RC=(14.6/(1+(SL/29)^{-7.84}))+1.955$	0.9810	MAX = 16.56
				MIN = 1.95
				IN = 29.33
		$V\ RC=(11.7/(1+(SL/30)^{-10.63}))+1.01$	0.9873	MAX = 12.72
				MIN = 1.01
				IN = 30.13
A. vachelli	ERM	$D\ RC = 30.44(1-e^{-0.0745})-8.314$	0.9748	TC = 13.43
				MAX = 22.12
A. doederleini	ERM	$D\ RC = 50.1(1-e^{-0.0895})-27.46$	0.9759	TC = 11.18
				MAX = 22.63
		$V\ RC = 32.88(1-e^{-0.0820})-18.29$	0.9843	TC = 12.20
				MAX = 14.59

Fig. I.15. Changes in the ratio of rods to cones during the growth of *Pomacentrus moluccensis, Stethojulis strigiventer, Pomacentrus bankanensis, Upeneus tragula, Ambassis vachelli*, and *Apogon doederleini*. Open symbols, dorsal retina; filled symbols, ventral retina; circles, pre-settlement; triangles, settled; SL, standard length. The error bars give the 95% confidence limits.

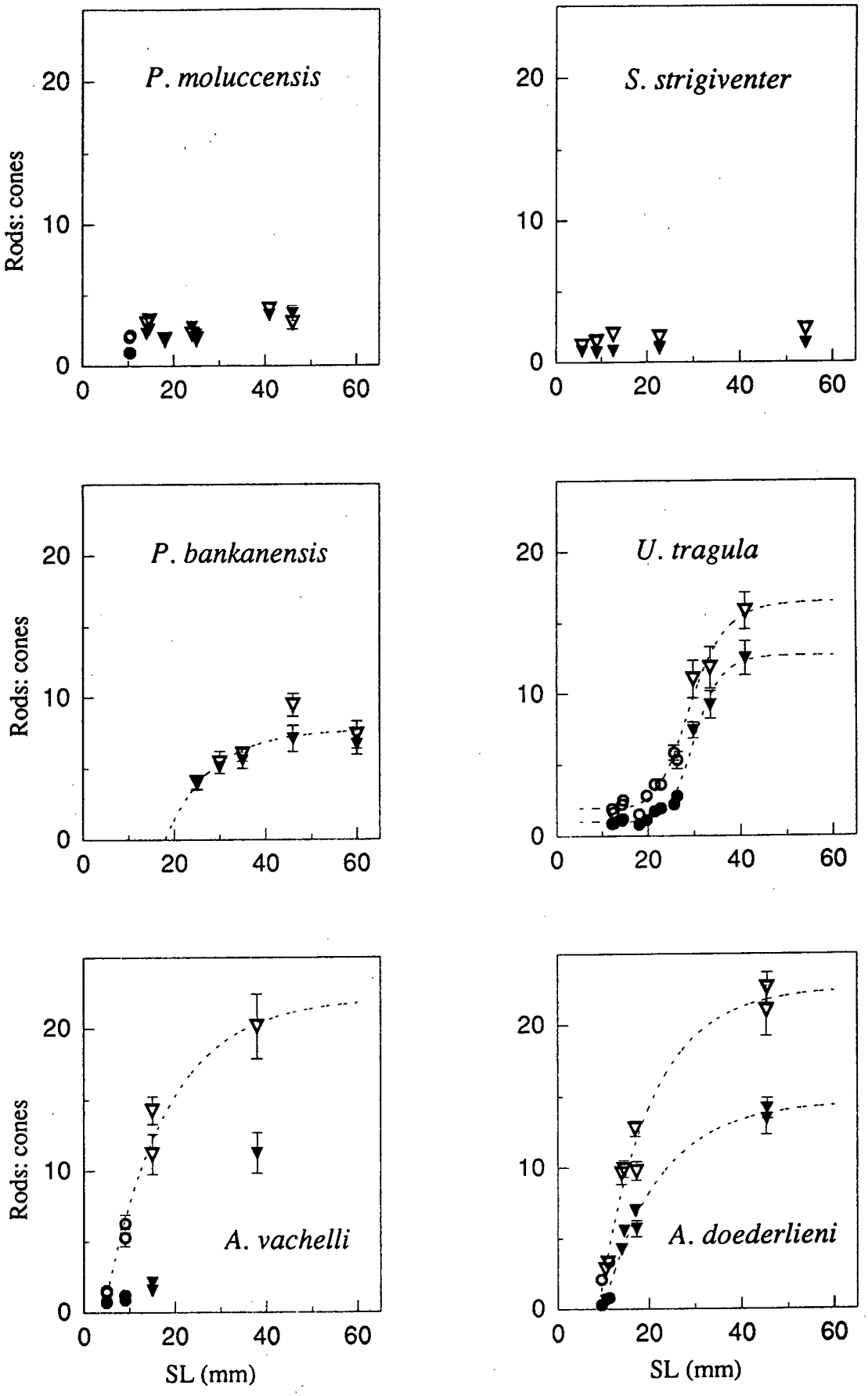
P. moluccensis
S. strigiventer
P. bankanensis
U. tragula
A. vachelli
A. doederlieni
Rods: cones
SL (mm)
0
10
20
40
60

Table I.15. Equations and regression coefficients for the curves fitted to the changes in the ratio of cone cells to cells in the inner nuclear layer (CINL) during growth (SL) as shown opposite. Curves fitted to *U. tragula* only, all other species gave no correlations. Curve is exponential decay to a minimum (EDM), with time constant (TC) and minimum asymptote (MIN) given. D, dorsal; V, ventral.

Species	Curve type	Equation	r^2	Notes
U. tragula	EDM	D CINL = $0.5845e^{-0.0112} - 0.2797$	0.7607	TC = 89.28
				MIN = -0.28
		V CINL = $0.3541e^{-0.0638} - 0.0879$	0.9100	TC = 15.67
				MIN = 0.0879

Fig. I.16. Changes in the ratio of cones to cells in the inner nuclear layer (INL) during the growth of *Pomacentrus moluccensis, Stethojulis strigiventer, Pomacentrus bankanensis, Upeneus tragula, Ambassis vachelli*, and *Apogon doederleini*. Open symbols, dorsal retina; filled symbols, ventral retina; circles, pre-settlement; triangles, settled; SL, standard length. The error bars give the 95% confidence limits.

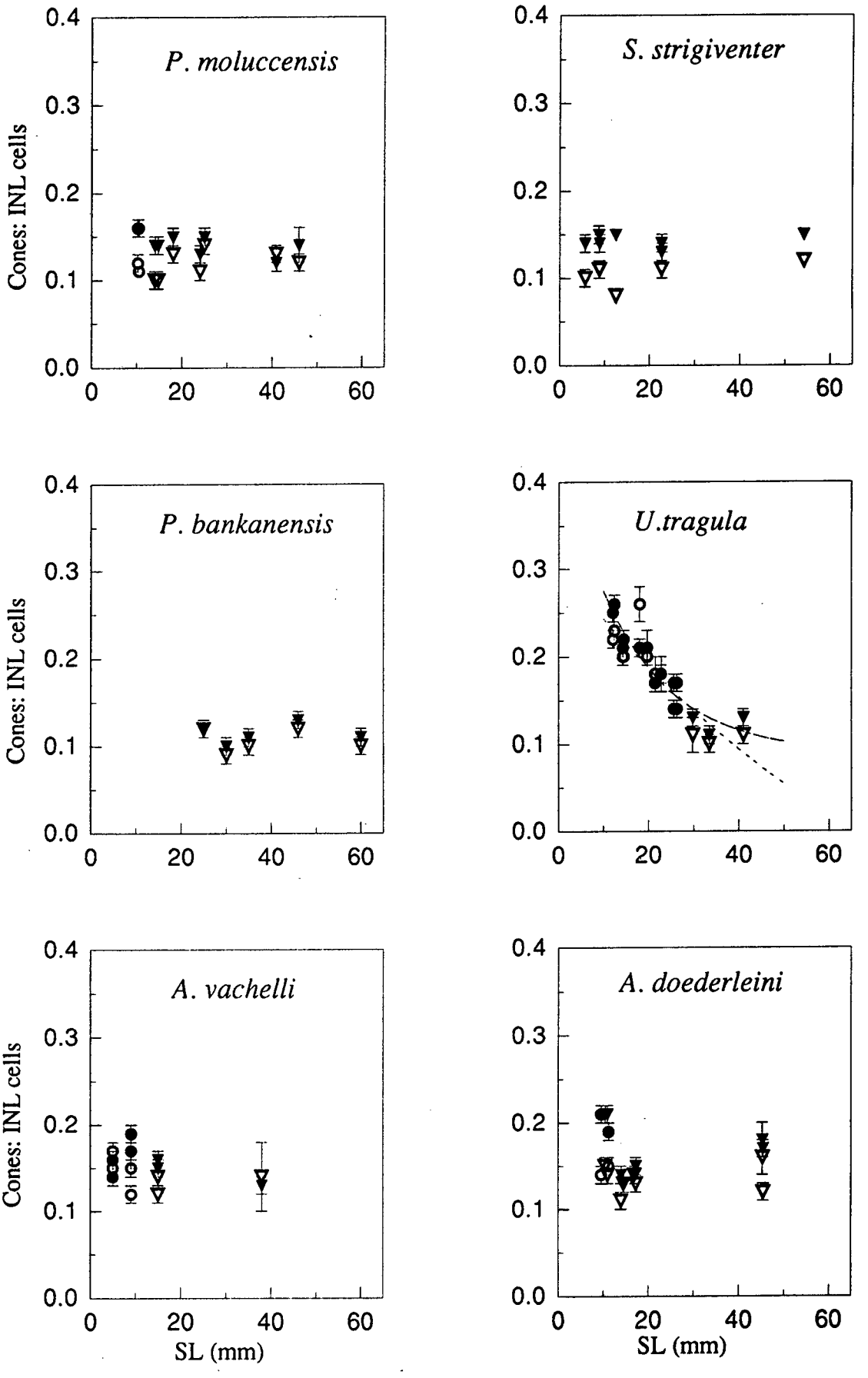
P. moluccensis
S. strigiventer
P. bankanensis
U.tragula
A. vachelli
A. doederleini
Cones: INL cells
SL (mm)
0.0
0.1
0.2
0.3
0.4
0
20
40
60

in smaller fish and declines prior to settlement when the relationship stabilises at a similar value to that found in the other species.

Photoreceptors (rods plus cones) to cells in the inner nuclear layer (Fig. I.17): The changes in rod densities influence the changes in convergence of photoreceptors to INL cells during growth since rod densities are higher than that of cones. Thus the changes in this ratio mirror the changes in rod densities (see Fig. I.12). The shallow water diurnal species with low rod densities (*P. moluccensis, S. strigiventer* and *P. bankanensis*) show a small increase in the ratio whereas the nocturnal species and *Upeneus tragula* show the greatest changes. The changes in this ratio in *Ambassis vachelli* and *Apogon doederleini* occur early in development whereas those in *U.tragula* are delayed until around the time of settlement.

Cones to cells in the ganglion cell layer (Fig. I.18): The changes in this ratio initially increase in all species. There are no distinct differences between species emerge although the highest degree of summation is in *Apogon doederleini*. *Upeneus tragula* appears to decrease the ratio following settlement. The variation in the ratio in the other species is in the range of approximately 1 to 2 cones per ganglion cell (Table I.9).

Photoreceptors to cells in the ganglion cell layer (Fig. I.19): The changes in this ratio during growth once again as a result of the changes in rod density. The increase in the ratio is therefore greatest in the fish with the greatest increase in rods.

Table I.16. Equations and regression coefficients for the curves fitted to the changes in the ratio of photoreceptors to cells in the inner nuclear layer (PINL) during growth (SL) as shown opposite. The curves are either: sigmoid (SIG) with maximum asymptote (MAX), minimum asymptote (MIN) and inflection point (IN): or exponential rise to a maximum (ERM) with time constant (TC) and maximum asymptote (MAX). D, dorsal; V, ventral.

Species	Curve type	Equation	r^2	Notes
P. moluccensis	no correlation			
S. strigiventer	no correlation			
P. bankanensis	no curve fitted			
U. tragula	SIG	D PINL=$(3.1/(1+(SL/45)^{-3.44}))+0.58$	0.9811	MAX = 3.68
				MIN = 0.58
				IN = 45.0
		V PINL=$(1.4/(1+(SL/32)^{-8.86}))+0.44$	0.9580	MAX = 1.81
				MIN = 0.44
				IN = 32.06
A. vachelli	ERM	D PINL = $4.389(1-e^{-0.0515SL})-0.631$	0.9846	TC = 19.40
				MAX = 3.76
A. doederleini	ERM	D PINL = $6.094(1-e^{-0.0731SL})-2.694$	0.9728	TC = 13.67
				MAX = 3.40
		V PINL = $4.548(1-e^{-0.0487SL})-1.494$	0.9945	TC = 20.55
				MAX = 3.054

Fig. I.17. Changes in the ratio of all photoreceptors to cells in the inner nuclear layer (INL) during the growth of *Pomacentrus moluccensis, Stethojulis strigiventer, Pomacentrus bankanensis, Upeneus tragula, Ambassis vachelli*, and *Apogon doederleini*. Open symbols, dorsal retina; filled symbols, ventral retina; circles, pre-settlement; triangles, settled; SL, standard length. The error bars give the 95% confidence limits.

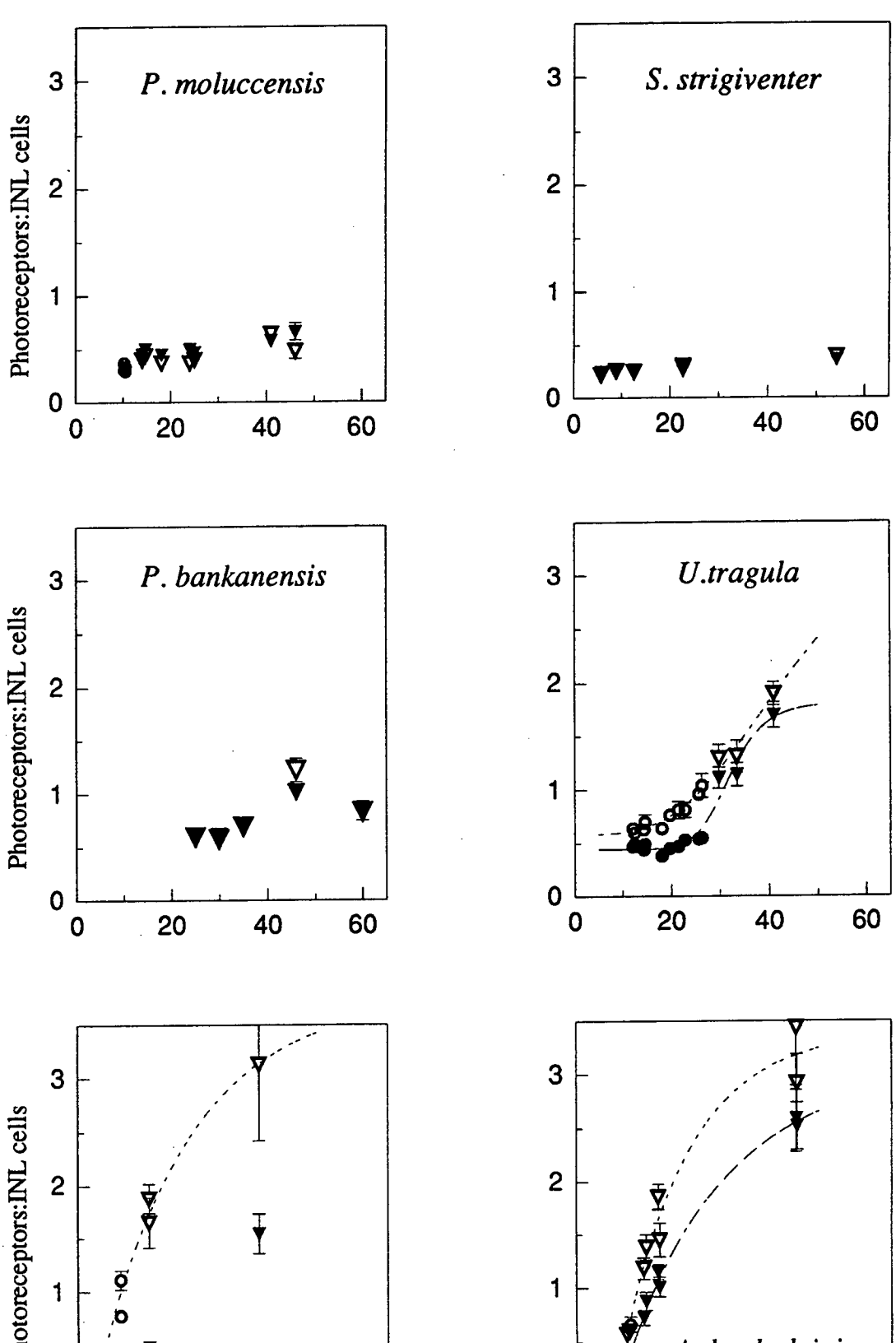
P. moluccensis
S. strigiventer
P. bankanensis
U.tragula
A. vachelli
A.doederleini
Photoreceptors:INL cells
SL (mm)
0
1
2
3
0
20
40
60

Table I.17. Equations and regression coefficients for the curves fitted to the changes in the ratios of cones to cells in the ganglion cell layer (CGCL) during growth (SL) as shown opposite. The curves fitted are: exponential rise to a maximum (ERM) with time constant (TC) and maximum asymptote (MAX); or quadratic curves (QUAD). D, dorsal; V, ventral.

Species	Curve type	Equation	r^2	Notes
P. moluccensis	ERM	D CGCL = $1.673(1-e^{-0.0788SL})-0.1465$	0.5995	TC = 12.68
				MAX = 1.53
S. strigiventer	ERM	D CGCL = $2.092(1-e^{-0.0512SL})-0.1643$	0.9842	TC = 19.54
				MAX = 1.93
		V CGCL = $2.656(1-e^{-0.0643SL})-0.3030$	0.9927	TC = 15.56
				MAX = 2.35
P. bankanensis	no curve fitted			
U. tragula	QUAD	D CGCL=$0.1475SL-0.0028SL^2-0.3524$	0.4483	
		V CGCL=$0.1726SL-0.0031SL^2-0.3967$	0.5426	
A. vachelli	ERM	D CGCL = $2.795(1-e^{-0.0148SL})+0.533$	0.9479	TC = 67.61
				MAX = 3.33
		V CGCL = $2.621(1-e^{-0.0498SL})+0.082$	0.9627	TC = 20.06
				MAX = 2.70
A. doederleini	no curve fitted			

Fig. I.18. Changes in the ratio of cones to cells in the ganglion cell layer during the growth of *Pomacentrus moluccensis, Stethojulis strigiventer, Pomacentrus bankanensis, Upeneus tragula, Ambassis vachelli*, and *Apogon doederleini*. Open symbols, dorsal retina; filled symbols, ventral retina; circles, pre-settlement; triangles, settled; SL, standard length. The error bars give the 95% confidence limits.

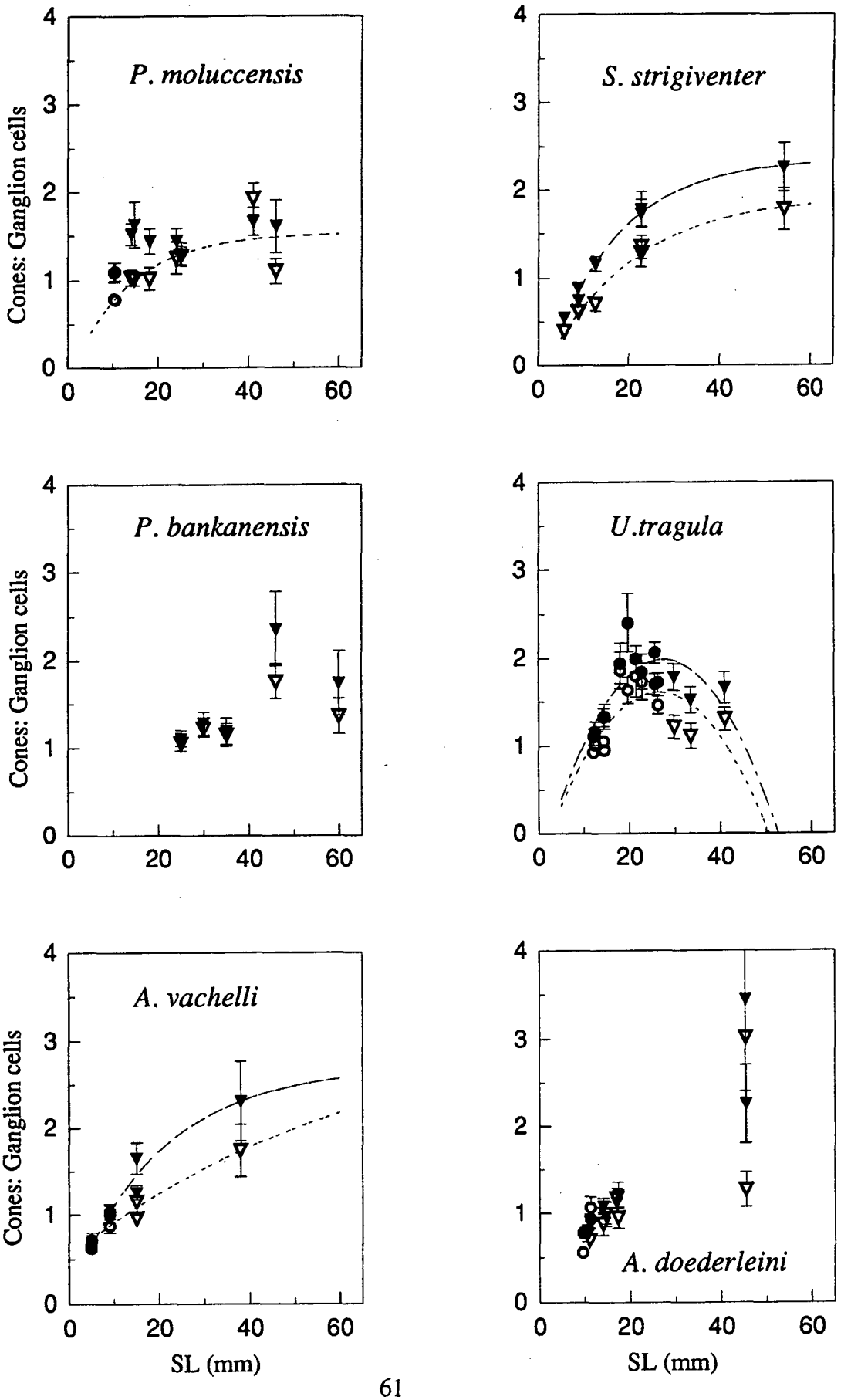
P. moluccensis
S. strigiventer
P. bankanensis
U.tragula
A. vachelli
A. doederleini
Cones: Ganglion cells
SL (mm)
0
1
2
3
4
0
20
40
60

Table I.18 Coefficients for the regression lines fitted to changes in ratios of photoreceptors to cells in the ganglion cell layer (PGCL) during growth (SL) as shown opposite. All regressions were linear. Dorsal and ventral curves for *P. moluccensis*, *S. strigiventer* and *U. tragula* were not significantly different so for these a single curve has been fitted using all points. D, dorsal; V, ventral.

Species	Equation for regression line	r^2
P. moluccensis	PGCL = 2.4371 + 0.1049SL	0.6093
S. strigiventer	PGCL = 0.8288 + 0.0955SL	0.9204
P. bankanensis	no curve fitted	
U. tragula	PGCL = -7.0467 + 0.6678SL	0.9210
A. vachelli	D PGCL = -2.9157 + 1.0688SL	0.9757
	V PGCL = -5.3243 + 0.8403SL	0.9411
A. doederleini	D PGCL = -3.4852 + 0.8074SL	0.9378
	V PGCL = -9.1174 + 1.0190SL	0.9888

Fig. I.19. Changes in the ratio of all photoreceptors to cells in the ganglion cell (GCL) layer during the growth of *Pomacentrus moluccensis*, *Stethojulis strigiventer*, *Pomacentrus bankanensis*, *Upeneus tragula*, *Ambassis vachelli*, and *Apogon doederleini*. Open symbols, dorsal retina; filled symbols, ventral retina; circles, pre-settlement; triangles, settled; SL, standard length. The error bars give the 95% confidence limits.

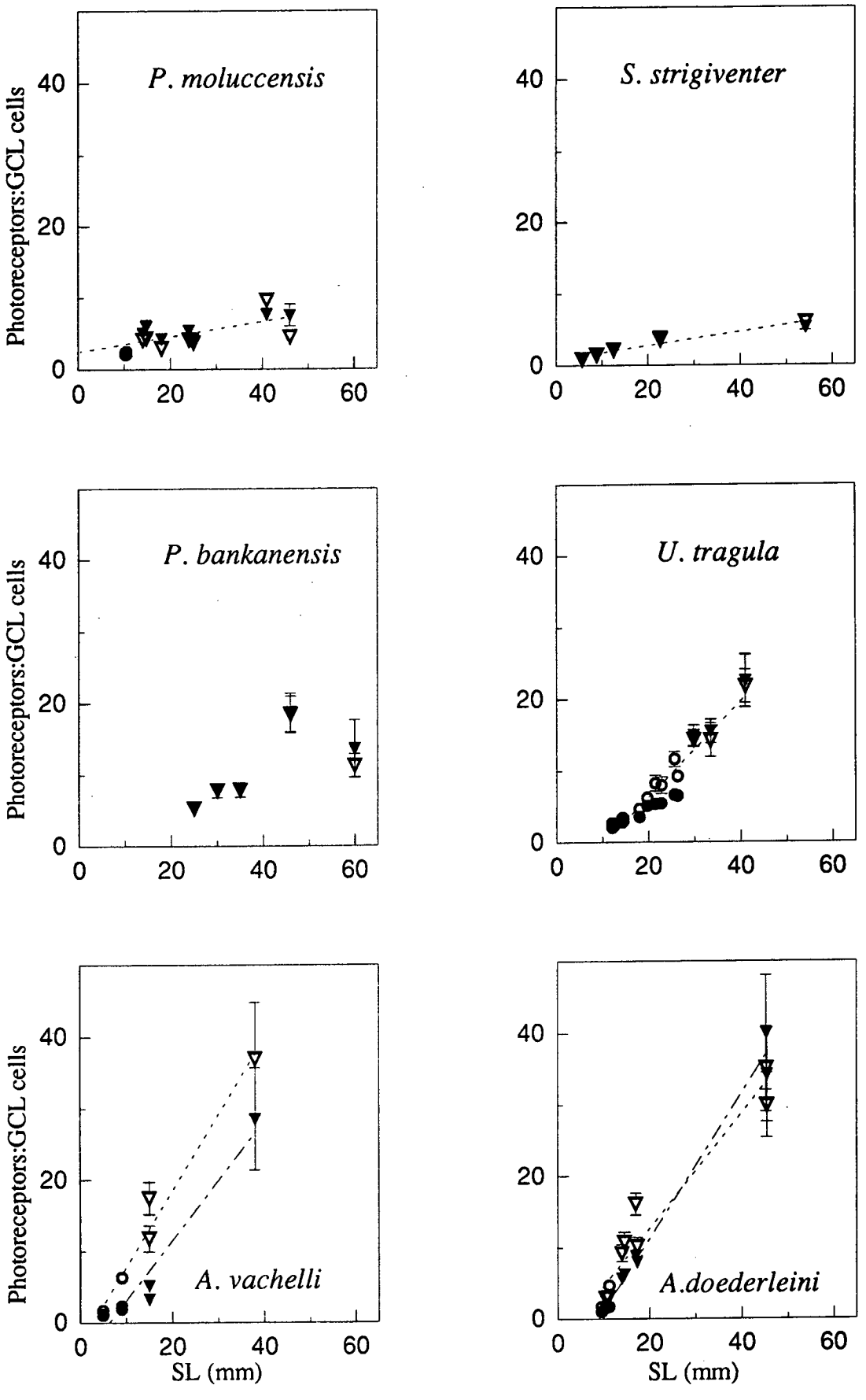
P. moluccensis
S. strigiventer
P. bankanensis
U. tragula
A. vachelli
A.doederleini
Photoreceptors:GCL cells
SL (mm)
0
20
40
60

Visual Acuity

Using data on cone densities and lens size, the minimum separable angle (MSA) was calculated. Changes in MSA for the six species over a range of sizes are shown in Fig. I.20. At small eye sizes the MSA is large and therefore the visual acuity is poor despite the high cone densities recorded from small fish. Acuity rapidly improves as the eye increases in size even though cone densities decline (Fig. I.11). There is a similar trend in all fish although the asymptote is reached at different stages of development. If the same data are plotted for all six species against lens diameter, rather than standard length, the acuity of all species is similar at a given lens size (Fig. I.21). This implies that eye size is the important factor. Thus for decreasing the MSA (and so increasing acuity) fish that can rapidly increase eye, and so lens size, will have an advantage. The data in Fig. I.21 has been fitted with a regression curve, the equation for which is:

$$MSA = 29.04LD^{-0.81113} \qquad r^2 = 0.972$$

By extrapolating this regression curve to a lens diameter value of 20 mm the curve in Fig. I.22 is obtained. The acuity data for the additional species listed in Table I.9 has been added to the graph, along with data obtained from the literature.

Fig. I.20. Changes in the minimum separable angle (MSA), calculated for the ventral retina, duing the growth of *Pomacentrus moluccensis, Stethojulis strigiventer, Pomacentrus bankanensis, Upeneus tragula, Ambassis vachelli*, and *Apogon doederleini*. A decrease in MSA implies an increase in visual acuity. Open symbols, pre-settlement; filled symbols, settled; SL, standard length.

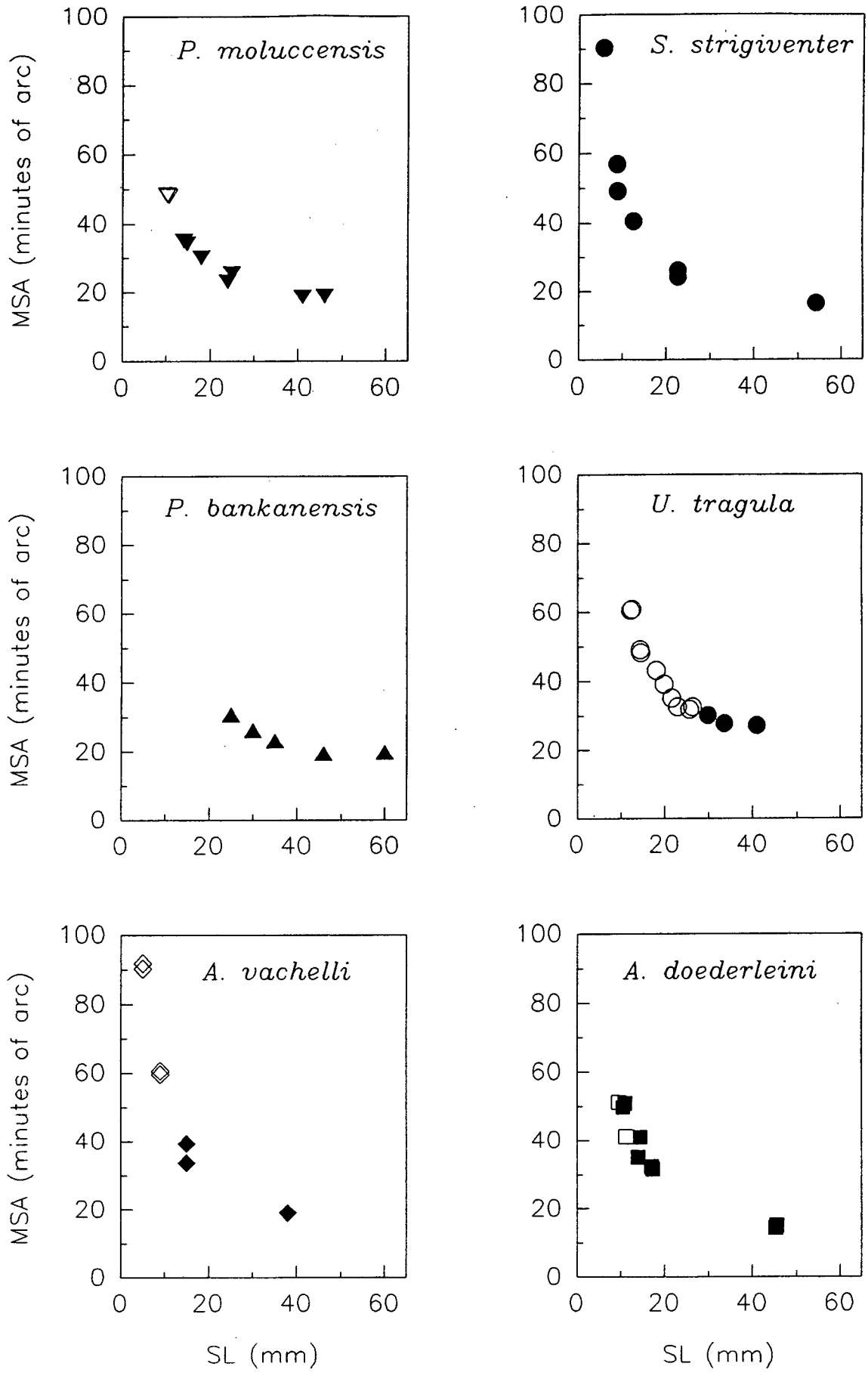
P. moluccensis
S. strigiventer
P. bankanensis
U. tragula
A. vachelli
A. doederleini
MSA (minutes of arc)
SL (mm)
0
20
40
60
80
100

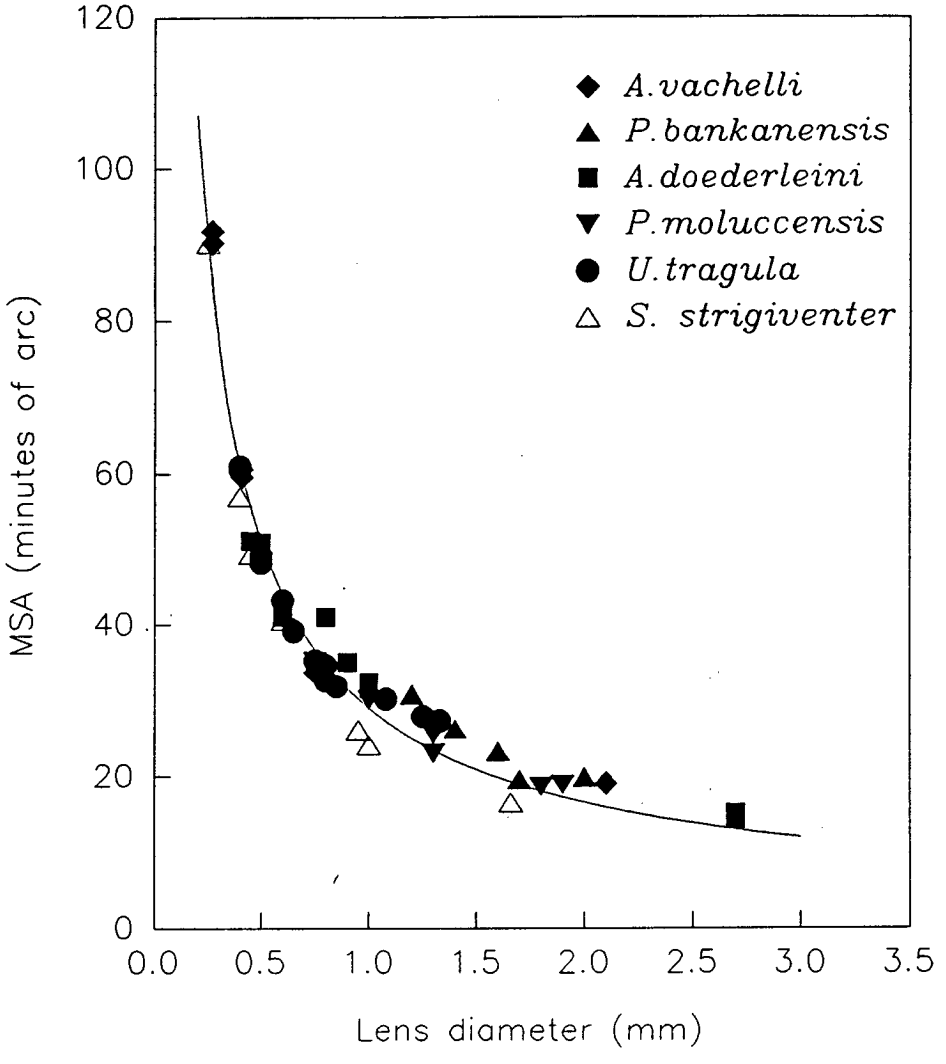

Fig. I.21. The same data for the changes in the minimum separable angle (MSA) during growth of the eye as given in Fig. I.20 but plotted against lens diameter rather than standard length. The solid line is a calculated regression curve. See text for the equation and coefficients of the curve.

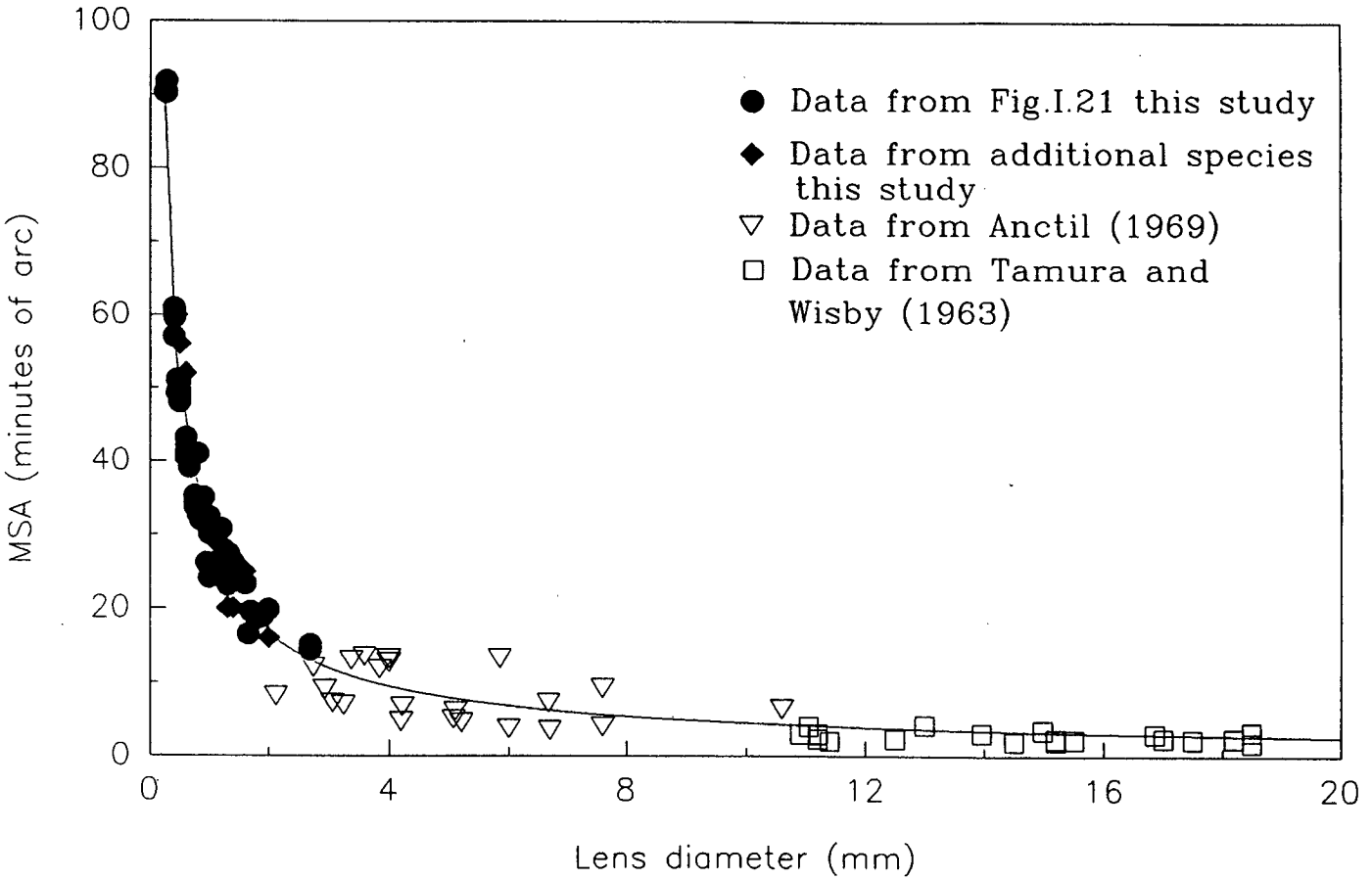

Fig. I.22. An extrapolation of the regression line calculated from the data presented in Fig. I.21. Data from additional species in this study and the literature has been added to the graph.

Upeneus tragula: a more detailed investigation

Much of the comparative cell density data during growth indicates that this species develops differently. In addition the structure of the dorsal retina of pre-settlement fish has an unusual double layer of cones which is not present in benthic settled juveniles. The retina of partially-settled and very recently aquarium-settled fish shows that the amalgamation of the two cone layers is closely related to the settlement event. Plate I.7A-D shows the structure of the retina at four stages:

A) *Before settlement.* The cone inner segments form two distinct layers. This double layer is not present in fish smaller than 15 mm SL and in fish between 15-17 mm SL the layering is found only at the retinal margins. In pre-settlement fish between 17-30 mm SL, the double layer covers the entire area of the dorsal retina. In these larger pre-settlement fish the melanin granules of the pigmented epithelium surround the outer segments of the cones in the outer (sclerad) layer but do not extend to surround the outer segments of the inner (vitread) layer (Plate I.7A).

B) *Partially-settled fish.* They still have a double layer of cones visible but the melanin granules of the pigment epithelium also extend around the outer segments of the vitread layer (Plate I.7B).

C) *Aquarium-settled fish.* Those settled for between 6 - 24 hr no longer show the distinct double layer of cones in the dorsal retina (Plate I.7C).

D) *Wild-caught settled fish.* None were found to possess the double layer of cones in the dorsal retina (Plate I.7D).

Examination of the cone mosaic of pre-settlement fish (Plate I.8A) shows that all the cells in the vitread layer are single cones, but those in the sclerad layer are double. The outer segment of the single cone projects into the middle of a square array formed by the inner segments of four double cones. In settled fish (Plate

Plate I.7. Radial sections of dorsal retinae of *Upeneus tragula* at various stages of development: **A)** pre-settlement fish of 21.5 mm SL in which the cone inner segments form two layers. Those in the vitread layer are single cones, and those in the sclerad layer are double cones. **B)** aquarium held fish of 29.3 mm SL which was beginning to obtain some skin pigmentation and settle to the bottom of the tank. Two layers of cone inner segments are still present, but melanin granules are extending around the outer segments of the vitread layer; **C)** aquarium-settled fish of 28.1 mm SL. The two layers of cone inner segments can no longer be distinguished; **D)** wild-caught settled fish of 41 mm SL, in which the cone inner segments are found arranged in one layer only. PE, pigment epithelium; C, cones; ONL, outer nuclear layer; INL; inner nuclear layer; B, bipolar cell bodies; GCL, ganglion cell layer. Scale bars = 50 μm.

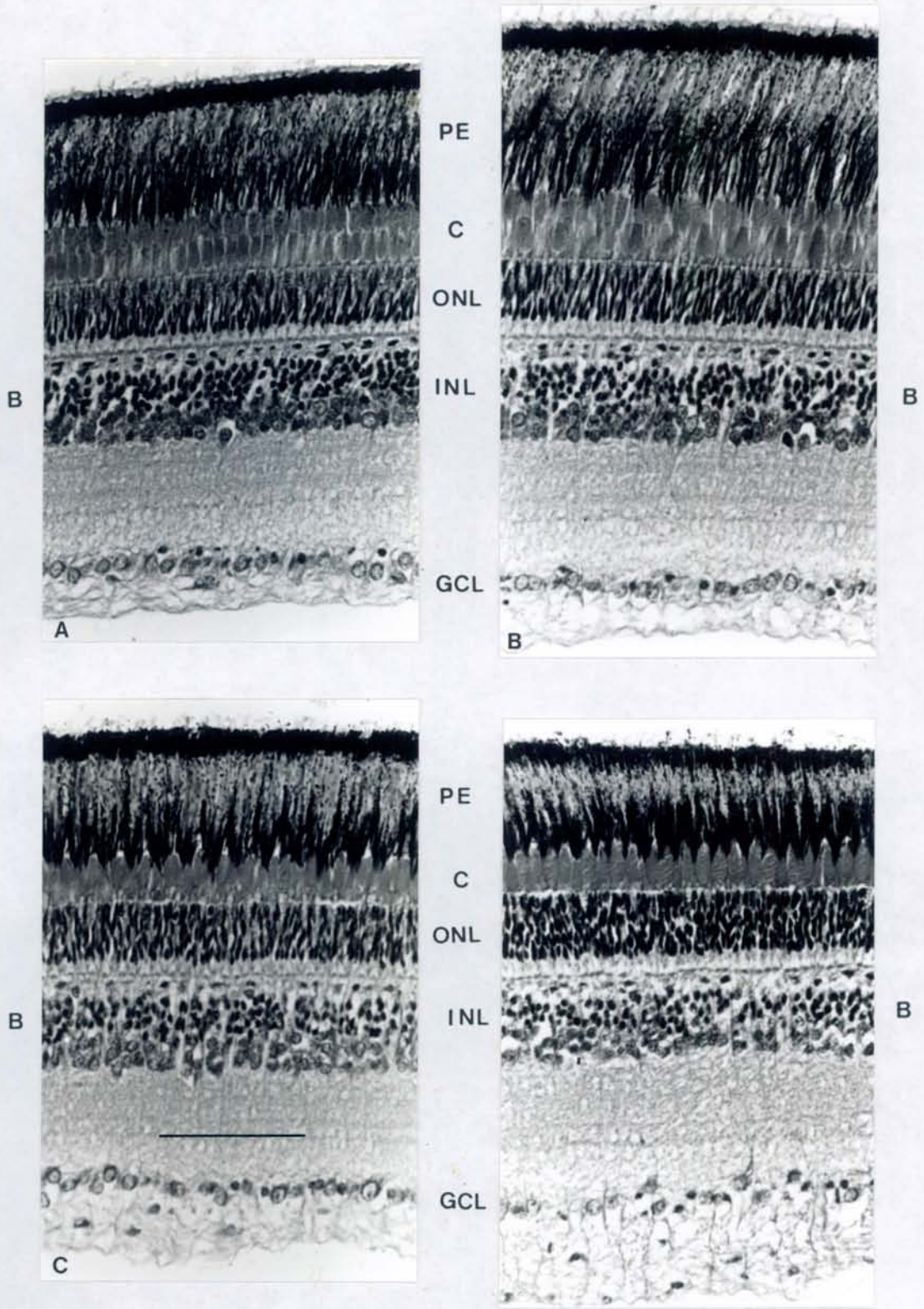
PE
C
ONL
INL
GCL
B
B
A
B
C

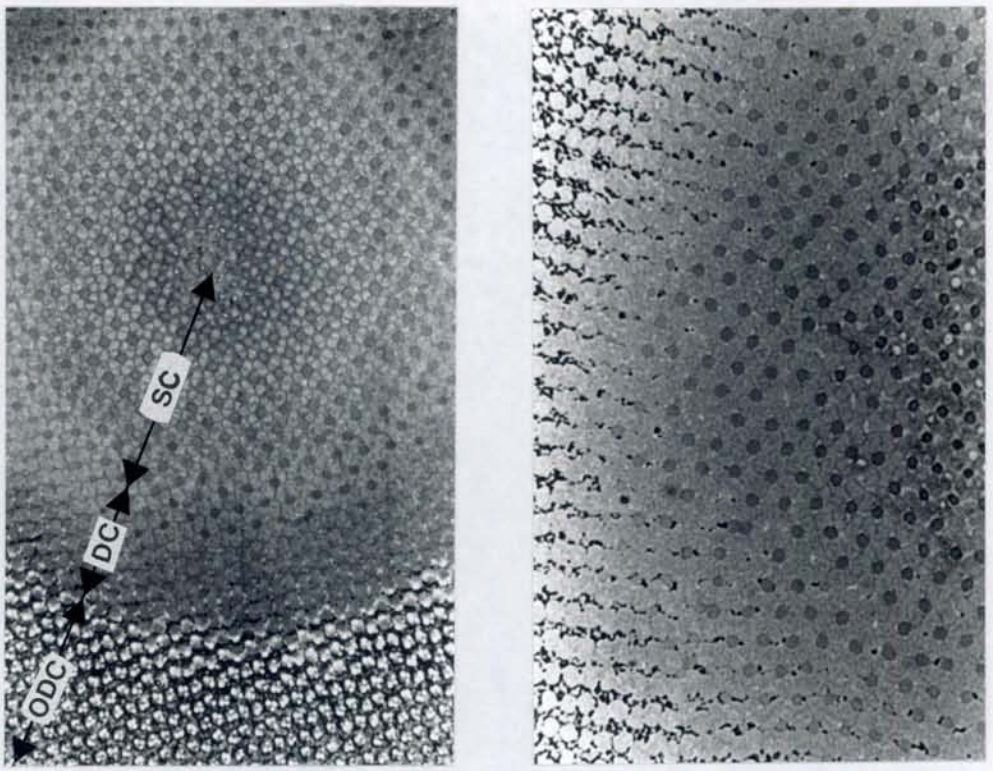

Plate I.8. Tangential sections at the level of the photoreceptors of dorsal retinae of *Upeneus tragula*: **A)** pre-settlement fish of 23.5 mm SL. As the retina is curved the section cuts through several retinal layers with those at the edges most oblique. From the centre to the edge they are: inner segments of the vitread layer of single cones plus the myoids of the sclerad layer of the double cones (SC); inner segments of the sclerad layer of double cones plus the outer segments of the single cones (DC); outer segments of the sclerad layer of double cones and surrounding melanin granules (ODC). Melanin granules do not extend around the inner segments of either cone layer; **B)** settled fish of 29 mm SL. The inner segments of both the double and single cones are now in the same plane. The melanin granules extend around the outer segments of both cone types and around the tops of the longer double cone inner segments (see also Plate I.7D). Single cones are not present within every unit of four double cones. Scale bars = 50 μm.

I.8B) it appears that the inner segments of the single cones have slotted into the array formed by the double cones so that the inner segments of all cone types are adjacent. However the central single cone is not present within every array of the mosaic.

Cone densities decrease as the fish grows but the rate of decline shows a sudden acceleration over the settlement period (Fig. I.23A). Cone densities in partially-settled fish are greater than in similar sized settled fish. This was similar for both dorsal and ventral areas of the retina but for clarity Fig. I.23B shows records from the dorsal retina only.

Another difference between *Upeneus tragula* and the other species is in the densities of cells in the inner nuclear layer (Fig. I.13). In *U. tragula* the bipolar nuclei of the inner nuclear layer increase in density in both dorsal and ventral areas to a size of 25 mm SL i.e. about the time of settlement. Following settlement bipolar nuclei density in both areas decreases (Fig. I.24A). Fig. I.24B also shows data from aquarium-held fish, in which the fully-settled fish show a greater decline in cell density than partially-settled fish of larger size.

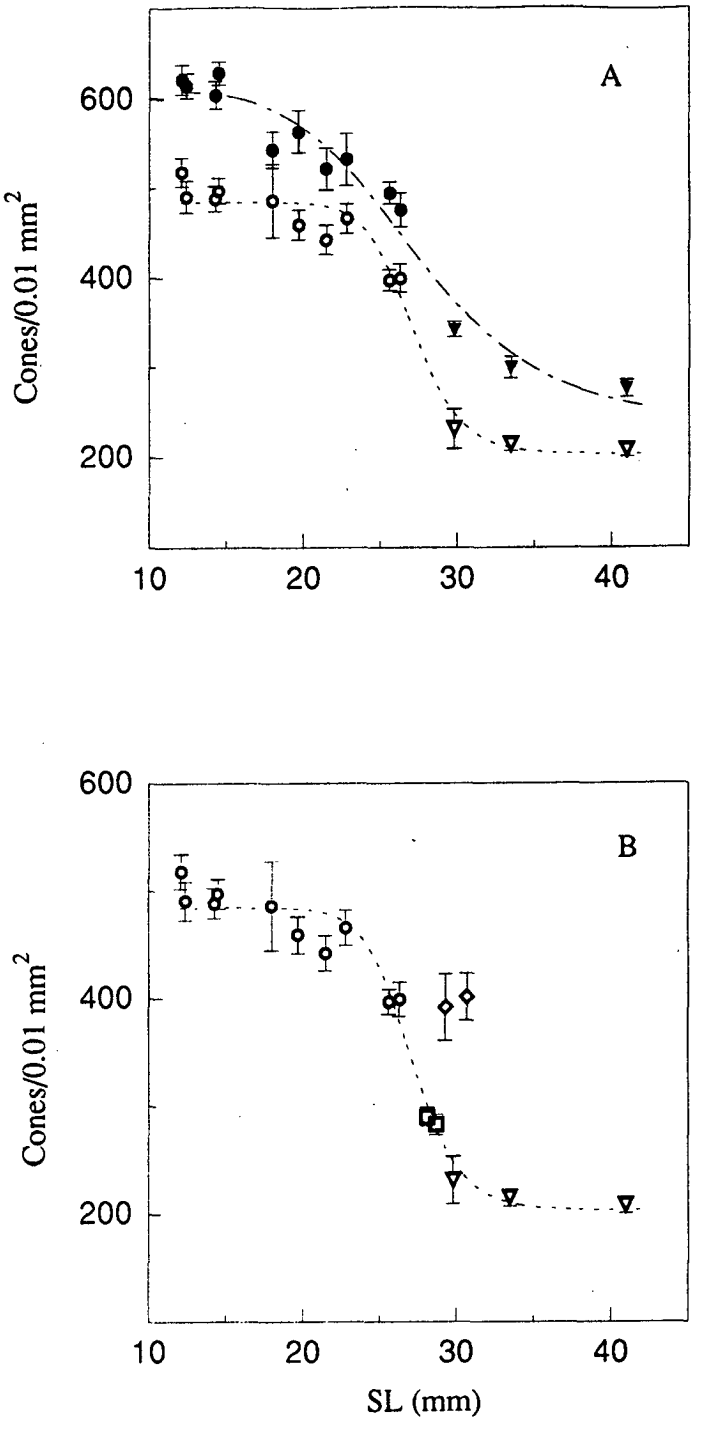

Fig. I.23. Changes in cone density in the retina of *Upeneus tragula* during growth: **A)** open symbols, dorsal retina; filled symbols, ventral retina; circles, pre-settlement; triangles, settled fish; **B)** The same data but for the dorsal retina only and including records from the aquarium-settled fish. Diamonds, partially-settled; squares, aquarium-settled; SL, standard length. The equations for the curves are given in Table I.10.

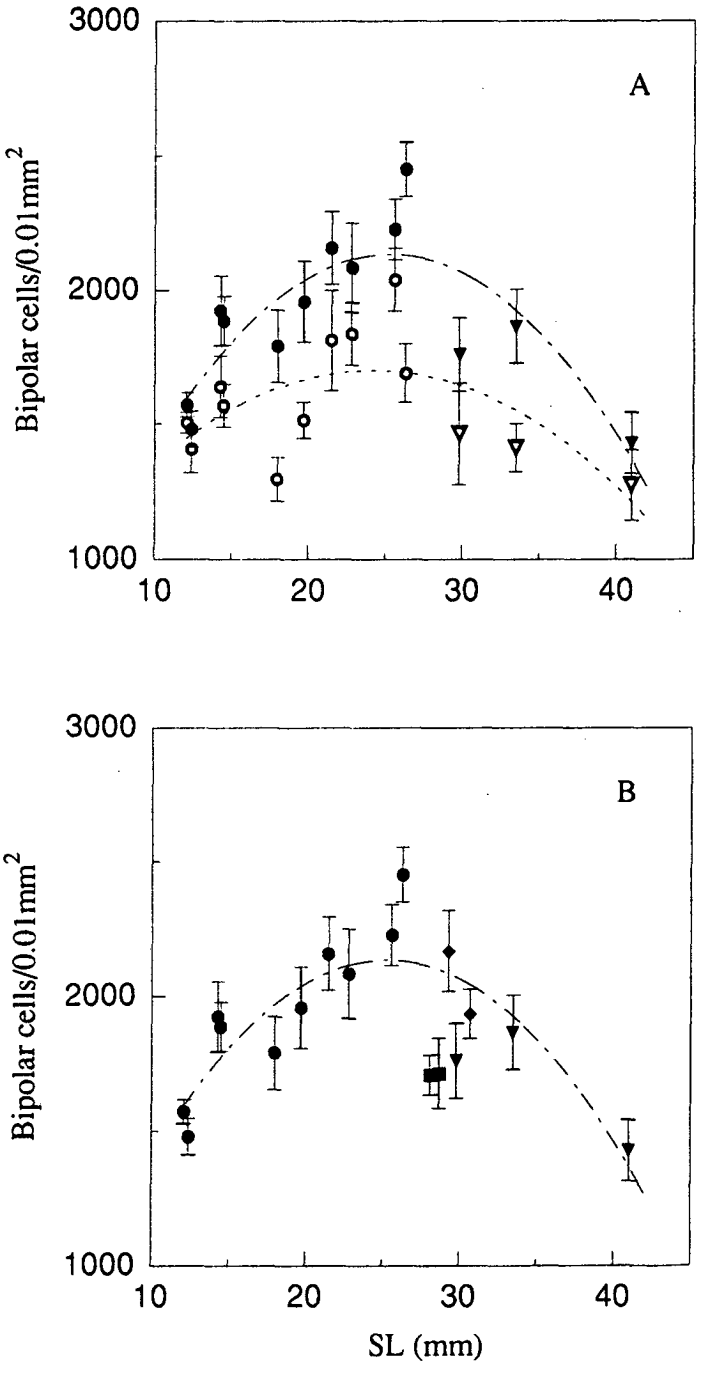

Fig. I.24. Changes in the density of bipolar cell nuclei in the retina of *Upeneus tragula* during growth: **A)** open symbols, dorsal retina; filled symbols, ventral retina; circles, pre-settlement; triangles, settled fish; **B)** The same data but for the ventral retina only and including records from the aquarium-settled fish. Diamonds, partially-settled; squares, aquarium-settled; BP, bipolar cells; SL, standard length. The fitted curves are quadratic with the equations:

dorsal, $BP = 83.79SL - 1.731SL^2 + 685.2$, $r^2 = 0.3931$

ventral, $BP = 157 - 3.104SL^2 + 148.2$, $r^2 = 0.6976$.

Observations of other species sampled

A number of other species were investigated before and following settlement although they were not necessarily sampled at regular intervals during their development (see Table I.9).

1) *Meiacanthus grammistes*: This blenny congregates under rafts in the same way as *Upeneus tragula* and settles at a relatively large size (20-28 mm SL). The retina was investigated to see whether it too possessed a double layer of cones in the dorsal retina prior to settlement. None was observed. Following settlement the cone density did not decrease during growth as in all other species examined. Densities remained high in the ventral retina and increased in the dorsal retina (Table I.9).

2) *Hemiramphus sp.*: The ventral retina of the garfish was much reduced in width compared with the dorsal retina which was up to 4 times wider. The cones in the dorsal retina were long. In the dorsal retina the outer segments were about 26 μm long and 3 μm in diameter. Long outer segments were also found in the adult garfish examined by microspectrophotometry (Part II).

3) *Neoniphon sammara*: Pre-settlement squirrelfish of this species were of a large size (30 mm SL) and possessed large eyes (diameter of 4 mm). The dorsal retina of the pre-settlement specimens had a high density of long thin cones, 26 μm long and 2 μm in diameter. The ventral retina had low rod to cone ratios (3:1) compared with those found in the thickened dorsal retina (15:1). Following settlement the cone density in the ventral retina rapidly decreased and the diameter of the cones in the dorsal retina increased to about 5 μm. Rod densities in both the ventral and dorsal retina increased so that the rod to cone ratios became 15:1 and 25:1 respectively.

4) Pomacentrids: The rod densities in pre-settlement *Pomacentrus amboinensis* and *Chromis atripectoralis* (8 - 10 mm SL) were relatively high compared with

those of pre-settlement *Pomacentrus moluccensis* (10 mm SL). Following settlement rod densities of all three species were similar and did not increase greatly. The herbivorous pomacentrid, *Pomacentrus bankanensis* had the highest rod densities of all the settled pomacentrid species investigated.

Fish with distinctive areas of retinal specialisation

Central area: All the species of labrids and scarids, at all stages of development, have an area centralis (Plate I.9A & B). This is a thickening of the photoreceptor layer and increase in density of the cones, cells of the inner nuclear layer and cells of the ganglion cell layer. The thickening of the photoreceptor layer causes the retina to become raised (convex). The cones in this area are very small and could not be counted in the usual way. In addition, the labrids and scarids were found to have red pigment granules in the pigment epithelium, as well as the usual brown melanin granules. The absorbance spectrum of the red pigment has been measured in a species of labrid from New Zealand, *Pseudolabrus celidotus* (Fineran and Nicol, 1974) and has a peak absorption at about 500 nm.

Clupeid specialised area: The temporal area of the ventral retina of *Spratelloides delicatulus* conformed to that described by Engstrom (1963) for the sprat, *Clupea sprattus* and Blaxter and Jones (1967) for the herring, *Clupea harengus*. In all these species the temporal area, ventral to the optic nerve, is specialised. There are high cone densities, few or no rods and high densities of cells in the inner nuclear and ganglion cell layers (Plate I.10A). Thus the area appears to be adapted for acute photopic vision. Dorsal to the optic nerve, in both the rostral and temporal regions, and in the rostral ventral area the retina is composed of larger cones. There are also high densities of rods and low densities of cells in the nuclear layers (Plate 10B). Thus these areas could be considered to be adapted for vision in low light conditions. Counts of the cones in the specialised area could not be made because of their small size and retracted position but comparisons of the numbers of cells in the inner nuclear layer (INL) and ganglion cell layer

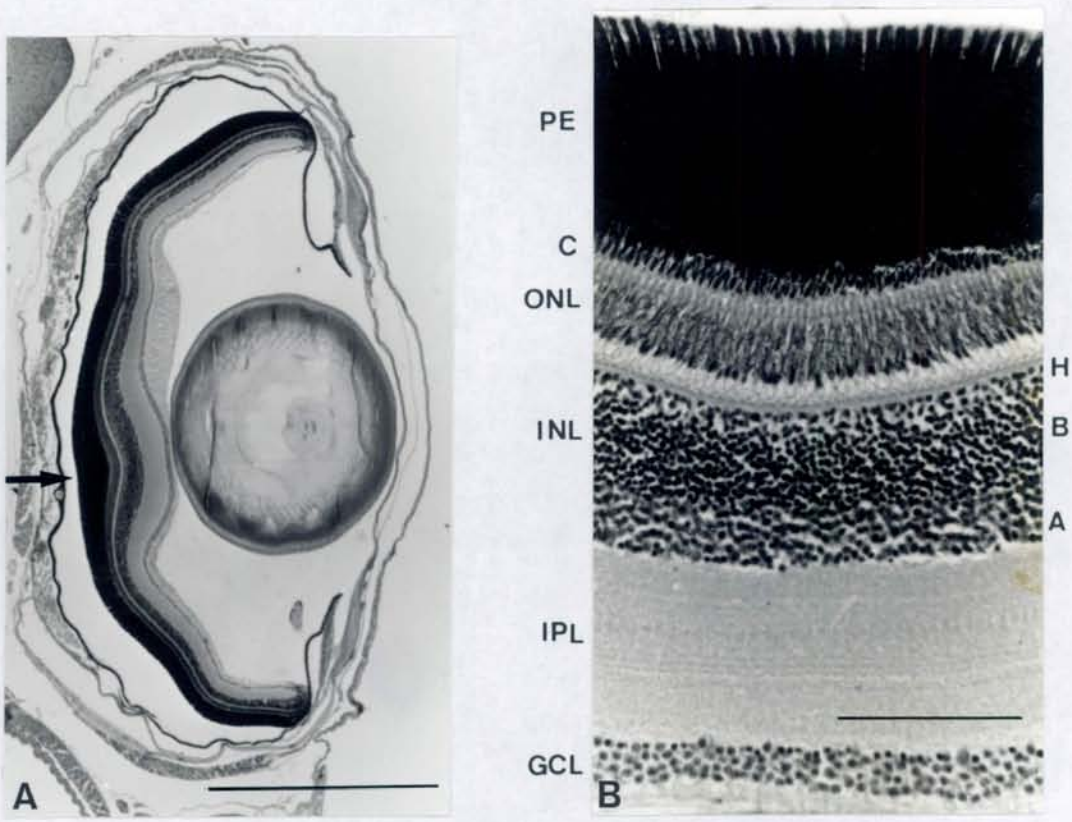

Plate I.9. Radial sections through the eye of a labrid, *Stethojulis strigiventer*: **A)** low power plan of the eye showing the position of the area centralis. The layers containing the cones, inner nuclear layer cell bodies and the ganglion cell layer cell bodies become thickened, due to an increase in the density of these cell types, resulting in the convex area of retina (arrow). Scale bar = 500 μm; **B)** Detail of the area centralis shown in A. The cones are very small in this species and individuals are not clearly visible. Scale bar = 50 μm. PE, pigment epithelium; C, cones; ONL, outer nuclear layer; INL; inner nuclear layer; H, horizontal cell bodies; B, bipolar cell bodies; A, amacrine cell bodies; IPL, inner plexiform layer; GCL, ganglion cell layer.

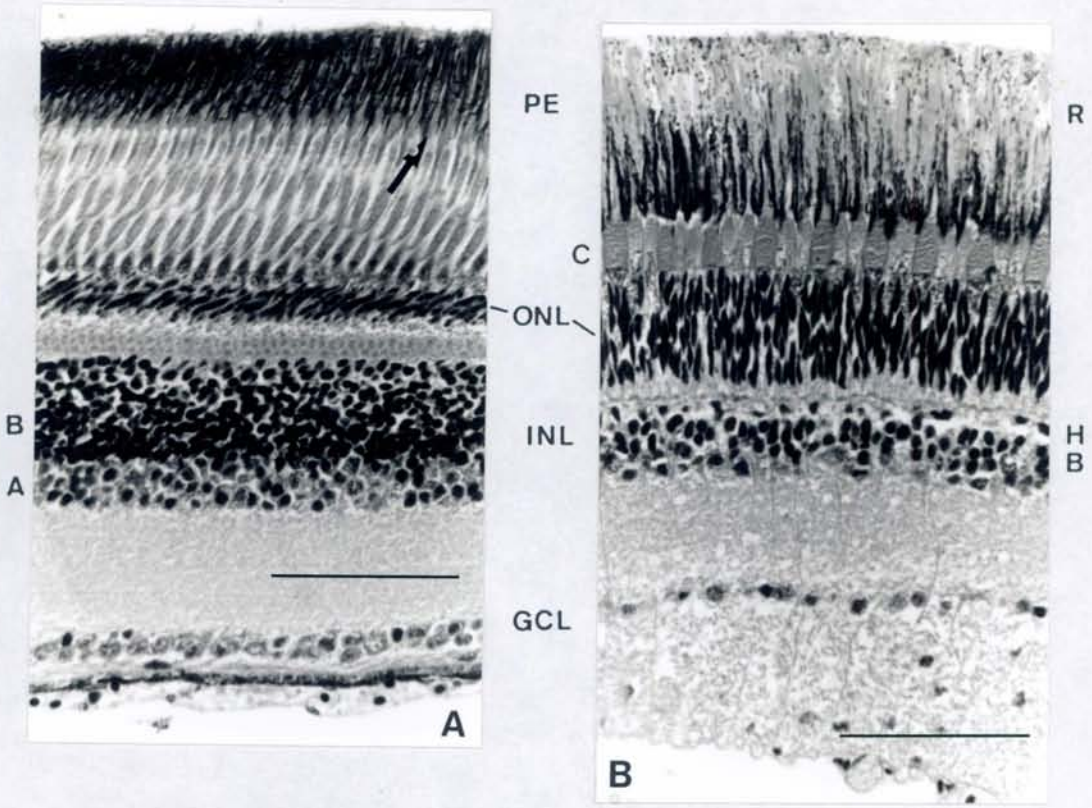

Plate I.10. Radial sections of the retina of *Spratelloides delicatulus*: **A)** the specialised area of retina found in the temporal-ventral region of the eye. It is not clear whether the photoreceptor layer contains rods as well as cones but one layer of cones is visible in the sclerad position amongst the melanin granules of the pigment epithelium (arrows). The densities of cells in the outer nuclear layer are low but those in the inner nuclear layer are high; **B)** the unspecialised area of retina from the dorsal region of the eye. Although this micrograph is from the same section as A, the melanin of the pigment epithelium and the large cones are not displaced to a sclerad position. There is a high density of rods (see Table I.9) and low density of neural cells (see text). PE, pigment epithelium; C, cones; ONL, outer nuclear layer; INL; inner nuclear layer; H, horizontal cell bodies; B, bipolar cell bodies; A, amacrine cell bodies; GCL, ganglion cell layer. Scale bars = 50 μm.

(GCL) from one specimen give the following densities per 0.01 mm^2 ± standard errors:

	Unspecialised ventral	Specialised ventral
INL	1295 ± 79	5536 ± 128
GCL	132 ± 15	396 ± 33

The specimens used in this study were caught at night from light traps and the pigment epithelium and cones in the specialised ventral area are retracted (Plate I.10A) (in the position typical of a dark-adapted retina (see Plate I.2B) whereas in the unspecialised areas the cones and pigment epithelium are in positions characteristic of a light-adapted retina (Plate I.10B, see also Plate I.2A). The fish would have been exposed to up to 1 hr of light in the traps and further illumination on board ship prior to killing and fixation. Why the two retinal areas should show different extents of light adaptation is unclear but the retinomotor movements of the specialised area may be under endogenous circadian control, such as that recorded in the retina of *Paracheirodon innesi* (Lythgoe and Shand, 1983). From these samples it would appear that the unspecialised area of retina responds to the direct action of light. The orientation of the cones in the two areas also appears to vary with those in the specialised area at an angle oblique to the direction of the light by about 45° and with the outer segments directed in a posterior orientation.

The way the specialised ventral area gives way to the dorsal unspecialised area is unusual and apparently unique to this genus. Plate I.11A - F shows a series of sections moving from the temporal to rostral regions of the retina of *Spratelloides delicatulus*. Fig. I.25 shows from where in the eye the sections were taken. The specialised area gradually becomes displaced towards the sclera, the unspecialised retina begins to appear in a layer in front and a blindly ending pocket is formed in more nasal positions of the eye. The function of the specialised area in the pocket is unclear as it appears to be shielded from light by the unspecialised area. Further investigation into the structure of the clupeid retina needs to carried out at

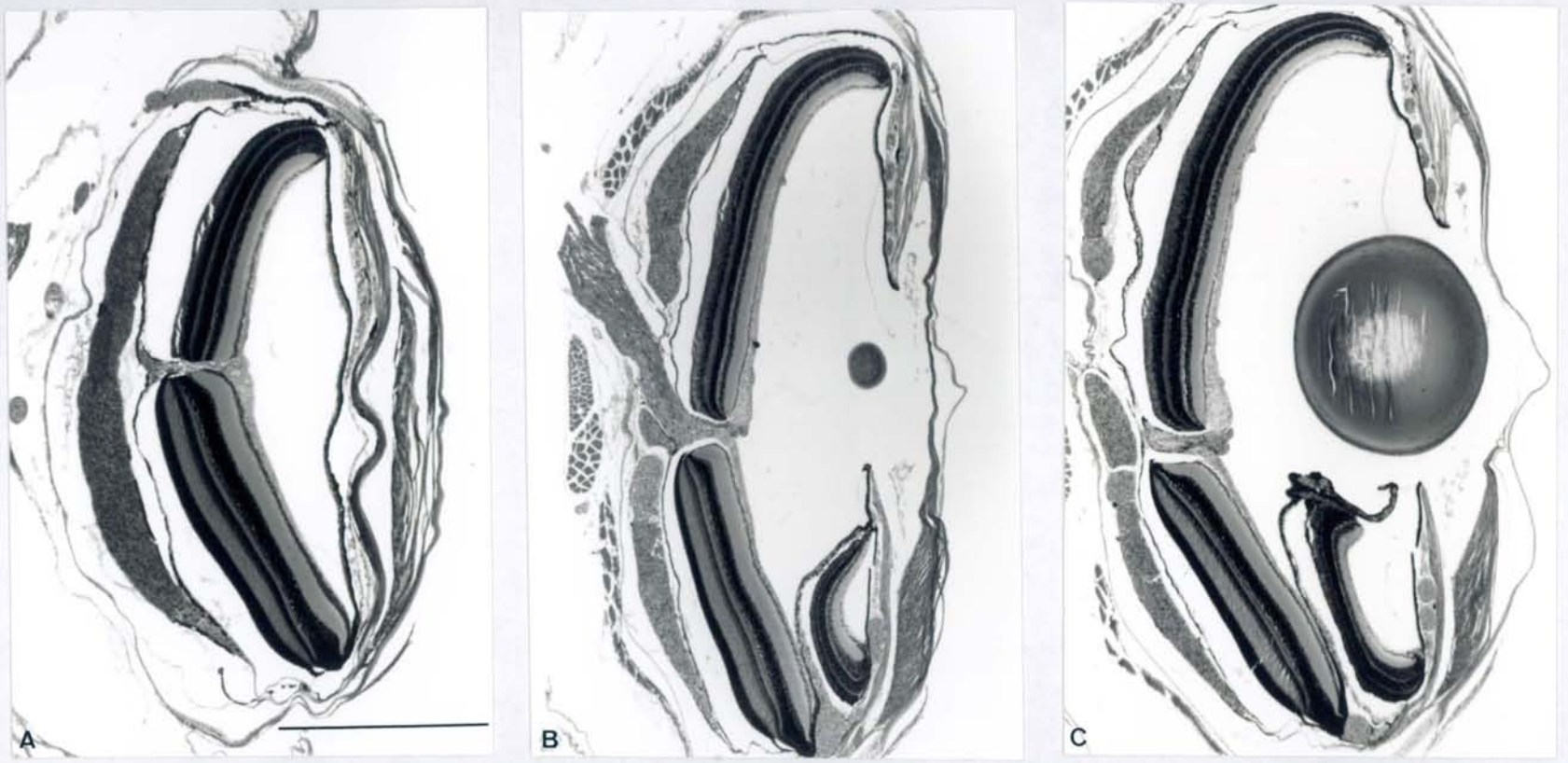

Plate I.11. A series of transverse sections, from temporal to rostral positions, through the eye of *Spratelloides delicatulus* showing the location of the specialised area in relation to the unspecialised area (Fig. I.25 gives details of from where in the eye the sections are taken): **A)** A temporal position with the specialised area ventral to the optic nerve (see Plate I.10A for more detailed view); **B)** the region where the ventral unspecialised area is beginning to extend across in front of the specialised area; **C)** the ventral unspecialised area extends across the specialised area towards the optic nerve exit;

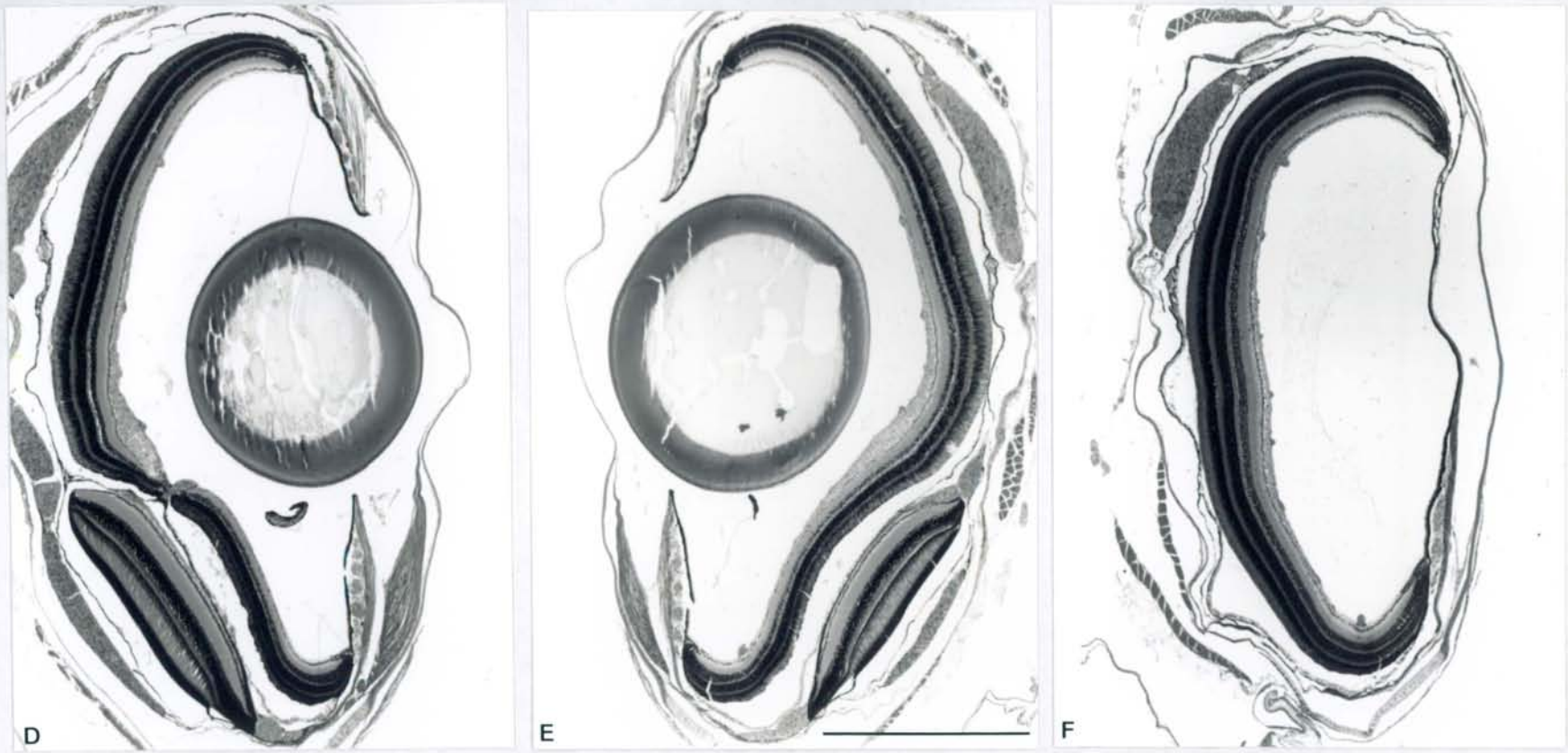

D) the unspecialised retina is continuous with the dorsal retina in this region and the specialised area is located in a sclerad position; **E)** The specialised area is reduced moving from central to rostral positions until it is eliminated; **F)** a rostral region of the eye where the retina is composed entirely of the unspecialised area. Scale bars = 500 μm.

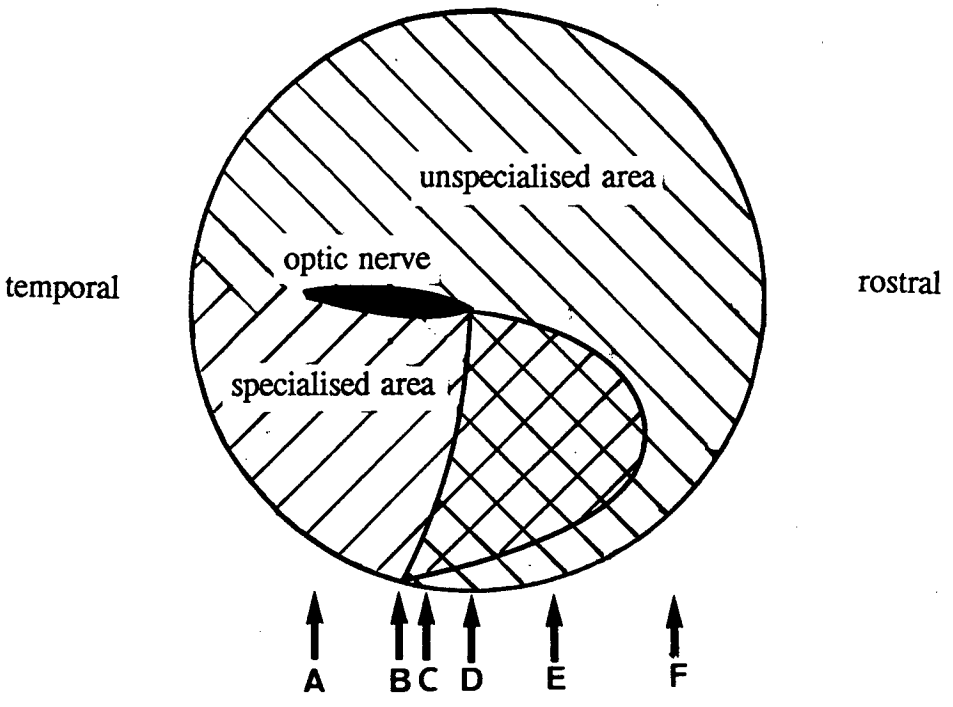

Fig. I.25. Schematic drawing of the eye of *Spratelloides delicatulus*, looking from above with the front of the eye cut away. A pocket is formed where the two areas overlap in the ventro-rostral region. The specialised area is behind the unspecialised area. The positions of the photomicrographs in Plate I.11A-F are shown.

the electron microscope level to clarify the arrangement of the specialised ventral area and its possible functions.

Discussion

In coral reef fish vision is important for both feeding and predator avoidance in coral reef fish and this is particularly true in larval fish. This stage of a fish's life cycle is one of high mortality with smaller larvae being more susceptible to starvation and predation (Hunter, 1981; Miller *et al.*, 1988). The development of the visual system can therefore have direct consequences for survival since both feeding and predator avoidance are visually mediated tasks (Blaxter, 1986). Structural changes in the visual system are discussed here in relation to constraints of small eye size, growth, the behaviour of pelagic larvae and the ecology of the juveniles and adults following settlement.

External morphology

Larval duration and size at settlement varies widely between species although why some should remain pelagic for longer periods than others is not understood (Victor, 1991). The larval pelagic phase is presumed to be one of dispersal. The adaptive reasons for this are a matter of conjecture but include proposals relating to the effects of predation; better survival in a patchy pelagic environment; and energy saving mechanisms (see Leis, 1991a for summary). Whatever the reasons, larval life history is likely to play an important role in determining the distribution and abundance of coral reef-fish populations (Williams, 1980; Doherty, 1983; Victor, 1983; Doherty and Williams 1988).

Of the species investigated in detail in this study, *Stethojulis strigiventer* settled at a very small size (SL, 5.5 mm; eye diameter, 0.6 - 0.7 mm), *Pomacentrus moluccensis, Pomacentrus bankanensis, Ambassis vachelli* and *Apogon doederleini* settled at an intermediate size (SL, 10 - 12 mm; eye diameter 1.2 - 1.5 mm) whereas *Upeneus tragula* settled when much larger (SL 27 mm; eye diameter 2.2 - 2.4 mm). The ages of the fish used in this study were not determined. However, *S. strigiventer* from the Eastern Pacific is reported to spend a mean of

23.4 days in the plankton, but the size ranges of the fish from which these data were obtained were not provided (Victor, 1986). The ages of *P. moluccensis* and *P. bankanensis* at settlement are in the vicinity of 19 days and 18 days respectively (Brothers *et al.*, 1983; Thresher *et al.*, 1989; Wellington and Victor, 1989). *A. doederleini* settles after about 23 days in the plankton (Brothers *et al.*, 1983) and *U. tragula* has a mean age of 31 days and mean SL of 27 mm at settlement (McCormick, 1994). The reason why *S. strigiventer* should be so much smaller at settlement is unclear but it seems that labrids do not feed as effectively as, for example, pomacentrids during their planktonic duration. This is borne out by looking at age and growth data for the labrid *Thalassoma lunare* which after an average of 55 days in the plankton attains a size of only 11 mm SL (Brothers *et al.*, 1983).

The size of the eye has implications for the functioning of the visual system. A small eye can never be of such high resolution as a large eye. This is because resolution of fine detail is affected by a number of physical properties such as diffraction by small apertures, focal length, fineness of the retinal mosaic and optical imperfections of the lens. These parameters are detailed and discussed in Appendix 2. Briefly and of concern here: Matthiessen's ratio, which is the ratio of focal length (assumed to be the distance from the centre of the lens to the retina) to lens radius is about 2.55 in teleosts (Matthiessen, 1882 cited by Fernald 1988). In fact a range of 2.2 - 2.8 has been recorded, but the ratio is thought to be constant within a species (Fernald and Wright, 1983; Fernald, 1990b). This in turn means that the F-numbers of teleost eyes (focal length / aperture diameter, or Matthiessen's ratio / 2) are in the range 1.1 - 1.4. As it has been shown that eyes with F-numbers below 4 are unaffected by diffraction (Kirschfeld, 1976; Land, 1981) (see Appendix 2 for detailed explanation) the small size of the pupils in larval fish is not of consequence to the resolving ability of their eyes. However, increasing the size of the eye (and hence focal length) is of significance to the resolving ability as the magnification on the retina is increased. This means a given image is sampled by a higher number of receptors (assuming the density has remained the same), thus improving the retinal grain. Increasing the density of

receptors will also increase resolution by giving a finer retinal grain. However, there is a limit to the minimum receptor size as below diameters of 1 - 2 μm light begins travel down the outside of the receptors and they can no longer operate independently (Kirschfeld, 1976). Optical imperfections of the lens such as spherical and chromatic aberration have not been found to limit resolution in fish eyes. In fact the resolving power of the teleost lens has been found to exceed that capable of being resolved by the cone mosaic (Northmore and Dvorak, 1979; Fernald and Wright, 1985; see Appendix 2 for explanation).

Sensitivity to low levels of light is governed by aperture size, focal length and receptor size (Land, 1981; see Appendix 2). If Matthiessen's ratio remains constant as the eye grows, the brightness of the image reaching the retina will not increase (Fernald, 1988). To increase sensitivity by optical means, a lowering of the ratio of focal length to aperture size is required during growth of the eye because retinal illuminance is inversely proportional to the square of Matthiessen's ratio (Fernald, 1988; see Appendix 2 for details). Sensitivity can also be improved by increasing the diameter and length of the receptors (Land, 1981).

Unlike mammals and birds, the eyes of teleosts are known to continue their growth into adulthood (Powers and Raymond, 1990). This growth is negatively allometric in relation to body length in the trout i.e. large trout have relatively smaller eyes than small ones (Lyall, 1957). Eye size relative to body length for the species investigated here gave inconclusive results so has not been presented. This may have resulted from to changes in the proportions of the fish over the settlement period. Measurements of the eyes of a number of species investigated here show that both eye size and lens size increase during growth over the size ranges obtained. Comparison of results from four pomacentrid species with similar body shape show that the increase in lens size (and hence eye size) is more rapid for the three planktivorous species than for *Pomacentrus bankanensis*, which is a herbivore (Fig. I.9). Thus an advantage to the planktivorous species in terms of resolution could be obtained.

Ratios of eye to lens diameters give an approximation of Matthiessen's ratio without actually measuring focal length. It is assumed that the eye cup is hemispherical and that the distance from the centre of the lens to the retina is half the eye diameter. Sadler (1973) points out that Matthiessen's ratio relates strictly to the distance between lens centre and retina, and measurements here give an estimation of this distance not the focal length of the lenses themselves. In the smallest fish measured in this study, the estimations of Matthiessen's ratio are variable but with a tendency to be higher than in settled fish. This variability may, in part, result from inaccuracies during measurement of such small eyes. In settled fish, with a lens diameter greater than 1 mm, the ratio begins to stabilise with the exception of *Upeneus tragula*, in which the ratio continues to decrease. However, more measurements from larger fish are needed to confirm this trend. If the relationship between focal length and lens radius remains constant during growth, as has been recorded in fish with lenses greater than 1 mm diameter (Sadler, 1973; Fernald and Wright, 1983), then the small eyes with a high Matthiessen's ratio may be myopic. This has been suggested for small eyes of *Fosterygion varium* in which estimations of Matthiessen's ratio during ocular growth, made from histological sections, were found to decrease from about 2.8 to 2.2 in the 14 days following hatching (Pankhurst *et al.*, 1993). As pointed out by Pankhurst *et al.* (1993) myopia would not be a problem if the accommodative system of the fish were functional, but in very young fish (up to 16 days post-hatching) the suspensory ligaments were not present. Accurate measurements of both focal length and the distance between the centre of the lens and the retina during growth are desirable to establish whether Matthiessen's ratio does change during growth and whether or not the eyes are myopic.

Estimations of Matthiessen's ratio from fish with a lens diameter greater than 1 mm (all fish that have settled) give a range of mean values of 2.3 - 2.6 for individual species. Despite the crude method of estimation, the values obtained are within the range recorded for other teleosts i.e. from 2.2 - 2.8 (Fernald, 1988 for list). The variation between species is not great never-the-less the trend is for the nocturnal species to have lower values (Table I.8). Increased sensitivity may

therefore be obtained by the species with the lower values. McFarland (1991) notes that two nocturnal reef fish *Holocentrus rufus* and *Myripristis jacobus* have ratios of 2.2 and 2.1 respectively. Without detailing his calculations McFarland (1991) states that these ratios would increase retinal illumination by 20 to 22 percent compared with teleosts with the average ratio of 2.55. Using the equation for retinal illuminance given by Land (1981) and modified by Fernald (1988) for teleosts (see Appendix 2 for details):

$$E = (\pi/m^2) \times L \qquad \text{Eqn. I.8}$$

where E is retinal illuminance, m is Matthiessen's ratio and L is luminance of the source, it is calculated that the lowering of Matthiessen's ratio from the average of 2.55 to 2.2 gives a 25% increase in retinal illuminance.

Acuity

Calculations of acuity, made from histological data of cone densities and records of lens size, show a rapid increase in resolving power of the eye (measured by a decrease in the minimum separable angle) during the early stages of growth. The increase in acuity occurs despite the reduction in cone densities over the same period and is, therefore, a result of the longer focal length increasing magnification on the retina. Similar patterns have been observed during the growth of other species e.g. the herring, *Clupea harengus* (Blaxter and Jones, 1967), the perch, *Perca fluviatilis* (Guma'a, 1982), the bluegill sunfish, *Lepomis macrochirus* (Hairston *et al.*), the yellow perch, *Perca flavescens* (Wahl *et al.* 1993). When making comparisons of absolute values with those published by other researchers it is necessary to be aware of the different formulae used to calculate the minimum separable angle as it is possible to obtain values which give half the angular subtense given by the formula used in this study (see Appendix 2 for detailed explanation of different interpretations of the Helmholtz Hypothesis and formulae used). Even so the resolving power reached in the settled fish is not as good as corrected values obtained for other teleosts (e.g. Tamura and Wisbey, 1963; Anctil, 1969; Pankhurst, 1989). This is likely to be a result of the

comparatively small size of fish and hence small eye and lens size of the species investigated. Examination of the data plotted against lens diameter, rather than SL (Fig. I.21) demonstrates how all fish with a similar lens diameter have similar acuity whatever their mode of life. This is especially true during the early stages of development. During these early stages growth of the lens from 0.25 to 1 mm diameter gives an improvement in theoretical MSA of 60 minutes of arc. Growth from 1 to 2 mm lens diameter gives an 18 minutes of arc increase in MSA. Thus rapid growth of the eye at the earliest stages of development is critical. Addition of results, from fish with larger eyes than those used in this study, to the extrapolated curve in Fig. I.22 shows that the highest acuity (lowest values of MSA) are obtained in fish with the largest eyes. Similarly, when calculating acuity from ganglion cell densities, Collin and Pettigrew (1989) noted that species with the highest ganglion cell densities did not have the highest acuity but that acuity varied directly with lens diameter. The curve presented here could be used to give some idea of the acuity range of fish with eyes of a particular size. However it should be noted that a single value for Matthiessen's ratio has been used in all these calculations and as discussed above the ratio may in fact vary between species and during growth. The effects of a variable Matthiessen's ratio have not been quantified. In addition the role of paired cones needs to be established. In this study it is assumed that both members of a pair sample the same image space and a pair is considered to be a single unit as suggested by (Northmore and Dvorak, 1979). However Wahl *et al.* (1993) have suggested that during early development, paired cones may function independently. If this turns out to be the case then the finer retinal grain obtained as a result would increase acuity. Similarly, improvements to acuity, at a given eye size, can be obtained at the level of the retina by areas of high cone density such as those observed in *Stethojulis strigiventer* and *Spratelloides delicatulus*. Areas of high cone density are known to correspond to the main visual axis (Browman *et al.* 1990) as are areas of high ganglion cell density (Collin and Pettigrew, 1988a,b).

In many adult teleosts, good agreement has been found between behavioural and morphological estimations of acuity (Yamanouchi, 1956; Muntz, 1974; Douglas

and Hawryshyn, 1990) but where a discrepancy has been found it has been suggested that convergence to ganglion cells is a limiting factor (Browman *et al.*, 1990). Measurements of acuity obtained from behavioural experiments with larvae have however found a mismatch with that estimated from histological data. The behavioural estimates usually give poorer acuity results (Neave, 1984; Miller *et al.*, 1993; Pankhurst *et al.*, 1993). This may be because of incomplete differentiation of the optic tectum (Rahmann *et al.*, 1979; Neave, 1984; Schmitt and Kunz, 1989) or myopia of larval eyes (Pankhurst *et al.*, 1993). Thus it should be remembered that the theoretical calculations of visual acuity give an estimate of the potential acuity an eye could reach. However it is only behavioural experiments that will provide a measure of the performance of the whole visual system that includes optical, accommodative and neurological factors.

Owing to starvation and predation, the larval stage of fish is the time when greatest mortality occurs. Thus, feeding and predator avoidance are the most important visually mediated tasks facing larvae (Hunter, 1981). At first feeding, capture of prey items occurs over short reaction distances (up to one body length) and is of limited success with only small prey being caught (e.g. Blaxter and Staines, 1971). This will also be a function of swimming muscle and mouth part development. However, an increase in visual acuity will allow for an increased search area by detection of small prey items at greater distances. McFarland (1991) shows how the decrease in minimum separable angle during growth of *Thalassoma bifasciatum* allows a 13-fold theoretical increase in the search volume for prey of a given size. Indeed, an increase in the reaction distance and rate of encounter with prey during growth has been shown experimentally for a number of species (Blaxter and Staines, 1971; Hairston *et al.*, 1982; Breck and Gitter, 1983; Wanzenböck and Schiemer, 1989). Similarly, an increase in predator avoidance has been demonstrated during ontogeny (Margulies, 1989; Batty, 1989; Blaxter and Fuiman, 1990).

Iridescence and pigmentation of the cornea

The phenomenon of corneal colouration, either from yellow pigments or structural iridescent colours, is present in a number of diurnal coral reef fish (Muntz, 1976; Lythgoe, 1971, Shand, 1988). The phenomena may be a result of phylogenetic trends as the visual significance is not always clear. However, it has been suggested that yellow corneas could help to reduce chromatic aberration (Muntz, 1976) and iridescent corneas could reduce intra-ocular flare in bright light conditions (Lythgoe, 1975). The fact that some species are able to "turn off" the colouration in low light intensities supports this (Orlov and Gamburtzeva, 1976; Appleby and Muntz, 1979; Shand and Lythgoe 1987; Shand, 1988)). Yellow corneas and lenses (ignoring those of some deep-sea fishes) and iridescent corneas are most common in diurnal and benthic dwelling species and are rare in nocturnal and pelagic fishes. Of the species investigated here only the labrids and scarids were found with coloured corneas and the colouration was present in the smallest fish examined. Labrids and scarids able to alter the colouration of their corneas have not been found (Shand, 1988). The presence of a coloured cornea may effect the feeding efficiency of these fish when in the pelagic environment.

Retinal Morphology during Growth and Settlement

The larvae of most diurnal teleosts have been found to hatch with cone dominated retinae e.g. herring, *Clupea harengus* (Blaxter and Jones, 1967; Blaxter and Staines, 1970); goldfish (Johns, 1982); zebrafish, *Brachydanio rerio* (Branchek and Bremiller, 1984); rainbow trout, *Salmo gairdneri* (Schmitt and Kunz, 1989); *Forsterygion varium* (Pankhurst *et al.*, 1993). Exceptions to this pattern include the presence of a well developed duplex retina in the viviparous guppy *Poecilia reticulata* (Kunz *et al.*, 1983) and rods only in the leptocephalus larvae of the eel *Anguilla anguilla* (Pankhurst, 1984). Rod densities increase from continual mitotic activity within differentiated areas of retina (Scholes, 1976; Sandy and Blaxter, 1980; Johns and Fernald, 1981; Johns, 1982; Fernald, 1989b). Cones and

ganglion cells decrease in density as the eye expands, presumably because the rate of cell neurogenisis at the retinal margins does not keep pace with the stretching of the retina (Lyall, 1957; Ali, 1964; Johns and Easter, 1977; Kock, 1982; Powers and Raymond, 1990). This sequence of events was also found here in the newly hatched diurnal planktivore *Pomacentrus amboinensis*. The cones are clearly visible at hatching but it is two days before the rods appear and the melanin of the pigment epithelium increases in density to become functional.

Larvae of all species investigated were found to have similar and high cone densities but the rate of reduction in density and value at the asymptote varied between species. In the species that settle at small and intermediate sizes the reduction in cone densities begins prior to settlement. The turbid water and nocturnal species, *Ambassis vachelli* and *Apogon doederleini* respectively, having the greatest reduction in numbers while the diurnal species, *Pomacentrus moluccensis* (a planktivore) and *Stethojulis strigiventer* (a microcarnivore) maintained the highest densities. Records from the larvae of the herbivore *Pomacentrus bankanensis* were not obtained but settled fish were found to have intermediate cone densities. Sampling prior to settlement was limited in fish that settled at small sizes so *Upeneus tragula* is the only species in which the cone densities show a distinctive pre-and post-settlement pattern. Of all the species sampled the blenny, *Meiacanthus grammistes* (a microcarnivore) was the only species in which cone densities were found to increase following settlement.

The rate of addition of rods in the different species also varies from an early age. The nocturnal species have the greatest rate of addition while the densities of rods in the diurnal species remains low. The rod densities of *Upeneus tragula* increase in line with those of the nocturnal species. This appears at variance with its diurnal lifestyle however it is possible that the high densities in this species are in preparation for life in deep (20 - 30 m) water where there will be less light. Differences in the rate of addition of rods have been found between three hake species inhabiting different depths, with the deepest living species having the highest rod densities (Mas-Riera, 1991).

Rates of change of cells in the inner nuclear layer and the ganglion cell layer also vary with species. However, when the ratio of cones to cells in the inner nuclear layer (INL) is examined it appears that the rates of reduction of cones and INL cells occur in proportion to each other so that a constant ratio is maintained. This is the situation in all species with the exception of *Upeneus tragula*. This is not the case with the ratios of rods to cells in the INL. The nocturnal species have an increase in the summation of rods to INL cells as rod densities increase during growth. The summation of rods is likely to increase the sensitivity of nocturnal retinae (Powers and Easter, 1978). The ratio of cones to ganglion cells tends to increase with growth in all species and is greatest in the nocturnal species. This is also true for the amount of rod summation to ganglion cells. The high summation of rods to ganglion cells may also be a means for increasing sensitivity in the nocturnal species. The high densities and low summation of cones to ganglion cells in the retinae of the youngest fish of all species may be an advantage as far as resolution is concerned, when the constraints of a small eye make acuity inherently poor.

The rate at which cone densities decrease and rod densities increase during early development appears to be influenced by the subsequent lifestyle of the settled fish. The differences between the presumptive nocturnal and presumptive diurnal species therefore begin early in the species that settle at small sizes. *Upeneus tragula* which remains pelagic until well developed (McCormick, 1992), does not follow this pattern.

Upeneus tragula

At the time of settlement *Upeneus tragula* undergoes a metamorphosis in body shape, skin pigmentation and barbel growth within a period of 6 - 12 hrs, following which the mode of feeding switches from planktivorous to benthic with the aid of sensory chin barbels (McCormick, 1992; 1993). Cone densities in this fish remain high until settlement and the bipolar cell densities actually increase

until settlement. These features of the pre-settlement fish are not size dependant as the changes are only initiated when metamorphosis to the benthic mode of life begins. The decrease in cone density is probably brought about by a reduction in the number of new cells being added at the retinal margins and an increase in the inter-cone spacing resulting from stretching of the retina beginning at the time of settlement. In addition, some of the single cones appear to be lost from the cone mosaic. It is possible that the high cone densities are maintained in the retina of pre-settlement fish as an adaptation to planktivorous feeding. Investigations of retinal topography in a number of species have found correlations with foraging ecology. For example the zooplanktivorous fish *Pomoxis annularis* has higher cone densities in an area of visual field corresponding to its search and pursuit axis (Browman *et al.*, 1990). In addition, behavioural evidence for the capture of smaller prey by fish with higher acuity has come from the study of the development of the sunfish *Lepomis macrochirus* (Hairston *et al.*, 1982).

Cones of the dorsal retina of pre-settlement *Upeneus tragula* are found to be arranged in a double layer, which slot together to form a single layer at the time of settlement. The functional significance of this is unclear. Displacement of cone inner segments from a single layer have been found in a number of fish, and it has been suggested that they could form a mechanism for overcoming longitudinal chromatic aberration of the lens (see Appendix 2 for an explanation of the effects of chromatic aberration) (Eberle, 1967, 1968; Scholes, 1975; Fernald and Wright, 1985). A number of measurements of chromatic aberration in fish lenses have now been made (Fernald, 1990b for list) and these are found to vary between 2 and 5% of the focal length at the C and F Fraunhofer lines (485 and 656 nm respectively). Eberle (1968) proposed that if longer cones were sensitive to longer wavelengths, compensation for chromatic aberration could be achieved, and claimed this to be the case in the guppy *Lebistes reticulatus*. However, measurements from the retina of the rudd (Scholes, 1975) and a cichlid (Fernald and Wright, 1985) do not show the cones of these fish to be displaced a sufficient distance from each other to compensate for longitudinal chromatic aberration.

In *Upeneus tragula* the base of the outer segments of the single cones comprising the vitread layer are 13-14 μm vitread to the double cones of the sclerad layer in fish of 20 mm SL. This distance increases to 16-17 μm in 30 mm SL fish. Microspectrophotometric measurements of the individual cones of *U. tragula* indicate that the single cones of the pre-settled fish are absorbing at wavelengths of less than 400 nm, whereas the double cones of the sclerad layer have their maximum absorption at wavelengths of 480 and 580 nm (Shand, 1993, Appendix 5; see Part II). Using the curve given by Sroczyński (1976) for longitudinal chromatic aberration in the rainbow trout (a fish with 3% chromatic aberration between 485 and 656 nm), it is possible to obtain an estimate of chromatic aberration between 400 nm and 480 nm. Expressed as a percentage of focal length this gives 4.5%, which is equivalent to approximately 36 μm and 55 μm in 20 mm and 30 mm SL fish, respectively. Thus the displacement of cones into the two layers does not provide enough distance between the single short-wavelength absorbing cones and the double cones absorbing at longer wavelengths to compensate adequately for the differences in focal plane resulting from chromatic aberration.

Retinal specialisations and ecological correlations

Investigations of the retinal structure of a range of larval fish and pelagic species have not found a layering of the cones as in *Upeneus tragula* (this study; Ali and Anctil, 1976). The double layer in *U. tragula* only becomes evident at eye sizes of 1.5 mm and greater and the larvae of the other species are settling at sizes similar to this. The only other fish sampled, that settles at a large size, is *Neoniphon sammara*. However a detailed investigation of a size range did not take place. This becomes nocturnal following settlement and has high numbers of rods both prior to and following settlement. The cone densities, in particular in the ventral retina, in the pre-settlement fish are high but decline in recently settled fish.

Spratelloides delicatulus is a pelagic planktivore that looks similar and schools like pre-settled *Upeneus tragula* but no evidence of a double layer of cones was found in this species. In fact *S. delicatulus*, in common with other clupeids, shows a remarkable arrangement in its ventral retina with a highly specialised area of cones in the ventral-temporal retina. It has been suggested that area provides high acuity and is an adaptation to catching prey by looking up and silhouetting items against brighter spacelight from the surface (Engstrom, 1963; Blaxter and Jones, 1967; Wagner, 1990). *U. tragula* does not possess such a specialised ventral retina although cone densities are higher than in the dorsal retina. The retina of the garfish, a surface dwelling species also has distinct differences between dorsal and ventral areas.

The scarids examined here have low cone and high rod densities, at all sizes examined, compared with the labrids. This occurs despite similarities in their behaviour during the early juvenile phase. Scarids, like labrids, settle at small sizes and are initially microcarnivores (Bellwood, 1988; Bellwood and Choat, 1989). However their diet progressively changes to one of herbivory. Of the labrids examined, *Stethojulis strigiventer*, remains a microcarnivore and *Thalassoma amblycephalum* is a planktivore. Thus it would appear that the visual system of scarids is not particularly well suited to their early settlement feeding behaviour, however they do possess a specialised area of high cone density which could aid detection of small prey items. Further investigation of feeding success and growth rates, combined with examination of retinal structure, of the two families during the early post-settlement period would be of interest. The low rod densities of all labrids suggest low sensitivity in these species. This observation coincides with the behaviour of labrids at dusk when they are one of the first groups of fishes to leave the water column to take up hibernation for the night (Hobson, 1965; 1972).

The position of different larval species in the water column is known to vary (Leis, 1991b) and may also reflect the differences in retinal structure. For example those species with higher rod densities (and thus greater sensitivity) may

occur in deeper water. More detail on the behaviour of larvae is required to confirm this. Similarly the attraction of a selective size range of selective species to light traps (Victor, 1991; Choat *et al.*, 1993, McCormick and Milicich, 1993) may be affected by the stage of development, and density, of rods in the retina. Of note, pomacentrids, apogonids and holocentrids, that are commonly attracted to light traps, all have a well developed duplex retina at the stages they are caught. A functional divergence of rods and cones is known to occur in zebrafish larvae when an increase in sensitivity corresponds to a dramatic increase in rod outer segment length (Brancheck, 1984).

In summary, small eyes give poor acuity but high cone densities and their low convergence ratios to neural cells may compensate when the focal length is limiting. The distinctive environmental changes at settlement have consequences for the development of the retina of fish that settle at small sizes (i.e. eyes below 1.5 mm diameter). Interspecific variation in development of the retina begins prior to settlement and is apparently influenced by the lifestyle the fish will adopt as an adult. The fact that these species are settling at small sizes meant that sampling prior to settlement was limited. It would seem that as the eye grows and the changes are occurring in anticipation of, and preparation for, their post-settlement existence. Following settlement the divergence of the "retinal types" continues as the eyes of the juveniles increase in size and the fish take up their different lifestyles. The very small size of settlement of *Stethojulis strigiventer* may also be influenced by the presence of coloured corneas, which are not thought to be suited to a pelagic mode of life, however further investigation into the eyes of other species with iridescent corneas needs to be carried out to substantiate this. In contrast, the mullid, *Upeneus tragula* which remains pelagic until a later stage of development does not show distinctive changes during early development but undergoes rapid changes over the settlement period. This indicates a visual adaptation to the pelagic environment is necessary to sustain a late-stage pelagic existence. However, the exact significance of the double layer of cones in pre-settlement mullids has yet to be determined.

PART II

Microspectrophotometry of Visual Pigments

Introduction

The outer segments of the retinal photoreceptors of vertebrates contain photolabile pigments known as visual pigments. It is these pigments that absorb photons of light and so begin a series of events that ultimately lead to a signal sent via the optic nerve to the brain. In large measure, it is the ability of these pigments to absorb light of different wavelengths selectively that governs the spectral sensitivity of an animal. Light with wavelengths not absorbed at this stage plays no part in the visual process. Early workers predicted that in the photon-limited environment of the deep-sea, the rods of fish would contain a visual pigment sensitive to the narrow band of wavelengths transmitted (Clarke, 1936; Bayliss *et al.*, 1936). The discovery that this was the case (Denton and Warren, 1957; Munz, 1958) marked the beginning of investigations into the ecological significance of the spectral location of visual pigments. The visual pigments of fishes have continued to be examined, mainly because of the extensive and diverse range of habitats in which fishes are found and to the natural variation in the colour of light underwater.

Pure water is blue, having a maximum transmission (minimum attenuation coefficient) in the region of 460 nm (Jerlov, 1976). This property is unaffected by dissolved salts (Morel, 1974). Because the attenuation coefficient is small the blue colour is only obvious for long path lengths. However, natural bodies of water are rarely pure. Varying amounts of chlorophyll in phytoplankton and dissolved organic matter from the breakdown products of plant decay (yellow substances or Glebstoff) affect the absorption characteristics and shift the maximum transmission to longer wavelengths. So, for example: oceanic water is blue, transmitting most strongly between 470-490 nm; coastal water is green, transmitting in the region of 520-550 nm; and freshwater peat stained lakes and rivers are yellow-red sometimes best transmitting wavelengths as long as 600 nm (Jerlov, 1976; Baker and Smith, 1982; Lythgoe, 1988). Absorption of light with increasing path length is an important factor in determining the colour of water and the spectrum available for vision. In shallow water (less than 0.5 m) of any

type there is little absorption and the spectral qualities of downwelling light are similar to those of the terrestrial situation with both ultra-violet (less than 390 nm) and far red (600 to 700 nm) wavelengths present. However, with increasing depth the light is progressively and selectively absorbed causing a narrowing of the bandwidth of transmitted light (Jerlov, 1976). The greatest rates of change of attenuation coefficients occur below 400 nm and above 600 nm. The wavelengths of maximum transmission, and the depth to which visibly useful amounts of light penetrate are determined by the quantities of phytoplankton and dissolved organic matter present (Dartnall, 1975). It is also necessary to consider the passage of light in horizontal directions when discussing vision as the colour of the background spacelight will differ from that of the downwelling light. This is because it is derived from light that has travelled a longer path through water than the downwelling light and hence has been subject to more absorption. In addition, scattered light (that deflected from its original path by suspended particles) will reduce visibility over short distances by degrading the contrast of an image in the same way that fog degrades contrast in the terrestrial environment. Scattering of light does not have any effect on the overall colour of the water. However it is highly dependant on wavelength, with short wavelengths being scattered most by large particles (Mei scattering, proportional to $1/\lambda$) and by particles of a size similar to the wavelength of light (Rayleigh/Tyndall scattering, proportional to $1/\lambda^4$). As a result ultra-violet images are quickly degraded implying that ultra-violet vision will only be useful over short ranges. Detailed discussion of the effects of both absorption and scatter of light underwater in relation to visual tasks is provided by Lythgoe (1979; 1988), Loew and McFarland (1990) and Partridge (1990).

The possession of visual pigments that enhance the contrast of objects against the background will be beneficial in the aquatic environment (Lythgoe, 1966; 1968; 1979; Munz and McFarland, 1973; 1977). Considering a grey target, the ways in which this could be achieved would be to 1) have a visual pigment matched to the background so making the target appear darker than the background, or 2) have a visual pigment absorbing at wavelengths offset from those of the background and

so increase the contrast by making the target appear brighter than the background (Loew and Lythgoe, 1978; Lythgoe, 1979). A combination of three pigments, one matched to the background spacelight, one offset to longer wavelengths and one offset to shorter wavelengths could then be the best system for covering a variety of visual tasks (Loew and Lythgoe, 1978; Lythgoe, 1979). It is even possible that the foundations for the evolution of colour vision were set by combinations of visual pigments originally selected to maximise contrast in the aquatic environment (McFarland and Munz, 1975a; Munz and McFarland, 1977).

The visual pigments of rod outer segments were the first to be investigated as they, unlike cone pigments, could be easily obtained by extraction techniques using solvents such as digitonin. It has now become evident that, while fish from clear blue water and the deep-sea have rod visual pigments well suited to absorb the predominant wavelengths of ambient light, coastal and freshwater fishes do not necessarily have rod pigments that confer maximum sensitivity in the respective water types (Denton and Warren, 1957; Munz, 1958; Lythgoe, 1968; 1979; Lythgoe *et al.*, 1994; Munz and McFarland, 1973; Crescitelli *et al.*, 1985; Partridge *et al.*, 1988; 1989). The wavelengths of maximum absorption (λmax) of the rods of coral reef fishes lie between 480 and 502 nm, with the deeper living species having the more blue sensitive (shorter wavelength) pigments and the shallow living species the longer wavelength pigments (Munz and McFarland, 1973). It is argued that this range of rod λmax values would confer optimal photon capture along all lines of sight during twilight (Munz and McFarland, 1973; 1977; McFarland, 1991), a particularly vulnerable time on the reef for potential prey species (Hobson, 1972). However, the rods are certainly poorly matched to the predominant wavelengths of the ambient light during much of the day. This mismatch between ambient spectral irradiance and the λmax values of rods is greatest in freshwater fishes, with the longest λmax of rod pigments being at about 540 nm but with wavelengths of maximum ambient light extending to 600 nm and beyond in some bodies of water (Lythgoe, 1988). This anomaly could be a result of phylogenetic constraints. Alternatively, it could be that spontaneous isomerizations resulting from thermal excitation are greatest in long wavelength

pigments (Barlow, 1957; Aho *et al.*, 1988). Since rods usually function in a photon-limited situation such isomerizations might be indistinguishable from the light signals and hence introduce noise to the system (Lythgoe, 1984; 1988).

Cones, being involved in photopic vision, are, in most animals, the photoreceptors responsible for wavelength discrimination and thus also provide the potential for colour vision. Several morphological types of cone are found in the retinae of fishes (see Part I). Although cone visual pigments can now be extracted using solvents the purification of mixed pigments is difficult and, as a result, the technique by which the λmax of these pigments has to be determined is that of microspectrophotometry (MSP) (Liebman, 1972). This technique involves the measurement of the spectral absorption of individual outer segments and so also provides information about the relationship between λmax and cell type. It has been found that there are usually two or three different cone visual pigments in the retinae of fishes although up to six have been found (Partridge, 1990). These pigments can have a λmax range from the ultra-violet to the far-red (Bowmaker, 1984). In general, ultraviolet and blue absorbing visual pigments are found in single cones and the double cones have pigments absorbing at longer wavelengths (Bowmaker, 1990). Several MSP surveys of the visual pigments of cones of fishes from different habitats have been carried out (Loew and Lythgoe, 1978; Levine and MacNichol, 1979; Lythgoe *et al.*, 1994) and these show that double cones are likely to have visual pigments with the λmax related to the spectral qualities of the ambient light. In collating data from the early surveys Lythgoe (1984) showed that deeper-living fish have a narrower spectral range of visual pigments and more blue-sensitive visual pigments than shallow living species. In fact, when comparing the visual pigments from terrestrial species with those of very shallow fresh water and coastal marine fishes, there appears to be very little difference in the location of the pigments in the spectrum (Lythgoe and Partridge, 1989).

It is known that some fish have the ability to alter the λmax of their visual pigments prior, or in response, to changes in habitat and depth. The eel (*Anguilla anguilla*) undertakes breeding migrations from the rivers of Europe to the depths

of the Sargasso Sea. It alters the λmax of the rod pigment to that of a 'deep-sea' blue-sensitive pigment prior to leaving the rivers (Carlisle and Denton, 1959). A reverse of this pigment shift has been found in the elvers as they enter fresh water from the sea (Wood *et al.*, 1992). Seasonal changes in spectral sensitivity have been found in the trout, *Salmo trutta*, when it moves between shallow water in the winter and deeper water in the winter (Muntz and Mouat, 1984). Changes in sensitivity of the cones of rudd, *Scardinius erythrophthalmus*, have been found in response to changing daylength and it is thought this could be a mechanism for dealing with seasonal changes in turbidity (Whitmore and Bowmaker, 1989 for review and resent investigation). Changes in visual pigment λmax that occur during the early life history of fishes have been correlated with changes in both preferred depth and feeding behaviour. For example the loss of a class of short wavelength absorbing cones has been reported for juvenile trout (*Salmo trutta*) and perch (*Perca flavescens*) when the fish move to deeper water and cease feeding on plankton (Bowmaker and Kunz, 1987; Loew and Wahl, 1991 respectively). Similarly, changes in the spectral absorption of short wavelength cones have been reported in the juvenile pollack in which the λmax of the single cones gradually shifts from 420 to 460 nm at a time when the fish are moving to deeper water and beginning to take larger prey (Shand *et al.*, 1988).

There are surprisingly few MSP studies of tropical marine reef fish. This may be because many diurnal coral reef fish have very small photoreceptors which make accurate measurements hard to obtain. Many of the diurnal coral reef species examined histologically in this study have small cones. However, mullids, which show unusual structural changes in the dorsal retina at settlement (see Part I) have cells of sizes that lend themselves to MSP investigation. This together with the temporary siting of an MSP at the Australian Institute of Marine Science (AIMS), provided an opportunity to study the visual pigments of *Upeneus tragula* at various times prior to, during and following settlement. The results of this specific investigation, together with the results from four additional species which were examined at the same time, and considered to be relevant to the discussion, are included in this section.

Materials and Methods

Study species

The species investigated by MSP are the goatfishes *Upeneus tragula* and *Upeneus moluccensis*, the glass perchlets *Ambassis vachelli* and *Ambassis nalua* and the garfish *Hemirhamphus* sp. For details of the methods and locations of capture see Part I, Table I.1, Fig. I.5. Pre-settlement *U. tragula* were caught at Lizard Island, from where they were transported to the Australian Institute of Marine Science (AIMS), Townsville, within a day of capture. The wild-settled *U.tragula* were transported to Monash University, Melbourne, because at the time these fish became available the MSP had been moved from AIMS. All other species were caught in Townsville waters and could be directly investigated. All fish not used on the day of capture were maintained in a natural light regime and fed on live *Artemia* sp. or chopped fish muscle.

As individual pre-settlement *Upeneus tragula* began to obtain skin pigmentation and settle to the bottom of the tanks, they were separated and the length of time between settlement and MSP investigation recorded. Settlement of all fish occurred within 10 days of capture, so that pre-settlement fish were the first to be used for MSP. Partially-settled fish (incomplete skin pigmentation) were next investigated, followed by those settled from 3 to 23 days.

Preparation of material

Retinal material was prepared at least 2 hr after dark adaptation of the live fish. This was particularly important with pre-settled *Upeneus tragula* as failure to do this resulted in large amounts of screening pigment remaining attached to the outer segments, which frustrated the measurement of the visual pigments. Fish were decapitated, the eyes removed and the retinae dissected out of the eye cups.

Dissection of the eyes was carried out under infra-red (IR) light (Kodak Wratten 87c IR-pass filter in front of a tungsten light source) using an IR image converter. A 1-2 mm^2 piece of retina, or in the case of the small eyes of *U. tragula* as much of each retina that could be obtained, was transferred to a drop of Dulbecco "A" calcium-free phosphate buffered saline (pH 7.3) containing 10% dextran (RMM 250) and diluted to 341 mOsm/Kg, on a microscope coverslip. The tissue was teased apart, covered with a second coverslip and the edges sealed with paraffin wax. This preparation was then transferred to the stage of the microspectrophotometer (MSP).

The microspectrophotometer

The single beam wavelength scanning MSP was set up at AIMS during 1989. A full description of the equipment, its use, and the analysis of visual pigments has been given by Partridge *et al.* (1992, see Appendix 5). Briefly: the measuring beam from a quartz-halogen light source is imaged into the plane of the specimen mounted on a micrometer-controlled stage. This is achieved via a 0.1 m F/3.5 holographic grating monochromator, a rotating film polariser and variable rectangular aperture, a series of lenses and a Zeiss Ultrafluar objective (x 32, NA 0.4). A Zeiss Neofluar objective (x 100, NA 1.3) objective above the specimen then images the monochromatic measuring beam onto the photocathode of a photomultiplier, the signal from which is converted to a pulse stream by a voltage\frequency converter. The frequency of the pulse stream is measured by a fast counter-timer board installed in the IBM/PC/XT microcomputer which controls the instrument. Wavelength calibration was regularly checked against didymium and holmium oxide filters and was estimated to be accurate to +/- 1 nm. To view the specimen and measuring beam a sliding prism can redirect the image formed by the Zeiss Neofluar to an IR sensitive video camera. The specimen is illuminated by far-red light from a tungsten light source in combination with an IR-pass filter (Kodak-Wratten 87c). The measuring beam, when the monochromator output wavelength is greater than c. 500 nm, and the

retinal preparation can then viewed on a video monitor. Measurements of the dimensions of the photoreceptors were made using an acetate overlay, marked with a calibrated scale, that could be aligned against the cells on the monitor.

To make spectral absorbance measurements the measuring beam was focussed (at 750 nm) in an area close to the outer segment to be sampled and a baseline scan was made at 1 nm intervals between 750 nm and 390 nm. The outer segment is then moved into the path of the measuring beam, with the *e*-vector of the polarised light orientated perpendicular to the long axis of the outer segment, and scanned over the same wavelength range. Bleaching of visual pigment during measurement was negligible. Data from both scans was stored on disc for subsequent analysis. Software controlling the MSP, the logging of data, its analysis and template generation was written in Microsoft QuickBASIC.

Analysis of visual pigment scans

The analysis of the data was carried out by the following procedure: The absorbance (A) was calculated from the baseline (B) and sample (S) scans as:

$$A(\lambda) = -\log_{10} (S(\lambda) / B(\lambda)) \qquad \text{Eqn. II.1}$$

and this was then normalised as a percentage of maximum absorbance (optical density). To obtain a value for the wavelength of maximum absorption (λmax) of each sample scan, a rhodopsin template was fitted to the normalised data. The template used was derived from the absorbance spectrum of bovine rhodopsin transformed on a scale of λmax/λ (Partridge and De Grip, 1991). To fit the template it was "moved" mathematically to intersect each data point on the long wavelength limb of the curve between 30% and 70% maximum absorbance. This provides a series of estimates of the λmax of the curve from which a mean and standard error can be obtained. A print-out of each normalised scan, together with the best-fitting rhodopsin template, was then obtained. This also contained relevant file information and details of the template-fitting statistics. An example of a print-out is shown in Fig. II.1. Records of individual scans and their λmax

FILE INFORMATION

File name	ambas 35		
Date of Experiment	19 oct 89		
Experiment Number	13		
Sample	glass perchlet		
Description	Adult		
Comments	rod		
High Tension Voltage	667		
Wavelength limits and Step	390 nm	750 nm	1 nm
19-Point Running Average LMax	510		

RHODOPSIN TEMPLATE

Mean Lambda Max	508.157
Standard Deviation	3.8184
Standard Error	0.7488
Maximum Corrected OD	+6.2050E-02
Longwave Offset OD	-1.1230E-03

Lmax Estimation from Longwave gradient:-

Lmax (Constant = 0.9131008)	507.862
Gradient of longwave limb (1/THz)	0.1316E-01
Number of valid points	26
Wavelength of 0.5 Max absorbance	556.195
Q value	7.0966

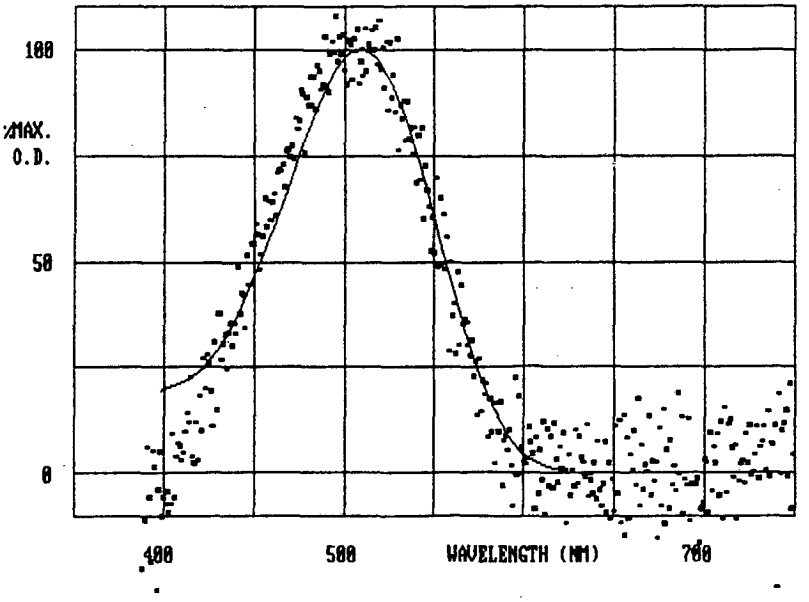

Fig. II.1. An example of the print-out obtained for each sample scan. The sample scan has been corrected and normalised and is presented as a percentage of the maximum optical density (O.D.). The continuous line represents the best fitting template, obtained as detailed in the text. The statistics for the accuracy of the fit are given under "Rhodopsin template". The "Lmax estimation from the longwave gradient" gives the statistics obtained when following the template fitting method of MacNichol (1986), results of which are provided for comparison only. For details of this procedure see MacNichol (1986).

were accepted only if the template-fitting met certain selection criteria. The criteria were: 1) the best-fitting template curve fell within the scatter of data points on the long wavelength limb; 2) the maximum was well defined; 3) the absorbance spectrum was flat for 100 nm beyond the wavelength at which the long wavelength limb first fell to an absorbance of zero. The rejection of unreliable curves is necessary to prevent over estimation of λmax variability (Levine and MacNichol, 1985). Accepted scans were used to determine visual pigment classes and to obtain average scans for each particular class. For presentation of the averaged scans, the corrected and normalised data were imported into Sigma Plot Scientific Graphing System (Jandel Corporation) together with the data for the relevant template. The specific λmax for the required template was obtained from the analysis procedure given above (presented on the print-outs), but the templates displayed in the figures were generated by a Chebyshev polynomial. This polynomial models the template derived from bovine rhodopsin (Partridge and De Grip, 1991).

Statistical analysis of λmax variation of rod photoreceptors between the four different stages of development of *Upeneus tragula* was performed using ANOVA. The mean λmax for each class of visual pigment found in the cones of *U. tragula* was calculated for individual fish and the averaged cone scans were obtained by combining all scans of a particular class, from all fish within each stage of development. Averaged scans for the other species were obtained by averaging the cells in each class of visual pigment.

Results

Upeneus tragula

Cell types

Preparations of retinal material from fish of all stages usually contained rods, single cones and double cones of a variety of sizes. The diameter of the rod outer segments (os) measured between 1.5 to 2 μm, but measurements of their lengths were not made as it was unclear whether they had been broken during preparation. In pre- and partially-settled fish there were single cones of two different sizes: Small, with base of os diameter and length of os 1-1.5 μm and 5-8 μm respectively; and large, 2.8-4 μm and 10-15 μm respectively. Similarly, two sizes of the double cones were found: small, with dimensions similar to the singles, and large with dimensions of 2.8-4.5 μm by 10-20 μm. The dimensions of the large cone outer segments of the aquarium-settled fish were smaller than in pre-settlement fish, the singles being 3-4 μm in diameter and 6-9 μm in length while the double cones were 3-4 μm by 6-12 μm. However, the double cones of the wild-settled fish were larger with a diameter of 3-5 μm and length of 12-17 μm. The differences in cone dimensions in pre-settlement fish are suggestive of the area of retina from where the cones originate. Histological examination of *Upeneus tragula* retina shows high densities of small cones in the ventral retina and lower densities of large cones located in the dorsal retina (see Part I).

λmax records

Scans of all types of photoreceptor were attempted but the small dimensions and low absorbance of the small cones led to noisy scans so that many of these records did not pass the selection criteria and were rejected.

Rods: Measurements of λmax obtained from individual rod outer segments and

Fig. II.2. Histograms of the measurements of λmax obtained from individual rods and the averaged spectral absorbance curves together with the best-fitting rhodopsin template (continuous line) in: **A)** pre-settlement; **B)** partially-settled; **C)** aquarium-settled; and **D)** wild-settled *Upeneus tragula*. Transverse maximum optical density measurements for the rod outer segments were about 0.025.

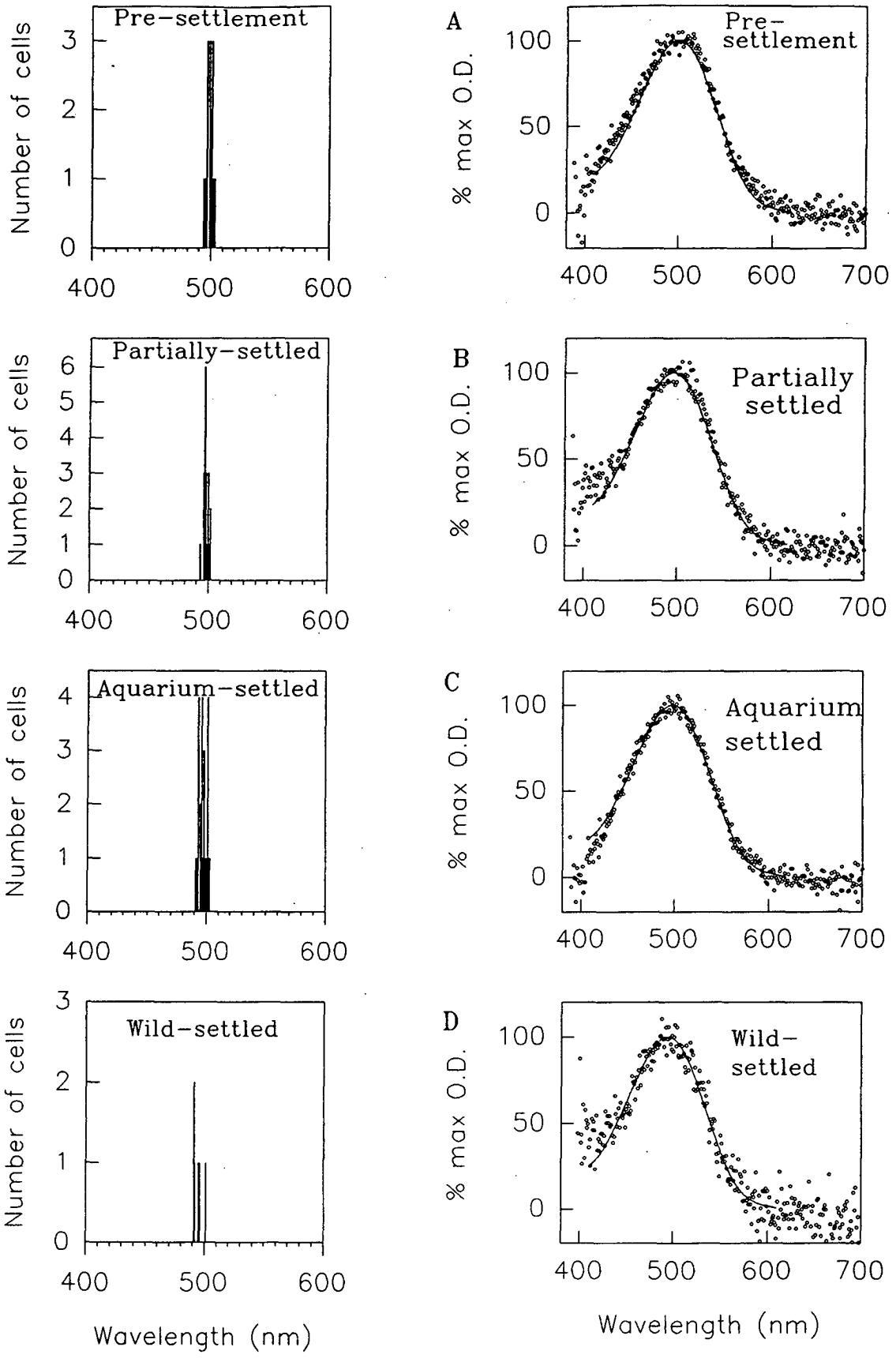
Pre-settlement
Number of cells
3
2
1
0
400
500
600
A
% max O.D.
100
50
0
Pre-
settlement
400
500
600
700
Partially-settled
6
5
4
3
2
1
0
B
Partially
settled
Aquarium-settled
4
3
2
1
0
C
Aquarium
settled
Wild-settled
3
2
1
0
D
Wild-
settled
Wavelength (nm)

the averaged scans for pre-settlement, partially-settled, aquarium-settled and wild-settled fish are shown in Fig. II.2. Means of the scans for each group of fish give λmax values of 499.1 nm, 498.1 nm, 497.0 nm and 495.7 nm respectively. No significant difference between the mean λmax values for each stage of development was found (ANOVA, $P = 0.0551$), however, there is the possibility that the λmax may be shifting to shorter wavelengths although there are too few data to confirm this.

Large cones: The mean λmax (with standard deviation) for each class of cones found in individual fish are shown in Fig. II.3. They are ranked according to standard length (SL) within each stage of development. Averaged visual pigment scans for each stage of development, fitted with a rhodopsin template, are shown in Fig. II.4. Histograms for all the λmax measurements obtained from individual cones of all fish within each stage of development are shown in Fig. II.5.

In pre-settlement fish (Fig. II.3A, II.4A, II.5A) three distinct classes of cone visual pigment were found. All single cones contained a pigment with λmax at or below 400 nm. It was not possible to establish the exact position of the λmax of this group as measurements below 400 nm are beyond the lower wavelength range of the MSP. However the righthand limb of the pigment curve was recorded and subsequent bleaching with white light of some cells indicated that these single cones contained a photolabile pigment (Fig. II.6). All double cones were found to have one member of the pair with a λmax near 490 nm and the other with λmax near 580 nm.

In partially settled fish the results from the double cones were different from those of the pre-settled fish with a total of four absorbance classes (Fig. II.3B, II.4B, II.5B). The single cone still has a λmax below 400 nm but double cones now contain combinations of two of four possible classes of cone absorbance. The average λmax values of these classes are: 487 nm, 515 nm, 530 nm, and 580 nm (Fig. II.3B). Fig. II.3B also shows that individual fish differed from each other with only the smallest and least pigmented fish (fish E) having the 580 nm

Fig. II.3. Mean λmax values and the standard deviation for the cone classes found in individual fish in: **A)** pre-settlement; **B)** partially-settled; **C)** aquarium-settled and **D)** wild-settled *Upeneus tragula*. The fish are ranked according to SL within each stage of development. Triangles, single cones; semi-circles, double cones, with possible pairs represented by opposite-facing semi-circles.

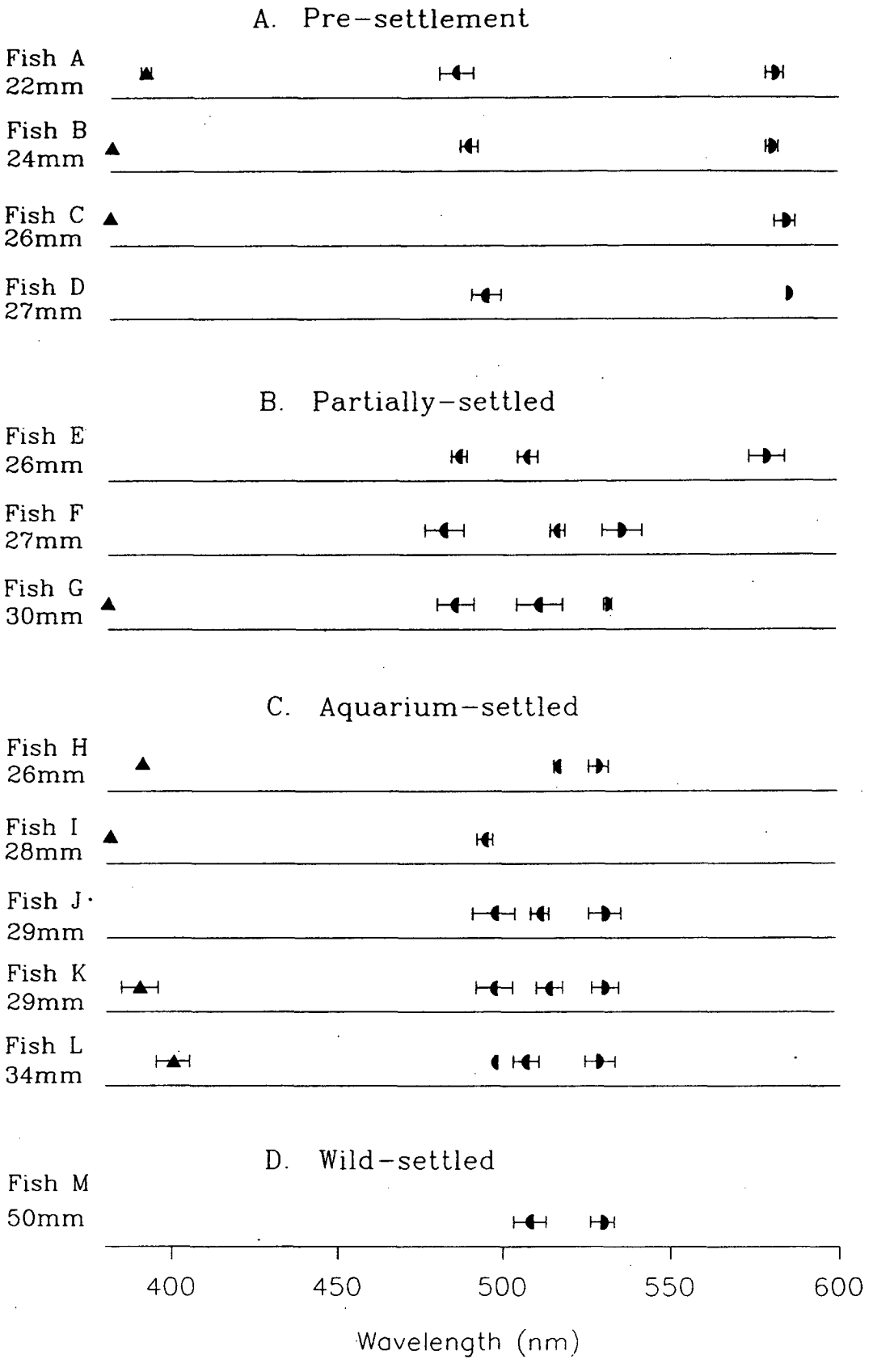
A. Pre-settlement
Fish A
22mm
Fish B
24mm
Fish C
26mm
Fish D
27mm
B. Partially-settled
Fish E
26mm
Fish F
27mm
Fish G
30mm
C. Aquarium-settled
Fish H
26mm
Fish I
28mm
Fish J
29mm
Fish K
29mm
Fish L
34mm
D. Wild-settled
Fish M
50mm
400
450
500
550
600
Wavelength (nm)

Fig. II.4. Averaged spectral absorbance curves, together with a best-fitting rhodopsin template (continuous line) for the classes of cones found in: **A)** pre-settlement; **B)** partially-settled; **C)** aquarium-settled and **D)** wild-settled *Upeneus tragula*. The short wavelength curve has been omitted from **B** for clarity. Transverse optical density measurements for the cone outer segments ranged from about 0.017 to 0.033.

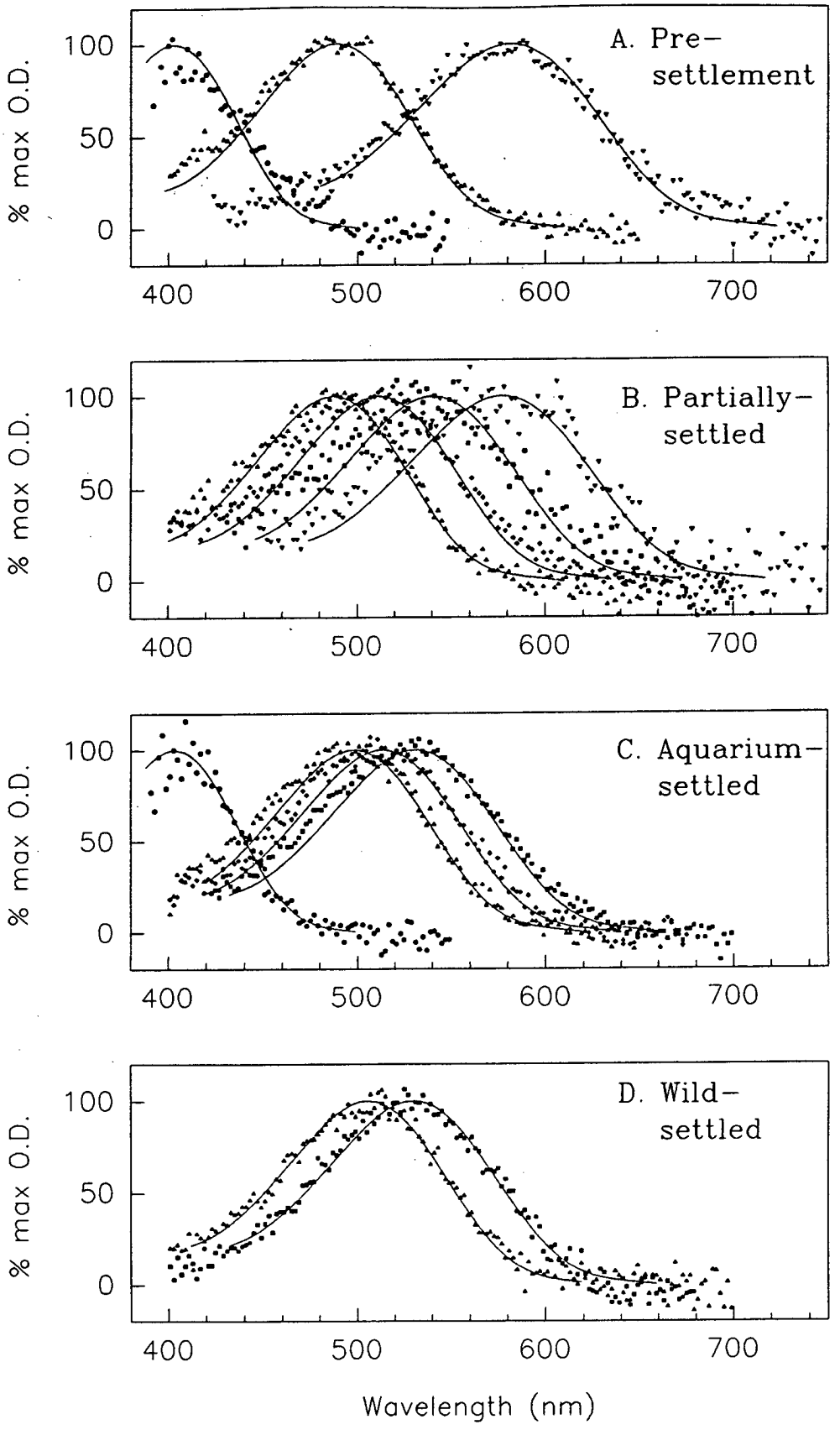
A. Pre–
settlement
B. Partially–
settled
C. Aquarium–
settled
D. Wild–
settled
% max O.D.
100
50
0
400
500
600
700
Wavelength (nm)

Fig. II.5. Histograms of the measurements of λmax obtained from individual large cones for: **A)** pre-settlement; **B)** partially-settled; **C)** aquarium-settled and **D)** wild-settled *Upeneus tragula*. The cells with λmax near 400 nm are single cones, all other records are from double cones.

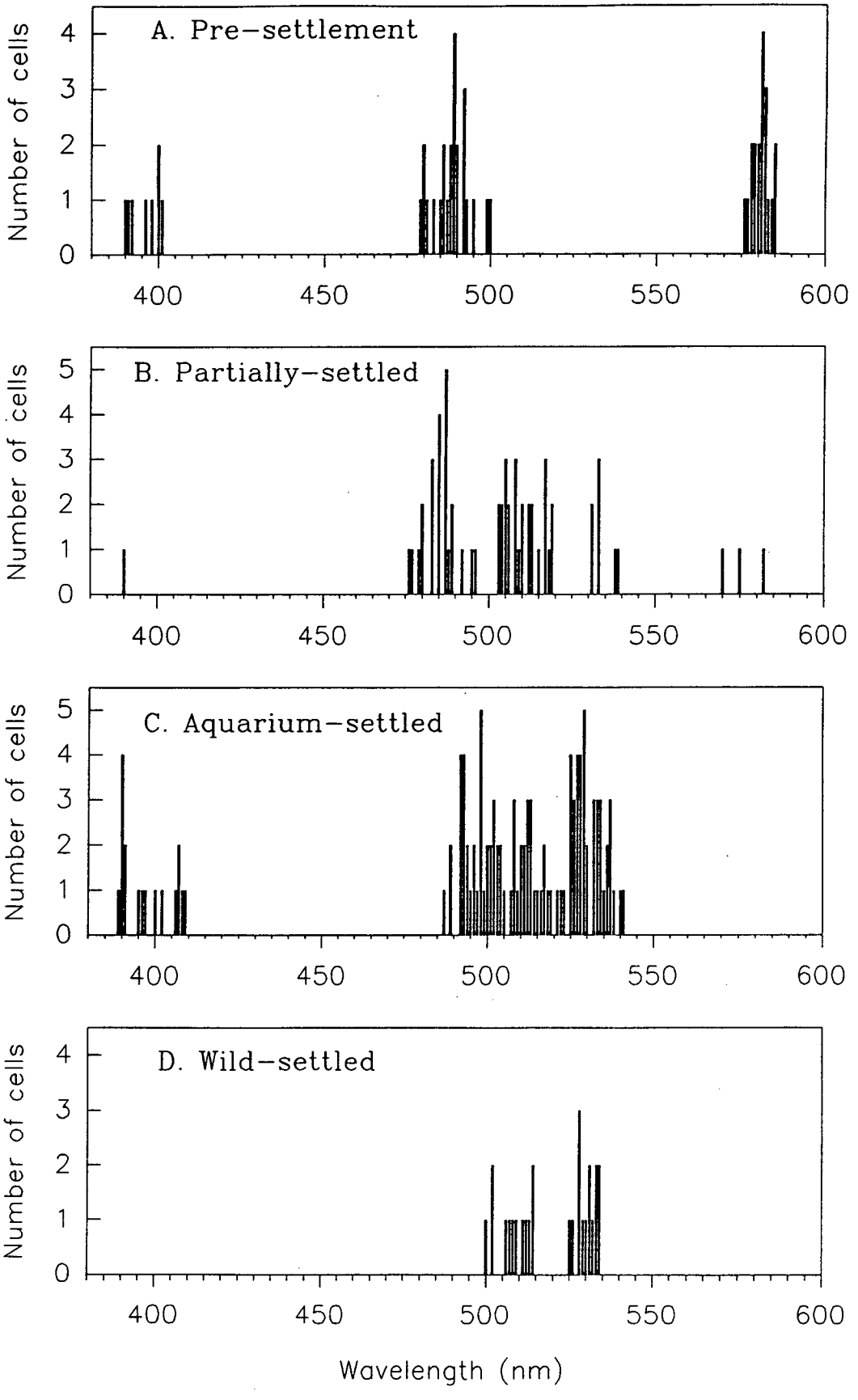
A. Pre-settlement
B. Partially-settled
C. Aquarium-settled
D. Wild-settled
Number of cells
Wavelength (nm)
400
450
500
550
600

pigment but no individual fish had all four absorbance classes. The arrangement of the λmax values within the double cones varied in combination: Fish E had 515/580 nm and 487/580 nm pairs; fish F had 487/530 nm pairs and a double cone containing a 515 nm pigment in one member of the pair (but for which records of the other member were not obtained); and fish G had 487/530 nm and 515/530 nm pairs.

Results from 5 aquarium-settled fish are shown in Fig. II.3C, II.4C, II.5C. The single cones have a pigment with λmax at about 400 nm. The situation in the double cones is less clear. Three absorbance classes continue to be measured from the double cones, however the 487 nm pigment found in the pre- and partially-settled fish appeared to have shifted in average λmax to 498 nm. The averages for the mid and long classes of the double cones were at about 515 nm and 530 nm respectively. Although variation between individual fish is evident, the way the pigments are paired is consistent; i.e. the shortest wavelength pigment (about 498 nm) was always paired with the longest (about 530 nm) and the mid wavelength pigment (about 515 nm) was also always found with the longest (530 nm) (Fig. II.3C). As in the partially-settled fish no records of the two shorter wavelength classes were found paired together, nor were there any records of double cones with the same pigment in each outer segment. This gave individual fish with the visual pigment classes shown in Fig. II.3C. Averaging scans of each pigment class (ie. for the double cones; the short, the mid or the long) from all aquarium-settled fish gave the curves in Fig. II.4C. The histogram of the λmax values obtained from all settled fish (Fig. II.5C) shows the class of single cones at about 400 nm and the spread of pigments from double cones because of the variation between individual fish.

The results from only one wild-settled fish were obtained and in the retinal preparations from this fish only double cones could be found although histological investigation shows single cones in fish of this size (see Part 1). The scans from this fish revealed double cones with λmax values which fell into two rather than three absorbance classes (Fig. II.3D, II.4D, II.5D). The average λmax values for

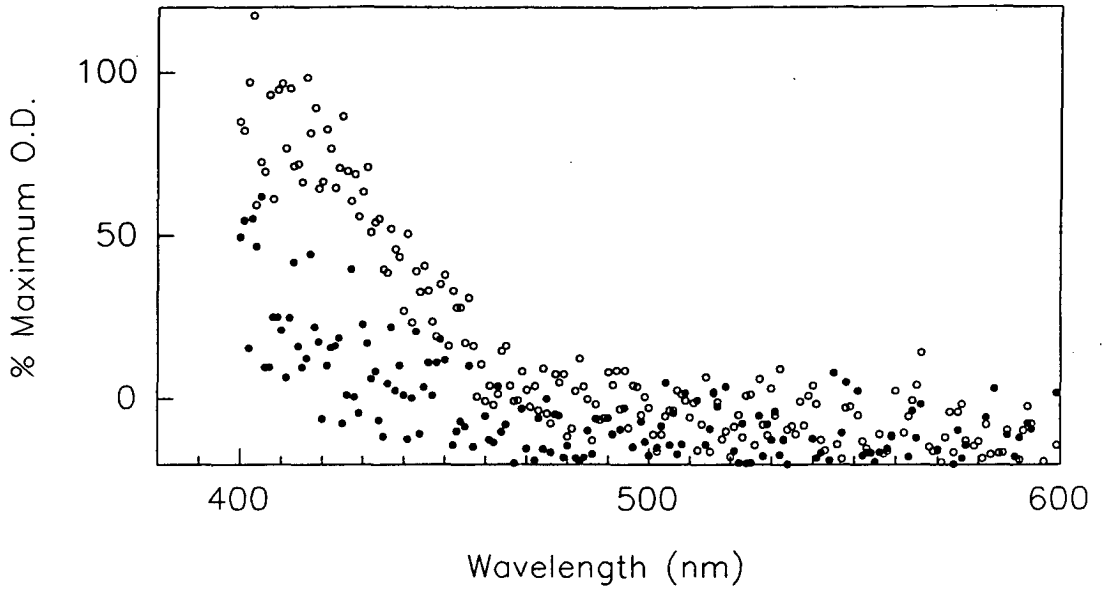

Fig. II.6. The spectral absorbance curve measured from a single cone of *Upeneus tragula* prior to (hollow symbols) and following (filled symbols) 2 min exposure to white light. The transverse maximum optical density measurement prior to bleaching was 0.018 and after bleaching was 0.008.

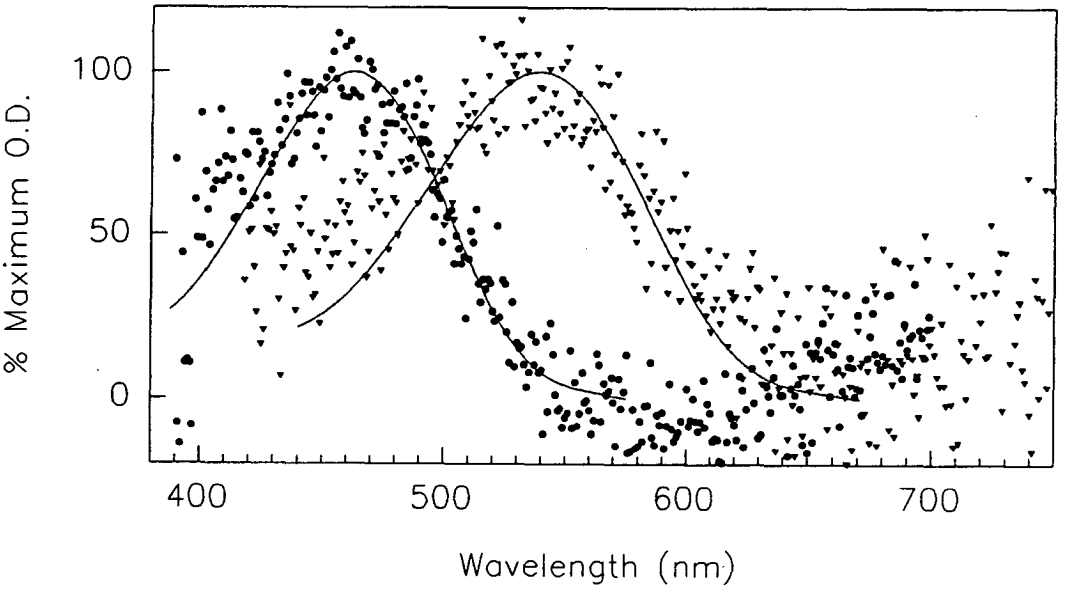

Fig. II.7. Spectral absorbance curves measured from a pair of small cones, presumed to have originated from the ventral retina, from a pre-settlement *Upeneus tragula*. The λmax of the template (continuous line) of the short wavelength measurement is 462 nm and that of the longer wavelength measurement is 540 nm. Transverse maximum optical density measurements were in the region of 0.020

these classes were 506 nm and 530 nm with each double cone having a 506 and 530 nm combination of pigments.

Small cones: Very few records of scans from the small cones (assumed, from histological records of cell dimensions, to be from the ventral retina) were obtained because of problems with the quality of the scans. Selection criteria rejected most scans. The records that were obtained indicated that small single cones also had a pigment with λmax at or below 400 nm in all groups of fish. In addition, one small pair of cones that was measured in a pre-settlement fish had a combination of pigments with λmax at approximately 460 nm and 540 nm (Fig. II.7).

Upeneus moluccensis

One specimen of *U. moluccensis* (SL 125 mm) was examined by MSP. The area of retina used in the preparation had large single and double cones. The length of the double cone outer segments was between 15 to 18 μm and the diameter at the base of the outer segment between 3 and 5 μm. The single cones were of similar diameter but the length varied between 14 to 17 μm. The diameter of the rods was between 1.5 and 3 μm. The location of the area of retina examined was not recorded as orientation of the eye was lost during preparation. Histograms of the λmax values obtained from the scans of the rods are shown in Fig. II.8A. The averaged rod scan is shown in Fig. II.8B. The λmax of the average scan is 496.6 nm. The λmax records obtained from the cones of *U. moluccensis* are shown in Fig. II.8C and the averaged scans in Fig. II.8D. Three classes of cone visual pigments can be distinguished: a short wavelength absorbing pigment, with an average λmax of 403 nm, which is found in the single cones only; a pigment with average λmax at 494.0 nm found in one member of the double cones; and a long wavelength pigment with λmax of 549.0 nm which is found paired with the 494 nm pigment in the double cones.

Fig. II.8. Histograms of the λmax values and averaged visual pigment curves for the photoreceptors of *Upeneus moluccensis*: **A)** and **B)** rods; **C)** and **D)** cones. The continuous line fitted to the curves is a template for rhodopsin. Transverse maximum optical density measurements for the rods were in the region of 0.021 and for the cones, 0.028.

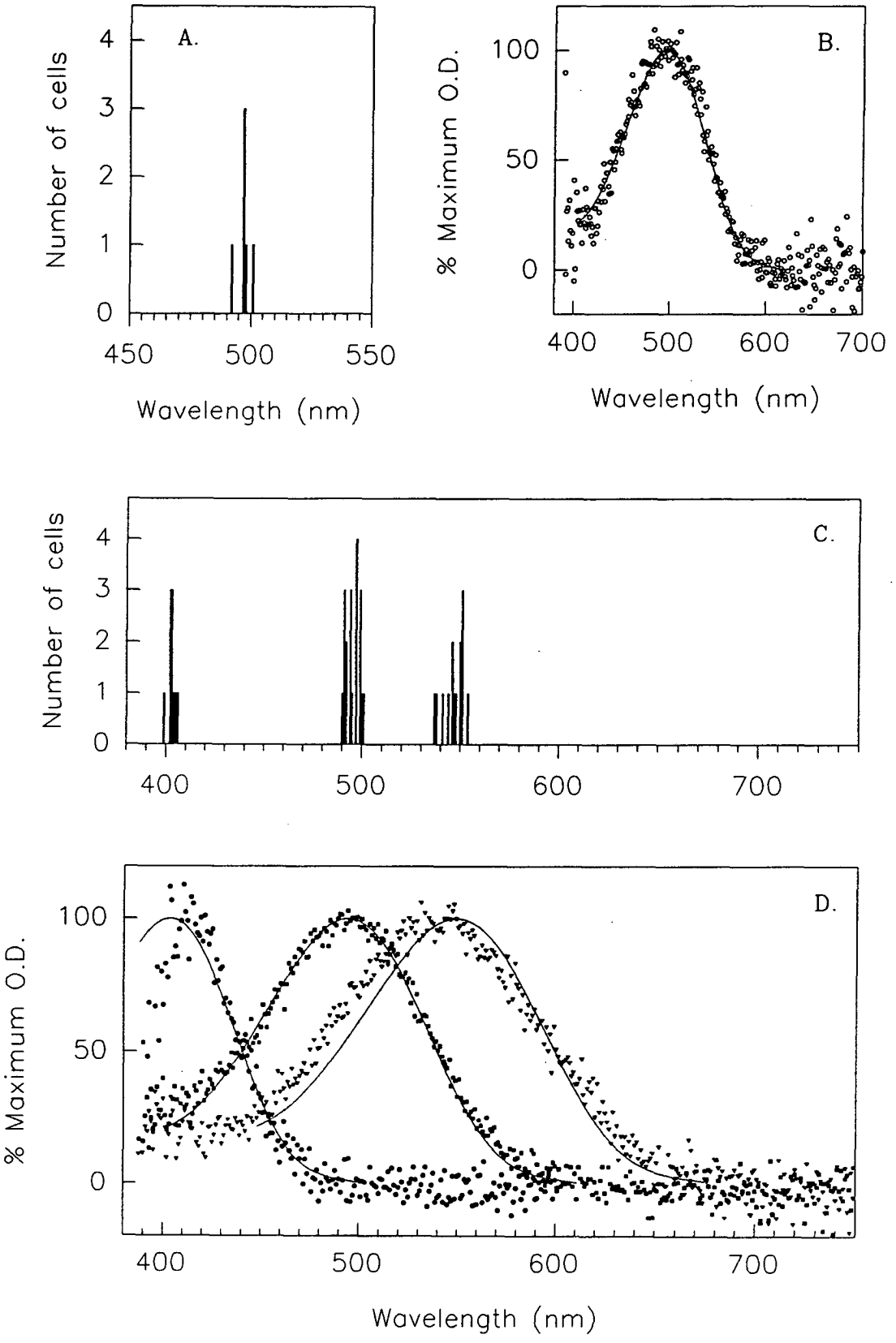
A.
Number of cells
0
1
2
3
4
450
500
550
Wavelength (nm)
B.
% Maximum O.D.
0
50
100
400
500
600
700
Wavelength (nm)
C.
Number of cells
0
1
2
3
4
400
500
600
700
D.
% Maximum O.D.
0
50
100
400
500
600
700
Wavelength (nm)

Ambassis nalua

The results of visual pigment investigations of *A. nalua* were obtained in collaboration with Dr J.C.Partridge (University of Bristol) during initial trials of the MSP. Accurate records of the dimensions of the photoreceptors scanned were not obtained but the general impression was that they were relatively large. Considerable variation between individuals of this species were found. This is shown in the histograms of λmax records obtained from the cones of three individual fish (Fig. II.9). Two of them (1 and 3) have single cones with λmax in the region of 475 nm, whereas fish 2 had a single cone with λmax of 445 nm. The double cones, absorbing at long wavelengths, also showed variation in λmax between individuals. Fish 1 and 3 had λmax values between 565 and 585 nm. Fish 2 appeared to have two long wavelength cone classes with λmax at 540 nm and 560 nm. However, more data would be needed to be sure of this distribution. The rods of fish 2 and 3 were similar with an average λmax of 507 nm. The averaged spectral absorbance curves for fishes 1 and 3 combined and fish 2 are shown in Fig. II.10A and II.10B respectively. In addition a class of cones appeared to be 'empty' i.e. spectral absorbance measurements between 390 and 750 nm resulted in a flat absorbance record. It is possible that these cells could contain a ultraviolet-absorbing pigment which does not have significant absorption within the wavelength range of the MSP.

Ambassis vachelli

Examination of the visual pigments of 5 specimens of *A. vachelli* revealed a spread in the λmax records from the long wavelength absorbing member of the double cones similar to that found in *A. nalua* i.e. from approximately 560 to 580 nm (Fig. II.11A). In one specimen, at least, the second member of the double cones had a λmax of 532 nm. Single cones were found with λmax values between 436 nm and 456 nm but whether there are one or two classes of pigment cannot be distinguished with the data available. No scans of rods were obtained from this

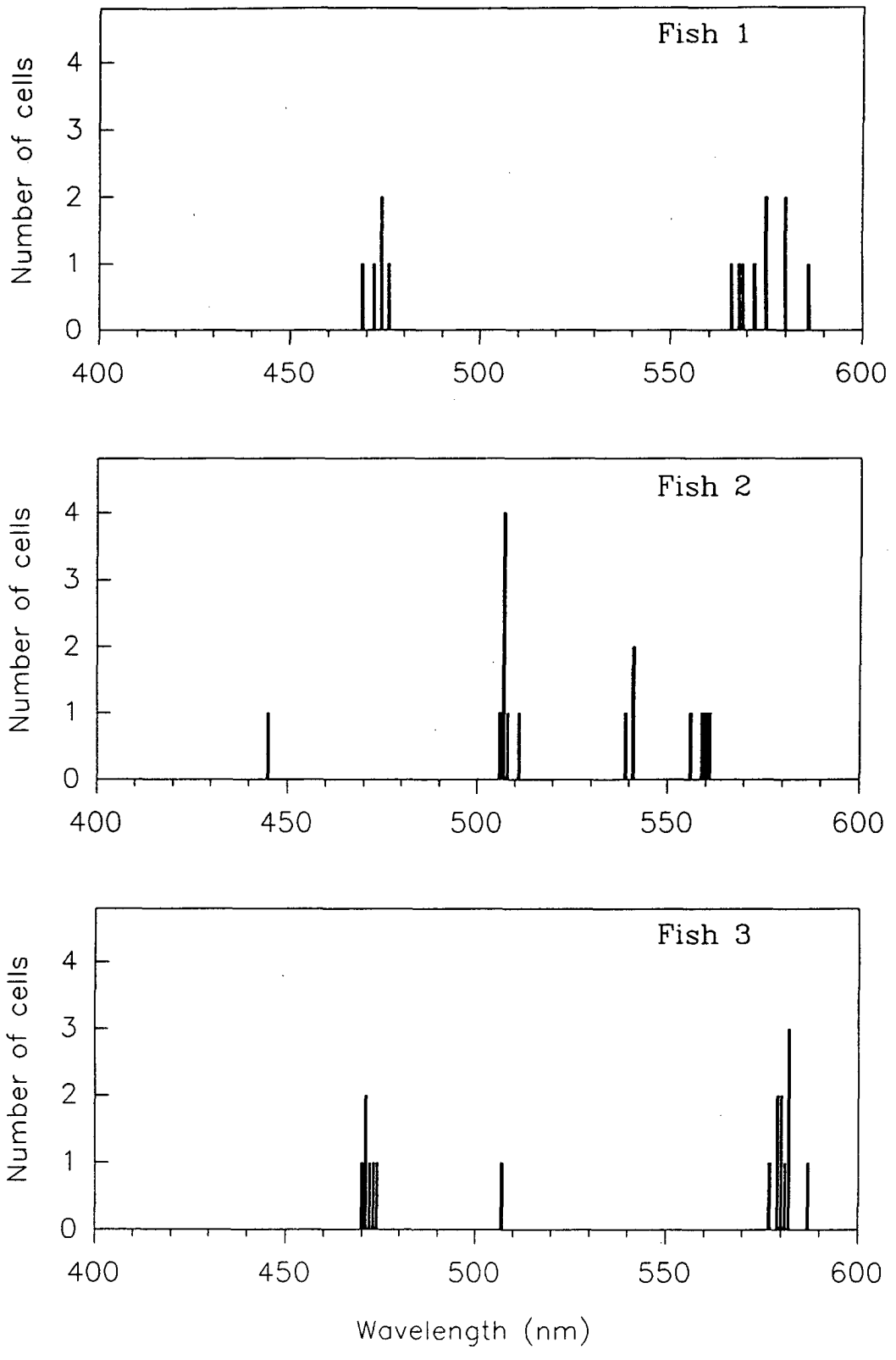

Fig. II.9. Histograms of the measurements of λmax obtained from the photoreceptors of three specimens of *Ambassis nalua*. The records near 505 nm are from rods, the short wavelength records are from single cones, all other records are from double cones.

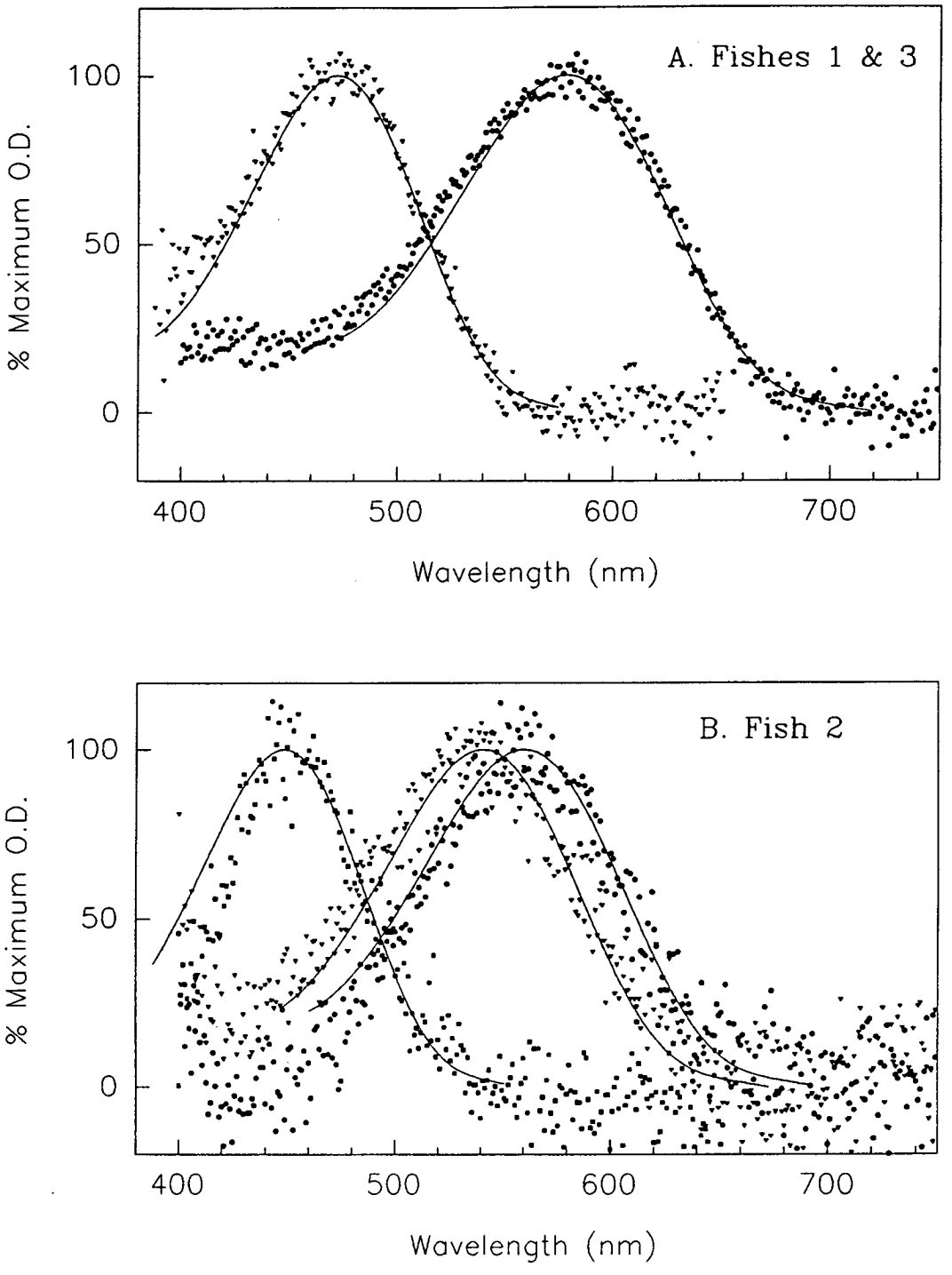

Fig. II.10. Averaged spectral absorbance curves, together with a best-fitting template for rhodopsin (continuous line), for the cone classes found in *Ambassis nalua*: **A)** fish 1 and 3 combined; **B)** fish 2. Transverse maximum optical density measurements ranged from 0.020 to 0.032.

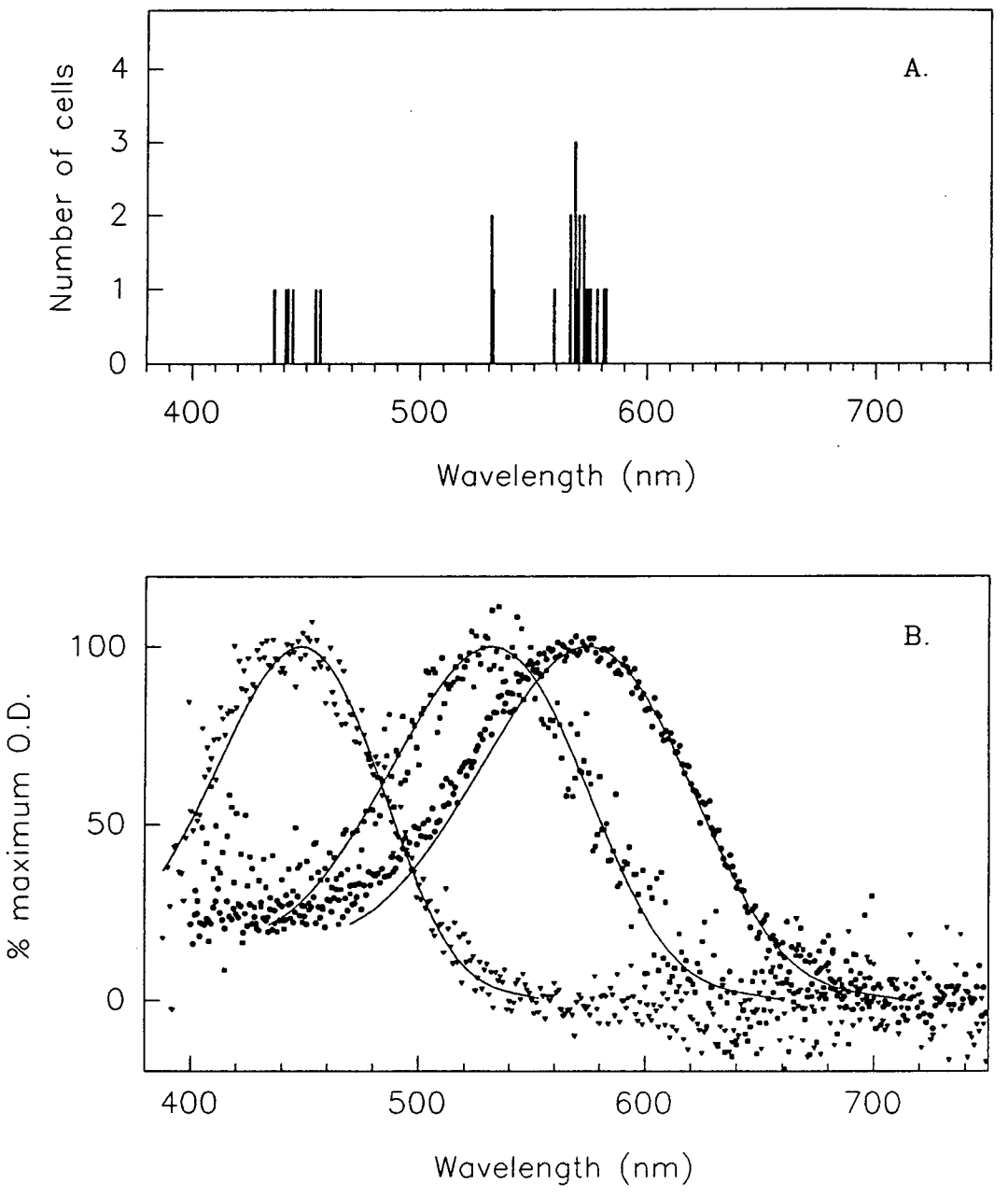

Fig. II.11. **A)** Histogram showing records of λmax recorded from the cones of *Ambassis vachelli* and **B)** averaged spectral absorbance curves, together with a best-fitting template for rhodopsin (continuous line). Transverse maximum optical density measurements ranged from 0.025 to 0.041.

species. The averaged visual pigment scans, fitted with a rhodopsin template, are shown in Fig. II.11B.

Hemirhamphus sp.

One specimen of garfish was examined (100 mm SL) and large cells were found in the area of retina examined. Long rod outer segments of up to 35 μm with a diameter of 2 to 3 μm were present. The single cones had lengths between 12 to 17 μm with base of outer segment diameters of 4 to 6 μm and the double cones had diameters of 2 to 4 μm with exceptionally long outer segments of between 22 to 29 μm. Histological examination of juvenile garfish *Hemirhamphus* sp. (27 mm SL) has shown that long rods and cones are only located in the dorsal retina (see Part I) thus it is likely that the area examined by MSP came from the dorsal retina of this specimen. The λmax records of both the rods and cones are shown in Fig. II.12A. Average scans of the cone classes distinguished are shown in Fig. II.12B. The rods have a λmax at 499 nm. The single cones were found to have an average λmax of 416 nm. Double cones with one outer segment having a λmax at 531.5 nm and the other with λmax at 586 nm were recorded. Despite the size of the double cone outer segments the quality of the scans of the long wavelength outer segment were poor and very few passed the selection criteria.

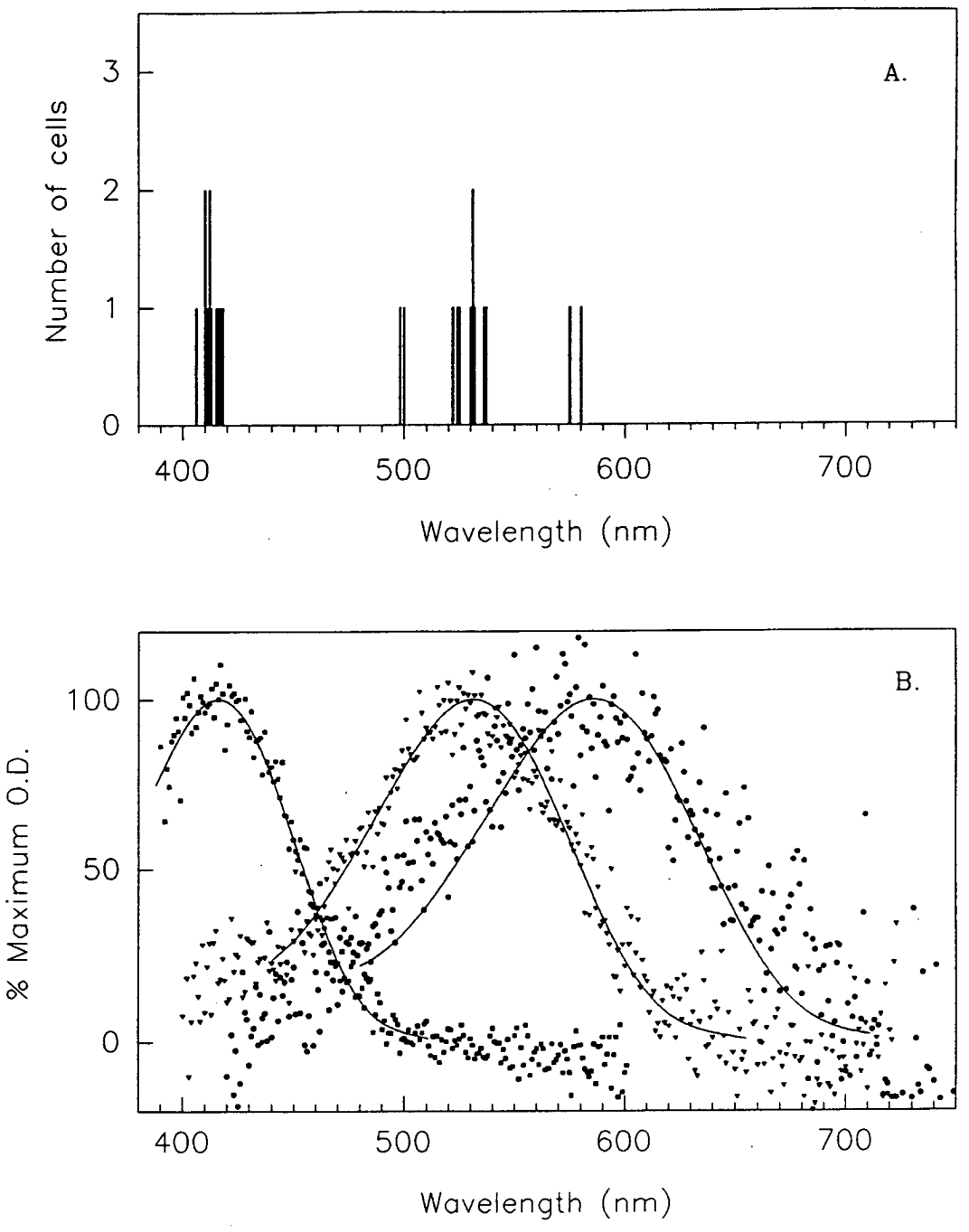

Fig. II.12. **A)** Histogram showing the λmax values and **B)** the averaged spectral absorbance curves, together with the best-fitting template for rhodopsin (continuous line) from the photoreceptors of the garfish *Hemirhamphus sp.* The records close to 500 nm are from rods, those near 410 nm from single cones and the 530 nm and 580 nm records from double cones. The averaged rod scan has been omitted from **B** for clarity. Transverse maximum optical density measurements ranged from 0.016 to 0.030.

Discussion

Upeneus tragula

Microspectrophotometry is the only method by which information about the visual pigments of individual photoreceptors can be obtained. One of the disadvantages of this technique, however, is that the absence of a class of visual pigments does not mean it is not present in a particular retina. Two possible reasons for this are: 1) An inadequate number of sample scans may lead to a cell type being overlooked; 2) Regionalisation of a class of pigments within the retina could mean they are missed because an area of retina is not present in the preparation. In fish with large eyes it is likely that the second possibility could occur as only small pieces of retinal tissue (1-2 mm^2) can be used in a preparation. Owing to the small size of the eyes of *Upeneus tragula* the preparations always aimed to contain the whole retina. However, the results are most likely to be from the dorsal retina where the larger cells yield better quality scans which are more likely to survive the selection criteria. The samples obtained from the other species were of unknown location and in the case of *U. moluccensis* and *Hemiramphus sp.* it is possible that cone classes were missed as only one specimen of each was examined.

In every pre-settlement *Upeneus tragula*, a red-absorbing cone pigment was found but in none of the settled fish was this pigment recorded. Moreover, it is only in the smallest of the partially-settled fish that a few records of this pigment were obtained. It is most likely, therefore, that during the metamorphosis associated with settlement of *U. tragula*, the red-sensitive pigment disappears from the double cones of the dorsal retina. Concomitant with the disappearance of this pigment is the appearance of visual pigment absorbance classes not previously encountered. The 580 nm pigment appears to be replaced by one of 530 nm which can be paired with either the 487 nm or a new 515 nm pigment. There is also the possibility that the 487 nm pigment, found in the pre- and partially-settled

fish, shifts in λmax to about 498 nm in the aquarium-settled fish and 506 nm in the wild-settled fish. Whether a double cone compliment of 506 nm and 530 nm, as found in the single wild-caught fish, is the final compliment in adults cannot be established without more data from larger settled fish.

Mechanism of visual pigment changes

The visual pigment molecule consists of a protein (opsin) and a chromophore, derived from either vitamin A1 or A2. If the A1 derivative (retinal) is present the visual pigment is a rhodopsin whereas the A2 derivative (dehydroretinal) forms porphyropsin. The methods by which the λmax of visual pigments are controlled are: 1) The chromophore part of the visual pigment molecule can be switched from retinal to dehydroretinal or the ratios of a mixture of the two can be altered (Knowles and Dartnall 1977); 2) The protein part of the molecule (opsin) can undergo changes in amino acid sequence (Nathans *et al.*, 1986). Porphyropsin pigments are broader in the width of their spectral sensitivity curve and long-wavelength sensitive porphyropsins have λmax values at longer wavelengths than their rhodopsin analogues (Dartnall and Lythgoe 1965; Whitmore and Bowmaker, 1989). It has been found that porphyropsin pigments are usually present in freshwater fishes with long wavelength sensitivity (see Crescitelli 1972 for review). It is an increase in the ratio of A2/A1 accounts for the shift in λmax to longer wavelengths in the rudd as daylengths shorten (Whitmore and Bowmaker, 1989 for recent summary). Porphyropsins are rare in marine fishes and most fishes that migrate from freshwater to the sea change their visual pigment chromophore from A2 to A1 as they leave the rivers (eg. Carlisle and Denton 1959 (eel); Beatty 1984 (salmonids)). From the evidence of template-fitting in this study, it appears that the visual pigments recorded in *Upeneus tragula* are all rhodopsins. The chromophore present in the other species found to have a pigment with λmax at 580 nm (the ambassids and the garfish) also appears to be retinal. This is supported by high performance liquid chromatography (HPLC) results that were obtained from both species of ambassid (Partridge and De Grip,

unpublished HPLC results) which failed to detect the presence of any dehydroretinal in the retinae of these species (J.C.Partridge, personal communication). A rhodopsin with λmax at 580 nm is in fact at the long wavelength limit predicted by Blatz and Liebman (1973) for this chromophore. Since dehydroretinal does not appear to be present in *U. tragula* it seems likely that opsin substitution, rather than chromophore replacement is bringing about the changes in λmax of the double cone pigments.

Loss of the 580 nm pigment in *Upeneus tragula* and its apparent replacement with a 530 nm pigment does not appear to involve a gradual shift in λmax to shorter wavelengths since no intermediate records were obtained. What is happening in the in the shorter wavelength-absorbing pigment of the cone pairs is not entirely clear. In partially- and aquarium-settled individuals there appear to be two possible absorbance classes, whereas in the wild-settled fish only one class was found. The considerable amount of variation in λmax from individual fish over the settlement period do not make it possible to say whether a gradual shift is taking place or whether the mid (515 nm) class is a new pigment or a mixture of the 487 nm and 530 nm pigments.

A spread of the λmax records from the double cones of the adult guppy, *Poecilia reticulata*, has been reported (Archer *et al.*, 1987; Archer and Lythgoe, 1990). In these fish long wavelength polymorphism was found. Individuals have up to three visual pigment classes in the green-yellow region of the spectrum with mean λmax values of 533, 543 and 572 nm. The middle class is thought to be formed by a mixture of rhodopsin from the longer and shorter wavelength pigments (Archer and Lythgoe, 1990). A similar spread of pigments is also observed in the ambassids investigated in this study, although more data from individual fish is required to clarify the situation in these species.

Cones are known to undergo continual regeneration in the same way as rods (O'Day and Young, 1978) with lamellae added at the base of the outer segment and detachment of packets of membranes from the ends. It is thought, for rods at

least, that this is the only way in which visual pigment is renewed. A major difference between rod and cone protein renewal is that in rods most of the protein is bound into new disc membranes at the base of the outer segment whereas in cones it is free to diffuse throughout the outer segment (Young, 1976; 1969; Bok and Young 1972). Autoradiographical studies of protein uptake in frogs have shown that concentrations of labelled protein reach peak concentrations in the cone outer segments within 24 hr of injection, but it is not clear whether it is actually the visual pigments that are being replaced by this diffuse renewal process (Bok and Young 1972). Loew and Dartnall (1976), when examining changes of A1/A2 mixtures in the rods and cones of the rudd following manipulation of daylength, found that the cones had incorporated the new mixtures throughout their length while there were still differences between the apical and basal portions of the rods. Different opsins within individual rods have recently been recorded in the eel (*Anguilla anguilla*) following artificial maturation with hormone injections (Wood and Partridge, 1993). A new opsin was found in the basal half of the rods within 30 - 40 days of injection. Evidence from *Upeneus tragula*, in which rapid changes in the cone pigments are occurring in the red-sensitive member of the double cones, suggests that a new opsin can be incorporated into these cones overnight.

The light environment

When in their pelagic phase in the surface waters, *Upeneus tragula* are in an environment in which downwelling light has the spectral characteristics of a terrestrial situation. The effects of absorption in shallow (less than 1 m) oceanic (Jerlov ocean type I) and continental (Jerlov ocean type III) water are minimal so that both the short wavelength (>400 nm) and the long (<600 nm) wavelengths are present. In addition fish swimming over deep water are subjected to upwelling light with a strong component of blue wavelengths (McFarland and Munz 1975b). The light environment will change following settlement to a benthic mode of life in deeper water (10 -30 m), where the ultra-violet and red components will be

reduced because of the selective absorption characteristics of water with depth (Jerlov 1976). McFarland (1986) has calculated that in continental seas, wavelengths of light about 400 nm can still be available for vision to depths of 50 m. The absorption of light greater than 600 nm increases rapidly below 5 m in continental seas although according to McFarland (1986) there will still be enough light of 600 nm left for vision at 30 m. When settled, *U. tragula* will no longer be exposed to the upwelling blue light as this will be replaced with reflections from sand and algae which are stronger in the green-yellow region of the spectrum (McFarland and Munz 1975b).

It is perhaps not surprising that a surface dwelling fish should have both short and long wavelength sensitivity. Although there are no published reports, from a marine fish, of rhodopsin visual pigments sensitive to ultraviolet wavelengths, or those with λmax values as long as 580 nm, it should be noted that tropical surface dwelling species have not been extensively investigated by MSP. In presenting collated data from very shallow living tide pool and tropical freshwater teleosts, Lythgoe and Partridge (1989) showed that the rhodopsins are located in regions of the spectrum similar to terrestrial species but with the longest wavelength pigment at about 574 nm. In addition, the brackish water four-eyed fish, *Anableps anableps*, which swims so that its eyes are semi submerged, was found to have a long wavelength sensitive pigment in the paired cones with a λmax of 576 nm, as well as a short wavelength pigment with λmax of 409 nm in single cones (Avery and Bowmaker, 1982). It is thought that these pigments are based on rhodopsin, but that some porphyropsin might also be present (Bowmaker, 1990). Results from the neustonic garfish, *Hemirhamphus* sp., also reveal a red sensitive pigment with λmax at 580 nm, as do the results from the shallow water ambassids, *Ambassis nalua* and *A. vachelli*. It is possible that a long wavelength absorbing pigment in marine fish is associated with a neustonic existence in an environment where there is a broad spectrum of light and that it is lost in direct response to the increase in depth at settlement. When comparing results from the ambassids and garfish it should be noted that these are inshore species which, as well as inhabiting shallow water, also inhabit a light environment in which longer

wavelengths are more predominant than in clearer offshore waters. Thus the red sensitivity of the double cones in these species could result from the influence of the longer wavelengths of ambient light found in inshore locations. Lythgoe *et al.*, (1994, see appendix 7) have shown that species of lutjanid caught from inshore locations have longer wavelength absorbing pigments than offshore species from clear reef environments. In the visual pigment survey of the lutjanids, four species from the estuarine and inshore habitats have a long wavelength absorbing cone pigment in the region of 570 nm. These species are not necessarily shallow-living although all the specimens investigated were caught in water less than 4 m in depth (Lythgoe *et al.* 1994, see appendix 7).

An alternative explanation for the possession of a long wavelength-absorbing visual pigment in the neustonic *Upeneus tragula* could involve the need to maximise contrast against the upwelling blue light. Since the pigment is located in the dorsal retina it might be advantageous in the detection of predators striking from below. The possession of an offset visual pigment could maximise the contrast of a target against a dark background (Lythgoe, 1979). McCormick and Milicich (1993) noted that schools of pelagic *U. tragula* were often attacked by predators such as the mackerel tuna, *Euthynnus affinus*. When this occurred the mullids formed tight balls typical of schooling fish.

Short-wavelength sensitivity

Ontogenetic changes in cone visual pigments have been documented for the brown trout (Bowmaker and Kunz 1987), the pollack (Shand *et al.* 1988) and the perch (Loew and Wahl 1991) as these fish migrate to deeper waters and change their feeding behaviour. All these studies have reported changes to the short wavelength absorbing single cones. In yearling trout a class of single cones absorbing at 355 nm was recorded but two-year old fish no longer possessed the ultra-violet absorbing cones (Bowmaker and Kunz, 1987). Similarly juvenile perch were found to lose small single cones absorbing at 400 nm at a stage of development

corresponding to a switch from planktivorous feeding in surface waters to a more demersal feeding mode (Loew and Wahl, 1991). The loss of the short wavelength sensitivity in these two species is attributed to movement of the fish to deeper water where there is less short wavelength light available for vision. Although no records from the single cones of wild-caught settled *Upeneus tragula* were obtained, the data from aquarium-settled fish do not suggest any changes occur in the λmax of these cones. Records at or below 400 nm were recorded in all aquarium-settled fish but the accuracy of the MSP records below 400 nm do not allow for detection of any changes that might be occurring in any uv-sensitive cones, if these exist in this species. The adult of the closely related *U. moluccensis* also has single cones with λmax at 403 nm. The larvae of *U. moluccensis* have a similar distribution to those of *U. tragula* but the adults have only been recorded from inshore locations whereas the adults of *U. tragula* are known to occur in both coastal and offshore areas (McCormick and Milicich, 1993). *U. tragula* were caught near Lizard Island (an offshore location), whereas adult *U. moluccensis* were caught in about 15 m at an inshore location near Townsville.

Although most ultra-violet absorbing pigments have been found in fresh water species, the presence of a short wavelength visual pigment in fishes inhabiting surface waters where there is more ultraviolet light is not now considered unusual. For example, in addition to the trout mentioned above, the roach (Avery *et al.*, 1983), the Japanese dace (Hárosi and Hashimoto, 1983) and the goldfish (Hawryshyn and Beauchamp, 1985; Bowmaker *et al.* 1991) are known to have ultra-violet sensitivity. The functional significance of ultra-violet/violet receptors is unclear. It has been suggested that they could be concerned with the contrast enhancement of planktonic prey (Bowmaker and Kunz, 1987; Loew and Wahl, 1991) resulting from the preferential scattering or absorption of short wavelengths so that, depending on direction of view, plankton appear brighter or darker than the background. Loew *et al.* (1993) have shown that juvenile yellow perch, *Perca flavescens*, which have a class of cones with λmax at 400 nm, can detect and strike prey in the presence of near-uv light only. The possibility that short

wavelength cones are involved in detection of polarized light also exists as *e* - vector discrimination has been reported in the goldfish with the ultra-violet receptor most sensitive to the horizontal *e* - vector axis (Hawryshyn and McFarland, 1987). This phenomenon has also been found in small rainbow trout (*Salmo gairdneri*) but is lost in larger fish that have also lost the ultra-violet sensitive cones (Hawryshyn *et al.*, 1990). Another possible role for ultra-violet receptors could be concerned with the detection of ultra-violet reflection patterns in intraspecific behavioural displays (Hárosi, 1985).

In the pelagic phase, *Upeneus tragula* are found in large schools feeding on planktonic prey and it is possible that the short wavelength receptor is involved in the detection of plankton. Alternatively the reflections from the silvery flanks of the fish could be polarized as has been found to some extent from the silvery exterior of the bleak, *Alburnus alburnus* (Denton and Nicol, 1965). Thus the short wavelength cones may be involved in the detection of polarized light as an aid to schooling. Unlike the trout and perch, the mullids appear to retain a short wavelength receptor when they move to deeper water and change to a benthic feeding mode. The role of these receptors then becomes confused when trying to rationalise the continued presence of the short wavelength cone in the settled mullids because, even though there may be enough light of around 400 nm present for vision (McFarland, 1986), the fish are no longer silvery sided and no longer feed on plankton. Exactly how these two species of mullid make use of a short wavelength absorbing cone once they have settled is therefore unknown. It is worth noting that *Lutjanus malabaricus* has a short wavelength absorbing cone with λmax of 408 nm (Lythgoe *et al.*, 1994, see appendix 7). This species also inhabits both coastal and offshore reefs of the Great Barrier Reef in depths of 12 to 100 m (Williams and Russ, 1991).

A prerequisite for ultra-violet mediated vision is the possession of a cornea and lens that will transmit short wavelengths. Since yellowing of the lens with age is not uncommon (Douglas, 1989; Thorpe and Douglas, 1993) it may be that loss of ultra-violet sensitivity in older fish is as a result of the loss of transmission

properties of the ocular media. No data for the transmission properties of the fish studied here are available but it would be of interest to know if the adult mullids and lutjanids are in fact able to see short wavelength light.

Rods

Munz and McFarland (1973) found differences in the λmax of larval and adult cardinal fish, *Apogon brachygrammus*. The larvae have pigment with λmax at 482 nm and the adults at 494 nm. Since the rods of deeper living coral reef species have a λmax displaced to shorter wavelengths than those from shallow-living species (Munz and McFarland, 1973), this indicates the larval *A. brachygrammus* might live deeper than the adults. There are however no ecological data to substantiate this. *Upeneus tragula* have shallow living larvae so any change in the λmax of the rods might be expected in the opposite direction and, although no significant change has been detected, the mean values for each stage do shift to slightly shorter wavelengths i.e from 499.1 nm in the pre-settlement fish to 495.7 nm in the wild-settled fish. The rods of the adult benthic *U. moluccensis* yield a mean λmax value of 496.6 nm and those of the pelagic garfish have an average λmax at 498 nm. The ambassids have rods absorbing at significantly longer wavelengths i.e. 507 nm. It is possible that the λmax of the rods of *A. nalua* has shifted to longer wavelengths because of the influence of longer wavelength ambient light in the inshore habitats. Surveys of rod pigments of fishes from freshwater habitats show some shift of their λmax to longer wavelengths although this seldom extends beyond 540 nm and does not extend to wavelengths long enough to provide maximum sensitivity in waters transmitting light as far into the red as 620 nm (Lythgoe, 1984). It appears that the positioning of the λmax of rods at shorter wavelengths than those capable of conferring maximum sensitivity is the normal condition in fish from most habitats, except those from the deep-sea and clear blue waters.

Correlation with structural changes in the retina

Changes in visual pigments have been correlated with changes in retinal structure in trout and perch when the loss of small single cones corresponds to loss of ultraviolet sensitivity (Bowmaker and Kunz, 1987; Loew and Wahl, 1991). At the time the visual pigment changes are taking place in *Upeneus tragula* there is also a structural reorganisation of the cone layers in the dorsal retina. While the fish are in their pelagic phase, cones are arranged in two layers, with the single cones in the vitread position and the double cones the sclerad position. At settlement these layers slot together to form only one layer (Shand, 1994, see Part I for details), a process that occurs in step with the other physiological changes associated with metamorphosis. However, loss of double cones that contained the red absorbing pigment does not occur, rather the pigment within them is replaced with the green-absorbing pigment. The single cones in the mosaic get smaller and some arrays appear to lose the single cone (see Part I), but no change in the sensitivity of the pigments contained in these cones is detected in the size range of fish investigated.

It is apparent that the visual pigment compliment in the two phases of the life history of *Upeneus tragula* exhibit adaptations to the respective modes of life. The rapid changes in the visual pigments that occur in step with the settlement process imply that the possession of particular visual pigments at different stages of the life-cycle is essential to the survival of the fish. At this stage the precise visual significance of the adaptations is not entirely clear.

GENERAL DISCUSSION

The extensive examination of the structure and physiology of the visual system of teleosts, since the early work in the last century (e.g. Cajal, 1892) to the present day, provides understanding of a sensory system and its functional role (Walls, 1942; Lythgoe, 1979). With the realisation that larval fish are not just passive planktonic animals but discriminating animals that feed and move within the water column, the study of the visual systems of larval fish has also begun with visual ecology in mind, rather than simply the development of a sensory organ. However, when interpreting visual adaptations of larval fish it is necessary to take into account the restrictions imposed by limitations of size as well as the effects of continuing rapid growth of the ocular tissues. This study also shows that information about the subsequent adult life is necessary when interpreting developmental sequences in the retina. This thesis has attempted to look at some of these parameters in a number of species with ecologically differing modes of life.

The choice of species relied to some extent upon what could be obtained and identified because the ecology of tropical reef teleost larvae is still in its early stages. However, the aim was to obtain a range of species with differing post-settlement lifestyles and to sample both prior to and following settlement, with particular attention to the period during the transition from the pelagic environment to the demersal juvenile phase. The extent of pre-settlement sampling was limited in the fish that settled at small sizes and in the case of the pre-settlement labrids none were obtained despite the settled species being amongst the smallest fish examined.

It is evident that in fish that settle at small sizes the retina undergoes changes in preparation for the post-settlement life-style at an early stage of development. This is shown by the differing rates of change of cone and rod densities in different species. In contrast, one species, the mullid *Upeneus tragula*, which remains

pelagic for an extended period, apparently maintains structural adaptations to a pelagic existence. Differences in the visual pigment compliment prior to and following settlement were also found in this species. It is hard to believe that structural and visual pigment changes occurring so precisely in step with settlement do not infer some adaptation to the light environment and mode of life at respective stages of their life history.

The precarious nature of the pelagic stage when larval fish are highly susceptible to starvation and predation is not helped by the physical limitations imposed by small eye size. Rapid growth of the eye would help to overcome poor acuity but presumably the size of the eyes is limited by energy requirements. There will be no gains in having high acuity or an increased search area if the fish is unable to process the information, swim an increased distance or ingest prey items. Larval development therefore has to be considered as an interaction between,and fine tuning of,neural and somatic development.

The coral reef environment is one of intense predation pressure for newly settled juvenile fish. The transition to this habitat often occurs rapidly (overnight) and the need to be well prepared for the demersal existence is obvious. The development of the visual system of reef teleosts that settle at small sizes appears to be geared towards the post-settlement life-style. Whereas a species that presumably gains some sort of advantage by remaining pelagic for a longer period is able to undergo rapid transition in retinal structure and visual pigment compliment at settlement.

There remain many unanswered questions. More information about larval behaviour in relation to feeding and depth distribution in correlation with studies of retinal structure would be desirable. Further visual pigment investigations on species that settle at smaller sizes, to see if changes such as those in *Upeneus tragula*, occur in other species. The role of the double layer of cones found in *Upeneus tragula* prior to settlement has still to be elucidated. The effects of delayed settlement on retinal structure and survival in the pelagic environment

would be of interest. Finally, behavioural experiments need to be carried out as theoretical estimates of visual ability can only act as a guide and do not actually tell us what a fish can see or how it will respond to visual cues.

BIBLIOGRAPHY

Abercrombie, M. (1946) Estimation of nuclear populations from microtome sections. *Anat. Rec.*, **94**, 239-247.

Ahlbert, I-B. (1973) Ontogeny of double cones in the retina of perch fry (*Perca fluviatilis*, Teleostei). *Acta Zool., Stockh.*, **54**, 241-254.

Ahlbert, I-B. (1976) Organization of the cone cells in the retinae of salmon (*Salmo salar*) and trout (*Salmo trutta trutta*) in relation to their feeding habits. *Acta Zool., Stockh.*, **57**, 13-35.

Aho, A.-C., Donner, K., Hydén, C., Larsen, L.O. and Reuter, T. (1988) Low retinal noise in animals with low body temperature allows high visual sensitivity. *Nature, Lond.*, **334**, 348-350.

Ali, M.A. (1959) The ocular structure, retinomotor and photobehavioral responses of juvenile Pacific salmon. *Can. J. Zool.*, **37**, 965-996.

Ali, M.A. (1964) Stretching of the retina during growth of salmon (*Salmo salar*). *Growth*, **28**, 83-89.

Ali, M.A. and Anctil, M. (1976) *Retinas of Fishes: An Atlas*. Springer-Verlag, Berlin.

Allen, G.R. and Burgess, W.E. (1990) A review of the glassfishes (Chandidae) of Australia and New Guinea. *Rec. West. Aust. Mus. Suppl.*, **34**, 139-206.

Allen, G.R. and Swainston, R. (1988) *The Marine Fishes of North-Western Australia*. Western Australia Museum, Perth.

Anctil, M. (1969) Structure de la rétine chez quelques téléosteéns marins du plateau continental. *J. Fish. Res. Bd. Can.*, **26**, 597-628.

Appleby, S.J. and Muntz, W.R.A. (1979) Occlusable yellow corneas in Tetraodontidae. *J. Exp. Biol.*, **83**, 249-259.

Archer, S.N. and Lythgoe, J.N. (1990) The visual pigment basis for cone polymorphism in the guppy, *Poecilia reticulata*. *Vision Res.*, **30**, 225-233.

Archer, S.N., Endler, J.A., Lythgoe, J.N. and Partridge, J.C. (1987) Visual pigment polymorphism in the guppy *Poecilia reticulata*. *Vision Res.*, **27**, 1243-1252.

Avery, J.A. and Bowmaker, J.K. (1982) Visual pigments in the four-eyed fish, *Anableps anableps*. *Nature, Lond.* **298**, 62-63.

Avery, J.A., Bowmaker, J.K., Djamgoz, M.B.A. and Downing, J.E.G. (1983) Ultra-violet sensitive receptors in a freshwater fish. *J. Physiol.*, **334**, 23-24P.

Baker, K.S. and Smith, R.C. (1982) Bio-optical classification and model of natural waters. 2. *Limnol. Oceanogr.*, **27**, 500-509.

Barlow, H.B. (1957) Purkinje shift and retinal noise. *Nature, Lond.*, **179**, 255-256.

Batty, R.S. (1989) Escape responses of herring larvae to visual stimuli. *J. Mar. Biol. Ass. U.K.*, **69**, 647-654.

Bayliss, L.E., Lythgoe, R.J. and Tansley, K. (1936) Some new forms of visual purple found in sea fishes with a note on the visual cells of origin. *Proc. R. Soc.*, **B**, **120**, 95-113.

Beatty, D.D. (1984) Visual pigments and the labile scotopic visual system of fish. *Vision Res.*, **24**, 1563-1573.

Beharse, J.C. (1982) The daily light-dark cycle and rhythmic metabolism in the photoreceptor-pigment epithelium complex, in *Progress in Retinal Research, Vol. 1* (eds N. Osborne and G. Chader), Pergamon Press, Oxford, pp. 81-118.

Bellwood, D.R. (1988) Ontogenetic changes in the diet of early post-settlement *Scarus* species (Pisces: Scaridae). *J. Fish Biol.*, **33**, 213-219.

Bellwood, D.R. and Choat, J.H. (1989) A description of the juvenile phase colour patterns of 24 parrotfish species (Family Scaridae) from the Great Barrier Reef, Australia. *Rec. Aust. Mus.*, **41**, 1-41.

Blatz, P.E. and Liebman, P.A. (1973) Wavelength regulation in visual pigments. *Exp. Eye Res.*, **17**, 573-580.

Blaxter, J.H.S. (1986) Development of sense organs and behaviour of teleost larvae with special reference to feeding and predator avoidance. *Trans. Am. Fish. Soc.*, **115**, 98-114.

Blaxter, J.H.S. (1988) Sensory performance, behaviour, and ecology of fish, in *Sensory Biology of Aquatic Animals* (eds J. Atema, R.R. Fay, A.N.

Popper and W.N. Tavolga), Springer-Verlag, New York, pp. 203-232.

Blaxter, J.H.S. and Fuiman, L.A. (1990) The role of sensory systems of herring larvae in evading predatory fishes. *J. Mar. Biol. Ass. U.K.*, **70**, 413-427.

Blaxter, J.H.S. and Jones, M.P. (1967) The development of the retina and retinomotor responses in the herring. *J. Mar. Biol. Ass. U.K.*, **47**, 677-697.

Blaxter, J.H.S. and Staines, M. (1970) Pure-cone retinae and retinomotor responses in larval teleosts. *J. Mar Biol. Ass. U.K.*, **50**, 449-460.

Blaxter, J.H.S. and Staines, M.E. (1971) Food searching potential in marine fish larvae, in *4th European Marine Biology Symposium Proceedings*. (ed. D.J. Crisp), Cambridge University Press, Cambridge, pp. 467-485.

Boehlert, G.W. (1978) Intraspecific evidence for the function of single and double cones in the teleost retina. *Science, New York*, **202**, 309-311.

Boehlert, G.W. (1979) Retinal development in postlarval through juvenile *Sebastes diploproa*: adaptations to a changing photic environment. *Rev. Can. Biol.*, **38**, 265-280.

Bok, D. and Young, R.W. (1972) The renewal of diffusely distributed protein in the outer segments of rods and cones. *Vision Res.*, **12**, 161-168.

Bowmaker, J.K. (1984) Microspectrophotometry of vertebrate photoreceptors. A brief review. *Vision Res.*, **24**, 1641-1650.

Bowmaker, J.K. (1990) Visual pigments of fishes, in *The Visual System of Fish* (eds. R.H. Douglas and M.B.A. Djamgoz), Chapman and Hall, London, pp. 81-107.

Bowmaker, J.K. (1991) The evolution of vertebrate visual pigments and photoreceptors, in *Evolution of the Eye and Visual System* (eds J.R. Cronly-Dillon and R.L. Gregory), *Vision and Visual Dysfunction, Vol 2*, CRC Press, Boca Raton, pp. 63-81.

Bowmaker, J.K. and Kunz, Y.W. (1987) Ultraviolet receptors, tetrachromatic colour vision and retinal mosaics in the brown trout (*Salmo trutta*): age-dependant changes. *Vision Res.*, **27**, 2101-2108.

Bowmaker, J.K., Thorpe, A. and Douglas, R.H. (1991) Ultraviolet-sensitive cones in the goldfish. *Vision Res.*, **31**, 349-352.

Branchek, T. (1984) The development of photoreceptors in the zebrafish, *Brachydanio rerio*. II. Function. *J. Comp. Neurol.*, **224**, 116-122.

Branchek, T. and Bremiller, R. (1984) The development of photoreceptors in the zebrafish, *Brachydanio rerio*. I. Structure. *J. Comp. Neurol.*, **224**, 107-115.

Breck, J.E. and Gitter, M.J. (1983) Effect of fish size on the reactive distance of bluegill (*Lepomis macrochirus*) sunfish. *Can. J. Fish. Aquat. Sci.*, **40**, 162-167.

Brothers, E.B., Williams, D.McB. and Sale, P.F. (1983) Length of larval life in twelve families of fishes at "One Tree Lagoon", Great Barrier Reef, Australia. *Marine Biol.*, **76**, 319-324.

Browman, H.I., Gordon, W.C., Evans, B.I. and O'Brien, W.J. (1990) Correlation between histological and behavioral measures of visual acuity in a zooplanktivorous fish, the white crappie (*Pomoxis annularis*). *Brain Behav. Evol.*, **35**, 85-97.

Cajal, S.R. (1892) La rétine des vértebrés. *Cellule*, **9**, 121-225.

Caldwell, M.C. (1962) Development and distribution of larval and juvenile fishes of the family Mullidae of the western north Atlantic. *Fish. Bull. US Fish. Widl. Serv.*, **62**, 403-457.

Cameron, D.A. and Pugh, E.N. Jr. (1991) Double cones as a basis for a new type of polarization vision in vertebrates. *Nature, Lond.*, **353**, 161-164.

Carlisle, D.B. and Denton, E.J. (1959) On the metamorphosis of the visual pigments of *Anguilla anguilla* (L.). *J. Mar Biol. Ass. U.K.*, **38**, 97-102.

Choat, J.H., Doherty, P.J., Kerrigan, B.A. and Leis, J.M. (1993) A comparison of towed nets, purse seine and light aggregation devices for sampling larvae and pelagic juveniles of coral reef fishes. *Fish. Bull.*, **91**, 195-209.

Clarke, G.L. (1936) On the depth at which fishes can see. *Ecology*, **17**, 452-456.

Coggeshall, R.E. (1992) A consideration of neural counting methods. *TINS*, **15**, 9-13.

Collin, S.P. and Pettigrew, J.D. (1988a) Retinal topography in reef teleosts. I. Some species with well-developed areae but poorly-developed streaks. *Brain Behav. Evol.*, **31**, 269-282.

Collin, S.P. and Pettigrew, J.D. (1988b) Retinal topography in reef teleosts. II. Some species with prominent horizontal streaks and high-density areae. *Brain Behav. Evol.*, **31**, 283-295.

Collin, S.P. and Pettigrew, J.D. (1989) Quantitative comparison of the limits on visual spatial resolution set by the ganglion cell layer in twelve species of reef teleosts. *Brain Behav. Evol.*, **34**, 184-192.

Crescitelli, F. (1972) The visual cells and visual pigments of the vertebrate eye, in *Handbook of Sensory Physiology, VII/1* (ed. H.J.A. Dartnall), Springer-Verlag, Berlin, pp. 245-365.

Crescitelli, F., McFall-Ngai, M. and Horwitz, J. (1985) The visual pigment sensitivity hypothesis: further evidence from fishes of varying habitats. *J. Comp. Physiol.*, **A. 157**, 323-333.

Dartnall, H.J.A. (1975) Assessing the fitness of visual pigments for their photic environments, in *Vision in Fishes* (ed. M.A. Ali), Plenum Press, New York, pp. 545-563.

Dartnall, H.J.A. (1957) *The Visual Pigments*. Methuen, London.

Dartnall, H.J.A. and Lythgoe, J.N. (1965) The spectral clustering of visual pigments. *Vision Res.*, **5**, 81-100.

Denton, E.J. and Nicol, J.A.C. (1965) Polarization of light reflected from the silvery exterior of the bleak, *Alburnus alburnus*. *J. Mar. Biol. Ass. U.K.*, **45**, 705-709.

Denton, E.J. and Warren, F.J. (1957) The photosensitive pigments in the retinae of deep-sea fish. *J. Mar. Biol. Ass. U.K.*, **36**, 651-662.

Doherty, P.J. (1987) Light-traps: selective but useful devices for quantifying the distributions and abundances of larval fishes. *Bull. Mar. Sci.*, **41**, 423-431.

Doherty, P.J. (1983) Tropical territorial damsel fishes: is density limited by agression or recruitment. *Ecology*, **64**, 176-190.

Doherty, P.J. and Williams, D.McB. (1988) The replenishment of coral reef fish populations. *Oceanogr. Mar. Biol.*, **26**, 487-551.

Douglas, R.H. (1989) The spectral transmission of the lens and cornea of the brown trout (*Salmo trutta*) and goldfish (*Carassius auratus*) - effect of age and implications for ultraviolet vision. *Vision Res.*, **29**, 861-869.

Douglas, R.H. and Hawryshyn, C.W. (1990) Behavioural studies of fish vision: an analysis of visual capabilities, in *The Visual System of Fish* (eds R.H. Douglas and M.B.A. Djamgoz), Chapman and Hall, Lond. pp. 373-418.

Dowling, J.E. (1987) *The Retina.* Belknap Press of Harvard University Press, Cambridge, Mass.

Duncan, G. (1990) *Physics in the Life Sciences.* 2nd Ed. Blackwell, Oxford.

Eberle, H. (1967) Cone length and chromatic aberration in the eye of *Lebistes reticulatus. Z. vergl. Physiol.*, **57**, 172-173.

Eberle, H. (1968) Zapfenbau, zapfenlange und chromatische aberration im auge von *Lebistes reticulatus* Peters (Guppy). *Zool. Jb. Physiol. Bd.*, **74**, 121-154.

Engström, K. (1963) Cone types and cone arrangements in teleost retinae. *Acta Zool., Stockh.* **44**, 179-243.

Evans, B.I. and Fernald, R.D. (1990) Metamorphosis and fish vision. *J. Neurobiol.*, **21**, 1037-1052.

Evans, B.I. and Fernald, R.D. (1993) Retinal transformation at metamorphosis in the winter flounder (*Pseudpleronectes americanus*). *Visual Neurosci.*, **10**, 1055-1064.

Evans, B.I., Hárosi, F.I. and Fernald, R.D. (1993) Photoreceptor spectral absorbance in larval and adult winter flounder (*Pseudpleronectes americanus*). *Visual Neurosci.*, **10**, 1065-1071.

Fernald, R.D. (1985) Growth of the teleost eye: novel solutions to complex constraints. *Environ. Biol. Fish.*, **13**, 113-123.

Fernald, R.D. (1988) Aquatic adaptations in fish eyes, in *Sensory Biology of Aquatic Animals* (eds J. Atema, R.R. Fay, A.N. Popper and W.N. Tavolga), Springer-Verlag, New York, pp. 436-466.

Fernald, R.D. (1989a) Fish vision, in *Development of the Vertebrate Retina* (eds B.L. Finlay and D.R. Sengelaub), Plenum Press, New York, pp. 247-265.

Fernald, R.D. (1989b) Retinal rod neurogenisis, in *Development of the Vertebrate Retina* (eds B.L. Finlay and D.R. Sengelaub), Plenum Press, New York, pp. 31-42.

Fernald, R.D. (1990a) *Haplochromis burtoni*: a case study, in *The Visual System*

of Fish (eds R.H. Douglas and M.B.A. Djamgoz), Chapman and Hall, London, pp. 443-464.

Fernald, R.D. (1990b) The optical system of fishes, in *The Visual System of Fish* (eds R.H. Douglas and M.B.A. Djamgoz), Chapman and Hall, London, pp. 45-61.

Fernald, R.D. and Wright, S.E. (1983) Maintenance of optical quality during crystalline lens growth. *Nature, Lond.*, **301**, 618-620.

Fernald, R.D. and Wright, S.E. (1985) Growth of the visual system in the African cichlid fish, *Haplochromis burtoni*. Optics. *Vision Res.*, **25**, 155-161.

Fineran, B.A. and Nicol, J.A.C. (1974) Studies on the eyes of New Zealand parrot-fishes (Labridae). *Proc. Roy. Soc.*, **B**, **186**, 217-247.

Goldsmith, T.H. (1990) Optimization, constraints, and history in the evolution of eyes. *Quart. Rev. Biol.*, **65**, 281-322.

Grun, A.G. (1982) The development of the vertebrate retina: a comparative study. *Adv. Anat. Embryol. Cell Biol.*, **78**, 1-85.

Guma'a, S.A. (1982) Retinal development and retinomotor responses in perch, *Perca fluviatilis* L. *J. Fish Biol.*, **20**, 611-618.

Hairston Jr, N.G., Li, K.T. and Easter, S.S. Jr. (1982) Fish vision and the detection of planktonic prey. *Science, N. Y.*, **218**, 1240-2142.

Hamner, W.M., Jones, M.S., Carleton, J.H., Hauri, I.R. and Williams, D.McB. (1988) Zooplankton, planktivorous fish, and water currents on a windward reef face: Great Barrier Reef, Australia. *Bull. Mar. Sci.*, **42**, 459-479.

Hárosi, F.J. (1985) Ultraviolet- and violet-absorbing vertebrate visual pigments: dichroic and bleaching properties, in *The Visual System* (eds A. Fein and J.S. Levine), Liss, New York, pp. 41-55.

Hárosi, F.I. and Hashimoto, Y. (1983) Ultraviolet visual pigment in a vertebrate: A tetrachromatic cone system in the dace. *Science, N. Y.*, **222**, 1021-1023.

Hawryshyn, C.W. and Beauchamp, R. (1985) Ultraviolet photosensitivity in goldfish: an independant u.v. retinal mechanism. *Vision Res.*, **25**, 11-20.

Hawryshyn, C.W. and McFarland, W.N. (1987) Cone photoreceptor mechanisms and the detection of polarized light in fish. *J. Comp. Physiol.*, **A**, **160**,

459-465.

Hawryshyn, C.W., Arnold, M.G., Bowering, E. and Cole, R.L. (1990) Spatial orientation of rainbow trout to plane-polarized light: the ontogeny of E-vector discrimination and spectral sensitivity characteristics. *J. Comp. Physiol.*, **A, 166**, 565-574.

Helmholtz, H. von (1924-25) *Physiological Optics, Vols I,II,III.* Optical Society of America, Rochester, New York.

Hobson, E.S. (1965) Diurnal-nocturnal activity of some inshore fishes in the Gulf of California. *Copeia*, **3**, 291-302.

Hobson, E.S. (1972) Activity of Hawaiian reef fishes during the evening and morning transitions between daylight and darkness. *Fish. Bull.*, **70**, 715-740.

Hunter, J.R. (1981) Feeding ecology and predation of marine fish larvae, in *Marine Fish Larvae* (ed. R. Lasker), Washington Sea Grant Program, University of Washington Press, Seattle, pp. 33-77.

Jerlov, N.G. (1976) *Marine Optics*. Elsevier, Amsterdam.

Johns, P.R. (1981) Growth of fish retinas. *Amer. Zool.*, **21**, 447-458.

Johns, P.R. (1982) Formation of photoreceptors in larval and adult goldfish. *J. Neurosci.*, **2**, 178-198.

Johns, P.R. and Easter, S.S. Jr. (1977) Growth of the adult goldfish eye II. Increase in retinal cell number. *J. Comp. Neurol.*, **176**, 331-342.

Johns, P.R. and Fernald, R.D. (1981) Genesis of rods in teleost fish retina. *Nature, Lond.*, **293**, 141-142.

Kawamura, G., Tsuda, R., Kumai, H. and Ohashi, S. (1984) The visual cell morphology of *Pagus major* and its adaptive changes with shift from pelagic to benthic habitats. *Bull. Jap. Soc. Sci. Fish.*, **50**, 1975-1980.

Kendall, A.W. Jr., Ahlstrom, E.H. and Moser, H.G. (1984) Early life history stages of fishes and their characters, in *Ontogeny and Systematics of Fishes* (eds H.G. Moser, W.J. Richards, D.M. Cohen, M.P. Facey, A.W. Kendall Jr. and S.L. Richardson) Amer. Soc. Ichthyol. Herpetol. Spec. Publ., pp. 11-22.

Kingsford, M.J. and Choat, J.H. (1985) The fauna associated with drift algae

captured with a plankton-mesh purse seine net. *Limnol. Oceanogr.*, **30**, 618-630.

Kirschfeld, K. (1976) The resolution of lens and compound eyes, in *Neural Principles in Vision* (eds F. Zettler and R. Weiler), Springer-Verlag, Berlin, pp. 354-370.

Knowles, A. and Dartnall, H.J.A. (1977) The photobiology of vision, in *The Eye*, (ed. H. Davson), Vol 2B. Academic, Lond., pp. 1-689.

Kock, J-H. (1982) Neuronal addition and retinal expansion during growth of the crucian carp eye. *J. Comp. Neurol.*, **209**, 264-274.

Kunz, Y.W., Ennis, S. and Wise, C. (1983) Ontogeny of the photoreceptors in the embryonic retina of the viviparus guppy, *Poecilia reticulata* P. (Teleostei). *Cell Tissue Res.*, **230**, 469-486.

Land, M.F. (1981) Optics and vision in invertebrates, in *Handbook of Sensory Physiology VII/6B* (ed. H. J. Autrum), Springer-Verlag, Berlin, pp. 471-592.

Land, M. F. (1987) Vision in air and water, in *Comparative Physiology: Life in Water and on Land* (eds. P. Dejours, L. Bolis, C.R. Taylor, and E.R. Weibel), Liviana, Padova, pp 289-302.

Leis, J.M. (1991a) The plagic stage of reef fishes: The larval biology of coral reef fishes, in *The Ecology of Fishes on Coral Reefs* (ed. P.F. Sale), Academic Press, San Diego pp. 183-230.

Leis, J.M. (1991b) Vertical distribution of fish larvae in the Great Barrier Reef Lagoon, Australia. *Marine Biol.*, **109**, 157-166.

Leis, J.M. and Rennis, D.S. (1983) *The Larvae of Indo-Pacific Coral Reef Fishes*. New South Wales University and University of Hawaii.

Leis, J.M. and Trnski, T. (1989) *The Larvae of Indo-Pacific shore Fishes*. New South Wales University, Kensington.

Levine, J.S. and MacNichol, E.F. Jr. (1979) Visual pigments in teleost fishes: Effects of habitat, microhabitat, and behavior on visual system evolution. *Sens. Processes*, 3, 95-131.

Levine, J.S. and MacNichol, E.F.Jr. (1985) Microspectrophotometry of primate photoreceptors: Art, artifact, and analysis, in *The Visual System* (eds A.

Fein and J.S. Levine), Liss, New York, pp. 73-87.

Liebman, P.A. (1972) Microspectrophotometry of photoreceptors, in *Handbook of Sensory Physiology, VII/1* (ed H.J.A. Dartnall), Springer-Verlag, New York, pp. 481-528.

Locket, N.A. (1977) Adaptations to the deep-sea environment, in *Handbook of Sensory Physiology, VII/5* (ed. F. Crescitelli), Springer-Verlag, New York, pp. 65-192.

Loew, E.R. and Dartnall, H.J.A. (1976) Vitamin A1/A2-based visual pigment mixtures in cones of the rudd. *Vision Res.*, **16**, 891-896.

Loew, E.R. and Lythgoe, J.N. (1978) The ecology of cone pigments in teleost fishes. *Vision Res.*, **18**, 715-722.

Loew, E.R. and McFarland, W.N. (1991) The underwater visual environment, in *The Visual System of Fish* (eds R.H. Douglas, and M.B.A. Djamgoz), Chapman and Hall, London. pp. 1-43.

Loew, E.R. and Wahl, C.M. (1991) A short-wavelength sensitive cone mechanism in juvenille yellow perch, *Perca flavescens. Vision Res.*, **31**, 353-360.

Loew, E.R., McFarland, W.N., Mills, E.L. and Hunter, D. (1993) A chromatic action spectrum for planktonic predation by juvenile yellow perch, *Perca flavescens. Can. J. Zool.*, **71**, 384-386.

Lyall, A.H. (1957) The growth of the trout retina. *Q. J. Microsc. Sci.* **98**, 101-110.

Lythgoe, J.N. (1966) Visual pigments and visual range underwater, in *Light as an Ecological Factor* (eds R. Bainbridge, G.C. Evans and O. Rackham), Blackwell, Oxford, pp. 375-391.

Lythgoe, J.N. (1968) Visual pigments and visual range underwater. *Vision Res.*, **8**, 997-1012.

Lythgoe, J.N. (1971) Iridescent corneas in fishes. *Nature, Lond.*, **233**, 205-207.

Lythgoe, J.N. (1975) The structure and function of iridescent corneas in teleost fishes. *Proc. R. Soc.*, **B**, **188**, 437-457.

Lythgoe, J.N. (1979) *The Ecology of Vision.* Clarendon Press, Oxford.

Lythgoe, J.N. (1984) Visual pigments and environmental light. *Vision Res.*, **24**,

1539-1550.

Lythgoe, J.N. (1988) Light and vision in the aquatic environment, in *Sensory Biology of Aquatic Animals* (eds J. Atema, R.R. Fay, A.N. Popper and W.N. Tavolga), Springer-Verlag, New York, pp. 57-82.

Lythgoe, J.N. and Partridge, J.C. (1989) Visual pigments and the aquisition of visual information. *J. Exp. Biol.*, **146**, 1-20.

Lythgoe, J.N. and Shand, J. (1983) Endogenous circadian retinomotor movements in the neon tetra (*Paracheirodon innesi*). *Invest. Opthalmol. Vis. Sci.*, **24**, 1203-1210.

Lythgoe, J.N., Muntz, W.R.A., Partridge, J.C., Shand, J. and Williams, D.McB. (1994) The ecology of the visual pigments of snappers (Lutjanidae) on the Great Barrier Reef. *J. Comp. Physiol.*, **A**, 174, (in press).

MacNichol, E.F. Jr. (1986) A unifying presentation of photopigment spectra. *Vision Res.*, **26**, 1543-1556.

Margulies, D. (1989) Size-specific vulnerability to predation and sensory system development of white seabass, *Atractoscion nobilis*, larvae. *Fish. Bull.*, **87**, 537-552.

Mas-Riera, J. (1991) Changes during growth in the retinal structure of three hake species, *Merluccius* spp. (Teleostei: Gadiformes) in relation to their depth distribution and feeding. *J. Exp. Mar. Biol. Ecol.* **152**, 91-104.

McCormick, M.I. (1992) *The influence of pelagic life history on the quality of tropical goatfish (family Mullidae) at settlement.* PhD Thesis, James Cook University of North Queensland, Townsville.

McCormick, M.I. (1993) Development and changes at settlement in the barbel structure of the reef fish, *Upeneus tragula* (Mullidae). *Environ. Biol. Fish.*, **37**, 269-282.

McCormick, M.I. (1994) Variability in age and size at settlement of the tropical goatfish *Upeneus tragula* (Mullidae) in the northern Great Barrier Reef Lagoon. *Mar. Ecol. Prog. Ser.*, (in press).

McCormick, M.I. and Milicich, M.J. (1993) Late pelagic stage goatfishes: distribution patterns and inferences on schooling behaviour. *J. Exp. Mar. Biol. Ecol.*, **174**, 15-42.

McFall-Ngai, M.J. (1990) Crypsis in the pelagic environment. *Amer. Zool.*, **30**, 175-188.

McFarland, W.N. (1986) Light in the sea - correlations with behaviours of fishes and invertebrates. Amer. Zool., **26**, 389-401.

McFarland, W.N. (1991) The visual world of coral reef fishes, in *The Ecology of Fishes on Coral Reefs* (ed. P.F. Sale), Academic Press, San Diego, pp. 16-38.

McFarland, W.N. and Munz, F.W. (1975a) The photic environment of clear tropical seas during the day. *Vision Res.*, **15**, 1063-1070.

McFarland, W.N. and Munz, F.W. (1975b) The evolution of photopic visual pigments in fishes. *Vision Res.*, **15**, 1071-1080.

Meekan, M.G. (1992) *The influence of pre- and post-settlement processes on the population dynamics of coral reef fishes*. PhD Thesis, Griffith University, Brisbane.

Miller, T.J., Crowder, L.B. and Rice, J.A. (1993) Ontogenetic changes in behavioural and histological measures of visual acuity in three species of fish. *Environ. Biol. Fish.*, **37**, 1-8.

Miller, T.J., Crowder, L.B., Rice, J.A. and Marschall, E.A. (1988) Larval size and recruitment mechanisms in fishes: toward a conceptual framework. *Can. J. Fish. Aquat. Sci.*, **45**, 1657-1670.

Molnar, L.M. (1974) Double embedding with nitrocellulose and paraffin. *Stain Technol.*, **49**, 311.

Morel, A. (1974) Optical properties of pure water and seawater, in *Optical aspects of Oceanography* (eds N.G.Jerlov and E. Steeman), Nielsen, Academic Press, London, pp 1-24.

Moser, H.G. (1981) Morphological and functional aspects of marine fish larvae, in *Marine Fish Larvae* (ed. R. Lasker), Washington Sea Grant Program, University of Washington Press, Seattle, pp. 89-131.

Munk, O. (1990) Changes in the visual cell layer of the duplex retina during growth of the eye of a deep-sea teleost, *Gempylus serpens* Cuvier, 1829. *Acta Zool.*, **71**, 89-95.

Muntz, W.R.A. (1974) Comparative aspects in behavioral studies of vertebrate

vision, in *The Eye, Vol. 6* (eds H. Davson and L.T. Graham Jr). Academic, New York, pp. 155-226.

Muntz, W.R.A. (1976) The visual consequences of yellow filtering pigments in the eyes of fishes occupying different habitats, in *Light as an Ecological Factor II.* (eds G.C. Evans, R. Bainbridge and O Rackham), Blackwell Scientific, Oxford, pp. 271-287.

Muntz, W.R.A. and Mouat, G.V.S. (1984) Annual variations in the visual pigments of brown trout inhabiting lochs providing different light environments. *Vision Res.*, **24**, 1575-1580.

Munz, F.W. (1958) Photosensitive pigments from the retinae of certain deep-sea fishes. *J. Physiol.*, **140**, 220-235.

Munz, F.W and McFarland, W.N. (1973) The significance of spectral position in the rhodopsins of tropical marine fishes. *Vision Res.*, **13**, 1829-1874.

Munz, F.W and McFarland, W.N. (1977) Evolutionary adaptations of fishes to the photic environment, in *Handbook of Sensory Physiology VII/5* (ed. F. Crescitelli), Springer-Verlag, New York, pp. 193-274.

Myers, R.F. (1989) *Micronesian Reef Fishes.* Coral Graphics, Guam.

Nathans, J., Thomas, D. and Hogness, D.S. (1986) Molecular genetics of human color vision: The genes encoding blue, green and red pigments. *Science, N. Y.*, **232**, 193-202.

Neave, D.A. (1984) The development of visual acuity in larval plaice (*Pleuronectes platessa* L.) and turbot (*Scophthalmus maximus* L.). *J. Exp. Mar. Biol. Ecol.* **78**, 167-175.

Nicol, J.A.C. (1989) *The Eyes of Fishes.* Clarendon Press, Oxford.

Noakes, D.L.G. and Godin, J-G.J. (1988) Ontogeny of behavior and concurrent developmental changes in sensory systems in teleost fishes, in *Fish Physiology Vol. XIB* (eds W.S. Hoar and D.J. Randall), Academic, London, pp 345-395.

Northmore, D.P.M. and Dvorak, C.A. (1979) Contrast sensitivity and acuity of the goldfish. *Vision Res.*, **19**, 255-261.

O'Day, W.T. and Young, R.W. (1978) Rhythmic shedding of outer-segment membranes by visual cells in the goldfish. *J. Cell Biol.*, **76**, 593-604.

Okiyama, M. 1988 (ed.) *An Atlas of the Early Stages of Fishes in Japan.* Tokai University Press.

Orlov, O.Y. and Gamburtzeva, A.G. (1976) Changeable coloration of cornea in the fish *Hexagrammos octogrammus. Nature, Lond.*, **263**, 405-407.

Pankhurst, N.W. (1982) The relation of visual changes to the onset of sexual maturation in the European eel *Anguilla anguilla* (L.). *J. Fish Biol.*, **21**, 127-140.

Pankhurst, N.W. (1984) Retinal development in larval and juvenile European eel *Anguilla anguilla* (L.). *Can. J. Zool.*, **62**, 335-343.

Pankhurst, N.W. (1987) Intra- and interspecific changes in retinal morphology among mesopelagic and demersal teleosts from the slope waters of New Zealand. *Environ. Biol. Fish.*, **19**, 269-280.

Pankhurst, N.W. (1989) The relationship of ocular morphology to feeding modes and activity periods in shallow marine teleosts from New Zealand. *Environ. Biol. Fish.*, **26**, 201-211.

Pankhurst, N.W. and Lythgoe, J.N. (1983) Changes in vision and olfaction during sexual maturation in the European eel *Anguilla anguilla* (L.). *J. Fish Biol.*, **23**, 229-240.

Pankhurst, P.M., Pankhurst, N.W. and Montgomery, J.C. (1993) Comparison of behavioural and morphological measures of visual acuity during ontogeny in the teleost fish *Forsterygion varium*, Tripterygiidae (Forster, 1801). *Brain Behav. Evol.*, **42**, 178-188.

Partridge, J.C. (1990) The colour sensitivity and vision of fishes, in *Light and Life in the Sea* (eds P.J. Herring, A.K. Campbell, M. Whitfield and L. Maddock), Cambridge University, Cambridge, pp. 167-184.

Partridge, J.C. and De Grip, W.J. (1991) A new template for rhodopsin (vitamin A_1 based) visual pigments. *Vision Res.*, **31**, 619-630.

Partridge, J.C., Archer, S.N. and Lythgoe, J.N. (1988) Visual pigments in the individual rods of deep-sea fishes. *J. Comp. Physiol.*, **A**, **162**, 543-550.

Partridge, J.C., Shand, J., Archer, S.N., Lythgoe, J.N. and van Groningen-Luyben, W.A.H.M. (1989) Interspecific variation in the visual pigments of deep-sea fishes. *J. Comp. Physiol.*, **A**, **164**, 513-529.

Partridge, J.C., Speare, P., Shand, J., Muntz, W.R.A. and Williams, D.McB. (1992) Microspectrophotometric determinations of rod visual pigments in some adult and larval Australian amphibians. *Visual Neurosci.*, **9**, 137-142.

Powers, M.K. and Easter, S.S. (1978) Absolute visual sensitivity of the goldfish. *Vision Res.*, **18**, 1137-1147.

Powers, M.K. and Raymond, P.A. (1990) Development of the visual system, in *The Visual System of Fish* (eds R.H. Douglas and M.B.A. Djamgoz), Chapman and Hall, Lond., pp. 419-442.

Powers, M.K., Bassi, C.J., Rone, L.A. and Raymond, P.A. (1988) Visual detection by the rod system in goldfish of different sizes. *Vision Res.*, **28**, 211-221.

Rahmann, H., Jeserich, G. and Zeutzius, I. (1979) Ontogeny of visual acuity of rainbow trout under normal conditions and light deprivation. *Behaviour*, **68**, 315-322.

Randall, J.E., Allen, G.R. and Steene, R.C. (1990) *Fishes of the Great Barrier Reef and Coral Sea.* Crawford, Bathurst.

Raymond, P.A. (1985) Cytodifferentiation of photoreceptors in larval goldfish: Delayed maturation of rods. *J. Comp. Neurol.*, **236**, 90-105.

Reynolds, E.S. (1963) The use of lead citrate at high pH as an electron opaque stain for electron microscopy. *J. Cell Biol.*, **17**, 208-212.

Sadler, J.D. (1973) The focal length of the fish lens and visual acuity. *Vision Res.*, **13**, 417-423.

Sandy, J.M. and Blaxter, J.H.S. (1980) A study of retinal development in larval herring and sole. *J. Mar. Biol. Ass. U.K.*, **60**, 59-71.

Schmitt, E. and Kunz, Y.W. (1989) Retinal morphogenesis in the rainbow trout, *Salmo gairdneri. Brain Behav. Evol.*, **34**, 48-64.

Scholes, J.H. (1975) Colour receptors, and their synaptic connexions, in the retina of a cyprinid fish. *Phil. Trans. R. Soc.*, **B, 270**, 61-118.

Scholes, J.H. (1976) Neuronal connections and cellular arrangement in the fish retina, in *Neural Principles in Vision* (eds. F. Zettler and R. Weiler), Springer-Verlag, New .York, pp. 63-93.

Shand, J. (1988) Corneal iridescence in fishes: light-induced colour changes in relation to structure. *J. Fish Biol.*, **32**, 625-632.

Shand, J. (1993) Changes in the spectral absorption of cone visual pigments during the settlement of the goatfish *Upeneus tragula*: the loss of red sensitivity as a benthic existence begins. *J. Comp. Physiol.*, **A, 173,** 115-121.

Shand, J. (1994) Changes in retinal structure during development and settlement of the goatfish Upeneus tragula. *Brain Behav. Evol.*, **43**, 51-60.

Shand, J. and Lythgoe, J.N. (1988) Light-induced changes in corneal iridescence in fish. *Vision Res.*, **27**, 303-305.

Shand, J., Partridge, J.C., Archer, S.N., Potts, G.W. and Lythgoe, J.N. (1988) Spectral absorbance changes in the violet/blue sensitive cones of the juvenile pollack, *Pollachius pollachius*. *J. Comp. Physiol.*, **A, 163,** 699-703.

Sharma, S.C. and Ungar, F. (1980) Histogenesis of the goldfish retina. *J. Comp. Neurol.*, **191**, 373-382.

Snyder, A.W. (1979) The physics of vision in compound eyes, in *Handbook of Sensory Physiology, Vol VII/6* (ed. H.J. Autrum), Springer-Verlag, Berlin, pp. 225-313.

Spurr, A.R. (1969) A low-viscocity epoxy resin embedding medium for electron microscopy. *J. Ultrstr. Res.*, **26**, 31-43.

Sroczyński, S. (1976) Die chromatische aberration der augenlinse der regenbogenforelle (*Salmo gairdneri* Rich). *Zool. Jb. Physiol.*, **80**, 432-450.

Tamura, T. (1957) A study of visual perception in fish, especially on resolving power and accommodation. *Bull. Jap. Soc. Sci. Fish.*, **22**, 536-557.

Tamura, T. and Wisbey, S.J. (1963) The visual sense of pelagic fishes especially the visual axis and accommodation. *Bull. Mar. Sci. Gulf Caribb.*, **13,** 433-448.

Thorpe, A. and Douglas, R.H. (1993) Spectral transmission and short-wave absorbing pigments in the fish lens -II. Effects of age. *Vision Res.*, **33,** 301-307.

Thresher, R.E., Colin, P.L. and Bell, L.J. (1989) Planktonic duration,

distribution and population structure of western and central Pacific damselfishes (Pomacentridae). *Copeia*, 420-434.

Victor, B.C. (1983) Recruitment and population dynamics of a coral reef fish. *Science, N. Y.*, **219**, 419-420.

Victor, B.C. 1986 Duration of the planktonic larval stage of one hundred species of Pacific and Atlantic wrasses (family Labridae). *Marine Biol.*, **90**, 317-326.

Victor, B.C. (1991) Settlement strategies and biogeography of reef fishes, in *The Ecology of Fishes on Coral Reefs* (ed. P.F. Sale), Academic Press, San Diego, pp. 231-260.

Wagner, H.-J. (1978) Cell types and connectivity patterns in mosaic retinas. *Adv. Anat. Embryol. Cell Biol.* **55**, 1-81.

Wagner, H.-J. (1990) Retinal structure of fishes, in *The Visual System of Fish* (eds R.H. Douglas and M.B.A. Djamgoz), Chapman and Hall, London., pp. 109-157.

Wahl, C.M., Mills, E.L., McFarland, W.N. and DeGisi, J.S. (1993) Ontogenetic changes in prey selection and visual acuity of the yellow perch, *Perca flavescens. Can. J. Fish. Aquat. Sci.*, **50**, 743-749.

Walls, G.L. (1942) *The Vertebrate Eye and its Adaptive Radiation.* Hafner, New York.

Wanzenböck, J. and Schiemer, F. (1989) Prey detection in cyprinids during early development. *Can. J. Fish. Aquat. Sci.*, **46**, 995-1001.

Wellington, G.M. and Victor, B.C. (1989) Planktonic larval duration of one hundred species of Pacific and Atlantic damselfishes (Pomacentridae). *Marine Biol.* **101**, 557-567.

Williams, D.McB. (1980) Dynamics of the pomacentrid community on small patch reefs in One Tree Lagoon (Great Barrier Reef). *Bull. Mar. Sci.*, **30**, 159-170.

Williams, D.McB. and Russ, G.R. (1991) Review of data on fishes of commercial and recreational fishing interest on the Great Barrier Reef. Unpublished report to the Great Barrier Reef Marine Park Authority, Townsville, Queensland.

Williamson, M. and Keast, A. (1988) Retinal structure relative to feeding in the rock bass (*Ambloplites rupestris*) and bluegill (*Lepomis macrochirus*). *Can. J. Zool.*, **66**, 2840-2846.

Winsor, L. (1984) *Manual of Basic Zoological Microtechniques for Light Microscopy*. 4th Edition, James Cook University of North Queensland, Townsville.

Winsor, L. (1994) Tissue processing, in *Laboratory Histopathology. A Complete Reference* (eds A.E. Woods and R.E. Ellis), Ch. 7, Churchill Livingstone (in press).

Wood, P. and Partridge, J.C. (1993) Opsin substitution induced in retinal rods of the eel (*Anguilla anguilla* (L.)): a model for G-protein-linked receptors. *Proc. R. Soc. Lond.*, **B**, **254**, 227-232.

Wood, P., Partridge, J.C. and De Grip, W.J. (1992) Rod visual pigment changes in the elver of the eel *Anguilla anguilla* L. measured by microspectrophotometry. *J. Fish Biol.*, **41**, 601-611.

Yamanouchi, T. (1956) The visual acuity of the coral fish *Microcanthus strigatus* (Cuvier and Valenciennes). *Publ. Seto Mar. Biol. Lab.*, **5**, 133-156.

Young, R.W. (1969) A difference between rods and cones in the renewal of outer segment protein. *Invest. Opthalmol.*, **8**, 222-231.

Young, R.W. (1976) Visual cells and the concept of renewal. *Invest. Opthalmol.* **15**, 700-725.

Youson J.H. (1988) First metamorphosis, in *Fish Physiology* (eds W.S. Hoar and D.J. Randall) Vol 11b, Academic, New York, pp. 135-196.

Zar, J.H. (1984) *Biostatistical Analysis*. 2nd Edition, Prentice-Hall, New Jersey.

Zaunreiter, M., Junger, H. and Kotrschal, K. (1991) Retinal morphology of cyprinid fishes: a quantitative histological study of ontogenetic changes and interspecific variation. *Vision Res.*, **31**, 383-394.

APPENDIX 1

Estimation of Shrinkage During Histological Processing

Introduction

Fixation, dehydration and embedding of biological specimens is known to cause shrinkage to the tissues involved (Baker, 1958). It is also known that such shrinkage can depend upon the type of tissue being treated and the fixative being used (Tarkhan, 1931; Stowell, 1941; Baker, 1958; Penttila *et al.*, 1975; Stickland, 1975; Winsor, 1994). In this thesis measurements of eye and lens diameter were made following fixation, and subsequent storage in ethanol, but prior to embedding. In addition, data such as retinal cell dimensions and their densities were obtained from embedded and sectioned material. These data were then incorporated into equations which give an insight into the visual capabilities of fish. For example, the visual acuity calculations include data on lens radius and cone density (see Part I). Before using the data for any calculations it was therefore necessary to consider the amount of shrinkage in the different tissues at the different stages of the histological procedure and to make corrections accordingly. This appendix describes how correction factors for shrinkage of a number of morphological dimensions, at different stages of the embedding procedure, were obtained.

Materials and Methods

The procedure followed was that used to fix, store and embed retinal material in wax blocks (Part I). No estimation of shrinkage in Spurr embedded material was made since dimensions and cell counts were not obtained from this material.

Nine *Terapon theraps* and six *Ambassis vachelli* of 4 different size classes were

used. The fish were assigned to the following size classes according to standard length (SL) and eye diameter (ED):

1) SL 7 - 16 mm ED 0.61 - 1.6 mm
2) SL 17 - 26 mm ED 1.61 - 2.6 mm
3) SL 27 - 36 mm ED 2.61 - 3.6 mm
4) SL 37 - 46 mm ED 3.61 - 4.6 mm

Dimensions of the following were recorded: SL; horizontal and vertical eye diameter; and lens diameter. Measurements were made prior to fixation in sea water Bouins (see Part I for formula) and at the following stages of the embedding procedure (referred to as treatments A - D below):

A) after 48 hr in Bouins but prior to immersion in 70% ethanol;
B) after 7 days in 70% ethanol;
C) after 75 days in ethanol;
D) after embedding in wax.

The 'in block' measurements were not made of SL as only the heads were embedded. To obtain measurements of the eye and lens from embedded material the eye was sectioned either vertically or horizontally until the mid-point was reached, thus one eye could only be used for a vertical or horizontal measurement. The results were analysed by two-way ANOVA, looking for differences between size classes and treatments or any interaction between the two. Correction factors for the amount of shrinkage in the different tissues were obtained by pooling the data and calculating a mean value or fitting a regression curve, whichever was appropriate following the ANOVA results.

In addition, the possibility of size reduction resulting from non-recovered compression during sectioning was considered by measuring the specimens in the wax blocks and comparing the measurements with similar dimensions on the stained slides.

Results

The percentage shrinkage at various stages of the embedding procedure for the three morphological measurements are given in Table A1.1. The percentage shrinkage (%SH) was calculated as:

$$\%SH = ((TM - M)/TM) \times 100 \qquad \text{Eqn. A1.1}$$

where TM is the true measurement (i.e. before fixation) and M is the measurement made after the treatments. The significance of the amount of shrinkage for each of the dimensions measured is considered separately below.

Standard Length: There is no significant difference in the amount of shrinkage in the SL between treatments (ANOVA F = 1.09; DF = 2/24; P = 0.3532) or between size classes of fish (ANOVA F = 3.77; DF = 3/24; P = 0.0239) at the 0.01% level. Although the difference in the amount of shrinkage between the size classes of fish is significant at the 0.05% level it followed no general pattern with the mean % shrinkage being 2.1 $\pm$ 0.3, 1.7 $\pm$ 1.2, 1.4 $\pm$ 0.5 and 3.3 $\pm$ 0.9 for size groups 1 - 4 respectively (see also Table A1.1). Thus, the mean % shrinkage (2.1 $\pm$ 0.8), derived from all the results, was used.

Eye diameter: The % shrinkage which occurred following the three treatments A, B, and C (see Table A1.1) was found not to be significantly different (ANOVA F = 0.09; DF = 2/132; P = 0.9064). However, comparisons between different size groups of fish, were found to be significantly different (F = 30.85; DF = 3/132; P < 0.000). There was no significant interaction between the treatments and size groups (F = 1.39; DF = 6/132; P = 0.2213). Since in this study all the measurements of eye diameter (ED) were made following fixation and subsequent storage in alcohol a correction factor needs to be applied before using the data. This was obtained by plotting the data for the % shrinkage after each of the first three treatments (but not after embedding) and fitting a regression curve. Four regression curves were fitted to the data (Fig. A1.1):

Table A1.1 The percentage shrinkage and standard deviation of standard length, eye diameter and lens diameter in four size groups of fish, at various stages of the fixation and embedding procedure.

Dimension measured Treatment at time of measurement	size group 1 SL 7 - 16 mm ED 0.61 - 1.6 mm	size group 2 SL 17 - 26 mm ED 1.61 - 2.6 mm	size group 3 SL 27 - 36 mm ED 2.61 - 3.6 mm	size group 4 SL 37 - 46 mm ED 3.61 - 4.6 mm
Standard length % shrinkage	n = 6	n = 3		
A After 40 hr bouins	1.8 ± 1.48	0.96 ± 0 .73	1.9 ± 1.68	4.3 ± 0.75
B After 7 days ethanol	2.4 ± 1.5	1.06 ± 0.73	0.96 ± 1.19	2.6 ± 2.07
C After 75 days ethanol	2.1 ± 1.73	3.06 ± 0.7	1.46 ± 1.0	3.0 ± 1.16
Eye diameter % shrinkage	n = 24	n = 12		
A After 40 hr bouins	7.5 ± 3.04	4.05 ± 1.7	2.65 ± 2.88	2.99 ± 2.4
B After 7 days ethanol	7.4 ± 3.45	4.33 ± 1.9	2.61 ± 2.87	2.76 ± 1.3
C After 75 days ethanol	6.5 ± 3.13	6.68 ± 2.5	4.125 ± 3.8	1.94 ± 1.9
D After embedding	14 ± 3.13 (n=12)	11.3 ± 1.7 (n=4)	11.75 ± 4.07 (n=5)	11.26 ± 1.3 (n=3)
Lens diameter % shrinkage	n = 12	n = 6		
A After 40 hr bouins	0	0	0	0
B After 7 days ethanol	0	0	0	0
C After 75 days ethanol	0	0	0	0
D After embedding	4.8 ± 6.0	8.25 ± 5.6 (n=4)	10 ± 4.7 (n=2)	7.8 ± 3.4 (n=3)

(1) Linear: % shrinkage = 9.0603 - 1.7694(ED); r^2 = 0.36; F = 99.77; DF = 1/176; P< <0.

(2) Log curve: % shrinkage = 7.396 - 8.101 log(ED); r^2 = 0.36; F = 99.148; DF = 1/176; P< <0.

(3) Exponential decay: % shrinkage = $10.59e^{-0.3627ED}$; r^2 = 0.35; F = 92.897; DF = 1/176; P< <0.

(4) Power curve; % shrinkage = $7.356ED^{-0.6761}$; r^2 = 0.35; F = 94.7055; DF = 1/176; P< <0.

All curves fit the data similarly within the range of measured eye size (Fig. A1.1). But, the log (2) and power curve (4) both give increasingly high values for % shrinkage when extrapolated beyond the data at small measurements of ED, while the linear fit (1) gives very low % shrinkage at higher values of eye size. Thus the exponential decay curve was used to calculate a correction factor since it is the more conservative when extrapolated beyond the data points. The following procedure was used to obtain the true eye diameter (TED) from the measured eye diameter (ED) and the % shrinkage (%SH):

since $\%SH = ((TED - ED)/TED) \times 100$ Eqn. A1.1

then $TED \times (\%SH/100) = TED - ED$

which gives: $TED = ED\ (1/(1 - (\%SH/100)))$

Substituting the exponential regression curve (3) for %SH gives:

$$TED = ED\ (1/(1 - (10.59 \times 10^{-2}\ e^{-0.3627ED}))) \qquad \text{Eqn. A1.2}$$

All measurements of eye diameter were corrected using this equation.

Following embedding (treatment D) a significant increase in shrinkage occurred so that the comparisons between treatments gave P < 0.000 (F = 31.2; DF = 3/32). But after this treatment there was no difference between the size classes of fish (F = 0.79; DF = 3/32; P = 0.5075) or interaction between treatment and size group (F = 1.0; DF = 9/32; P = 0.4631). Thus all the results obtained

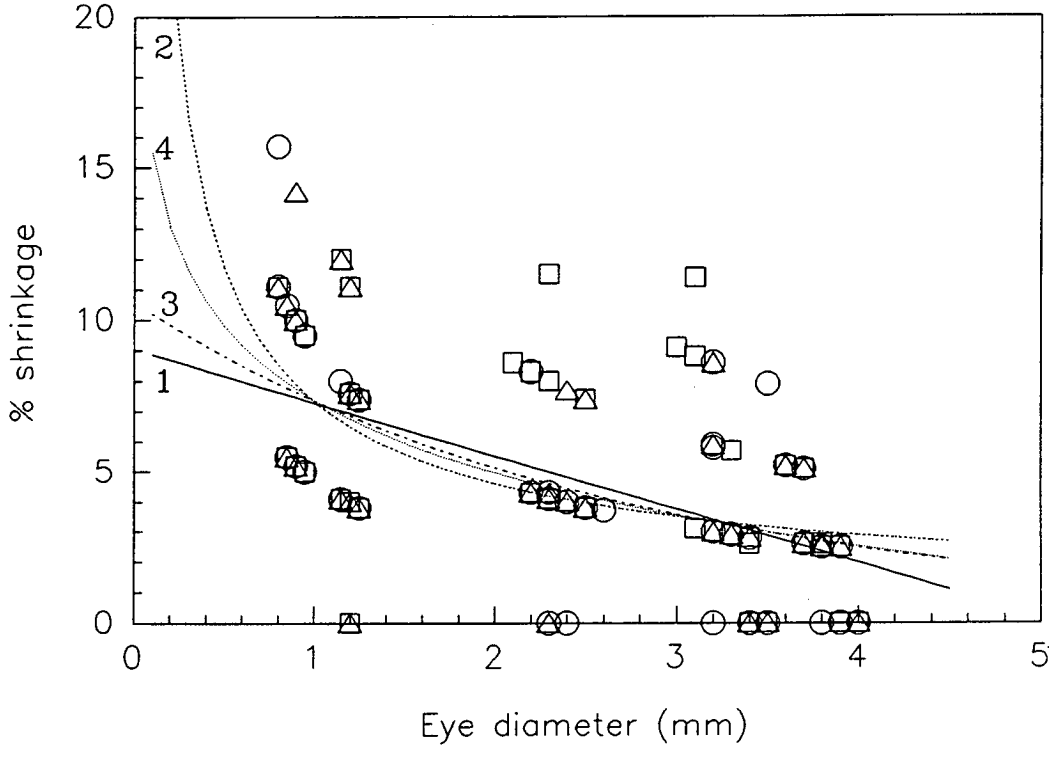

Fig. A.1.1 Graph showing the four possible regression curves fitted to the data for the percentage shrinkage of eye diameter following each of the three treatments (A, circles; B, triangles; C, squares). Curve 1, linear; 2, log; 3, exponential decay; 4, power. The exponential decay curve was selected for calculating the correction factor to the eye diameter since it is the most conservative when extrapolated beyond the data points.

from all fish following embedding were pooled and one correction factor calculated. The shrinkage following embedding was 12.08%. This correction was employed when measurements from embedded material were used, such as in the calculations of visual acuity (Part I).

Lens diameter: Following treatments A, B, and C no shrinkage in the lens was recorded (Table A1.1). Thus no correction factor needs to be applied to the measurements of lens diameter made during this study. An increase in shrinkage was measured after treatment D (embedding) however, since no measurements of lens diameter were made from embedded material at any stage of this thesis it is not necessary to calculate a correction for this shrinkage.

Shrinkage due to compression during sectioning: No differences were found when comparing the dimensions of the tissues in the wax blocks with those measured from the stained sections.

Discussion

The measurements of primary importance investigated during this experiment were those used in calculations of visual capability i.e. the lens and eye dimensions obtained prior to embedding in wax and the retinal cell density records obtained from embedded material. As might be expected the crystalline lens did not shrink prior to embedding, whereas the softer tissue of the eye cup did shrink. Furthermore, the shrinkage of the eye cup was related to the size of the eye. Following embedding, increased shrinkage occurred but with no apparent relationship to eye size. The average shrinkage following embedding of 12 % compares with that of 12 % stated by Mas-Riera (1991) in the eyes of three hake species and 10 % obtained by Neave (1984) in the eyes of flatfish. However, these values are much less than the 25% stated by Tamura and Wisbey (1963) for a range of marine species. All these studies used Bouins as the fixative and paraffin wax as the embedding material.

The shrinkage of fish standard length after fixation was relatively low across the size range investigated (approximately 2%) and followed no discernible pattern in relation to size of the fish. Since in this study SL is not used in any comparisons with age of fish it was not considered necessary to expand the sample size and investigate the possibilities of size dependent shrinkage any further. However it should be noted that several studies have found changes in SL of fish larvae according to both the amount of time the fish are held in alcohol and the type of fixation (Kruse and Dalley, 1990 for review). Many of these studies are aimed at obtaining age and growth data and thus use 95 % alcohol as a fixative which does not dissolve the calcareous ear bones (otoliths) used in ageing. Anhydrous or 95% alcohol can cause up to approximately 14% shrinkage in the SL of capelin larvae after 24 weeks in the solution, a value that is at least twice that of formalin induced shrinkage (Kruse and Dalley, 1990). In turn, Bouins is known to cause less shrinkage than when formalin alone is used as a fixative since a degree of protection against subsequent contraction and hardening during processing to paraffin wax is obtained from the picric acid component of Bouins (Winsor, 1994).

References

Baker, J.R. (1958) *Principles of Biological Microtechnique*. Methuen, London.

Kruse, G.H. and Dalley, E.L. (1990) Length changes in capelin, *Mallatus villosus* (Muller), larvae due to preservation in formalin and anhydrous alcohol. *J. Fish Biol.*, **36**, 619-621.

Mas-Riera, J. (1991) Changes during growth in the retinal structure of three hake species, *Merluccius* spp. (Teleostei: Gadiformes), in relation to their depth distribution and feeding. *J. Exp. Mar. Biol. Ecol.*, **152**, 91-104.

Neave, D.A. (1984) The development of visual acuity in larval plaice (*Pleuronectes platessa* L.) and turbot (*Scophthalmus maximus* L.). *J. Exp. Mar. Biol. Ecol.*, **78**, 167-175.

Penttila, A., McDowell, E.M. and Trump, B.F. (1975) Effects of fixation and

postfixation treatments on volume of injured cells. *J. Histochem. Cytochem.*, **23**, 251-270.

Stickland, N.C. (1975) A detailed analysis of the effects of various fixatives on animal tissue with particular reference to muscle tissue. *Stain Technol.*, **50**, 255-264.

Stowell, R.E. (1941) Effect on tissue volume of various methods of fixation, dehydration, and embedding. *Stain Technol.*, **16**, 67-83.

Tamura, T. and Wisbey, W.J. (1963) The visual sense of pelagic fishes especially the visual axis and accommodation. *Bull. Mar. Sci.*, **13**, 433-448.

Tarkhan, A.A. (1931) The effects of fixatives and other reagents on cell-size and tissue-bulk. *J. Roy. Mic. Soc.*, **51**, 387-400.

Winsor, L. (1994) Tissue Processing, in *Laboratory Histopathology - A Complete Reference* (Eds, A.E. Woods and R.E. Ellis) Chp. 7, Churchill Livingstone, (in press).

APPENDIX 2

Sensitivity and Resolving Power of the Vertebrate Eye

The optical stage of the visual process is responsible for delivering an image of the outside world to the retina where it can be sampled by the light-sensitive visual cells. Information lost at this stage cannot be recovered by neural processing. The sensitivity of an eye relates to the capture of sufficient photons to provide a useable neural signal whereas resolution is concerned with producing a high definition image. This appendix outlines the optical limits to the design of vertebrate eyes and considers the parameters in relation to teleost eyes. The section concerned with resolving power is followed by discussion of the various formulae used by different workers in calculating visual acuity.

Sensitivity

The capture of sufficient light to form an image is a sampling problem (Land, 1981). The degree of reliability of the sampling is increased with the number of photons caught. Therefore the brightness of the retinal image is of prime concern. The detection of a point source of light such as a star or specks of bioluminescence, when all the light comes from a single point, is related to the intensity of the source and the area of aperture and is inversely proportional to the square of the distance (Land, 1981). Thus deep-sea fish which view bioluminescence would benefit from a larger eye with large pupil (Fernald, 1988). However most animals living in higher levels of illumination will view scenes by extended light sources. Land (1981) shows that in this case retinal illuminance is proportional to luminance of the source and the square of the aperture diameter and inversely proportional to the square of the focal length. This is represented by the equation:

$$E = L \times (\pi/4) \times (A^2/f^2) \qquad \text{Eqn. A2.1}$$

where E is the retinal illuminance, L is the luminance of the extended source, A is the pupil diameter and f focal length. Thus the image brightness is not related to absolute size of the eye but to the ratio of aperture diameter to focal length. This ratio is related to the F-number of a lens:

$$\text{F-number} = f/A \qquad \text{Eqn. A2.2}$$

Combining equations 1 and 2:

$$E = L \times (\pi/4) \times (1/\text{F-number})^2 \qquad \text{Eqn. A2.3}$$

Matthiessen (1882; cited in Fernald, 1988) noted that in eyes of fishes, focal length (f) divided by lens radius (r) equalled a constant (m). This is known as Matthiessen's ratio:

$$m = f/r \qquad \text{Eqn. A2.4}$$

In most fish the aperture diameter and lens diameter are the same because the iris does not cover the lens, so from equations 2 and 4:

$$\text{F-number} = m/2 \qquad \text{Eqn. A2.5}$$

and combining equations 3 and 5:

$$E = L \times (\pi/4) \times (2/m)^2$$
$$= L \times \pi/m^2 \qquad \text{Eqn. A2.6}$$

Thus in teleost eyes, retinal illuminance is proportional to the intensity of the source and inversely proportional to the square of Matthiessen's ratio (Fernald, 1988). In other words, when viewing an extended source, teleost eyes that follow Matthiessen's ratio do not have a brighter retinal image as a result of being larger. To obtain a brighter retinal image a lowering of Matthiessen's ratio would be required.

It is also possible to increase sensitivity at the level of the retina by increasing the width and length of photoreceptors so that a large proportion of the light transmitted optically is absorbed (Land, 1981). Pooling of responses from a number of receptors by the neuronal circuitry will also improve sensitivity. However both these mechanisms for increasing sensitivity will have consequences for the resolution of the image as is discussed below.

Resolving power

For an eye to define an image accurately several criteria must be met. Firstly the eye must be able to collect sufficient light. Assuming this is achieved then a well defined image must be delivered to the retina where the photoreceptor mosaic should be of sufficient "fineness" to sample the image and thus retain the required detail. The delivery of the image to the retina and the sampling by the retinal mosaic are subject to a number of physical constraints:

1) Diffraction, which occurs at the entrance aperture and is related to the size of the aperture.

2) The fineness of the retinal receptor mosaic (often referred to as the grain of the retina), which is governed by the minimum size at which receptors can function without optical cross-talk between neighbours.

3) The focal length of the lens; the longer the focal length the greater the magnification of the image on the retina.

4) Optical imperfections of the lens, of which spherical and chromatic aberration are the most significant.

It is possible to calculate the effects of the above parameters for given eye sizes, wavelengths, and receptor diameters. Basic laws of physics apply for all parameters and several reviews deal with these factors (ie. Kirschfeld, 1976 for diffraction and receptor spacing; Lythgoe, 1979 and Land, 1981 for general reviews; Fernald, 1988 for a review relating to fish). A brief summary only is attempted here which is followed by a more detailed appraisal of the ways in which visual acuity have been calculated from histological material. It should be noted that what happens once the image has been sampled and is subsequently being analysed by neural cells of both the retina and brain is not as predictable

and can perhaps only be determined by behavioural experiments.

Diffraction

Limits to the resolving power of an eye can be set by the effects of diffraction of light at the entrance aperture. The result of diffraction is an Airy pattern, of concentric light and dark rings, on the retina which can degrade the contrast of the image and hence limit resolution. The angle subtending the radius of the Airy disc (Δr_A) is given by:

$$\Delta r_A = 1.22\lambda/A \text{ radians} \qquad \text{Eqn. A2.7} \quad \text{(Fig. A2.1a)}$$

where λ is the wavelength of light and A is the aperture diameter Kirschfeld, 1976). The radius of the Airy disc (r_A) is given by:

$$r_A = 1.22\lambda f/A \text{ mm} \qquad \text{Eqn. A2.8} \quad \text{(Fig. A2.1b)}$$

where f is the focal length of the lens (Kirschfeld, 1976). From Equation A2.7 it can be seen that Δr_A is dependant on the inverse of aperture size so that the larger A, the smaller Δr_A, and so the better the resolution. From Equation A2.8 the actual radius of the Airy disc on the retina depends on the relation of f/A (ie. the ratio known as the F-number of a lens). If the F-number remains constant so does r_A. Thus eyes with the same F-number have the same size Airy disc whatever their size or aperture diameter.

Minimum receptor size

Kirschfeld (1976) discusses the reasons for a lower limit to receptor size of about 1 - 2 μm; the main one being that at smaller diameters the receptors no longer operate as light guides and the light travels along the outside of the cell. This means that the amount of light absorbed is reduced and that the receptors are no longer able to function independently. This in turn sets a limit to the fineness of the retinal mosaic and the resolving power of the retina.

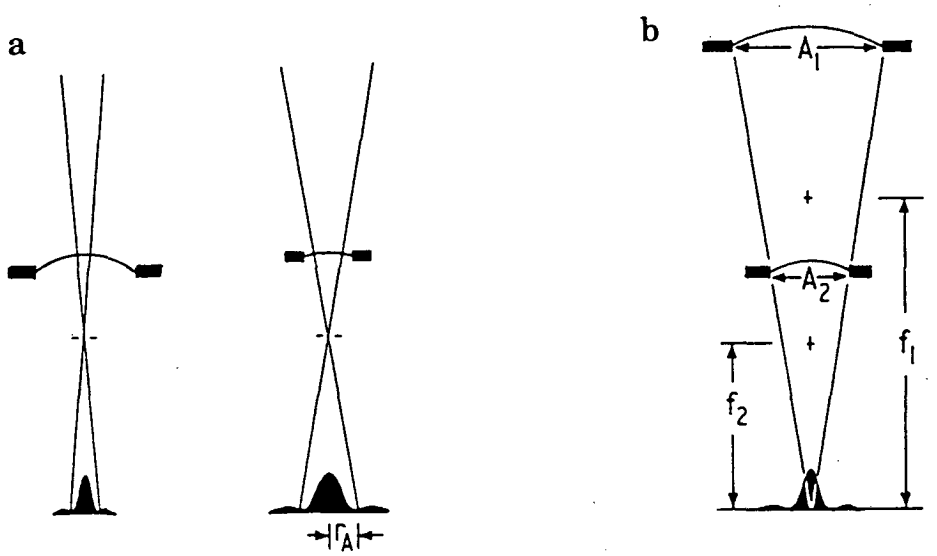

Fig. A2.1. Representation of the Airy diffraction pattern on the retina: **a)** the angular size increases and hence resolution decreases when the aperture size of the eye is reduced (Eqn. A2.7); **b)** the actual size of the pattern is the same for eyes with the same F-number (f/A in Eqn. A2.8). After Land, 1981, based on Kirschfeld, 1976).

Diffraction and receptor size

By combining the limits of receptor size and diffraction, Kirschfeld (1976) calculates an optimal F-number for which diffraction and receptor spacing are matched. At receptor spacings of 1 and 2 μm and at a wavelength of 500 nm the smallest useful F-numbers are calculated to be between 4 and 8 respectively. By relating the spatial cut-off frequency to the resolving power Land (1981) also shows 4 to be the F-number below which diffraction will be unimportant when receptor spacing is 1 μm (the spatial cut-off frequency is the point at which the contrast of a grating of black and white bars reaches zero, owing to a decrease in the spacing of the bars alone, and is also ultimately limited by diffraction). As implied from Kirschfeld's calculations, if the receptor spacing is greater, the F-number can also be greater without diffraction becoming limiting, (see also Land, 1981). Smaller F-numbers are of no use to the eye with respect to angular resolution but, as Kirschfeld states, smaller F-numbers might be of importance if temporal scanning is considered because absolute sensitivity is then increased. Land (1981) also points out that all optical systems reduce the contrast of the image compared with that of the object (the contrast transfer function) and that if the spatial frequency at which 50% object contrast is reached is taken as a limit to resolution then F-numbers of 2 with receptors of minimal size are more realistic as the optimal F-numbers. A list of F-numbers for a number of animals, given by Lythgoe (1979), shows that many animals do in fact have values close to 2, with nocturnal species having the smallest F-numbers.

In the animals investigated it would seem therefore that diffraction is not a factor that limits resolution. This would appear to be true for fish eyes as well for the following reason: the ratio, known as Matthiessen's ratio, between focal length and lens radius gives a constant value of 2.55 (in fact a range of between 2.1 and 2.8 has been reported; see Fernald, 1988 for a list). This implies that the F-number (f/A or Matthiessen's ratio/2) of the spherical fish lenses will be 1.275 (or between 1.1 and 1.4). At these low F-numbers diffraction will not interfere with the resolution set by even the finest photoreceptor mosaic.

Focal Length

As an eye increases in size the focal length of the lens also increases and this in turn increases the magnification of a given image on the retina. If the aperture size and receptor spacing also increase in proportion, the resolution will remain constant (Kirschfeld, 1976). This is because both the F-number (focal length/aperture) and number of receptors sampling a given image remain constant. If on the other hand the receptor spacing were to remain constant during an increase in eye size, resolution would improve as more receptors would be sampling the larger image. It follows therefore that in a small eye a higher density of receptors is required to obtain the same amount of information from the smaller image. However, as discussed above, there is a lower limit to the size of receptors (1 μm) which means their density can not be increased indefinitely. So, because of an increased focal length providing a larger image on the retina, large eyes always have the potential for better resolution than small eyes.

Spherical aberration

The spherical lens of teleosts could potentially be a source of spherical aberration, a defect which is results from rays further from the axis being focussed closer to the refracting surface (Land, 1981). On the assumption that spherical aberration becomes important once the resulting blur circle is larger than the Airy disc owing to diffraction, Land shows that spherical aberration of a homogenous lens is an important consideration once the focal length of the lens is over 100 μm. Thus it is an aberration that must be overcome optically in all single-lens corneal eyes. The method by which this is achieved in the spherical lenses of teleosts is to have an internal refractive index gradient with higher values towards the centre. This results in the light rays following a curved path through the lens (Pumphrey, 1961). Several mathematical models have been proposed to account for the correction of spherical aberration in the spherical fish lens and these are reviewed by Jagger (1992). Jagger also proposes a new polynomial gradient which

accurately describes image quality found in fish and one that would allow the high acuity, determined behaviourally, at 8 cycles/degree (7.5 minutes of arc) found in the tuna (Nakamura, 1968).

Chromatic aberration

This optical aberration occurs as a result of differences in refractive index for different wavelengths. Short wavelengths are refracted more than long, thus blue wavelengths come into focus before red. The size of the resulting blur circle is proportional to aperture diameter (Land, 1981). Using a dispersion factor of 0.029 (Abbe No. 34.5) Land (1981) shows that the size of the blur circle becomes significant at aperture diameters of 0.5 mm or more. It would be theoretically possible to correct for chromatic aberration by having a lens with material of decreasing dispersion towards the core, however this has not been found to occur in any biological material. Most fish lenses measured have been found to possess some degree of chromatic aberration with a range of between 2 and 5% of the focal length between the C and F Fraunhofer lines (485 and 656 nm) (see Fernald, 1988 for list). To account for this measured chromatic aberration of fish lenses Jagger (1992) finds that an increase in dispersion towards the centre of the lens would be required in the model of the spherical lens. Chromatic aberration increases rapidly at short wavelengths (below 450 nm) (Wald, 1950 for curve) and is thus likely to be more significant to fish with visual pigments absorbing at these short wavelengths, especially those living in clear shallow water where ultra violet and violet wavelengths are present. Fishes living at greater depths, where the spectral composition of light is of a narrower spectral range with the ultraviolet light absorbed, will be less affected. The presence of short wavelength absorbing pigments in the lens or cornea may be a means of reducing the effects of chromatic aberration (Muntz, 1976; Sivak and Bobier, 1978). Alternatively, the possession of a layered retina in which the short wavelength sensitive cones are located in front of those absorbing at longer wavelengths may reduce the effects of this aberration. Such a situation has been found in a number of fish; the guppy,

Lebistes reticulatus (Eberle, 1968); the rudd, *Scardinus erythrophalmus* (Scholes,1975); and the cichlid, *Haplochromis burtoni* (Fernald and Wright, 1985). However, with the exception of the guppy the displacement of the photoreceptors does not fully compensate for the observed differences in focal length (see Part I for further discussion relating to measurements of *Upeneus tragula* made during this study).

In summary: It would appear that of the potential sources of optical aberration affecting the resolution of the teleost, chromatic aberration is the factor most likely to cause image degradation once eye size, and hence focal length, reaches a critical point. However the significance of any chromatic aberration is dependant on the absorption characteristics of the visual pigments and the spectral qualities of the light environment so will be potentially more of a problem for fish inhabiting shallow water and possessing short wavelength sensitivity. Spherical aberration is known to be corrected by the refractive index gradient of the lens and the low F-number of fish lenses makes diffraction insignificant, assuming the low F-number is maintained in eyes of all sizes.

It has often been suggested that optical resolution, as set by diffraction, focal length and lens aberrations, should match the resolving ability of the photoreceptor mosaic. This appears to be true for man (Campbell and Green, 1965; Westheimer, 1972). However it does not appear to be the case in many of the other animals investigated (including fish) as optical resolution has often been found to exceed that capable of being resolved by the photoreceptors (eg. Fernald and Wright, 1985). Snyder *et al.*, (1986) have discussed this discrepancy and propose that a gain in image contrast at the level of the photoreceptors is obtained following improvement of optical image quality.

Visual Acuity

Visual acuity is a measure of the resolving power of an eye and hence the ability to distinguish fine detail. Estimates of an animals visual acuity can be obtained from behavioural experiments in which stimuli of ever decreasing dimensions are presented and some form of response is recorded. The threshold at which the stimulus elicits a response is then a measure of acuity (Muntz, 1974). Behavioural determination of visual acuity is a good measure of what an animal is actually seeing but training techniques involved can often be time consuming and difficult. Acuity is frequently calculated using data on cone densities obtained from histological preparations of the retina. This estimate is known as morphological (or anatomical) visual acuity and is based upon the suggestion by Helmholtz (1924-25) that acuity is related to "...the size of the retinal element stimulated by light". These elements are taken to be the cones. It is assumed that light falling on a single cone can produce nothing but a single light response, with no information about variation in light intensity across the cone being recorded. By using a grating of black and white bars Helmholtz concluded that images of the bright bars "...cannot be seen as separate unless there is an unstimulated retinal element between the retinal elements on which their images fall". As it is possible that some light from the bright bands could fall onto the central (unstimulated) cone, but be insufficient to cause any response. He concluded that the cones must be smaller than the interval between the middle of the bright bands falling on the retina. It is this distance, ie. the period of the grating, that Helmholtz used to calculate the smallest visual angle, also known as the minimum separable angle (MSA). Resolving power can also be quoted in cycles per degree which refers to the spatial frequency of a just-resolved grating (see for example Land, 1981). The reciprocal of this measure will give the minimum separable angle (acuity) in degrees.

It should be noted that the Helmholtz hypothesis represents the simplest approach to calculating acuity and does not take account of the effects of optical defects and diffraction which will affect the square-wave pattern of the grating on the retina,

nor is neural convergence within the retina taken into account (Muntz, 1974). Nevertheless this is the principle upon which most visual acuity calculations are now based. In many cases good agreement has been found between behavioural and morphological acuity (Muntz, 1974). However, when comparing measurements of morphological visual acuity obtained by different authors it is necessary to be aware that there appears to be a certain amount of confusion about interpretation of the Helmholtz hypothesis resulting in differing formulae for calculating acuity. This confusion stems from whether the minimum separable angle is subtended on the retina by the period or the half-period of the grating. To define the angle subtended by the period of a grating twice the intercone separation is required in the calculations (Interpretation 1, Fig. A2.2A) as this is the minimum dimension that will allow the stimulation of alternate cones with an unstimulated cone between them. To calculate the angle subtended by the half-period, only the intercone spacing is used (Interpretation 2, Fig. A2.2B) as only one cone is stimulated.

With reference to studies on fish: Tamura (1957) and Tamura and Wisbey (1963) in calculating acuity in a number of species use formulae in which they use twice the intercone spacing to calculate the acuity, thus interpreting the Helmholtz hypothesis to mean the period of the grating subtends the minimum separable angle. The formula of Tamura and Wisbey (1963) was followed by others i.e. Anctil, 1969; Blaxter (1975), Guma'a (1982), Pankhurst (1984), Mas-Riera (1991). Otten (1981) used ganglion cell receptive fields to define acuity with underlying assumption in his calculations that an unstimulated cell must lie between those stimulated, so that it is the period of a grating that is being defined. The same principle is followed by Meer and Anker (1984) and Zaunreiter *et al.* (1991) who use Otten's formula for calculating acuity. Collin and Pettigrew (1989) in using ganglion cell densities to estimate acuity also appear to use twice the inter-ganglion cell separation in their calculations. However, Northmore and Dvorak (1979) suggested that the Helmholtz hypothesis should be interpreted to mean the minimum separable angle is defined using the angle subtending the half-period of the grating and use a formula to calculate acuity that incorporates the

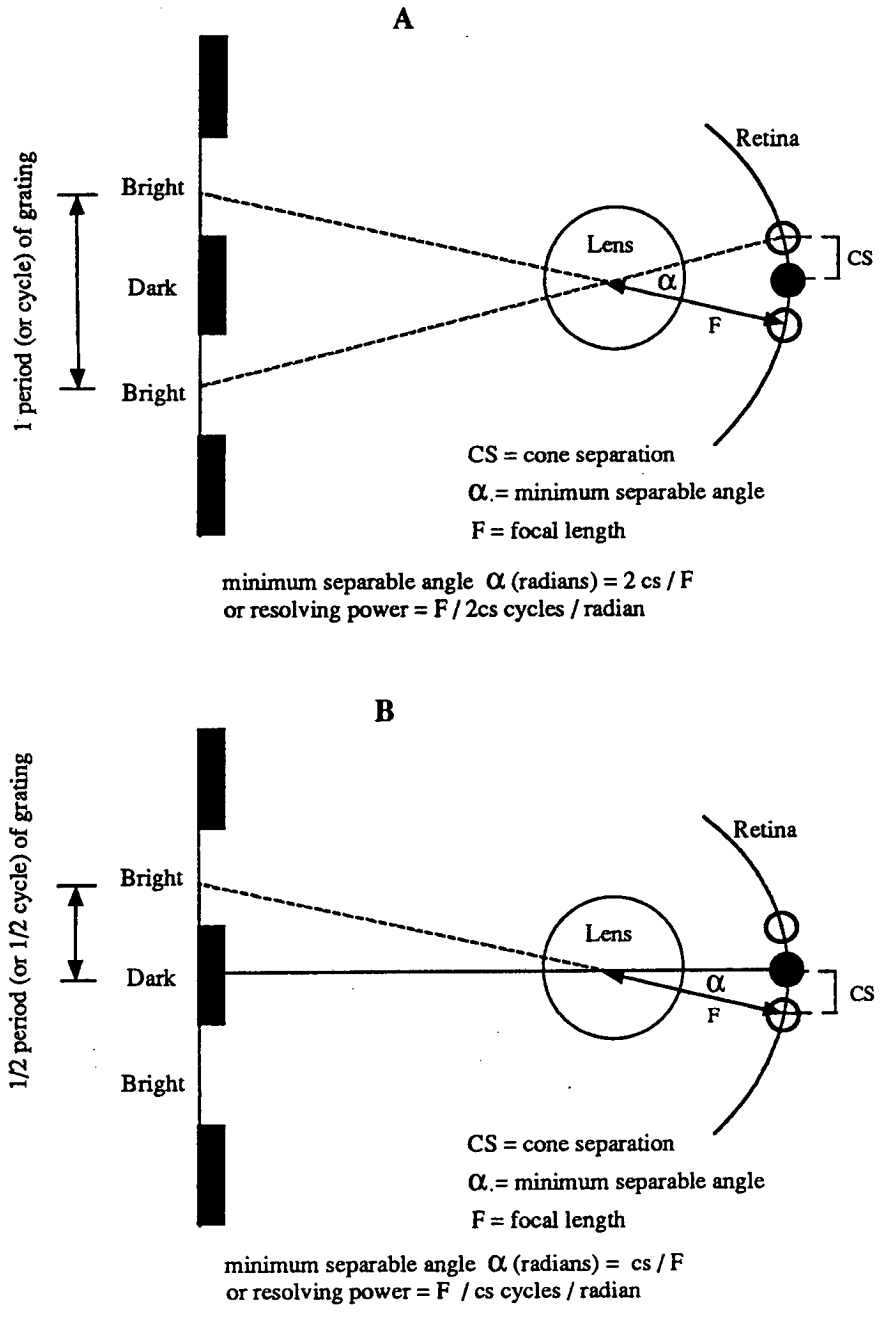

Fig. A2.2. Interpretations of the Helmholtz hypothesis. Schematic representation of cone stimulation by a grating of black and white bars. 1 unstimulated cone (filled circle) lies between 2 stimulated cones (hollow circles): **A)** Interpretation 1. One period of the grating from the middle of the bright bars is subtended by the minimum separable angle. This angle also subtends the minimum distance on the retina, of 2 x CS, that will distinguish a grating of these dimensions; **B)** Interpretation 2. A 1/2 period (or 1/2 cycle) of the grating from the middle of the bright bars to the middle of the dark bars is subtended by the minimum separable angle. This angle also subtends the distance on the retina of CS.

intercone spacing only. Others that use this interpretation of the hypothesis include Neave (1984), Williamson and Keast (1988), Margulies (1989), Browman *et al.* (1990) and Miller *et al.* (1993). This is also the angle recorded when acuity is being determined behaviourally (Douglas and Hawryshyn, 1990).

In this study the Helmholtz hypothesis is taken as meaning that the angle subtended by the period of the grating should be calculated and that to do this three cones are required. This is based on the assumption that two cells would define an edge, but not a grating, and that an edge on its own has little to do with visual acuity (W.R.A. Muntz, personal communication).

Formulae used in calculating visual acuity

A variety of formulae have been used to estimate the visual acuity of fish from measurements of cone (or ganglion cell) density. Worked examples of these formulae follow below substituting the same values for cone separation (cs = 0.006 mm) and lens radius (r = 1 mm) in each so that a comparison of the results can be made. Of the formulae that use the focal length (f) of the lens in the procedure the value for f (also known as the post nodal distance) is obtained from Matthiessen's ratio (f/r = 2.55). In fact Matthiessen reported a range of f/r from 2.4 - 2.8 (cited Fernald, 1988) and Fernald (1988) reports values from 2.1 to 2.6. However most estimates of focal length for calculations of the minimum separable angle are made using 2.55r.

1) Tamura (1957) calculates the minimum separable angle α using:

α (radians) = 2cs/2.55r Eqn. A2.9 (Fig. A2.3)

2) However Tamura and Wisbey (1963) use:

$\sin \alpha$ = 2cs/2.55r degrees Eqn. A2.10 (Fig. A2.4)

Although Equation A2.9 is not strictly mathematically correct as the retina forms

Equation A2.9:
minimum separable angle α (radians) = 2 cs / F

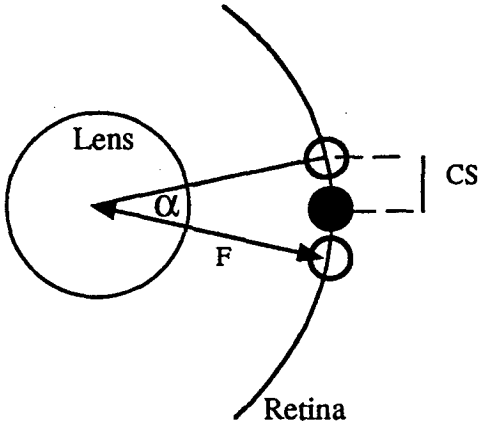

CS = 0.006 mm
F = 2.55r
r = 1 mm

α (radians) = 0.0047 α (degrees) = 16' 10.66"

Fig. A2.3. Illustration of the calculation of the minimum separable angle as proposed by Tamura (1957). The focal length (F) is obtained from Matthiessen's ratio of F = 2.55r, where r is the radius of the lens.

Equation A2.10: sin α = 2cs/F
minimum separable angle α = arc sin (2cs/F)

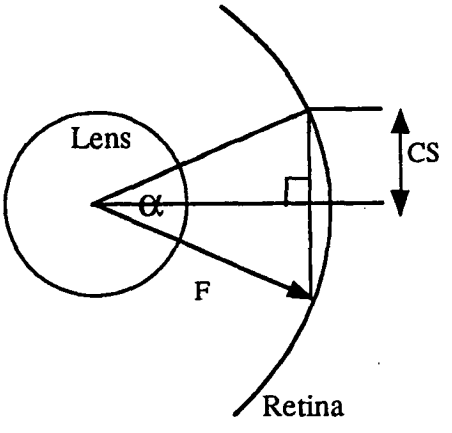

CS = 0.006 mm
F = 2.55r
r = 1 mm

α (degrees) = 16' 10.66"

Fig. A2.4. Illustration of the calculation of the minimum separable angle as proposed by Tamura and Wisbey (1963). The focal length (F) is obtained from Matthiessen's ratio of F = 2.55r, where r is the radius of the lens. The position of the cones is as for Fig. A2.3.

an arc (Fig. 4) the fact that the cone separation is so small compared with the focal length means the differences in the answers of the two formulae are minimal. As shown in Fig. A2.3 and 4: taking an intercone spacing of 0.006 mm and lens radius of 1 mm and substituting these into Equation A2.9 a value of 0.00470588 (radians) is obtained, which converted to degrees gives α = 16'10". The same values substituted into Equation A2.10 also give α = 16'10".

3) Neave (1984) uses:

$$\sin \alpha = cs/2.55r \text{ degrees} \qquad \text{Eqn. A2.11} \quad \text{(Fig. A2.5)}$$

which gives half the value obtained by Equation A2.9 and 10 ie. 8'5" as the intercone spacing alone is assumed to be subtending the minimum separable angle.

4) Northmore and Dvorak (1979) in calculating the angle subtending the half-period of the grating use a formula incorporating the magnification of the eye (M) in μm/degree, a value that is obtained from 20.5 x lens diameter (after Easter *et al.*, 1977). The formula used is:

$$\alpha \text{ (min of arc)} = 60000 \times cs/M \qquad \text{Eqn. A2.12} \quad \text{(Fig. A2.6)}$$

where 60000 is the factor for converting the units to minutes of arc. Calculating this formula with the same dimensions as used for previous examples gives:

$$\alpha = 60000 \times 0.006/20.5 \times 2 = 8'47"$$

which when multiplied by 2 to give the angle subtended by the period of the grating gives 17'34", a value slightly larger than that obtained by Equations A2.9 and 10 (see above).

5) Otten (1981) calculates visual acuity of *Haplochromis elegans* from the number of cones contributing to a ganglion cell receptive field. It is assumed that one mid receptive field needs to remain unstimulated for two points of an image to be distinguished. Based on the observation that there is a 5:1 ratio of cones to ganglion cells (paired cones counted as two) in this species, one receptive field is taken as 4 paired cones and a central single cone (Fig. A2.7). As paired cones can belong to two possible receptive fields bringing about an overlap of adjacent receptive fields (Fig. A2.7) it is the central single cone that Otten uses as the unit

Equation A2.11: $\sin \alpha = cs/F$

minumum separable angle

α (degrees) = arc sin cs/F

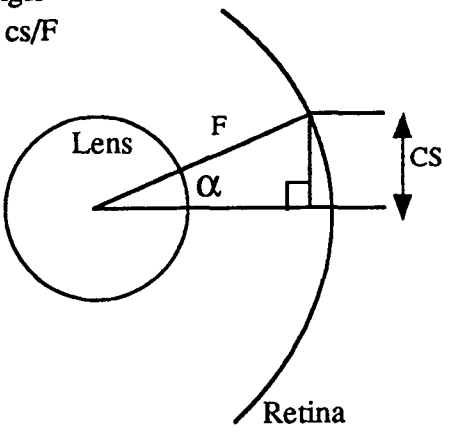

CS = 0.006 mm

F = 2.55r

r = 1 mm

α (degrees) = 8' 5. 33"

Fig. A2.5. Illustration of the calculation of the minimum separable angle as used by Neave (1984) in which the angle subtending the half-period of a grating is obtained. The focal length (F) is obtained from Matthiessen's ratio of F = 2.55r, where r is the radius of the lens. The position of the cones is as for Fig. A2.3.

Equation A2.12:

α (minutes of arc) = 60000 x cs/M

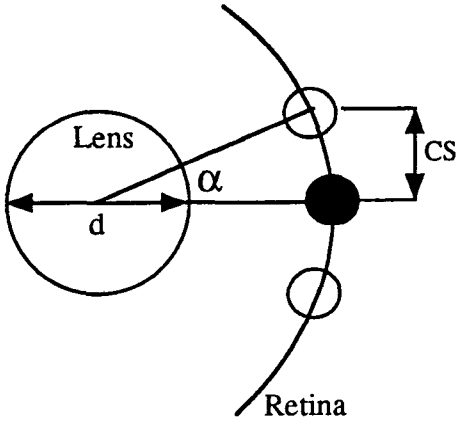

CS = 0.006 mm

M = 20.5d (μm/degree)

d= 2 mm

α (minutes) = 8' 46.83"

Fig. A2.6. Illustration of the calculation of the minimum separable angle as used by Northmore and Dvorak (1979) in which the angle subtending the half-period of the grating is obtained. The magnification on the retina (M) in μm/degree is obtained from 20.5 x lens diameter (after Easter et al., 1977).

A

Equation A2.14a: $\tan \beta = 1/F$

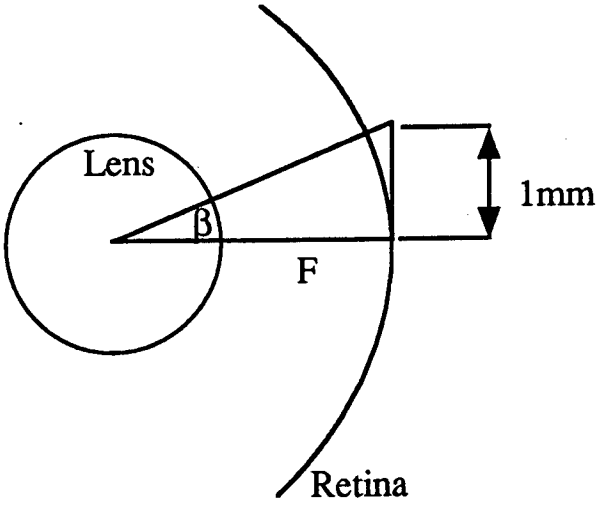

$F = 2.55r$
$r = 1mm$

$\beta = 21.413$ degrees

B

Equation A2.14aa: $\beta = 1/F$ radians

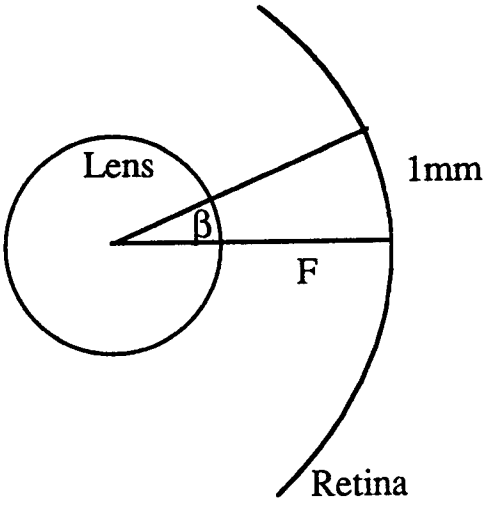

$F = 2.55r$
$r = 1mm$

$\beta = 22.46$ degrees

Fig. A2.8. Illustration of methods used for obtaining the angle subtending 1 mm on the retina: **A)** following equation A2.14a, as used by Collin and Pettigrew (1989); **B)** following equation A2.14aa. See text for procedure to obtain the minimum separable angle by the method used by Collin and Pettigrew (1989).

of reception. Therefore the distance between the single cones (q) is used in calculating the minimum separable angle, with the middle single cone being the unstimulated unit as required by the Helmholtz hypothesis if the period of the grating is to be calculated. Thus the formula used is:

α (radians) = 2q/2.55r Eqn. A2.13 (Fig.A2.7)

Assuming the intercone spacing between cone types to be the same, the value of q will be twice the value of cs used in the previous equations. Substituting the previously used values gives:

α (degrees) = (4 x 0.006/2.55) x (180/3.14)

which gives the minimum separable angle to be 32'21" ie. twice that obtained by Equations A2.9 and 10 where each individual cone is considered to be a sampling unit with its own pathway to the brain.

6) In a study of ganglion cell distribution in twelve reef species Collin and Pettigrew (1989) make visual acuity calculations based on ganglion cell densities in the areas of retina where the density is highest (assumed to be the visual axis). The procedure followed is:

i) The angle subtending 1 mm on the retina is initially calculated using Matthiessen's ratio and the lens radius by the formula:

$\tan \beta = 1/F$ Eqn. A2.14a (Fig. A2.8a)

For a lens radius of 1 mm, as used in the examples above,

β = arc tan 1/2.55 = 21.413 degrees.

ii) The number of cells/mm is then divided by the angle subtending 1 mm to give the number of cells/degree. So, continuing with the example and assuming the same receptive field as given by Otten (1981) where 2 x cs will give separate ganglion cell receptive fields, the number of cells/mm is:

1/0.012 = 83.3/mm

The number of cells/degree is:

83.3/21.413 = 3.892 Eqn. A2.14b

iii) At this point Collin and Pettigrew divide the number of cells/degree by 2 to give the highest resolvable frequency in cycles per degree:

3.892/2 = 1.9459 cycles/degree Eqn. A2.14c

Equation A.2.13: $\alpha = 2q/2.55r$

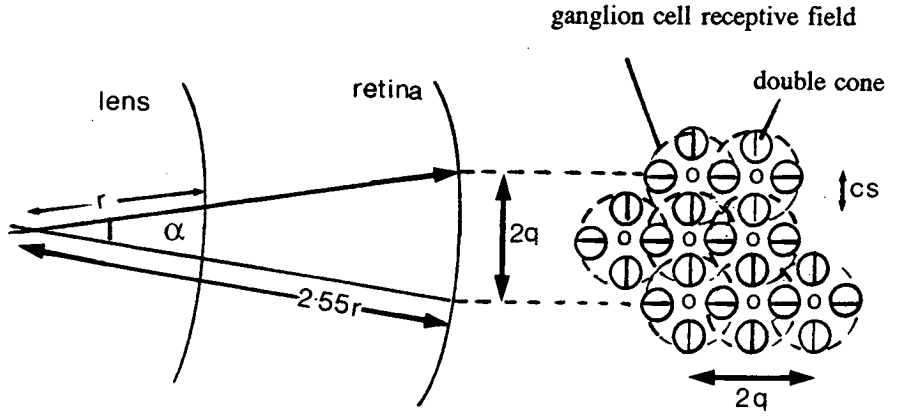

cs = 0.006

q = 2cs

r = lens radius = 1 mm

α = 32'21.32"

Fig. A2.7. Calculation of the minimum separable angle (α) based on ganglion cell receptive fields as proposed by Otten (1981). The focal length is obtained from Matthiessen's ratio of F = 2.55r. After Meer and Anker (1984) based on Otten (1981).

iv) This value can then be converted to minutes of arc subtending 1 cycle of the grating by:

$$60/1.9459 = 30'50" \qquad \text{Eqn. A2.14d}$$

This value is slightly less than given by the formula used by Otten (1981) ie. 32'21". This is due to the initial calculation of the angle subtended by 1 mm on the retina (Eqn. A2.14a) which uses arc tan instead of radians (Fig. A2.8a). Recalculating this angle using:

$$\beta = 1/F \text{ (radians)} \qquad \text{Eqn. A2.14aa} \quad \text{Fig. A2.8b}$$

and converting this value to degrees gives 22.46 degree (Fig. A2.8b). Working through the rest of the procedure using this value gives a final value for the minimum separable angle of 32'21", which is comparable with the value obtained by the formula used by Otten. At step iii) Collin and Pettigrew state that at least 2 cells are needed to resolve a cycle of the grating and they go on to divide by this value. In fact, dividing by this number at this stage is actually giving twice the intercell separation as the distance subtended by the minimum separable angle. Thus it is the period (or cycle) of the grating that is being resolved by this method (as discussed above). It should also be noted that the convergence ratio of cones to ganglion cells can vary between species and/or across the retina so the ratio substituted in this worked example of the Collin and Pettigrew method are for demonstration only as no data for this ratio were available for the species investigated by Collin and Pettigrew (1989).

In summary; the various interpretations of the Helmholtz hypothesis and the use of either cones or ganglion cells can give estimates of morphological visual acuity that vary up to 4-fold. The calculation of the angle subtended by the period of the grating gives twice the values of the angle subtending the half-period of the grating when using cone spacing. If ganglion cell receptive field is used with a ratio of 5:1 for cones to ganglion cells as in *Haplochromis elegans*, the values for the angle subtending the period of the grating is double that obtained when using cone densities.

The question of whether ganglion cell receptive fields or cone densities alone

should be used in visual acuity calculations is a matter of conjecture. In some species the ratios of cones to ganglion cells can vary across the retina with a ratio approaching 1:1 in areas of visual axis (Yamanouchi, 1966). In addition it is not known how much processing of visual information occurs in the neural cells (horizontal, bipolar and amacrine) of the retina, nor to what exactly the ganglion cells are responding when they send information to the brain. The exact interactions between cones and ganglion cells appear to vary from species to species and as also pointed out by Collin and Pettigrew (1989) there are a number of neuronal elements in the ganglion cell layer that do not have central projections. Thus, using ganglion cell densities to calculate acuity may not provide an accurate estimate of acuity.

In this study estimates of visual acuity have been obtained from cone densities alone as varying ratios of cones to ganglion cells were recorded both between species and during the growth of individual species. The formula used here in calculating the minimum separable angle is that originally proposed by Tamura (1957) (Eqn. A2.9). Northmore and Dvorak's method of using the magnification of the lens (M) was not used as the constant for calculating this magnification factor has only been worked out for the goldfish (Easter *et al.*, 1977). It is acknowledged that there are interspecific variations in Matthiessen's ratio which could lead to inaccuracies in the calculation of the focal length but the range of possible ratios is known (see for example Fernald, 1988), whereas interspecific variations in calculating M have not been quantified.

Additional assumptions concerning the function and arrangement of the photoreceptor mosaic underlie the above calculations. The double cones are taken to be one unit on the assumption that both members of the pair sample the same image space, as suggested by Northmore and Dvorak (1979). Whether or not this is the case remains to be established. It is also assumed that the cone mosaic forms a square pattern, while it is possible that this is not always the situation. If a hexagonal mosaic is present cs in the calculations should be replaced by $\sqrt{(3)}cs/2$ to take this into account (Snyder, 1979). The difference in the final

answer is not great and Northmore and Dvorak (1979) do not feel that is necessary to make any correction in view of the uncertainties involved in histological shrinkage. However where a hexagonal mosaic is observed in the species used in this study the correction factor is applied.

References

Anctil, M. (1969) Structure de la rétine chez quelques téléostéens marins du plateau continental. *F. Fish. Res. Bd. Can.*, **26**, 597-628.

Blaxter, J.H.S. (1975) The eyes of larval fish, in *Vision in Fishes* (ed. M.A. Ali), Plenum, New York, pp. 427-443.

Browman, H.I.,Gordon, W.C., Evans, B.I. and O'Brien, W.J. (1990) Correlation between histological and behavioral measures of visual acuity in a zooplanktivorous fish, the white crappie (*Pomoxis annularis*). *Brain Behav. Evol.* **35**, 85-97.

Campbell, F.W. and Green, D.G. (1965) Optical and retinal factors affecting visual resolution. *J. Physiol.*, **181**, 576-593.

Collin, S.P. and Pettigrew, J.D. (1989) Quantitative comparison of the limits on visual spatial resolution set by the ganglion cell layer in twelve species of reef teleosts. *Brain Behav. Evol.*, **34**, 184-192.

Douglas R.H. and Hawryshyn C.W. (1990) Behavioural studies of fish vision: an analysis of visual capabilities, in *The Visual System of Fish* (eds R.H. Douglas and M.B.A. Djamgoz), Chapman and Hall, London, pp. 373-418.

Easter, S.S.Jr., Johns, P.R. and Baumann, L.R. (1977) Growth of the adult goldfish eye. I: Optics. *Vision Res.*, **17**, 469-477.

Eberle, H. (1968) Zapfenbau, zapfenlange und chromatische aberration im auge von *Lebistes reticulatus* Peters (Guppy). *Zool. Jb. Physiol.Bd.*, **74**, 121-154.

Fernald, R.D. (1988) Aquatic adaptations in fish eyes, in *Sensory Biology of Aquatic Animals* (eds J. Atema, R.R. Fay, A.N. Popper and W.N. Tavolga), Springer-Verlag, New York, pp. 436-466.

Fernald, R.D. and Wright, S.E. (1985) Growth of the visual system in the African cichlid fish, *Haplochromis burtoni*. Optics. *Vision Res.*, **25**, 155-161.

Guma'a, S.A. (1982) Retinal development and retinomotor responses in perch, *Perca fluviatilis* L. *J. Fish Biol.*, **20**, 611-618.

Helmholtz, H. von (1924-25) *Physiological Optics, Vols 1,2,3*. Optical Society of America, Rochester, New York.

Jagger, W.S. (1992) The optics of the spherical fish lens. *Vision Res.*, **32**, 1271-1284.

Kirschfeld, K. (1976) The resolution of lens and compound eyes, in *Neural Principles in Vision* (eds F. Zetter and R. Weiler), Springer-Verlag, Berlin, pp. 345-370.

Land, M.F. (1981) Optics and vision in invertebrates, in *Handbook of Sensory Physiology VII/6B* (ed. H. J. Autrum), Springer-Verlag, Berlin, pp 471-592.

Lythgoe, J.N. (1979) *The Ecology of Vision*. Clarendon Press, Oxford.

Margulies, D. (1989) Size-specific vulnerability to predation and sensory system development of white seabass, *Atractoscion nobilis*, larvae. *Fish. Bull.*, **87**, 537-552.

Mas-Riera, J. (1991) Changes during growth in the retinal structure of three hake species, *Merluccius* spp. (Teleostei: Gadiformes) in relation to their depth distribution and feeding. *J. Exp. Mar. Biol. Ecol.*, **152**, 91-104.

Meer, van der, H.J. and Anker, G.C. (1984) Retinal resolving power and sensitivity of the photopic system in seven haplochromine species (Teleostei, Cichlidae). *Neth. J. Zool.*, **34**, 197-209.

Miller, T.J., Crowder, L.B. and Rice, J.A. 1993 Ontogenetic changes in behavioural and histological measures of visual acuity in three species of fish. *Environ. Biol. Fish.*, **37**, 1-8.

Muntz, W.R.A. (1974) Comparative aspects in behavioral studies of vertebrate vision, in *The Eye, Comparative Physiology Vol 6* (eds H. Davson and L.T. Graham Jr), Academic, New York, pp. 155-226.

Muntz, W.R.A. (1976) The visual consequences of yellow filtering pigments in

the eyes of fishes occupying different habitats, in *Light as an Ecological Factor II* (eds G.C. Evans, R. Bainbridge and O Rackham), Blackwell Scientific, Oxford pp. 271-287.

Nakamura, E.L. (1968) Visual acuity of two tunas, *Katsuwonus pelamis* and *Euthynnus affinis*. *Copeia*, 41-49.

Neave, D.A. (1984) The development of visual acuity in larval plaice (*Pleuronectes platessa* L.) and turbot (*Scophthalmus maximus* L.). *J. Exp Mar. Biol. Ecol.*, **78**, 167-175.

Northmore, D.P.M. and Dvorak, C.A. (1979) Contrast sensitivity and acuity of the goldfish. *Vision Res.*, **19**, 255-261.

Otten, E. (1981) Vision during growth of a generalized Haplochromis species: *H. elegans* Trewavas 1933 (Pisces, Cichlidae). *Neth. J. Zool.* **31**, 650-700.

Pankhurst, N.W. 1984 Retinal development in larval and juvenile European eel *Anguilla anguilla* (L.). Can. J. Zool. 62,335-343.

Pumphrey, R.J. (1961) Concerning vision, in *The Cell and the Organism* (eds J.A. Ramsey and V.B. Wigglesworth), Oxford University Press, Oxford, pp. 193-208.

Scholes, J.H. (1975) Colour receptors and the synaptic connexions in the retina of a cyprinid fish. *Phil. Trans. R. Soc.* **B. 270**, 61-118.

Sivak, J.G. and Bobier, W.R. (1978) Chromatic aberration of the fish eye and its effect on refractive state. *Vision Res.* **18**, 453-455.

Snyder, A.W. (1979) The physics of vision in compound eyes, in *Handbook of Sensory Physiology VII/6* (ed, H. J. Autrum), Springer-Verlag, Berlin, pp. 225-313.

Snyder, A.W., Bossomaier, T.R.J. and Hughes, A. (1986) Optical image quality and cone mosaic. *Science, N.Y.* **231**, 499-501.

Tamura, T. (1957) A study of visual perception in fish, especially on resolving power and accommodation. *Bull. Jap. Soc. Sci. Fish.*, **22**, 536-557.

Tamura, T. and Wisbey, S.J. (1963) The visual sense of pelagic fishes especially the visual axis and accommodation. *Bull. Mar. Sci. Gulf Caribb.*, **13**, 433-448.

Wald, G. (1950) Eye and camera in *From Cell to Organism* (ed. D. Kennedy),

Freeman, San Fransisco, pp. 142-151.

Westheimer, G. (1972) Visual acuity and spatial modulation thresholds, in *Handbook of Sensory Physiology, VII/2* (eds D. Jameson and L.M. Hurvich), Springer-Verlag, Berlin, pp. 449-482.

Williamson, M. and Keast, A. (1988) Retinal structure relative to feeding in the rock bass (*Ambloplites rupestris*) and bluegill (*Lepomis macrochirus*). *Can. J. Zool.* **66**, 2840-2846.

Yamanouchi, T. (1956) The visual acuity of the coral fish *Microcanthus strigatus* (Cuvier and Valaenciennes). *Publ. Seto Mar. Biol. Lab.*, **2**, 134-156.

Zaunreiter, M. Junger, H. and Kotrschal, K. (1991) Retinal morphology of cyprinid fishes: a quantitative histological study of ontogenetic changes and interspecific variation. *Vision Res.*, **31**, 383-394.

APPENDIX 3

Brain, Behavior and Evolution
Editor-in-Chief: R. Glenn Northcutt, La Jolla, Calif.

Reprint
Publisher: S. Karger AG, Basel
Printed in Switzerland

Original Paper

Brain Behav Evol 1994;43:51–60

Julia Shand

Department of Marine Biology, James Cook University of North Queensland, Townsville, Australia

Changes in Retinal Structure during Development and Settlement of the Goatfish *Upeneus tragula*

APPENDIX 4

Proceedings of the Seventh International Coral Reef Symposium, Guam, 1992, Vol. 1

Metamorphosis of the Visual and Barbel Sensory Systems at Settlement in the Reef Fish *Upeneus tragula* (Family Mullidae)

M. I. McCormick and J. Shand

Department of Marine Biology, James Cook University, Townsville, Q. 4811, Australia, Fax. No.: 61 77 25 1570

APPENDIX 5

Visual Neuroscience (1992), 9, 137–142. Printed in the USA.

Microspectrophotometric determinations of rod visual pigments in some adult and larval Australian amphibians

J. C. PARTRIDGE,[1] P. SPEARE,[2] J. SHAND,[2,3] W. R. A. MUNTZ,[4] AND D. McB. WILLIAMS[2]

[1]Department of Zoology, University of Bristol, Woodland Road, Bristol BS8, 1UG, U.K.
[2]Australian Institute of Marine Science, PMB No.3, Townsville, Queensland 4810, Australia
[3]Department of Marine Biology, James Cook University, Townsville, Queensland 4811, Australia
[4]Department of Ecology and Evolutionary Biology, Monash University, Clayton, Victoria 3168, Australia

(RECEIVED May 29, 1991; ACCEPTED December 17, 1991)

APPENDIX 6

J Comp Physiol A (1993) 173:115–121

Journal of Comparative Physiology A Sensory, Neural, and Behavioral Physiology

Changes in the spectral absorption of cone visual pigments during the settlement of the goatfish *Upeneus tragula:* the loss of red sensitivity as a benthic existence begins

J. Shand

Department of Marine Biology, James Cook University of North Queensland, Townsville, Qld. 4811, Australia

Accepted: 24 March 1993

APPENDIX 7

J Comp Physiol A (1994) 174:461–467

Journal of Comparative Physiology A
Sensory, Neural, and Behavioral Physiology

The ecology of the visual pigments of snappers (Lutjanidae) on the Great Barrier Reef

J.N. Lythgoe[1,*], W.R.A. Muntz[2], J.C. Partridge[1], J. Shand[3], D.McB. Williams[4]

[1] School of Biological Sciences, University of Bristol, Woodland Road, Bristol BS8 1UG, UK
[2] Department of Ecology and Evolutionary Biology, Monash University, Clayton, Victoria 3168, Australia
[3] Department of Marine Biology, James Cook University, Townsville, Queensland 4811, Australia
[4] Australian Institute of Marine Science, PMB 3, Townsville MC, Queensland 4810, Australia